9-1-2012

Quantum Corrections to the Gravitational Interaction of Massless Particles

Thomas J. Blackburn Jr.
University of Massachusetts - Amherst, blackburn@physics.umass.edu

QUANTUM CORRECTIONS TO THE GRAVITATIONAL INTERACTION OF MASSLESS PARTICLES

A Dissertation Presented

by

THOMAS J. BLACKBURN JR.

Submitted to the Graduate School of the
University of Massachusetts Amherst in partial fulfillment
of the requirements for the degree of

DOCTOR OF PHILOSOPHY

September 2012

Physics

QUANTUM CORRECTIONS TO THE GRAVITATIONAL INTERACTION OF MASSLESS PARTICLES

A Dissertation Presented

by

THOMAS J. BLACKBURN JR.

Approved as to style and content by:

Barry Holstein, Chair

John Donoghue, Member

David Kastor, Member

Martin Weinberg, Member

Donald Candela, Department Chair
Physics

ACKNOWLEDGMENTS

Special thanks to Barry Holstein for being my advisor for this dissertation. Thanks also to John Donoghue for initiating the research upon which it is based and for useful conversations along the way, as well as to the other members of my committee, David Kastor and Martin Weinberg

Special thanks also to my parents for their support throughout this process, without which this dissertation would not have been possible.

ABSTRACT

QUANTUM CORRECTIONS TO THE GRAVITATIONAL INTERACTION OF MASSLESS PARTICLES

SEPTEMBER 2012

THOMAS J. BLACKBURN JR.

B.Sc., UNIVERSITY OF MASSACHUSETTS AMHERST

Ph.D., UNIVERSITY OF MASSACHUSETTS AMHERST

Directed by: Professor Barry Holstein

Donoghue's effective field theory of quantum gravity is extended to include the interaction of massless particles. The collinear divergences which accompany massless particles are examined first in the context of QED and then in quantum gravity. A result of Weinberg is extended to show how these divergences vanish in the case of gravity. The scattering cross section for hypothetical massless scalar particles is computed first, because it is simpler, and the results are then extended to photons. Some terms in the cross section are shown to correspond to the Aichelburg-Sexl metric surrounding a massless particle and to quantum corrections to that metric. The scattering cross section is also applied to calculate quantum corrections to the bending of starlight, and though small, the result obtained is qualitatively different than in the classical case. Since effective field theory includes the low-energy degrees of freedom which generate collinear divergences, the results presented here will remain relevant in any future quantum theory of gravity.

TABLE OF CONTENTS

LIST OF FIGURES

Figure **Page**

CHAPTER 1
INTRODUCTION

It is well known that general relativity, unlike the other fundamental theories of the standard model, is non-renormalizable, and that this has been a major obstacle to its quantization. (See for instance [24].) The classical predictions of the theory have been verified by numerous observations, including the precession of Mercury, radar time delays, the bending of starlight, and the expansion of the universe. Because the expansion parameter for quantum corrections to the classical theory is the Planck length, these corrections should be extremely small at observable energies. However, as with all quantum field theories, even the lowest order quantum corrections are divergent. In renormalizable theories like those of the standard model, such divergences can be absorbed into a finite number of renormalized parameters, whose true values can be determined empirically, and the remaining predictions of the theory are then finite. In contrast, non-renormalizable theories like general relativity contain an infinite number of divergent parameters which must be determined empirically. Because of this, they were once thought of as non-predictive [2] and not sensible [1].

More recently though non-renormalizable theories have become accepted as effective field theories [1, 3]. In this approach, the high-energy, short-distance degrees of freedom which produce divergences are systematically separated from the low energy, long distance degrees of freedom, and the high energy degrees of freedom are integrated out. Then at low energies, only a finite number of renormalized parameters need be considered to any given order.

General relativity has previously been treated as an effective field theory by Donoghue [6, 7, 4, 5, 12, 20], who demonstrated that this method can be used to compute well-defined long-distance quantum corrections to the classical theory. Thus when interpreted as an effective field theory, general relativity is a perfectly valid quantum field theory, at least at low energies.

Donoghue and subsequent authors [33] have used this approach to compute the radiative corrections to the Newtonian scattering potential of two particles. Errors in the details of all these calculations were finally corrected by Bjerrum-Bohr, Donoghue, and Holstein in [7]. Some of the radiative corrections reported there were shown in [6, 12] to reproduce the known higher-order terms

in the classical metrics surrounding the particles, while others were shown to be quantum corrections to those metrics.

These calculations all focused on the case $q^2 \ll m^2$, where q is the momentum transfer and m the mass of the particles. This is obviously inapplicable to the case of massless particles, such as photons, for which $m = 0$. In quantum field theories with massless particles, new types of divergences appear and present a challenge [17, 16, 1, 18]. These new divergences, known as infrared (or IR) divergences, originate in the low-energy degrees of freedom. Some are familiar from QED and can be treated by well known methods, but others are more difficult to deal with.

The effective field theory method still can be applied to the massless case, but since the low-energy degrees of freedom are included in the effective theory, the IR divergences threaten the effective theory as well. If these divergences could not be removed somehow then the theory would be rendered meaningless. Since they occur in the regime where both quantum field theory and general relativity are expected to be valid, they present a real challenge to the existing theory of gravity and quantum physics.

On the other hand, since the divergences in the effective theory will be identical to those in the underlying high energy theory, the treatment of IR divergences in the effective theory will be relevant to the true theory of quantum gravity, whatever that may be. Also, one might hope that quantum corrections could be easier to detect empirically in the massless case if some effects are entirely null in the classical predictions for massless particles. Therefore the calculation of observables for massless particles in the effective theory of quantum gravity is an important task. This thesis considers the massless case and the special problems that it involves.

1.1 Overview of Effective Field Theory

Many non-renormalizable theories at least approximately describe nature at low energies. One of the oldest examples of this is the Fermi theory of weak interactions. Here the weak interactions of fermions with the W and Z bosons is replaced in the low energy regime by a direct four-fermion interaction. The exact matrix element for muon-electron scattering via a W, for instance, is of the form

$$\mathcal{M} \propto \bar{\nu_e}\gamma^\mu \left(1-\gamma^5\right) e \frac{g_{\mu\nu} - \frac{q_\mu q_\nu}{M_W^2}}{q^2 - M_W^2} \bar{\mu}\gamma^\nu \left(1-\gamma^5\right) \nu_\mu \tag{1.1}$$

where e, ν_e, μ, and ν_μ are the electron, muon, and neutrino spinors, and M_W is the W mass. All the interactions in this reaction are renormalizable. However, when $q^2 \ll M_W^2$, this becomes approximately

$$\mathcal{M} \propto \bar{\nu_e}\gamma^\mu \left(1-\gamma^5\right) \frac{e}{M_W^2} g_{\mu\nu} \bar{\mu}\gamma^\nu \left(1-\gamma^5\right) \nu_\mu \tag{1.2}$$

This is of the same form as a direct four-fermion coupling, which is non-renormalizable. Another example is furnished by chiral perturbation theory, which is the low energy approximation to QCD. In these examples the true high energy theory is renormalizable, but at low energy fields appear to interact via 'effective' non-renormalizable interactions. Effective field theory has been used to treat such theories for a long time. [1, 3]

Consider as an example a complex scalar field θ with a spontaneously broken $U(1)$ symmetry [1, 25]:

$$\mathcal{L} = -\partial_\mu \theta^* \partial^\mu \theta - \frac{\lambda^2}{4}\left(\theta^*\theta - v^2\right)^2 \tag{1.3}$$

This is an entirely renormalizable theory. Reparameterize the theory by a polar decomposition in terms of two real fields χ, ϕ

$$\theta = \chi e^{i\phi/v} \tag{1.4}$$

The Lagrangian then becomes

$$\mathcal{L} = -\partial_\mu \chi \partial^\mu \chi - \frac{1}{v^2}\chi^2 \partial_\mu \phi \partial^\mu \phi - \frac{\lambda^2}{4}\left(\chi^2 - v^2\right)^2 \tag{1.5}$$

The invariance of the θ field under $U(1)$ transformations

$$\theta \to \theta e^{i\omega} \tag{1.6}$$

has become invariance of the ϕ field under the transformation

$$\phi \to \phi + \omega v \tag{1.7}$$

Expanding χ about the potential minimum $\chi = v$ reveals that χ is a particle of mass $M \sim \lambda v$ while the field ϕ is massless. The ϕ and χ particles interact via various couplings.

Suppose one is interested only in the scattering of ϕ particles at low energy. Under the Lagrangian (1.5), this would occur via the exchange of various virtual ϕ and χ particles. The quantum field theory can be derived from the functional integral

$$W = \int \mathrm{D}\phi \mathrm{D}\chi e^{i\int \mathrm{d}^4 x \mathcal{L}(\chi,\phi)} \tag{1.8}$$

Divide the degrees of freedom of the fields into those with Euclidean momentum p such that $p^2 + m^2 \geq \Lambda^2$ and those with $p^2 + m^2 < \Lambda^2$, where Λ defines the cutoff between low and high energy scales.

The former includes all modes of the χ field and high-energy modes $\phi_>$of the ϕ field, while the latter only includes the low-energy ϕ modes $\phi_<$. Define an effective Lagrangian via

$$e^{i\int \mathrm{d}^4x\mathcal{L}_{eff}(\phi_<)} = \int \mathrm{D}\phi_>\mathrm{D}\chi e^{i\int \mathrm{d}^4x\mathcal{L}(\chi,\phi_<,\phi_>)} \tag{1.9}$$

Then trivially

$$W = \int \mathrm{D}\phi_<\mathrm{D}\phi_>\mathrm{D}\chi e^{i\int \mathrm{d}^4x\mathcal{L}(\chi,\phi_<,\phi_>)} = \int \mathrm{D}\phi_< e^{i\int \mathrm{d}^4x\mathcal{L}_{eff}(\phi_<)} \tag{1.10}$$

and so the effective Lagrangian functions is the Lagrangian for a quantum field theory which contains only the $\phi_<$ field and has the same scattering amplitudes as the full theory. The effective Lagrangian may be highly nonlinear, but in general it will be local and it must obey the symmetry (1.7) of the underlying theory, so it can depend on ϕ only through $\partial_\mu\phi$.

The most general effective Lagrangian respecting the symmetry of the theory is of the form

$$\mathcal{L}_{eff} = -\frac{1}{2}\partial_\mu\phi\partial^\mu\phi + \frac{a}{M^4}\left(\partial_\mu\phi\partial^\mu\phi\right)^2 + \frac{b}{M^6}\left(\partial_\mu\phi\partial^\mu\phi\right)\partial_\nu\partial^\nu\left(\partial_\mu\phi\partial^\mu\phi\right) + \frac{c}{M^8}\left(\partial_\mu\phi\partial^\mu\phi\right)^3 + \cdots \tag{1.11}$$

The constants a, b, $c\ldots$ are dimensionless, and since M is the only mass of the underlying theory, this must set the scale of the effective theory as well. This leaves out redundant interactions of the form

$$\mathcal{L}_{redundant} = -d\Box\phi\Box\phi + e\partial_\mu\phi\Box\partial^\mu\phi + \cdots \tag{1.12}$$

which may be removed by an integration by parts or by a field redefinition.

A general Feynman diagram constructed from this Lagrangian will be the integral of a rational function in the internal momenta p with coefficients formed from the external momenta q:

$$\int \mathrm{d}^4p_1\mathrm{d}^4p_2\cdots\frac{Ap^r + Bp^{r-1}q + \cdots + Cq^r}{Dp^s + Ep^{s-1}q + \cdots Fq^s} \tag{1.13}$$

Each vertex with d derivatives contributes a factor p^d to the numerator. Each propagator contributes a factor p^2 to the denominator. Each integration contributes d^4p to the volume element, and a diagram with I internal lines and V vertices has L integrations, where

$$L = I - V + 1 \tag{1.14}$$

is the number of loops in the diagram, so the total volume element is $\mathrm{d}^{4L}p$. Let d_i and n_i be the number of lines and derivatives of vertex i. Then the integral behaves asymptotically at large p like

$$\int p^{D-1}\mathrm{d}p \tag{1.15}$$

where

$$D = \sum_i d_i - 2I + 4\,(I - V + 1) = 4 + 2I + \sum_i (d_i - 4) \tag{1.16}$$

Using the identity

$$2I + E = \sum_i n_i \tag{1.17}$$

where E is the number of external lines, this can be expressed

$$D = 4 - E - \sum \Delta_i \tag{1.18}$$

where for each vertex

$$\Delta_i \equiv 4 - d_i - n_i \tag{1.19}$$

is the dimensionality in powers of mass of the corresponding coupling constant in the Lagrangian. If $D \geq 0$ the integral diverges like p^D (or logarithmically if $D = 0$) and thus will contain terms $\sum_{n=0}^{D} C_n q^n$ with divergent coefficients C.

The divergent parts of an individual diagram with E external lines are polynomials of degree D in the external momenta q. These have exactly the same form as the contribution from single vertex diagrams with $n_i = E$ lines and $d_i \leq D$ derivatives, and so they can be absorbed into renormalized parameters in the Lagrangian. Neither the bare coupling constants in the Lagrangian nor the the divergent parts of the diagrams can be observed individually. Only the combination of the two in the renormalized constants can be observed. The values of the renormalized coupling constants are not predicted by the theory, but must rather be determined either by matching onto the predictions of the high energy theory, or from experiment.

In a renormalizable theory, only a finite number of parameters. In a renormalizable theory, the Lagrangian contains only the finite number of possible terms with $\Delta_i \geq 0$, so $D \leq 4 - E$ for every diagram, and only terms in the Lagrangian with $\Delta_i = 4 - d_i - n_i = 4 - d_i - E \geq 4 - D - E \geq 0$ will be renormalized. However, because $\mathcal{L}_{eff}$ contains coupling constants with negative dimension $\Delta_i \leq 0$, the degree of divergence D will grow arbitrarily large with more complicated diagrams. Thus more and more terms will be renormalized in the effective Lagrangian, and so the Lagrangian must contain all terms allowed by the symmetry of the theory.

Besides polynomials in the q, each diagram also has non analytic parts of the form, for example, $\log q^2$. These can not be expanded in power of q, and so can not be combined with terms in the effective Lagrangian. Therefore they are observable by themselves and are physically meaningful predictions of the effective theory. Further, when Fourier transformed to the position representation, they contribute the long-range pieces of the result, whereas the analytic terms contribute only derivatives of delta-functions.

Although the full effective Lagrangian must contain an infinite number of terms, at low energy, only a finite number of them need be considered at a time. Each vertex of dimension Δ_i in a diagram with a given number of external lines will contribute a factor M^{Δ_i}, which dimensionally must be accompanied by a factor of $q^{-\Delta_i}$. Thus at low energy, each diagram will be suppressed by a factor $\left(\frac{q}{M}\right)^\nu$ where

$$\nu \equiv -\sum_i \Delta_i = E - 2 + 2L + \sum_i (d_i - 2) \tag{1.20}$$

by the topological identities above. Thus for a given type of diagram, the dominant behavior at low energy is given by the tree diagram with the fewest number of derivatives, and each additional loop or derivative suppresses the diagram by additional factors of $\frac{q}{M}$. One can therefore expand in powers of $\frac{q}{M}$, and to any given order, only a finite number of diagrams contribute.

1.2 Effective Field Theory of Gravity

Once the renormalized coupling constants have been determined, the low-energy behavior of an effective theory can be computed without even knowing the short-distance theory.

General relativity is an example of a non-renormalizable theory for which there is no known underlying renormalizable high-energy theory. Nevertheless, whatever the true high-energy theory of gravitation, one can integrate out the high energy modes in the same way as for the scalar theory above, defining an effective Lagrangian via [4, 5]

$$e^{i\int \mathrm{d}^4x\mathcal{L}(g_<)} = \int \mathrm{D}g_> e^{i\int \mathrm{d}^4x\mathcal{L}(g_<,g_>)} \tag{1.21}$$

where $g_>$ are the high-energy gravitational degrees of freedom, and $g_<$ the low-energy, which will be the metric tensor $g_{\mu\nu}$, at least in the realm where classical general relativity is valid. The symmetry of general relativity is general covariance. The only invariant quantity (besides $g_{\mu\nu}$ itself) of no more than second order in derivatives which can be formed from the metric tensor $g_{\mu\nu}$ is the curvature

tensor $R^{\rho}_{\sigma\mu\nu}$ [26]. Therefore the most general effective Lagrangian of pure gravity consistent with this symmetry is

$$\mathcal{L}_g = \sqrt{-g}\left\{-4\frac{\Lambda}{\kappa^2} + 2\frac{R}{\kappa^2} + c_1 R^2 + c_2 R^{\mu\nu}R_{\mu\nu} + \ldots\right\} \tag{1.22}$$

where g is the determinant of $g_{\mu\nu}$, $R_{\mu\nu} = R^{\rho}_{\mu\rho\nu}$ the Ricci tensor, $R = R^{\mu}_{\mu}$ the scalar curvature, and $\kappa^2/32\pi \equiv G$ Newton's constant. Each factor of $R^{\rho}_{\mu\rho\nu}$ has two derivatives of the field $g_{\mu\nu}$, and so higher order terms in the curvature contain greater powers of the derivatives, and are suppressed by more factors of κ^2. The coefficients c_i are normalized to be dimensionless. As explained in chapter 4, this theory is quantized about a background field $\bar{g}_{\mu\nu}$ as $g_{\mu\nu} = \bar{g}_{\mu\nu} + \kappa h_{\mu\nu}$. Then $h_{\mu\nu}$ has the conventional units and all the coupling constants have negative dimension Δ_i.

As usual, diagrams constructed from this Lagrangian will contain analytic terms with possibly divergent coefficients as well as non-analytic terms. The divergent pieces can again be absorbed into the bare parameters in the Lagrangian, and only the finite renormalized parameters have physical meaning. By the same reasoning as in the scalar case, the degree of divergence of a diagram will again be given by (1.18). Since the coupling constants have negative dimension Δ_i, in principal all possible terms in the Lagrangian must be included. Although more and more bare parameters will be renormalized at higher orders, any given diagram at any given order will only renormalize finitely many. At one loop, the renormalization of the coupling constants under dimensional regularization due to gravity have previously been calculated and are[13, 5]

$$\begin{aligned} c_1^r &= c_1 + \frac{1}{960\pi^2\epsilon} \\ c_2^r &= c_2 + \frac{7}{160\pi^2\epsilon} \end{aligned} \tag{1.23}$$

The values of the renormalized coefficients are not fixed by the theory. However, it is known empirically that after renormalization, the cosmological constant Λ^r is very small; why this is so is unknown. Effective field theory adds nothing to the resolution of this mystery, but is consistent with taking $\Lambda^r = 0$. On the other hand, effective field theory does offer a natural explanation why all of the higher order terms are effectively zero; even beginning with nonzero values of the constants c^r, the curvature of physical space-time is so small compared to the Planck length$\sim \kappa$ that for any reasonable values of c^r, the higher order terms will have completely negligible effect [5].

Once the renormalized parameters are specified, the non-analytic terms should give physically meaningful predictions.

Just as in the case of the scalar field, each diagram will be suppressed by a factor of $(\kappa q)^{\nu}$ with ν given by (1.20), and to any given order in κq only a finite number of diagrams need be considered.

The leading terms in the expression for any diagram will be those with the fewest numbers of loops and the least number of derivatives, with each additional loop or derivative suppressing the result by additional factors of κq.

[27] has shown that the traditional problems with higher order curvature terms in the gravitational Lagrangian do not occur in the low energy region appropriate for effective field theory. In the high energy region, when the R^2 terms become comparable with R, still higher order terms in the Lagrangian would have to be included, the energy expansion would be invalid, and one can not say anything about the full series in R.[5]

Gravity has previously been treated successfully as an effective field theory and used to calculate scattering amplitudes of massive particles of spin 0, 1/2, and 1 [4, 5, 7, 6, 12, 33]. It was also shown that some diagrams in the scattering amplitude could be interpreted as a correction to the metric surrounding one of the particles.

These calculations produced leading non-analytic terms of the form $\log q^2$ and $\sqrt{q^2}$ in the scattering amplitudes. When Fourier transformed to the position representation, these produced long-distance results. The square root terms were shown to produce classical, $\hbar$ independent terms in the position representation, while the $\log q^2$ terms produced quantum terms of first order in $\hbar$. The classical terms in the metric were shown [6] to correspond to the known classical corrections to the linearized Einstein theory in the Schwarzschild and Kerr metrics.

Thus the effective field theory of gravity predicts unambiguous long distance quantum corrections to classical general relativity. Furthermore, these corrections must be present in any quantum theory of gravity which reproduces Einstein's theory at low energy.

1.3 Massless Particles and Infrared Divergences

These previous calculations were done in the limit of $q \ll m^2$ for particles of mass m. Massless particles also interact gravitationally. Classically, their scattering cross sections could in theory be calculated, and the classical metric of a massless scalar particle was given by Aichelburg and Sexl[8, 9]. Quantum corrections to these results should be calculable by effective field theory, if only q remains much less than the Planck energy.

However, naive application of quantum field theory to this case, as in the case of other massless quantum field theories, leads to new, infrared (IR) divergences[19, 1, 18, 16, 17]. Some of these are just the familiar infrared singularities from QED, which can be removed in the usual way, by the

inclusion of bremsstrahlung. However, there are additional divergences present known as collinear or mass singularities. When a Feynman integral of the form

$$\int \frac{1}{k^2 \left(p-k\right)^2 \cdots} \frac{d^4k}{\left(2\pi\right)^4} = \int \frac{1}{k^2 \left(-2p_1 \cdot k + k^2\right) \cdots} \frac{\mathrm{d}^4k}{\left(2\pi\right)^4} \tag{1.24}$$

where $p^2 = 0$, is integrated over k_0, the pole in k^2 leaves a residue

$$\int \frac{1}{2\left|\vec{k}\right| \left(2p \cdot k\right) \ldots} \frac{\mathrm{d}^3k}{\left(2\pi\right)^3} = \int \frac{\vec{k}^2 \mathrm{d}\left|\vec{k}\right| \mathrm{d}\phi \mathrm{d}\left(\cos\theta\right)}{4\vec{k}^2 \left|\overrightarrow{p}\right| \left(1-\cos\theta\right) \cdots} \tag{1.25}$$

where the polar angle θ is measured from the direction of the vector $\vec{p}$, and this diverges logarithmically around $\cos\theta = 1$, that is, when $\vec{p}$ is collinear with $\vec{k}$.

Such divergences present an additional challenge to the calculation and interpretation of observables in massless quantum gravity. Since they arise from low-energy regions of virtual momenta, they can not be ascribed to the integrated degrees of freedom of the underlying high-energy theory. Further, in general they will occur in the coefficients of non-analytic terms from the remaining integration, and so they can not be removed by renormalization of parameters in the Lagrangian. Therefore they are not resolved by effective field theory.

Nevertheless massless particles, namely photons, do exist in nature. Since these divergences occur in the region where both quantum field theory and general relativity are expected to be valid, a problem with the calculation of the gravitational effects of photons would represent a real challenge to the existing theory of gravity and quantum physics at low energies. Also, one might hope that quantum corrections may be more easy to detect empirically in the massless case, since classically some effects may be entirely null for massless particles, for instance polarization effects in the gravitational bending of light rays. Therefore the calculation of observables for massless particles in quantum gravity is an important task.

1.4 Overview of Thesis

This thesis presents calculations to one-loop order of the quantum corrections to the energy-momentum tensor of massless particles, to the Aichelburg-Sexl metric, and to the cross section for scattering of massless particles by particles of arbitrary mass. After the nature of infrared divergences in general is explored in chapter 2, they are examined in the more familiar context of QED in chapter 3, before moving on to the main problem of quantum gravity. The gravitational

cross sections are calculated in chapter 4, first for the simpler case of a massless particle of spin 0, because the gravitational interaction of particles with spin is algebraically more complicated, and then these results are extended to the massless spin 1 (photon) case. There the collinear divergence problem is solved by extending a result due to Weinberg [19], who showed that certain collinear divergences cancel in the total cross section when all diagrams are added together. These results are then applied and interpreted in chapter 5. It is examined whether certain diagrams can be interpreted in terms of the metric surrounding a massless particle, as could be done for massive particles, but it is found that the collinear singularities do not disappear from the result for this subset of diagrams. The cross section results are also applied to calculate the quantum corrections to the bending of starlight. Some concluding remarks are offered in chapter 6.

CHAPTER 2

FEYNMAN INTEGRALS AND INFRARED DIVERGENCES

The main problem of gravitationally interacting massless particles is the occurrence of infrared divergences in certain Feynman integrals. In order to understand how this problem is resolved, it is necessary to understand how these divergences arise. To this end, the integrals involved are examined and evaluated in this chapter without regard to any specific field theory, paying particular attention to the origin and treatment of IR divergences. The results will be used in later chapters in the computation of matrix elements in QED and gravity.

2.1 Preliminary Reduction of Tensor Integrals

With the exception of the bremsstrahlung integrals listed below, the integrals to be calculated are all of the form

$$I^{\mu\nu\cdots} \equiv \int \frac{k^\mu k^\nu \cdots (k\cdot p_1)\,(k\cdot p_2)\cdots}{(k^2-\lambda^2)\left((p_1-k)^2-M^2\right)\left((k-q)^2-\lambda^2\right)\left((p_2+k)^2-m^2\right)\cdots}\frac{d^Dk}{(2\pi)^D}, \tag{2.1}$$

with up to four propagators, and with multiple factors of the integration momentum k in the numerator. These integrals are computed by reducing them to combinations of simpler scalar integrals with unity in the numerator and various combinations of propagators comprising the denominator. Since the IR divergences all originate in the denominators, they are most easily examined after this reduction has been performed.

2.1.1 Form Factors

First, Feynman diagrams with external lines that have spin are expressed in terms of scalar 'invariant amplitudes' [23] or form factors. These invariant amplitudes can be calculated individually by projecting onto appropriately constructed tensors.

For example, the matrix element for the energy-momentum tensor of a scalar particle in chapter 5 can be written

$$\langle p_2|T_{\mu\nu}(x)|p_1\rangle = \frac{e^{i(p_2-p_1)x}}{\sqrt{4E_1E_2}}\left[2P_\mu P_\nu F_1 + (q_\mu q_\nu - \eta_{\mu\nu}q^2)F_2\right] \tag{2.2}$$

where $p_1^2 = p_2^2 = M^2$, $P = \frac{p_1+p_2}{2}$, $q = p_1 - p_2$, and F_1 and F_2 are scalar form factors depending on q^2. The expression determining the matrix element on the left hand side is a sum of tensor integrals of the form (2.1). By contracting both sides of (2.2) with $P^\mu P^\nu$, one obtains on the left a sum of scalar integrals, and on the right the quantity $2P^4F_1 - P^2q^2F_2$. Similarly, by contracting both sides with $\eta^{\mu\nu}$, one obtains a scalar equation for the quantity $2P^2F_1 - 3q^2F_2$. These two expressions can then be evaluated independently of one another, and the results used to solve for $F_1$and F_2.

Similarly, the matrix element for photon-scalar scattering in chapter 4 can be written

$$-i\mathcal{M} = H^{\mu\nu}\epsilon_\mu(p_4)\,\epsilon_\nu(p_2) \tag{2.3}$$

where p_1 and p_3 are the momenta of the initial and final scalars, p_2 and p_4 the momenta of the initial and final photons, $\epsilon(p_2)$ and $\epsilon(p_4)$ are the polarization vectors of the initial and final photons, and H has the form

$$H^{\mu\nu} = H_1\frac{P^\mu P^\nu}{P^2} + H_2\left(\eta^{\mu\nu} - \frac{P^\mu P^\nu}{P^2} - \frac{K^\mu K^\nu}{K^2} - \frac{q^\mu q^\nu}{q^2}\right) \tag{2.4}$$

where

$$\begin{aligned} P &= p_1 + p_3 - \frac{(p_1+p_3)\cdot K}{K^2}K \\ K &= p_2 + p_4 \\ q &= p_1 - p_3 = p_4 - p_2 \end{aligned} \tag{2.5}$$

By contracting the expression for $H^{\mu\nu}$ with $P^\mu P^\nu/P^2$, one obtains an expression for the scalar H_1, which can be evaluated independently of H_2. Contracting $H^{\mu\nu}$ with the other tensor form in (2.4) determines an expression for H_2.

2.1.2 Cancellation of Scalar Products

After this, each integral is a scalar with propagators comprising the denominator and with scalar products of various external and internal momenta in the numerator. Scalar products not involving the integration momentum k can be brought outside the integral. Integrals with scalar products in

their numerators that do involve k may be reducible to simpler integrals by reworking the products so as to cancel with factors in the denominator. For example,

$$\begin{aligned}\int \frac{k\cdot p_1}{\left((k-p_1)^2-M^2\right)(q-k)^2\,k^2}\mathrm{d}^4k &= \int \frac{\frac{1}{2}\left(k^2+M^2-(k-p_1)^2\right)}{\left((k-p_1)^2-M^2\right)(q-k)^2\,k^2}\mathrm{d}^4k \\ &= \frac{1}{2}\int \frac{\mathrm{d}^4k}{\left((k-p_1)^2-M^2\right)(q-k)^2} \\ &\quad -\frac{1}{2}\int \frac{\mathrm{d}^4k}{(q-k)^2\,k^2} \end{aligned} \tag{2.6}$$

where $p_1^2 = M^2$. Other formulae can be proven similarly. A list of all such cancellation formulae used is given in the appendix.

When there are several scalar products in the numerator, the cancellation process can be applied iteratively. For instance, if the numerator on the left-hand side of (2.6) were $(k\cdot p)(k\cdot q)$ instead of just $k\cdot p$, then after eliminating the factor of $k\cdot p$ as above:

$$\begin{aligned}\int \frac{(k\cdot p_1)(k\cdot q)}{\left((k-p_1)^2-M^2\right)(q-k)^2\,k^2}\mathrm{d}^4k &= \frac{1}{2}\int \frac{k\cdot q\mathrm{d}^4k}{\left((k-p_1)^2-M^2\right)(q-k)^2} \\ &\quad -\frac{1}{2}\int \frac{k\cdot q\mathrm{d}^4k}{(q-k)^2\,k^2} \end{aligned} \tag{2.7}$$

the same process can be used again in the latter integral on the right-hand side of (2.7):

$$\int \frac{(k\cdot q)\,\mathrm{d}^4k}{(q-k)^2\,k^2} = \frac{1}{2}\int \frac{\mathrm{d}^4k}{k^2} - \frac{q^2}{2}\int \frac{\mathrm{d}^4k}{(q-k)^2\,k^2} - \frac{1}{2}\int \frac{\mathrm{d}^4k}{(q-k)^2} \tag{2.8}$$

2.1.3 Tensor Reduction

However, not all factors of k can be canceled in this way. For instance, if one were to attempt the same process in the first integral in (2.7),

$$\begin{aligned}\int \frac{k\cdot q}{\left((k-p_1)^2-M^2\right)(k-q)^2}\mathrm{d}^4k &= \int \frac{\frac{1}{2}\left(k^2+q^2-(k-q)^2\right)}{\left((k-p_1)^2-M^2\right)(k-q)^2}\mathrm{d}^4k \\ &= \frac{1}{2}\int \frac{k^2\mathrm{d}^4k}{\left((k-p_1)^2-M^2\right)(k-q)^2} \\ &\quad +\frac{q^2}{2}\int \frac{\mathrm{d}^4k}{\left((k-p_1)^2-M^2\right)(k-q)^2} \end{aligned}$$

$$-\frac{1}{2}\int \frac{\mathrm{d}^4 k}{\left(\left(k-p_1\right)^2 - M^2\right)} \tag{2.9}$$

then there would be nothing left in the denominator of the first integral on the right to cancel the remaining factor of k^2. One is thus forced to evaluate certain integrals such as

$$\int \frac{k^\mu}{\left(\left(k-p_1\right)^2 - M^2\right)\left(k-q\right)^2}\mathrm{d}^4 k \tag{2.10}$$

These tensor integrals, with various powers of k remaining in their numerators, are reduced to standard scalar integrals using the tensor integral reduction method of Passarino and Veltman[14]. For instance,

$$I_\mu^{(1)}(q) = \int \frac{\mathrm{d}^4 k}{(2\pi)^4}\frac{k_\mu}{(k^2-\lambda^2)\left(\left(k-q\right)^2-\lambda^2\right)} = \frac{I^{(1)}(q)}{2}q_\mu \tag{2.11}$$

$$\begin{aligned} I_{\mu\nu}^{(1)}(q) &= \int \frac{\mathrm{d}^4 k}{(2\pi)^4}\frac{k_\mu k_\nu}{(k^2-\lambda^2)\left(\left(k-q\right)^2-\lambda^2\right)} \\ &= \frac{I^{(1)}(q)}{3}q_\mu q_\nu - \frac{I^{(1)}(q)}{12}q^2\eta_{\mu\nu} \end{aligned} \tag{2.12}$$

etc. The advantage in projecting out the individual form factors in a diagram first is that with more scalar products in the numerator, more cancellations may occur, reducing the number of tensor integrals which must be computed. If instead evaluating the expression for the full diagram directly, one may have to calculate certain tensor integrals which are orthogonal to those that actually occur in the final result, thus wasting effort.

Each of the formulae (2.12) can be derived by projecting both sides onto appropriately constructed tensors, and canceling the resulting scalar products, as above. For instance, by Lorentz invariance, the result for $I_{\mu\nu}^{(1)}(q)$ must be expressible in terms of q_μ and the metric tensor $\eta_{\mu\nu}$:

$$I_{\mu\nu}^{(1)}(q) = \int \frac{\mathrm{d}^4 k}{(2\pi)^4}\frac{k_\mu k_\nu}{(k^2-\lambda^2)\left(\left(k-q\right)^2-\lambda^2\right)} = aq_\mu q_\nu + bq^2\eta_{\mu\nu} \tag{2.13}$$

Contracting this equation with $q_\mu q_\nu$ produces

$$\begin{aligned} (a+b)\,q^4 &= \int \frac{\mathrm{d}^4 k}{(2\pi)^4}\frac{(q\cdot k)^2}{(k^2-\lambda^2)\left(\left(k-q\right)^2-\lambda^2\right)} \\ &= -\frac{1}{2}\int \frac{\mathrm{d}^4 k}{(2\pi)^4}\frac{\left(\left(k-q\right)^2-\lambda^2-q^2-\left(k^2-\lambda^2\right)\right)(q\cdot k)}{(k^2-\lambda^2)\left(\left(k-q\right)^2-\lambda^2\right)} \end{aligned}$$

$$
\begin{aligned}
&= \frac{q^2}{2}\int \frac{\mathrm{d}^4k}{(2\pi)^4}\frac{(q\cdot k)}{(k^2-\lambda^2)\left((k-q)^2-\lambda^2\right)} + \text{analytic terms} \\
&= \frac{q^4}{4}\int \frac{\mathrm{d}^4k}{(2\pi)^4}\frac{1}{(k^2-\lambda^2)\left((k-q)^2-\lambda^2\right)} + \text{analytic terms} \\
&= \frac{q^4}{4} I^{(1)}(q) + \text{analytic terms} \qquad (2.14)
\end{aligned}
$$

while contracting with $\eta_{\mu\nu}$ produces

$$
\begin{aligned}
(a+4b)\,q^2 &= \int \frac{\mathrm{d}^4k}{(2\pi)^4}\frac{k^2-\lambda^2+\lambda^2}{(k^2-\lambda^2)\left((k-q)^2-\lambda^2\right)} \\
&= 0 + \text{analytic terms} + o\left(\lambda^2\right) \qquad (2.15)
\end{aligned}
$$

Solving these two equations for the two unknowns a and b results in (2.11). If some of the scalar products do not cancel, then the tensor reduction process must be applied iteratively to the remaining integrals. Because the result for each integral only involves vectors which are present in the denominator of that integral, at least one of the scalar products will cancel at every stage, and the iterative process will eventually terminate.

For integrals with several indices and involving several different momenta, the number of possible tensor forms in the result becomes very large, and the expressions occurring in the equations for the coefficients become very complicated. One is thus faced with solving a large system of linear equations with complicated symbolic coefficients, which is potentially a very slow process. Here, to increase the efficiency of the whole tensor reduction process, Graham-Schmidt orthogonalization of the tensors is performed first. Thus, for example, instead of expressing (2.13) in terms of $q_\mu q_\nu$ and $\eta_{\mu\nu}$, one expresses it in terms of $q_\mu q_\nu$ and the orthogonal tensor $\eta_{\mu\nu} - q_\mu q_\nu/q^2$:

$$
I^{(1)}_{\mu\nu}(q) = \int \frac{\mathrm{d}^4k}{(2\pi)^D}\frac{k_\mu k_\nu}{(k^2-\lambda^2)\left((k-q)^2-\lambda^2\right)} = a' q_\mu q_\nu + b' q^2\left(\eta_{\mu\nu} - q_\mu q_\nu/q^2\right) \qquad (2.16)
$$

Since $q^\mu\left(\eta_{\mu\nu} - q_\mu q_\nu/q^2\right) = 0$, contracting both sides with $q_\mu q_\nu$ produces

$$
a' q^4 = \int \frac{\mathrm{d}^4k}{(2\pi)^D}\frac{(q\cdot k)^2}{(k^2-\lambda^2)\left((k-q)^2-\lambda^2\right)}
$$

$$= \frac{q^4}{4} I^{(1)}(q) + \text{analytic terms}, \tag{2.17}$$

while contracting with $\eta_{\mu\nu} - q_\mu q_\nu / q^2$ produces

$$\begin{aligned} 3b'q^2 &= \int \frac{\mathrm{d}^4 k}{(2\pi)^D} \frac{k^2 - \lambda^2 + \lambda^2}{(k^2-\lambda^2)\left((k-q)^2 - \lambda^2\right)} - \frac{1}{q^2} \int \frac{\mathrm{d}^4 k}{(2\pi)^D} \frac{(q\cdot k)^2}{(k^2-\lambda^2)\left((k-q)^2-\lambda^2\right)} \\ &= 0 - \frac{q^2}{4} I^{(1)}(q) + \text{analytic terms} + o\left(\lambda^2\right) \end{aligned} \tag{2.18}$$

Thus each equation directly determines the corresponding coefficient, without the need ever to solve a linear system. To give an idea of the savings achieved consider the fourth rank four-point integral $K_{\mu\nu\sigma\rho}(p_1, p_2, q)$. Even with a computer, previous calculation of similar integrals [12] took a day on a modern personal computer. With the method described here the computation of $K_{\mu\nu\sigma\rho}(p_1, p_2, q)$ takes only about five minutes.

After all this, all of the integrals will have been reduced to combinations of the standard scalar integrals, with unity in the numerator, listed below:

$$\begin{aligned} K(p_1,p_2,q) &= \mu^{4-D} \int \frac{1}{\left((k-q)^2-\lambda^2\right)\left((p_2+k)^2-m^2\right)} \\ &\quad \cdot \frac{1}{\left((k-q)^2-\lambda^2\right)\left((p_2+k)^2-m^2\right)} \frac{d^D k}{(2\pi)^D} \\ J^{(1)}(p_1,q) &= \mu^{4-D} \int \frac{1}{(k^2-\lambda^2)\left((k-q)^2-\lambda^2\right)\left((p_1-k)^2-M^2\right)} \frac{d^D k}{(2\pi)^D} \\ J^{(1)}(p_2,q) &= \mu^{4-D} \int \frac{1}{(k^2-\lambda^2)\left((k-q)^2-\lambda^2\right)\left((p_2+k)^2-m^2\right)} \frac{d^D k}{(2\pi)^D} \\ J^{(2)}(p_1,p_2) &= \mu^{4-D} \int \frac{1}{(k^2-\lambda^2)\left((p_1-k)^2-M^2\right)\left((p_2+k)^2-m^2\right)} \frac{d^D k}{(2\pi)^D} \\ I^{(1)}(q) &= \mu^{4-D} \int \frac{1}{(k^2-\lambda^2)\left((k-q)^2-\lambda^2\right)} \frac{d^D k}{(2\pi)^D} \\ I^{(2)}(p_1,p_2) &= \mu^{4-D} \int \frac{1}{\left((p_1-k)^2-M^2\right)\left((p_2+k)^2-m^2\right)} \frac{d^D k}{(2\pi)^D} \\ I^{(3)}(p_2) &= \mu^{4-D} \int \frac{1}{\left((p_2+k)^2-m^2\right)k^2} \frac{d^D k}{(2\pi)^D} \end{aligned} \tag{2.19}$$

where $M^2 \equiv p_1^2 = (p_1 - q)^2$, $m^2 \equiv p_2^2 = (p_2 + q)^2$.

2.2 IR Divergences and Regularization Methods

Most of the scalar integrals listed above contain the usual ultraviolet divergences of quantum field theory, arising from the infinite range of integration of k. These are dealt with in the usual way, by using dimensional regularization in $D = 4 - \epsilon_{UV}$ dimensions, and eventually absorbing the divergent pieces into renormalized parameters [1, 17]. However the scalar integrals $K(p_1, p_2, q)$ and $J^{(2)}(p_1, p_2)$ contain divergences, which will be collectively referred to as infrared (IR) divergences, arising instead from finite regions of integration.

In general, a Feynman diagram with massless propagators will contain infra-red divergences of two different types [18, 16, 1, 17]. For example, consider the scalar integral $J^{(2)}(p_1, p_2)$ in (2.19), which can be written

$$\int \frac{1}{k^2\left((p_1-k)^2-M^2\right)\left((p_2+k)^2-m^2\right)}\frac{d^4k}{(2\pi)^4} = \int \frac{1}{k^2\left(-2p_1\cdot k+k^2\right)\left(2p_2\cdot k+k^2\right)}\frac{\mathrm{d}^4k}{(2\pi)^4} \quad (2.20)$$

in the case $\lambda^2 = 0$. In the range of integration where k is soft (that is, where all the components of k are small), this becomes

$$\begin{aligned}\int \frac{1}{k^2\left((p_1-k)^2-M^2\right)\left((p_2+k)^2-m^2\right)}\frac{d^4k}{(2\pi)^4} &= \int \frac{1}{k^2\left(-2p_1\cdot k\right)\left(2p_2\cdot k\right)}\frac{\mathrm{d}^4k}{(2\pi)^4} \\ &\propto \int \frac{k^3\mathrm{d}k}{k^4} \end{aligned} \quad (2.21)$$

which diverges logarithmically near $k = 0$. This is the familiar IR divergence of, for example, QED, and occurs regardless of the value of m or M. Such divergences will here be called soft.

But in diagrams with more than one massless propagator, there will also be divergences arising from the range of integration where k is on-shell and collinear with one of the external massless momenta p. Consider (2.20) in the case $M^2 = m^2 = 0$. After the integration over k_0, the residue from the pole at $k^2 = 0$ leaves a term

$$\int \frac{1}{2\left|\vec{k}\right|\left(2p_1\cdot k\right)\left(2p_2\cdot k\right)}\frac{\mathrm{d}^3k}{(2\pi)^3} = \int \frac{\vec{k}^2\mathrm{d}\left|\vec{k}\right|\mathrm{d}\phi\mathrm{d}\left(\cos\theta\right)}{8\vec{k}^2\left(p_2\cdot k\right)\left|\overrightarrow{p_1}\right|\left(1-\cos\theta\right)} \quad (2.22)$$

(measuring the direction of the three-vector $\vec{k}$ from the three-vector $\vec{p_1}$), and the integral over $\cos\theta$ diverges logarithmically near $\cos\theta = 1$. (There is a similar divergence from the region of $\vec{k}$ near $\vec{p_2}$.) This divergence occurs for k hard as well as soft, as long as k is on-shell. Such divergences will be called collinear.

These infrared divergences will cancel in the final results for all physical quantities below, but in the intermediate calculations they must be dealt with by some sort of regularization. The intermediate results then depend on the regularization method used, and to study the effects of this regulator dependence, three different infra-red regularization methods are examined:

a) regularization by giving a small fictitious mass λ to the quantum mediating the interaction (photon in the case of QED or graviton in the case of gravity) while maintaining a (real or fictitious) mass m for the particles undergoing scattering,

b) dimensional regularization in $D = 4 + \epsilon_{IR}$ dimensions, with $\epsilon_{IR} > 0$, setting the mediating quantum mass $\lambda = 0$ but still maintaining the non-zero mass m of the scattered particles, and

c) dimensional regularization alone, setting both m and λ equal to 0.

To see the effect of these regularization methods on soft divergences, consider (2.21) and (2.22) again. In case **a**, (2.21) becomes

$$\int \frac{1}{\left(k^2-\lambda^2\right)\left(-2p_1\cdot k\right)\left(2p_2\cdot k\right)}\frac{\mathrm{d}^4k}{\left(2\pi\right)^4} \propto \int \frac{k^3\mathrm{d}k}{\left(k^2-\lambda^2\right)k^2} \propto \log\left(\lambda^2\right) \tag{2.23}$$

The integral is effectively cut off on the lower end at λ^2, and the logarithmic divergence is replaced by the large but finite quantity $\log\lambda^2$. (λ is chosen to be much smaller than all other quantities in the process considered, and one examines the asymptotic behavior as λ approaches 0.) To motivate case **b** or **c**, consider that the integral

$$\int \frac{1}{k^2\left(-2p_1\cdot k\right)\left(2p_2\cdot k\right)}\frac{d^Dk}{\left(2\pi\right)^4} \propto \int \frac{k^{D-1}\mathrm{d}k}{k^4} \tag{2.24}$$

is convergent in $D > 4$ dimensions and divergent in $D \leq 4$ dimensions. Thus formally replacing D by $4 + \epsilon_{IR}$, ϵ_{IR} a small positive real number, (2.21) becomes

$$\int \frac{1}{k^2\left(-2p_1\cdot k\right)\left(2p_2\cdot k\right)}\frac{d^Dk}{\left(2\pi\right)^D} \propto \int \frac{k^{D-1}\mathrm{d}k}{k^4} = \int k^{\epsilon_{IR}-1}\mathrm{d}k \propto \frac{1}{\epsilon_{IR}} \tag{2.25}$$

In this case the logarithmic divergence is replaced with a convergent power-law behavior, but with a coefficient of $1/\epsilon_{IR}$. Again one is interested only in the asymptotic behavior, this time as ϵ_{IR} approaches 0. (Note that the sign of ϵ_{IR} required for convergence is opposite to the case of UV divergences.)

Next consider the effect of these regularization methods on collinear divergences. In case **a** or **b** (2.22) becomes

$$\int \frac{1}{2\left|\vec{k}\right|(2p_1\cdot k)(2p_2\cdot k)}\frac{\mathrm{d}^3k}{(2\pi)^3} = \int \frac{\vec{k}^2\mathrm{d}\left|\vec{k}\right|\mathrm{d}\phi\mathrm{d}(\cos\theta)}{8\vec{k}^2(p_2\cdot k)\left(\sqrt{\overrightarrow{p_1}^2+m^2}-|\overrightarrow{p_1}|\cos\theta\right)} \propto \log m^2 \tag{2.26}$$

assuming m is much less than all other quantities (except possibly for λ above), while in case **c**, introducing spherical coordinates in D dimensions [17], it becomes

$$\begin{aligned}
\int \frac{1}{2\left|\vec{k}\right|(2p_1\cdot k)(2p_2\cdot k)}\frac{\mathrm{d}^{D-1}k}{(2\pi)^{D-1}} &= \frac{\pi^{\frac{D}{2}-2}}{\Gamma\left(\frac{D}{2}-1\right)(2\pi)^{D-1}}\int \mathrm{d}\left|\vec{k}\right|\left|\vec{k}\right|^{D-2}\int \mathrm{d}\phi \\
&\quad\cdot\int \mathrm{d}(\cos\theta)\left(1-\cos^2\theta\right)^{\frac{D}{2}-2}\frac{1}{8\vec{k}^2(p_2\cdot k)|\overrightarrow{p_1}|(1-\cos\theta)} \\
&= \frac{\pi^{\epsilon_{IR}/2}}{\Gamma\left(\frac{\epsilon_{IR}}{2}+1\right)(2\pi)^{\epsilon_{IR}+3}}\int \mathrm{d}\left|\vec{k}\right|\left|\vec{k}\right|^{\epsilon_{IR}+2}\int \mathrm{d}\phi \\
&\quad\cdot\int \mathrm{d}(\cos\theta)\left(1-\cos^2\theta\right)^{\epsilon_{IR}/2}\frac{1}{8\vec{k}^2(p_2\cdot k)|\overrightarrow{p_1}|(1-\cos\theta)} \\
&\propto \frac{\pi^{\epsilon_{IR}/2}}{\Gamma\left(\frac{\epsilon_{IR}}{2}+1\right)(2\pi)^{\epsilon_{IR}+3}}\int \mathrm{d}\left|\vec{k}\right|\left|\vec{k}\right|^{\epsilon_{IR}-1}\frac{2}{\epsilon_{IR}}
\end{aligned} \tag{2.27}$$

(Of course, this integral also has a $1/\epsilon_{IR}$ singularity from the k integration, and so the final result will have a double pole in ϵ_{IR}.)

2.3 Evaluation of Scalar Integrals

Finally, the scalar integrals I, J, and K can be evaluated using the regularization methods listed above. While the two- and four-point integrals needed here can be reduced to logarithms, the three-point integrals can not, and can only be reduced to Spence functions instead. The Spence function is defined by

$$\mathrm{Li}_2(x) \equiv -\int_0^1 \frac{1}{y}\log(1-xy)\,dy \tag{2.28}$$

It satisfies (amongst others) the identity[28, 29]

$$\mathrm{Li}_2(x) = -\mathrm{Li}_2(1-x) + \frac{\pi^2}{6} - \log(x)\log(1-x) \tag{2.29}$$

The logarithm and Spence function have branch cuts, corresponding to the existence of real intermediate states in the integrals, and so it is important to pay careful attention to avoid landing on the wrong branch of the complex plane. In particular the reduction to Spence functions is very

intricate, and it is easy to make such a mistake. It is easiest to evaluate these integrals first in a region where real intermediate states can not exist, and where the integrals have no branch cuts, and then extend the results to the rest of the complex plane by analytic continuation.

Frequently below the integrals will be reduced to the form

$$\int_0^1 \frac{\log(y-a) - \log(y_0-a)}{y-y_0} dy \tag{2.30}$$

This can be further reduced as follows

$$\begin{aligned}
& \int_0^1 \frac{\log(y-a) - \log(y_0-a)}{y-y_0} dy \\
= & \int_0^1 \frac{1}{y-y_0} \log\frac{y-a}{y_0-a} dy - \theta(a-y_0)\, 2\pi i \int_0^1 \frac{1}{y-y_0} dy \\
= & \int_{-y_0}^{1-y_0} \frac{1}{y'} \log\left(\frac{y'}{y_0-a}+1\right) dy' - \theta(a-y_0)\, 2\pi i \log\frac{y_0-1}{y_0} \\
= & \int_0^{1-y_0} \frac{1}{y'} \log\left(1+\frac{y'}{y_0-a}\right) dy' - \int_0^{-y_0} \frac{1}{y'} \log\left(1+\frac{y'}{y_0-a}\right) dy' \\
& -\theta(a-y_0)\, 2\pi i \log\frac{y_0-1}{y_0} \\
= & \int_0^1 \frac{1}{y''} \log\left(1+\frac{1-y_0}{y_0-a}y''\right) dy'' - \int_0^1 \frac{1}{y'''} \log\left(1-\frac{y_0}{y_0-a}y'''\right) dy''' \\
& -\theta(a-y_0)\, 2\pi i \log\frac{y_0-1}{y_0} \\
= & \ \mathrm{Li}_2\left(\frac{y_0}{y_0-a}\right) - \ \mathrm{Li}_2\left(\frac{y_0-1}{y_0-a}\right) - \theta(a-y_0)\, 2\pi i \log\frac{y_0-1}{y_0}
\end{aligned} \tag{2.31}$$

where $y' = y - y_0$, $y'' = {}^{y'}/_{1-y_0}$, $y''' = {}^{y'}/_{-y_0}$.

2.3.1 One- and Two-Point Integrals

Consider first the one-point integral

$$H_1 \equiv \mu^{4-D} \int \frac{1}{k^2 - M^2} \frac{d^D k}{(2\pi)^D} \tag{2.32}$$

Performing the integration and writing the result in terms of $\epsilon_{UV} = 4 - D$,

$$H_1 = \frac{-i}{16\pi^2} M^2 \Gamma(-1 + \epsilon_{UV}/2) \left(\frac{M^2}{4\pi\mu^2}\right)^{-\epsilon_{UV}/2} \tag{2.33}$$

Expanding in powers of ϵ_{UV},

$$H_1 = \frac{i}{16\pi^2} M^2 \left(\frac{2}{\epsilon_{UV}} - \gamma + 1 - \log\frac{M^2}{4\pi\mu^2}\right) \tag{2.34}$$

Next consider the generic two point integral

$$I^{(0)}\left(q^2,m_1^2,m_2^2\right) \equiv \mu^{4-D}\int \frac{1}{\left(k^2-m_1^2\right)\left(\left(k-q\right)^2-m_2^2\right)}\frac{\mathrm{d}^D k}{\left(2\pi\right)^D} \tag{2.35}$$

Introducing Feynman parameters via the rule

$$\frac{1}{ab}=\int_0^1 \frac{\mathrm{d}x}{\left(ax+b\left(1-x\right)\right)^2} \tag{2.36}$$

this becomes

$$\begin{aligned} I^{(0)}\left(q^2,m_1^2,m_2^2\right) &= \mu^{4-D}\int \frac{\mathrm{d}^D k}{\left(2\pi\right)^D}\int_0^1 dx \frac{1}{\left(x\left(k^2-m_1^2\right)+\left(1-x\right)\left(\left(k-q\right)^2-m_2^2\right)\right)^2} \\ &= \mu^{4-D}\int_0^1 \mathrm{d}x\int \frac{\mathrm{d}^D k}{\left(2\pi\right)^D}\frac{1}{\left(k^2-2\left(1-x\right)k\cdot q+\left(1-x\right)q^2-\left(1-x\right)m_2^2-xm_1^2\right)^2} \end{aligned} \tag{2.37}$$

Performing the k integration

$$I^{(0)}\left(q^2,m_1^2,m_2^2\right) = \frac{i}{16\pi^2}\Gamma\left(\epsilon_{UV}/2\right)\int_0^1 \left(\frac{4\pi\mu^2}{q^2x^2+\left(-q^2+m_1^2-m_2^2\right)x+m_2^2}\right)^{\epsilon_{UV}/2}\mathrm{d}x \tag{2.38}$$

where $\epsilon_{UV}=4-D$. Expanding in terms of ϵ_{UV}

$$\begin{aligned} I^{(0)}\left(q^2,m_1^2,m_2^2\right) &= \frac{i}{16\pi^2}\left(\frac{2}{\epsilon_{UV}}-\gamma-\int_0^1 \mathrm{d}x\log\frac{q^2x^2+\left(-q^2+m_1^2-m_2^2\right)x+m_2^2}{4\pi\mu^2}\right) \\ &= \frac{i}{16\pi^2}\left(\frac{2}{\epsilon_{UV}}-\gamma-\log\frac{q^2}{4\pi\mu^2}-\log\left(1-x_+\right)+x_+\log\frac{x_+-1}{x_+}\right. \\ &\quad \left.-\log\left(1-x_-\right)+x_-\log\frac{x_--1}{x_-}+2\right) \end{aligned} \tag{2.39}$$

where $x_\pm$ are the two roots of $q^2x_\pm^2+\left(-q^2+m_1^2-m_2^2\right)x_\pm+m_2^2=0$.

Particular cases of (2.39) used below are

$$\begin{aligned} I^{(1)}\left(q\right) &= \mu^{4-D}\int \frac{1}{k^2\left(k-q\right)^2}\frac{d^D k}{\left(2\pi\right)^D} \\ &= \frac{i}{16\pi^2}\left(\frac{2}{\epsilon_{UV}}-\gamma-\log\frac{-q^2}{4\pi\mu^2}+2\right) \end{aligned} \tag{2.40}$$

$$I^{(2)}\left(p_1,p_1-q\right) = \mu^{4-D}\int \frac{1}{\left(\left(p_1-k\right)^2-M^2\right)\left(\left(p_1-q-k\right)^2-M^2\right)}\frac{d^D k}{\left(2\pi\right)^D}$$

$$= \frac{i}{16\pi^2}\left(\frac{2}{\epsilon_{UV}} - \gamma - \log\frac{M^2}{4\pi\mu^2} - \frac{\sqrt{4M^2-q^2}}{\sqrt{-q^2}}\log\frac{\left(\sqrt{-q^2}+\sqrt{4M^2-q^2}\right)^2}{4M^2} + 2\right) \quad (2.41)$$

where here $M^2 \equiv p_1^2 = (p_1 - q)^2$,

$$\begin{aligned} I^{(2)}(p_1, p_3) &= \mu^{4-D}\int \frac{1}{\left((p_1-k)^2 - M^2\right)\left((p_3+k)^2 - m^2\right)}\frac{d^Dk}{(2\pi)^D} \\ &= \frac{i}{16\pi^2}\left(\frac{2}{\epsilon_{UV}} - \gamma - \log\frac{M^2}{4\pi\mu^2} + \frac{M^2-s}{s}\log\frac{M^2-s}{M^2} + 2\right) \end{aligned} \quad (2.42)$$

where here $s \equiv (p_1+p_3)^2$, $M^2 \equiv p_1^2$, $m^2 \equiv p_3^2$,

$$\begin{aligned} I^{(3)}(p_1) &= \mu^{4-D}\int \frac{1}{\left((p_1-k)^2 - M^2\right)k^2}\frac{d^Dk}{(2\pi)^D} \\ &= \frac{i}{16\pi^2}\left(\frac{2}{\epsilon_{UV}} - \gamma - \log\frac{M^2}{4\pi\mu^2} + 2\right) \end{aligned} \quad (2.43)$$

where $M^2 \equiv p_1^2$, and

$$\begin{aligned} I^{(4)}(p) &\equiv \int \frac{1}{(k^2-m^2)(p-k)^2}\frac{d^Dk}{(2\pi)^D} \\ &= \frac{i}{16\pi^2}\left(\frac{2}{\epsilon_{UV}} - \gamma - \log\frac{m^2}{4\pi\mu^2} + \frac{m^2-p^2}{p^2}\log\frac{m^2-p^2}{m} + 2\right) \end{aligned} \quad (2.44)$$

The case

$$I^{(3)}(p_2) = \mu^{4-D}\int \frac{1}{(p_2+k)^2k^2}\frac{d^Dk}{(2\pi)^D} \quad (2.45)$$

when $p_2^2 = m^2 = 0$ requires special attention. After introducing Feynman parameters,

$$\begin{aligned} I^{(3)}(p_2) &= \mu^{4-D}\int_0^1\int \frac{1}{(k^2 + 2(1-x)k\cdot p_2)^2}\frac{d^Dk}{(2\pi)^D}dx \\ &= \mu^{4-D}\int_0^1\int \frac{1}{\left((k+(1-x)p_2)^2\right)^2}\frac{d^Dk}{(2\pi)^D}dx \end{aligned}$$

$$= \mu^{4-D} \int \frac{1}{(k^2)^2} \frac{d^D k}{(2\pi)^D} \tag{2.46}$$

Changing to spherical coordinates in D dimensions and performing the angular integration,

$$I^{(3)}(p_2) = \mu^{4-D} i \frac{2\pi^{D/2}}{\Gamma(D/2)(2\pi)^D} \int_0^\infty \frac{k^{D-1} dk}{k^4} \tag{2.47}$$

This is both ultraviolet and infrared divergent, and so must be split in to two regions of integration, with $D = 4 + \epsilon_{IR}$ in the first and $D = 4 - \epsilon_{UV}$ in the second.

$$\begin{aligned} I^{(3)}(p_2) &= \frac{i}{8\pi^2} \frac{\mu^{-\epsilon_{IR}} \pi^{\epsilon_{IR}/2}}{\Gamma(2 + \epsilon_{IR}/2)(2\pi)^{\epsilon_{IR}}} \int_0^\mu k^{\epsilon_{IR}-1} dk \\ &\quad + \frac{i}{8\pi^2} \frac{\mu^{\epsilon_{UV}} \pi^{-\epsilon_{UV}/2}}{\Gamma(2 - \epsilon_{UV}/2)(2\pi)^{-\epsilon_{UV}}} \int_\mu^\infty k^{-\epsilon_{UV}-1} dk \\ &= \frac{i}{8\pi^2} \frac{\pi^{\epsilon_{IR}/2}}{\Gamma(2 + \epsilon_{IR}/2)(2\pi)^{\epsilon_{IR}}} \frac{1}{\epsilon_{IR}} + \frac{i}{8\pi^2} \frac{\pi^{-\epsilon_{UV}/2}}{\Gamma(2 - \epsilon_{UV}/2)(2\pi)^{-\epsilon_{UV}}} \frac{1}{\epsilon_{UV}} \end{aligned} \tag{2.48}$$

Finally, expanding in ϵ_{IR} and ϵ_{UV},

$$I^{(3)}(p_2) = \frac{i}{8\pi^2} \frac{1}{\epsilon_{IR}} + \frac{i}{8\pi^2} \frac{1}{\epsilon_{UV}} \tag{2.49}$$

Lastly, the integral

$$\begin{aligned} J^{(3)}(p) &\equiv \mu^{4-D} \int \frac{1}{k^2 (p-k)^2 (p-k)^2} \frac{d^D k}{(2\pi)^D} \\ &= \mu^{4-D} \int \frac{1}{k^2 (p^2 - 2p\cdot k + k^2)(p^2 - 2p\cdot k + k^2)} \frac{d^D k}{(2\pi)^D} \end{aligned} \tag{2.50}$$

though it has three denominators, is more like a two-point integral since two denominators are repeated. Introducing Feynman parameters,

$$\begin{aligned} J^{(3)}(p) &= \mu^{4-D} 2 \int_0^1 \mathrm{d}x \int \frac{x}{\left(k^2(1-x) + (p^2 - 2p\cdot k + k^2)x\right)^3} \frac{d^D k}{(2\pi)^D} \\ &= 2\mu^{4-D} \int_0^1 \mathrm{d}x \int \frac{x}{\left(k^2 - 2p\cdot kx + p^2 x\right)^3} \frac{d^D k}{(2\pi)^D} \end{aligned} \tag{2.51}$$

Performing the k integration,

$$J^{(3)}(p) = \frac{i}{16\pi^2 p^2} \Gamma(1 - \epsilon_{IR}/2) \left(\frac{-p^2}{4\pi\mu^2}\right)^{\epsilon_{IR}/2} \int_0^1 \mathrm{d}x \frac{x}{(x - x^2)^{1-\epsilon_{IR}/2}} \tag{2.52}$$

Performing the x integration,

$$J^{(3)}(p) = \frac{i}{16\pi^2 p^2}\Gamma(1-\epsilon_{IR}/2)\left(\frac{-p^2}{4\pi\mu^2}\right)^{\epsilon_{IR}/2}\frac{\Gamma\left(1+\frac{\epsilon_{IR}}{2}\right)\Gamma\left(\frac{\epsilon_{IR}}{2}\right)}{\Gamma(1+\epsilon_{IR})} \tag{2.53}$$

Expanding in powers of ϵ_{IR},

$$J^{(3)}(p) = \frac{i}{16\pi^2 p^2}\left(\frac{2}{\epsilon_{IR}}+\gamma+\log\frac{-p^2}{4\pi\mu^2}\right) \tag{2.54}$$

2.3.2 Three-Point Integral J2

The three-point integral $J^{(2)}(p_1,p_2)$ has both soft and, if m approaches 0, collinear singularities. In any of the IR regularization methods **a**, **b**, or **c**, it has the form

$$\begin{aligned} J^{(2)}(p_1,p_2) &= \mu^{4-D}\int\frac{d^Dk}{(2\pi)^D}\frac{1}{(k^2-\lambda^2)\left((p_1-k)^2-M^2\right)\left((p_2+k)^2-m^2\right)} \\ &= \mu^{4-D}\int\frac{d^Dk}{(2\pi)^D}\frac{1}{(k^2-\lambda^2)(k^2-2k\cdot p_1)(k^2+2k\cdot p_2)} \end{aligned} \tag{2.55}$$

where $M^2 \equiv p_1^2$, $m^2 \equiv p_2^2$. In case **a**, $D=4$ and $\epsilon_{IR}=0$, but $\lambda \neq 0$, while in case **b** or **c**, $\lambda = 0$ but $D = 4+\epsilon_{IR}$ with $\epsilon_{IR} > 0$. In either case, (2.55) is most easily evaluated by performing the integration first in the range $s < 0$ and then extending the result by analytic continuation. Introducing Feynman parameters via the rule

$$\frac{1}{abc} = 2\int_0^1 \mathrm{d}x\int_0^1 \mathrm{d}y\frac{x}{\left(a(1-x)+bx(1-y)+cxy\right)^3} \tag{2.56}$$

(2.55) becomes

$$\begin{aligned} J^{(2)}(p_1,p_2) &= \mu^{4-D}\int\frac{d^Dk}{(2\pi)^D} \\ &\quad\cdot 2\int_0^1 dx\int_0^1 dy\frac{x}{\left((k^2-\lambda^2)(1-x)+(k^2-2k\cdot p_1)x(1-y)+(k^2+2k\cdot p_2)xy\right)^3} \\ &= 2\mu^{4-D}\int_0^1 dx\int_0^1 dy\int\frac{d^Dk}{(2\pi)^D}\frac{x}{\left(k^2+2k\cdot(p_2y-p_1(1-y))x-\lambda^2(1-x)\right)^3} \end{aligned} \tag{2.57}$$

Performing the k integration and writing the result in terms of $\epsilon_{IR} = D-4$,

$$J^{(2)}(p_1,p_2) = 2\mu^{-\epsilon_{IR}}\int_0^1 dx\int_0^1 dy\frac{i(-\pi)^{2+\epsilon_{IR}/2}}{(2\pi)^{4+\epsilon_{IR}}}\frac{\Gamma(1-\epsilon_{IR}/2)}{\Gamma(3)}$$

$$
\begin{aligned}
& \cdot \frac{x}{\left(-\lambda^2(1-x) - x^2(p_2 y - p_1(1-y))^2\right)^{1-\epsilon_{IR}/2}} \\
= \quad & \frac{i}{16\pi^2}\int_0^1 dx \int_0^1 dy \frac{\Gamma(1-\epsilon_{IR}/2)}{(-4\pi\mu^2)^{\epsilon_{IR}/2}} \\
& \cdot \frac{x}{\left(-\lambda^2(1-x) - x^2\left(M^2 + (m^2 - M^2 - s)y + sy^2\right)\right)^{1-\epsilon_{IR}/2}}
\end{aligned} \tag{2.58}
$$

where here $s \equiv (p_1 + p_2)^2$. The next step depends on the regularization method used.

Using a nonzero λ, the integral is convergent with $\epsilon_{IR} = 0$ and becomes

$$
J^{(2)}(p_1, p_2) = \frac{-i}{16\pi^2}\int_0^1 dx \int_0^1 dy \frac{x}{\lambda^2(1-x) + x^2\left(M^2 + (m^2 - M^2 - s)y + sy^2\right)} \tag{2.59}
$$

Performing the x integration, in the limit of small λ, this becomes

$$
\begin{aligned}
J^{(2)}(p_1, p_2) &= \frac{-i}{32\pi^2}\int_0^1 dy \frac{1}{\left(M^2 + (m^2 - M^2 - s)y + sy^2\right)} \\
&\quad \cdot \log\left(\frac{M^2 + \left(m^2 - M^2 - s\right)y + sy^2}{\lambda^2}\right) + \mathcal{O}(\lambda) \\
&= \frac{-i}{32\pi^2 s}\int_0^1 dy \frac{1}{(y - y_+)(y - y_-)} \log\frac{s}{\lambda^2}(y - y_+)(y - y_-) + \mathcal{O}(\lambda)
\end{aligned} \tag{2.60}
$$

where

$$
\begin{aligned}
y_\pm &= \frac{M^2 - m^2 - s \pm \sqrt{(m^2 - M^2 - s)^2 - 4M^2 s}}{-2s} \\
&= \frac{M^2 - m^2 - s \pm \sqrt{\left((m^2 + M^2) - s\right)^2 - 4m^2 M^2}}{-2s}
\end{aligned} \tag{2.61}
$$

Note that $y_+ = 1 - y_-$ $(M \leftrightarrow m)$.

On the other hand, with $\lambda = 0$ but $\epsilon_{IR} > 0$, one can factor out the power of x in the denominator of (2.58) and perform the x integration separately:

$$
\begin{aligned}
J^{(2)}(p_1, p_2) &= \frac{-i}{16\pi^2}\int_0^1 dy \Gamma(1-\epsilon_{IR}/2)\int_0^1 dx x^{\epsilon_{IR}-1} \frac{1}{M^2 + (m^2 - M^2 - s)y + sy^2} \\
&\quad \cdot \left(\frac{M^2 + \left(m^2 - M^2 - s\right)y + sy^2}{4\pi\mu^2}\right)^{\epsilon_{IR}/2} \\
&= \frac{-i}{16\pi^2}\int_0^1 dy \Gamma(1-\epsilon_{IR}/2)\frac{1}{\epsilon_{IR}} \frac{1}{M^2 + (m^2 - M^2 - s)y + sy^2}
\end{aligned}
$$

$$\cdot \left(\frac{M^2 + \left(m^2 - M^2 - s\right) y + s y^2}{4\pi\mu^2} \right)^{\epsilon_{IR}/2} \tag{2.62}$$

Then expanding in powers of ϵ_{IR}, one finds

$$\begin{aligned} J^{(2)}(p_1, p_2) &= \frac{-i}{32\pi^2} \int_0^1 dy \frac{1}{M^2 + (m^2 - M^2 - s) y + s y^2} \\ &\quad \left(\frac{2}{\epsilon_{IR}} + \gamma + \log \frac{M^2 + \left(m^2 - M^2 - s\right) y + s y^2}{4\pi\mu^2} \right) + \mathcal{O}(\epsilon_{IR}) \\ &= \frac{-i}{32\pi^2 s} \int_0^1 dy \frac{1}{(y - y_+)(y - y_-)} \\ &\quad \left(\frac{2}{\epsilon_{IR}} + \gamma + \log \frac{s}{4\pi\mu^2} (y - y_+)(y - y_-) \right) + \mathcal{O}(\epsilon_{IR}) \end{aligned} \tag{2.63}$$

Comparing (2.60) and (2.63), the remaining y integration is finite in either case, and thus the only difference between the two regularization methods is that $\log \lambda^2$ in one case is replaced by $\log 4\pi\mu^2 + \frac{2}{\epsilon_{IR}} + \gamma$ in the other.

Continuing with the evaluation using dimensional regularization, writing the argument of the logarithm as a product of positive quantities ($y_+ \geq 1$, $y_- \leq 0$),

$$\begin{aligned} J^{(2)}(p_1, p_2) &= \frac{-i}{32\pi^2 s} \int_0^1 dy \frac{1}{(y - y_+)(y - y_-)} \\ &\quad \cdot \left(\frac{2}{\epsilon_{IR}} + \gamma + \log \frac{-s}{4\pi\mu^2} (y_+ - y)(y - y_-) \right) \\ &= \frac{-i}{32\pi^2 s} \frac{1}{y_+ - y_-} \int_0^1 dy \left(\frac{1}{(y - y_+)} - \frac{1}{(y - y_-)} \right) \\ &\quad \cdot \left(\frac{2}{\epsilon_{IR}} + \gamma + \log \frac{-s}{4\pi\mu^2} + \log(y_+ - y) + \log(y - y_-) \right) \end{aligned} \tag{2.64}$$

Adding and subtracting a term $\log(y_+ - y_-)$ inside the second parentheses and expanding,

$$\begin{aligned} J^{(2)}(p_1, p_2) &= \frac{-i}{32\pi^2 s} \frac{1}{y_+ - y_-} \\ &\quad \left(\left(\frac{2}{\epsilon_{IR}} + \gamma + \log \frac{-s}{4\pi\mu^2} + \log(y_+ - y_-) \right) \int_0^1 dy \left(\frac{1}{(y - y_+)} - \frac{1}{(y - y_-)} \right) \right. \\ &\quad + \int_0^1 dy \left(- \frac{\log(y_+ - y)}{(y_+ - y)} - \frac{\log(y - y_-)}{(y - y_-)} \right) \\ &\quad \left. + \int_0^1 dy \left(\frac{\log(y - y_-) - \log(y_+ - y_-)}{(y - y_+)} - \frac{\log(y_+ - y) - \log(y_+ - y_-)}{(y - y_-)} \right) \right) \end{aligned} \tag{2.65}$$

and using (2.31) this becomes

$$\begin{aligned} J^{(2)}(p_1,p_2) &= \frac{-i}{32\pi^2 s}\frac{1}{y_+-y_-} \\ &\left(\left(\frac{2}{\epsilon_{IR}}+\gamma+\log\frac{-s}{4\pi\mu^2}+\log(y_+-y_-)\right)\left(\log\frac{y_+-1}{y_+}-\log\frac{1-y_-}{-y_-}\right)\right. \\ &+\left(\frac{1}{2}\log^2(y_+-1)-\frac{1}{2}\log^2 y_+-\frac{1}{2}\log^2(1-y_-)+\frac{1}{2}\log^2 -y_-\right) \\ &\left.+\left(\mathrm{Li}_2\left(\frac{y_+}{y_+-y_-}\right)-\mathrm{Li}_2\left(\frac{y_+-1}{y_+-y_-}\right)-\mathrm{Li}_2\left(\frac{y_-}{y_--y_+}\right)+\mathrm{Li}_2\left(\frac{y_--1}{y_--y_+}\right)\right)\right) \end{aligned} \tag{2.66}$$

where $\mathrm{Li}_2(x)$ is defined in 2.28. Using 2.29 this becomes

$$\begin{aligned} J^{(2)}(p_1,p_2) &= \frac{-i}{32\pi^2 s}\frac{1}{y_+-y_-} \\ &\left(\left(\frac{2}{\epsilon_{IR}}+\gamma+\log\frac{-s}{4\pi\mu^2}+\log(y_+-y_-)\right)\left(\log\frac{y_+-1}{y_+}-\log\frac{1-y_-}{-y_-}\right)\right. \\ &+\frac{1}{2}\log^2(y_+-1)-\frac{1}{2}\log^2 y_+-\frac{1}{2}\log^2(1-y_-)+\frac{1}{2}\log^2 -y_- \\ &+2\,\mathrm{Li}_2\left(\frac{y_+}{y_+-y_-}\right)-2\,\mathrm{Li}_2\left(\frac{y_+-1}{y_+-y_-}\right) \\ &\left.+\log\frac{y_-}{y_--y_+}\log\left(\frac{y_+}{y_+-y_-}\right)-\log\frac{y_--1}{y_--y_+}\log\left(\frac{y_+-1}{y_+-y_-}\right)\right) \\ &= \frac{-i}{32\pi^2 s}\frac{1}{y_+-y_-}\left(\left(\frac{2}{\epsilon_{IR}}+\gamma+\log\frac{-s}{4\pi\mu^2}\right)\left(\log\frac{y_+-1}{y_+}-\log\frac{1-y_-}{-y_-}\right)\right. \\ &+\left(2\log(y_+-y_-)\left(\log\frac{y_+-1}{y_+}\right)+\log -y_-\log y_+-\log(1-y_-)\log(y_+-1)\right) \\ &+\left(\frac{1}{2}\log^2(y_+-1)-\frac{1}{2}\log^2 y_+-\frac{1}{2}\log^2(1-y_-)+\frac{1}{2}\log^2 -y_-\right) \\ &\left.+2\,\mathrm{Li}_2\left(\frac{y_+}{y_+-y_-}\right)-2\,\mathrm{Li}_2\left(\frac{y_+-1}{y_+-y_-}\right)\right) \end{aligned} \tag{2.67}$$

which agrees with [28].

Some frequently used particular cases follow. Continuing from (2.66) in case $m^2 \ll M^2, |s|$,

$$y_\pm \;\to\; 1-\frac{M^2}{s}, \frac{-m^2}{M^2-s} \tag{2.68}$$

and using (2.29)

$$\begin{aligned} J^{(2)}(p_1,p_2) &= \frac{-i}{32\pi^2(s-M^2)}\left(\frac{2}{\epsilon_{IR}}+\gamma+\log\frac{M^2-s}{4\pi\mu^2}\right)\left(\log\frac{M^2}{M^2-s}+\log\frac{m^2}{M^2-s}\right) \\ &+\frac{-i}{32\pi^2(s-M^2)}\left(\frac{1}{2}\log^2\frac{M^2}{-s}-\frac{1}{2}\log^2\frac{M^2-s}{-s}+\frac{1}{2}\log^2\frac{m^2}{M^2-s}\right) \end{aligned}$$

$$
\begin{aligned}
&+\frac{-i}{32\pi^2\left(s-M^2\right)}\left(\frac{\pi^2}{6}-\ \mathrm{Li}_2\left(\frac{M^2}{M^2-s}\right)+\ \mathrm{Li}_2\left(\frac{-s}{M^2-s}\right)\right)\\
= &\ \frac{-i}{32\pi^2\left(s-M^2\right)}\left(\frac{2}{\epsilon_{IR}}+\gamma+\log\frac{M^2-s}{4\pi\mu^2}\right)\left(\log\frac{M^2}{M^2-s}+\log\frac{m^2}{M^2-s}\right)\\
&+\frac{-i}{32\pi^2\left(s-M^2\right)}\left(\frac{1}{2}\log^2\frac{M^2}{M^2-s}+\frac{1}{2}\log^2\frac{m^2}{M^2-s}+2\ \mathrm{Li}_2\frac{-s}{M^2-s}\right) \qquad (2.69)
\end{aligned}
$$

which can easily be analytically continued to $s > M^2$. Continuing instead from 2.66 in case $M^2 = m^2$,

$$
y_\pm \ = \ \frac{1}{2}\pm\frac{\sqrt{4m^2-s}}{2\sqrt{-s}} \qquad (2.70)
$$

and

$$
\begin{aligned}
J^{(2)}\left(p_1,p_2\right) \ = \ & \frac{-i}{32\pi^2 s}\frac{1}{\frac{\sqrt{4m^2-s}}{\sqrt{-s}}}\\
&\cdot\left(\left(\frac{2}{\epsilon_{IR}}+\gamma+\log\frac{-s}{4\pi\mu^2}+\log\frac{\sqrt{4m^2-s}}{\sqrt{-s}}\right)\left(-2\log\frac{\frac{1}{2}+\frac{\sqrt{4m^2-s}}{2\sqrt{-s}}}{-\left(\frac{1}{2}-\frac{\sqrt{4m^2-s}}{2\sqrt{-s}}\right)}\right)\right.\\
&+\log^2-\left(\frac{1}{2}-\frac{\sqrt{4m^2-s}}{2\sqrt{-s}}\right)-\log^2\left(\frac{1}{2}+\frac{\sqrt{4m^2-s}}{2\sqrt{-s}}\right)\\
&\left.+2\ \mathrm{Li}_2\left(\frac{\frac{1}{2}+\frac{\sqrt{4m^2-s}}{2\sqrt{-s}}}{\frac{\sqrt{4m^2-s}}{\sqrt{-s}}}\right)-2\ \mathrm{Li}_2\left(\frac{-\left(\frac{1}{2}-\frac{\sqrt{4m^2-s}}{2\sqrt{-s}}\right)}{\frac{\sqrt{4m^2-s}}{\sqrt{-s}}}\right)\right)\\
= \ & \frac{i}{32\pi^2\sqrt{-s}\sqrt{4m^2-s}}\\
&\cdot\left(-2\left(\frac{2}{\epsilon_{IR}}+\gamma+\log\frac{\sqrt{-s}\sqrt{4m^2-s}}{4\pi\mu^2}\right)\log\left(1+\frac{-s+\sqrt{-s}\sqrt{4m^2-s}}{2m^2}\right)\right.\\
&+\log^2\left(-\frac{1}{2}+\frac{\sqrt{4m^2-s}}{2\sqrt{-s}}\right)-\log^2\left(\frac{1}{2}+\frac{\sqrt{4m^2-s}}{2\sqrt{-s}}\right)\\
&\left.+2\ \mathrm{Li}_2\left(\frac{1}{2}+\frac{\sqrt{-s}}{2\sqrt{4m^2-s}}\right)-2\ \mathrm{Li}_2\left(\frac{1}{2}-\frac{\sqrt{-s}}{2\sqrt{4m^2-s}}\right)\right) \qquad (2.71)
\end{aligned}
$$

which can be analytically continued.

Finally, in the case $m = M = 0$, where the collinear divergences are regularized by dimensional regularization, one can also factor out the power of $-s$ in (2.62) and then perform the y integration separately:

$$
J^{(2)}\left(p_1,p_2\right) \ = \ \frac{i}{16\pi^2 s}\Gamma\left(1-\epsilon_{IR}/2\right)\left(\frac{-s}{4\pi\mu^2}\right)^{\epsilon_{IR}/2}\frac{1}{\epsilon_{IR}}\int_0^1 dy\left(y-y^2\right)^{\epsilon_{IR}/2-1}
$$

$$
\begin{aligned}
&= \frac{i}{16\pi^2 s}\Gamma\left(1-\epsilon_{IR}/2\right)\left(\frac{-s}{4\pi\mu^2}\right)^{\epsilon_{IR}/2} \\
&\quad \frac{1}{\epsilon_{IR}}\frac{2^{1-\epsilon_{IR}}\cos\left(\frac{\pi\epsilon_{IR}}{2}\right)\Gamma\left(1/2-\epsilon_{IR}/2\right)\Gamma\left(\epsilon_{IR}/2\right)}{\sqrt{\pi}} \\
&= \frac{i}{16\pi^2 s}\left(\frac{4}{\epsilon_{IR}^2}+\frac{2}{\epsilon_{IR}}\log\frac{-s}{4\pi\mu^2}+\frac{2\gamma}{\epsilon_{IR}}+\frac{1}{2}\log^2\frac{-s}{4\pi\mu^2}\right. \\
&\quad \left.+\gamma\log\frac{-s}{4\pi\mu^2}+\frac{\gamma^2}{2}-\frac{\pi^2}{12}+\cdots\right) \\
&= \frac{i}{16\pi^2 s}\left(\frac{1}{2}\left(\log\frac{-s}{4\pi\mu^2}+\gamma+\frac{2}{\epsilon_{IR}}\right)^2+\frac{2}{\epsilon_{IR}^2}-\frac{\pi^2}{12}\right) \qquad (2.72)
\end{aligned}
$$

The logarithmic singularities which would exist in (2.71) in the limit $m \to 0$ are replaced in (2.72) by additional single and double poles in ϵ_{IR}, but not just by a simple substitution as when going from (2.60) to (2.63). However, (2.72) may be obtained by both substituting $\log m^2 \to \log 4\pi\mu^2 - 2/\epsilon_{IR} - \gamma$ and adding an additional term $i/16\pi^2 q^2\left(2/\epsilon_{IR}^2+\frac{\pi^2}{12}\right)$.

2.3.3 Three-Point Integral J1

$J^{(1)}(p_1,q)$ is evaluated following the method of [13].

$$
\begin{aligned}
J^{(1)}(p_1,q) &\equiv \mu^{4-D}\int\frac{d^Dk}{(2\pi)^D}\frac{1}{k^2\left(k-q\right)^2\left(\left(p_1-k\right)^2-M^2\right)} \\
&= \mu^{4-D}\int\frac{d^Dk}{(2\pi)^D}\frac{1}{k^2\left(k^2-2k\cdot q+q^2\right)\left(k^2-2k\cdot p_1\right)} \qquad (2.73)
\end{aligned}
$$

where $M^2 \equiv p_1^2 = \left(p_2-q\right)^2$. There is no soft divergence in this integral, so λ has been set equal to zero. In the case $M^2 = 0$, there is a collinear divergence, which can be regularized either by method **b,** maintaining an infinitesimal mass M, or by method **c**, using dimensional regularization. Again this is most easily evaluated in either case in the region $q^2 < 0$. Introducing Feynman parameters, this time via

$$
\frac{1}{abc} = 2\int_0^1 \mathrm{d}x\int_0^x \mathrm{d}y\frac{1}{\left(a\left(x-y\right)+by+c\left(1-x\right)\right)^3} \qquad (2.74)
$$

the integral becomes

$$
\begin{aligned}
J^{(1)}(p_1,q) &= \mu^{4-D}\int\frac{d^Dk}{(2\pi)^D}2\int_0^1 dx \\
&\quad \int_0^x dy\frac{1}{\left(k^2\left(x-y\right)+\left(k^2-2k\cdot q+q^2\right)y+\left(k^2-2k\cdot p_1\right)\left(1-x\right)\right)^3}
\end{aligned}
$$

$$= 2\mu^{4-D}\int\frac{d^Dk}{(2\pi)^D}\int_0^1 dx\int_0^x dy\frac{1}{\left(k^2-2k\cdot(qy+p_1(1-x))+q^2y\right)^3} \quad (2.75)$$

Performing the k integration and writing the result in terms of $\epsilon_{IR}=D-4$,

$$\begin{aligned} J^{(1)}(p_1,q) &= 2\mu^{-\epsilon_{IR}}\int_0^1 dx\int_0^x dy\frac{i(-\pi)^{2+\epsilon_{IR}/2}\Gamma(1-\epsilon_{IR}/2)}{(2\pi)^{4+\epsilon_{IR}}\Gamma(3)} \\ &\quad \frac{1}{\left(q^2y-(qy+p_1(1-x))^2\right)^{1-\epsilon_{IR}/2}} \\ &= \frac{i}{16\pi^2}\int_0^1 dx\int_0^x dy\frac{\Gamma(1-\epsilon_{IR}/2)}{(-4\pi\mu^2)^{\epsilon_{IR}/2}}\frac{1}{\left(q^2y(x-y)-M^2(1-x)^2\right)^{1-\epsilon_{IR}/2}} \end{aligned} \quad (2.76)$$

bearing in mind that $2q\cdot p_1=q^2$. The next step depends on the value of M and the regularization method used.

If $M=0$, then, making the change of variables $y'=y/x$, the denominator can be factored and the x and y integrals done separately:

$$\begin{aligned} J^{(1)}(p_1,q) &= \frac{i}{16\pi^2}\int_0^1 dx\int_0^1 dy'\frac{\Gamma(1-\epsilon_{IR}/2)}{(-4\pi\mu^2)^{\epsilon_{IR}/2}}\frac{x}{\left(q^2x^2y'(1-y')\right)^{1-\epsilon_{IR}/2}} \\ &= \frac{i}{16\pi^2q^2}\Gamma(1-\epsilon_{IR}/2)\left(\frac{-q^2}{4\pi\mu^2}\right)^{\epsilon_{IR}/2}\int_0^1 dx x^{\epsilon_{IR}-1}\int_0^1 dy'\left(y'(1-y')\right)^{\epsilon_{IR}/2-1} \\ &= \frac{i}{16\pi^2q^2}\Gamma(1-\epsilon_{IR}/2)\left(\frac{-q^2}{4\pi\mu^2}\right)^{\epsilon_{IR}/2}\frac{1}{\epsilon_{IR}}\frac{2^{1-\epsilon_{IR}}\cos\left(\frac{\pi\epsilon_{IR}}{2}\right)\Gamma(1/2-\epsilon_{IR}/2)\Gamma(\epsilon_{IR}/2)}{\sqrt{\pi}} \\ &= \frac{i}{16\pi^2q^2}\left(\frac{4}{\epsilon_{IR}^2}+\frac{2}{\epsilon_{IR}}\log\frac{-q^2}{4\pi\mu^2}+\frac{2\gamma}{\epsilon_{IR}}+\frac{1}{2}\log^2\frac{-q^2}{4\pi\mu^2}+\gamma\log\frac{-q^2}{4\pi\mu^2}+\frac{\gamma^2}{2}-\frac{\pi^2}{12}+\cdots\right) \end{aligned} \quad (2.77)$$

This is the same as (2.72).

With a nonzero M, (2.76) is convergent with $\epsilon_{IR}=0$ and becomes

$$J^{(1)}(p_1,q) = \frac{i}{16\pi^2}\int_0^1 dx\int_0^x dy\frac{1}{q^2y(x-y)-M^2(1-x)^2} \quad (2.78)$$

Since q^2 is assumed negative, the integrand is finite for all x and y in the range of integration (except $x=y=1$). Let $y'=y-\alpha x$, where

$$q^2\alpha^2-q^2\alpha+M^2=0 \quad (2.79)$$

$$\alpha=\frac{q^2+\sqrt{q^4-4M^2q^2}}{2q^2}=\frac{1}{2}\left(1-\frac{\sqrt{4M^2-q^2}}{\sqrt{-q^2}}\right) \quad (2.80)$$

Then changing variables and using (2.79) the integral becomes

$$\begin{aligned} J^{(1)}(p_1,q) &= \frac{-i}{16\pi^2}\int_0^1 dx \int_{-\alpha x}^{x-\alpha x} dy' \frac{1}{M^2(1-x)^2 - q^2\left((y'+\alpha x)x - (y'+\alpha x)^2\right)} \\ &= \frac{-i}{16\pi^2}\int_0^1 dx \int_{-\alpha x}^{(1-\alpha)x} dy' \frac{1}{M^2 + q^2 y'^2 - (2M^2 + q^2(1-2\alpha)y')x} \end{aligned} \tag{2.81}$$

Next change the order of integration, which can be done without complication, since there are no singularities in the entire region of integration:

$$\begin{aligned} J^{(1)}(p_1,q) &= \frac{-i}{16\pi^2}\left(\int_0^{-\alpha} dy' \int_{y'/(1-\alpha)}^{-y'/\alpha} dx + \int_{-\alpha}^{1-\alpha} dy' \int_{y'/(1-\alpha)}^{1} dx\right) \\ &\quad \cdot \frac{1}{M^2 + q^2 y'^2 - (2M^2 + q^2(1-2\alpha)y')x} \end{aligned} \tag{2.82}$$

Performing the x integration one finds

$$\begin{aligned} J^{(1)}(p_1,q) &= \frac{-i}{16\pi^2}\int_0^{-\alpha} dy' \frac{1}{-(2M^2 + q^2(1-2\alpha)y')} \\ &\quad \cdot \left(\log\left(M^2 + q^2 y'^2 - \left(2M^2 + q^2(1-2\alpha)y'\right)\frac{-y'}{\alpha}\right)\right. \\ &\quad \left. - \log\left(M^2 + q^2 y'^2 - \left(2M^2 + q^2(1-2\alpha)y'\right)\frac{y'}{1-\alpha}\right)\right) \\ &\quad + \frac{-i}{16\pi^2}\int_{-\alpha}^{1-\alpha} dy' \frac{1}{-(2M^2 + q^2(1-2\alpha)y')} \\ &\quad \cdot \left(\log\left(M^2 + q^2 y'^2 - \left(2M^2 + q^2(1-2\alpha)y'\right)\right)\right. \\ &\quad \left. - \log\left(M^2 + q^2 y'^2 - \left(2M^2 + q^2(1-2\alpha)y'\right)\frac{y'}{1-\alpha}\right)\right) \end{aligned} \tag{2.83}$$

Add and subtract a term $\log\left(M^2 + q^2\left(\frac{2M^2}{-q^2(1-2\alpha)}\right)^2\right) = \log\frac{-M^2q^2}{4M^2-q^2}$ inside the parentheses in each integral, which removes the poles from the integrands, and then regroup the resulting terms:

$$\begin{aligned} J^{(1)}(p_1,q) &= \frac{-i}{16\pi^2}\int_{-\alpha}^{1-\alpha} dy' \frac{1}{-(2M^2 + q^2(1-2\alpha)y')} \cdot \\ &\quad \left(\log\left(-M^2 - q^2(1-2\alpha)y' + q^2 y'^2\right) - \log\frac{-M^2q^2}{4M^2-q^2}\right) \\ &\quad + \frac{i}{16\pi^2}\int_0^{1-\alpha} \frac{1}{-(2M^2 + q^2(1-2\alpha)y')} \cdot \\ &\quad \left(\log\left(M^2 - \left(2M^2 + q^2(1-2\alpha)y'\right)\frac{y'}{1-\alpha} + q^2 y'^2\right) - \log\frac{-M^2q^2}{4M^2-q^2}\right) \\ &\quad + \frac{-i}{16\pi^2}\int_0^{-\alpha} dy' \frac{1}{-(2M^2 + q^2(1-2\alpha)y')} \cdot \end{aligned}$$

$$\left(\log\left(M^2-\left(2M^2+q^2\left(1-2\alpha\right)y'\right)\frac{-y'}{\alpha}+q^2y'^2\right)-\log\frac{-M^2q^2}{4M^2-q^2}\right) \quad (2.84)$$

Make the change of variables $y=y'+\alpha$, $y=y'/(1-\alpha)$, and $y=y'/-\alpha$ in the first, second, and third integral, respectively, and simplify, again using (2.79),

$$\begin{aligned}
J^{(1)}\left(p_1,q\right) &= \frac{-i}{16\pi^2}\int_0^1 dy\frac{1}{-2M^2-q^2\left(1-2\alpha\right)\left(y-\alpha\right)} \\
&\quad\cdot\left(\log\left(-M^2-q^2\left(1-2\alpha\right)\left(y-\alpha\right)+q^2\left(y-\alpha\right)^2\right)-\log\frac{-M^2q^2}{4M^2-q^2}\right) \\
&\quad+\frac{i}{16\pi^2}\int_0^1 dy\frac{1-\alpha}{-2M^2-q^2\left(1-2\alpha\right)\left(1-\alpha\right)y} \\
&\quad\cdot\left(\log\left(M^2-\left(2M^2+q^2\left(1-2\alpha\right)\left(1-\alpha\right)y\right)y+q^2\left(1-\alpha\right)^2y^2\right)-\log\frac{-M^2q^2}{4M^2-q^2}\right) \\
&\quad+\frac{-i}{16\pi^2}\int_0^1 dy\frac{-\alpha}{-2M^2+q^2\left(1-2\alpha\right)y\alpha} \\
&\quad\cdot\left(\log\left(M^2-\left(2M^2-q^2\left(1-2\alpha\right)\alpha y\right)y+q^2\alpha^2y^2\right)-\log\frac{-M^2q^2}{4M^2-q^2}\right) \\
&= \frac{-i}{16\pi^2}\int_0^1 dy\frac{1}{-q^2\left(1-2\alpha\right)y-q^2\alpha}\left(\log\left(-q^2y+q^2y^2\right)-\log\frac{-M^2q^2}{4M^2-q^2}\right) \\
&\quad+\frac{i}{16\pi^2}\int_0^1 dy\frac{1-\alpha}{-q^2\left(1-2\alpha\right)\left(1-\alpha\right)y-2M^2} \\
&\quad\cdot\left(\log\left(M^2-2M^2y+M^2y^2\right)-\log\frac{-M^2q^2}{4M^2-q^2}\right) \\
&\quad+\frac{-i}{16\pi^2}\int_0^1 dy\frac{-\alpha}{q^2\left(1-2\alpha\right)y\alpha-2M^2} \\
&\quad\cdot\left(\log\left(M^2-2M^2y+M^2y^2\right)-\log\frac{-M^2q^2}{4M^2-q^2}\right) \qquad (2.85)
\end{aligned}$$

Factoring the arguments of the logarithms into positive quantities,

$$\begin{aligned}
J^{(1)}\left(p_1,q\right) &= \frac{-i}{-16\pi^2q^2\left(1-2\alpha\right)}\left(\int_0^1\frac{dy}{y-y_1}\left(\log-q^2y\left(1-y\right)-\log-q^2y_1\left(1-y_1\right)\right)\right. \\
&\quad-\int_0^1\frac{dy}{y-y_2}\left(\log M^2\left(1-y\right)^2-\log M^2\left(1-y_2\right)^2\right) \\
&\quad\left.+\int_0^1\frac{dy}{y-y_3}\left(\log M^2\left(1-y\right)^2-\log M^2\left(y_3-1\right)^2\right)\right) \qquad (2.86)
\end{aligned}$$

where

$$\begin{aligned}
y_1 &= \frac{\alpha}{2\alpha-1}=\frac{1}{2}\left(1-\frac{\sqrt{-q^2}}{\sqrt{4M^2-q^2}}\right),0\le y_1\le\frac{1}{2} \\
y_2 &= \frac{2M^2}{-q^2\left(1-2\alpha\right)\left(1-\alpha\right)}=1-\frac{\sqrt{-q^2}}{\sqrt{4M^2-q^2}},0\le y_2\le 1
\end{aligned}$$

$$y_3 = \frac{2M^2}{-q^2\left(2\alpha-1\right)\alpha} = 1+\frac{\sqrt{-q^2}}{\sqrt{4M^2-q^2}}, 1 \leq y_3 \leq 2 \tag{2.87}$$

Note that

$$1-y_1 = \frac{1-\alpha}{1-2\alpha} = \frac{1}{2}\left(1+\frac{\sqrt{-q^2}}{\sqrt{4M^2-q^2}}\right), \frac{1}{2} \leq 1-y_1 \leq 1 \tag{2.88}$$

Expanding the logarithms, the first term in parentheses in (2.86) is

$$\begin{aligned}
&\int_0^1 \frac{dy}{y-y_1}\left(\log -q^2 y\left(1-y\right) - \log -q^2 y_1\left(1-y_1\right)\right) \\
&= \int_0^1 \frac{dy}{y-y_1}\left(\log y - \log y_1\right) + \int_0^1 \frac{dy}{y-y_1}\left(\log\left(1-y\right) - \log\left(1-y_1\right)\right)
\end{aligned} \tag{2.89}$$

Making the change of variables $y' = 1-y$ in the second integral and using (2.31), this becomes

$$\begin{aligned}
&\int_0^1 \frac{dy}{y-y_1}\left(\log y - \log y_1\right) - \int_0^1 \frac{dy}{y-\left(1-y_1\right)}\left(\log y - \log\left(1-y_1\right)\right) \\
&= \mathrm{Li}_2\left(1-\frac{1}{1-y_1}\right) - \mathrm{Li}_2\left(1-\frac{1}{y_1}\right) \\
&= \mathrm{Li}_2\left(\frac{q^2-2M^2+\sqrt{-q^2}\sqrt{4M^2-q^2}}{2M^2}\right) - \mathrm{Li}_2\left(\frac{q^2-2M^2-\sqrt{-q^2}\sqrt{4M^2-q^2}}{2M^2}\right)
\end{aligned} \tag{2.90}$$

Similarly, the second term in parentheses in (2.86) is

$$\int_0^1 \frac{dy}{y-y_2}\left(\log M^2\left(1-y\right)^2 - \log M^2\left(1-y_2\right)^2\right) = 2\int_0^1 \frac{dy}{y-y_2}\left(\log\left(1-y\right) - \log\left(1-y_2\right)\right) \tag{2.91}$$

Changing variables again to $y' = 1-y$ this becomes

$$\begin{aligned}
-2\int_0^1 \frac{dy'}{y'-\left(1-y_2\right)}\left(\log y' - \log\left(1-y_2\right)\right) &= -2\left(\mathrm{Li}_2 1 - \mathrm{Li}_2\left(\frac{y_2}{y_2-1}\right)\right) \\
&= 2\,\mathrm{Li}_2\left(1-\frac{\sqrt{4M^2-q^2}}{\sqrt{-q^2}}\right) - \frac{\pi^2}{3}
\end{aligned} \tag{2.92}$$

The last term in parentheses in (2.86) is

$$\begin{aligned}
&\int_0^1 \frac{dy}{y-y_3}\left(\log M^2\left(1-y\right)^2 - \log M^2\left(y_3-1\right)^2\right) \\
&= 2\int_0^1 \frac{dy}{y-y_3}\left(\log\left(1-y\right) - \log\left(y_3-1\right)\right) \\
&= 2\int_0^1 \frac{dy}{y-y_3}\left(\log\left(1-y\right) - \log\left(1-y_3\right) + \pi i\right)
\end{aligned}$$

$$= 2\int_0^1 \frac{dy}{y-y_3}\left(\log(1-y)-\log(1-y_3)\right)+2\pi i\log\left(\frac{y_3-1}{y_3}\right)$$
$$= -2\int_0^1 \frac{dy'}{y'-(1-y_3)}\left(\log y'-\log(1-y_3)\right)+2\pi i\log\left(\frac{y_3-1}{y_3}\right) \quad (2.93)$$

where again $y' = 1-y$. Using 2.31 this becomes

$$\int_0^1 \frac{dy}{y-y_3}\left(\log M^2(1-y)^2-\log M^2(y_3-1)^2\right)$$
$$= -\frac{\pi^2}{3}+2\,\mathrm{Li}_2\left(\frac{y_3}{y_3-1}\right)+2\pi i\log\frac{y_3}{y_3-1}$$
$$= -\frac{\pi^2}{3}+2\,\mathrm{Li}_2\left(1+\frac{\sqrt{4M^2-q^2}}{\sqrt{-q^2}}\right)+2\pi i\log\left(1+\frac{\sqrt{4M^2-q^2}}{\sqrt{-q^2}}\right) \quad (2.94)$$

Note that the explicit imaginary term cancels the imaginary part of the Spence function.

Finally, substituting (2.90), (2.92), and (2.94) in (2.86),

$$\begin{aligned} J^{(1)}(p_1,q) &= \frac{-i}{16\pi^2\sqrt{-q^2}\sqrt{4M^2-q^2}}\left(\mathrm{Li}_2\left(\frac{q^2-2M^2+\sqrt{-q^2}\sqrt{4M^2-q^2}}{2M^2}\right)\right. \\ &\quad -\mathrm{Li}_2\left(\frac{q^2-2M^2-\sqrt{-q^2}\sqrt{4M^2-q^2}}{2M^2}\right)-2\,\mathrm{Li}_2\left(1-\frac{\sqrt{4M^2-q^2}}{\sqrt{-q^2}}\right) \\ &\quad \left.+2\,\mathrm{Li}_2\left(1+\frac{\sqrt{4M^2-q^2}}{\sqrt{-q^2}}\right)+2\pi i\log\left(1+\frac{\sqrt{4M^2-q^2}}{\sqrt{-q^2}}\right)\right) \quad (2.95) \end{aligned}$$

2.3.4 Four-Point Integral

The result for the four-point integral is taken from [28]. In the region $q^2<0$, $s>(M+m)^2$,

$$\begin{aligned} K(p_1,p_2,q) &\equiv \mu^{4-D}\int \frac{1}{(k^2-\lambda^2)\left((p_1-k)^2-M^2\right)\left((k-q)^2-\lambda^2\right)\left((p_2+k)^2-m^2\right)}\frac{d^Dk}{(2\pi)^D} \\ &= \frac{i}{8\pi^2q^2\sqrt{s^2-2s(m^2+M^2)+(m^2-M^2)^2}} \\ &\quad \cdot\left(\log\frac{s-(M+m)^2-\sqrt{s^2-2s(m^2+M^2)+(m^2-M^2)^2}}{s-(M+m)^2+\sqrt{s^2-2s(m^2+M^2)+(m^2-M^2)^2}}\right)\log\frac{-q^2}{\lambda^2} \quad (2.96) \end{aligned}$$

where $s\equiv(p_1+p_2)^2$, $t\equiv q^2$, $M^2\equiv p_1^2=(p_1-q)^2$, $m^2\equiv p_2^2=(p_2+q)^2$. In case $m\approx 0$, this becomes

$$K(p_1,p_2,q) = \frac{i}{16\pi^2(s-M^2)q^2}\left(\log\frac{s-M^2}{m^2}+\log\frac{s-M^2}{M^2}\right)\log\frac{-q^2}{\lambda^2} \quad (2.97)$$

If dimensional regularization is used instead of a photon mass, the result is the same after the substitution $\log\lambda^2 \to \log 4\pi\mu^2 + \frac{2}{\epsilon_{IR}} + \gamma$.

2.4 Bremsstrahlung Integrals

In addition to the covariant integrals listed above, it will also prove necessary to calculate non-covariant integrals of the form

$$B_{ij} \equiv \mu^{4-D} \int_0^{k_{max}} \frac{\mathrm{d}^{D-1}k}{(2\pi)^{D-1}} \frac{1}{k_0} \frac{1}{(p_i \cdot k)(p_j \cdot k)} \tag{2.98}$$

where $p_{i,j}$ are future-directed timelike vectors on their mass shell, $p_i^2 = M^2$, $p_j^2 = m^2$. These contain soft and, if $m = 0$, collinear divergences. Introducing Feynman parameters,

$$\begin{aligned} B_{ij} &= \mu^{4-D} \int_0^{k_{max}} \frac{\mathrm{d}^{D-1}k}{(2\pi)^{D-1}} \frac{1}{k_0} \int_0^1 \mathrm{d}x \frac{1}{((p_i \cdot k)\, x + (p_j \cdot k)\,(1-x))^2} \\ &= \mu^{4-D} \int_0^1 \mathrm{d}x \int_0^{k_{max}} \frac{\mathrm{d}^{D-1}k}{(2\pi)^{D-1}} \frac{1}{k_0} \frac{1}{\left((E_i x + E_j\,(1-x))\, k_0 - (\vec{p_i} x + \vec{p_j}\,(1-x)) \cdot \vec{k}\right)^2} \end{aligned} \tag{2.99}$$

Introducing polar coordinates in $D-1$ dimensions [17] with polar axis along the vector $\vec{p_i} x + \vec{p_j}\,(1-x)$,

$$\begin{aligned} B_{ij} &= \mu^{4-D} \int_0^1 \mathrm{d}x \frac{2\pi^{D/2-1}}{\Gamma(D/2-1)\,(2\pi)^{D-1}} \int_0^{k_{max}} \mathrm{d}\left|\vec{k}\right| \left|\vec{k}\right|^{D-2} \frac{1}{k_0} \\ &\quad \cdot \int_{-1}^1 \mathrm{d}z \frac{\left(1-z^2\right)^{D/2-2}}{\left((E_i x + E_j\,(1-x))\, k_0 - |\vec{p_i} x + \vec{p_j}\,(1-x)| \left|\vec{k}\right| z\right)^2} \end{aligned} \tag{2.100}$$

Again, the order in which to proceed depends on the regularization method used for the IR divergences.

If $\lambda \neq 0$, $\epsilon_{IR} = 0$, then

$$\begin{aligned} B_{ij} &= \frac{1}{4\pi^2} \int_0^1 \mathrm{d}x \int_0^{k_{max}} \frac{\mathrm{d}\left|\vec{k}\right| \vec{k}^2}{\sqrt{\vec{k}^2 + \lambda^2}} \\ &\quad \int_{-1}^1 \mathrm{d}z \frac{1}{\left((E_i x + E_j\,(1-x))\sqrt{\vec{k}^2 + \lambda^2} - |\vec{p_i} x + \vec{p_j}\,(1-x)| \left|\vec{k}\right| z\right)^2} \end{aligned} \tag{2.101}$$

Performing the z integration,

$$B_{ij} = \frac{1}{2\pi^2} \int_0^1 \mathrm{d}x \int_0^{k_{max}} \frac{\mathrm{d}\left|\vec{k}\right| \vec{k}^2}{\sqrt{\vec{k}^2 + \lambda^2}}$$

$$\frac{1}{\left(E_i x + E_j\left(1-x\right)\right)^2 \lambda^2 + \left(\left(E_i x + E_j\left(1-x\right)\right)^2 - \left(\vec{p_i} x + \vec{p_j}\left(1-x\right)\right)^2\right)\vec{k}^2} \tag{2.102}$$

Decomposing the integrand in partial fractions in $\vec{k}^2$ and letting λ^2 approach 0,

$$\begin{aligned}
B_{ij} &= \frac{1}{2\pi^2}\int_0^1 \mathrm{d}x \frac{1}{\left(\left(E_i x + E_j\left(1-x\right)\right)^2 - \left(\vec{p_i} x + \vec{p_j}\left(1-x\right)\right)^2\right)} \\
&\quad \cdot \int_0^{k_{max}} \frac{\mathrm{d}\left|\vec{k}\right|}{\sqrt{\vec{k}^2 + \lambda^2}} \\
&\quad \left(1 - \frac{\left(E_i x + E_j\left(1-x\right)\right)^2 \lambda^2}{\left(E_i x + E_j\left(1-x\right)\right)^2 \lambda^2 + \left(\left(E_i x + E_j\left(1-x\right)\right)^2 - \left(\vec{p_i} x + \vec{p_j}\left(1-x\right)\right)^2\right)\vec{k}^2}\right) \\
&\approx \frac{1}{2\pi^2}\int_0^1 \mathrm{d}x \frac{1}{\left(E_i x + E_j\left(1-x\right)\right)^2 - \left(\vec{p_i} x + \vec{p_j}\left(1-x\right)\right)^2} \\
&\quad \cdot \left(\frac{1}{2}\log\frac{4k_{max}^2}{\lambda^2} - \int_0^\infty \frac{\mathrm{d}y}{\sqrt{y^2+1}}\right. \\
&\quad \left.\frac{\left(E_i x + E_j\left(1-x\right)\right)^2}{\left(E_i x + E_j\left(1-x\right)\right)^2 + \left(\left(E_i x + E_j\left(1-x\right)\right)^2 - \left(\vec{p_i} x + \vec{p_j}\left(1-x\right)\right)^2\right) y^2}\right)
\end{aligned} \tag{2.103}$$

where $y = |\vec{k}|/\lambda$. Performing the y integration,

$$\begin{aligned}
B_{ij} &= \frac{1}{4\pi^2}\int_0^1 \mathrm{d}x \frac{1}{\left(E_i x + E_j\left(1-x\right)\right)^2 - \left(\vec{p_i} x + \vec{p_j}\left(1-x\right)\right)^2} \\
&\quad \cdot \left(\log\frac{4k_{max}^2}{\lambda^2} - \frac{E_i x + E_j\left(1-x\right)}{\left|\vec{p_i} x + \vec{p_j}\left(1-x\right)\right|}\log\frac{E_i x + E_j\left(1-x\right) + \left|\vec{p_i} x + \vec{p_j}\left(1-x\right)\right|}{E_i x + E_j\left(1-x\right) - \left|\vec{p_i} x + \vec{p_j}\left(1-x\right)\right|}\right)
\end{aligned} \tag{2.104}$$

On the other hand, if $\lambda = 0$, $\epsilon_{IR} \neq 0$, then, performing the k integration in (2.100),

$$\begin{aligned}
B_{ij} &= \int_0^1 \mathrm{d}x \frac{1}{4\pi^2\Gamma\left(1+\epsilon_{IR}/2\right)\left(4\pi\mu^2\right)^{\epsilon_{IR}/2}} \int_0^{k_{max}} \mathrm{d}\left|\vec{k}\right| \left|\vec{k}\right|^{\epsilon_{IR}-1} \\
&\quad \int_{-1}^1 \mathrm{d}z \frac{\left(1-z^2\right)^{\epsilon_{IR}/2}}{\left(E_i x + E_j\left(1-x\right) - \left|\vec{p_i} x + \vec{p_j}\left(1-x\right)\right| z\right)^2} \\
&= \frac{1}{4\pi^2\Gamma\left(1+\epsilon_{IR}/2\right)\epsilon_{IR}}\left(\frac{k_{max}^2}{4\pi\mu^2}\right)^{\epsilon_{IR}/2} \\
&\quad \cdot \int_0^1 \mathrm{d}x \int_{-1}^1 \mathrm{d}z \frac{\left(1-z^2\right)^{\epsilon_{IR}/2}}{\left(E_i x + E_j\left(1-x\right) - \left|\vec{p_i} x + \vec{p_j}\left(1-x\right)\right| z\right)^2}
\end{aligned} \tag{2.105}$$

If both $M^2, m^2 \neq 0$, expand in powers of ϵ_{IR}:

$$B_{ij} \approx \frac{1}{4\pi^2\epsilon_{IR}}\left(1 + \frac{\gamma\epsilon_{IR}}{2}\right)\left(1 + \frac{\epsilon_{IR}}{2}\log\frac{k_{max}^2}{4\pi\mu^2}\right)$$

$$\int_0^1 \mathrm{d}x \int_{-1}^1 \mathrm{d}z \frac{1+\frac{\epsilon_{IR}}{2}\log\left(1-z^2\right)}{\left(E_i x+E_j\left(1-x\right)-\left|\vec{p_i}x+\vec{p_j}\left(1-x\right)\right|z\right)^2} \tag{2.106}$$

Performing the z integration,

$$\begin{aligned}
B_{ij} &= \frac{1}{4\pi^2\epsilon_{IR}}\left(1+\frac{\gamma\epsilon_{IR}}{2}\right)\left(1+\frac{\epsilon_{IR}}{2}\log\frac{k_{max}^2}{4\pi\mu^2}\right) \\
&\quad \cdot \int_0^1 \mathrm{d}x \frac{1}{\left(E_i x+E_j\left(1-x\right)\right)^2-\left(\vec{p_i}x+\vec{p_j}\left(1-x\right)\right)^2} \\
&\quad \cdot \left(2+\epsilon_{IR}\left(\log 4+\frac{E_i x+E_j\left(1-x\right)}{\left|\vec{p_i}x+\vec{p_j}\left(1-x\right)\right|}\log\frac{\left(E_i x+E_j\left(1-x\right)\right)-\left|\vec{p_i}x+\vec{p_j}\left(1-x\right)\right|}{\left(E_i x+E_j\left(1-x\right)\right)+\left|\vec{p_i}x+\vec{p_j}\left(1-x\right)\right|}\right)\right) \\
&= \frac{1}{4\pi^2}\int_0^1 \mathrm{d}x \frac{1}{\left(E_i x+E_j\left(1-x\right)\right)^2-\left(\vec{p_i}x+\vec{p_j}\left(1-x\right)\right)^2} \\
&\quad \cdot \left(\frac{2}{\epsilon_{IR}}+\gamma+\log\frac{k_{max}^2}{\pi\mu^2}+\frac{E_i x+E_j\left(1-x\right)}{\left|\vec{p_i}x+\vec{p_j}\left(1-x\right)\right|}\log\frac{\left(E_i x+E_j\left(1-x\right)\right)-\left|\vec{p_i}x+\vec{p_j}\left(1-x\right)\right|}{\left(E_i x+E_j\left(1-x\right)\right)+\left|\vec{p_i}x+\vec{p_j}\left(1-x\right)\right|}\right)
\end{aligned} \tag{2.107}$$

Comparing this to (2.104), one once again observes the substitution $\log\lambda^2 \to \log 4\pi\mu^2+\frac{2}{\epsilon_{IR}}+\gamma$.

Simplifying (2.107) using

$$\begin{aligned}
\left(\vec{p_i}x+\vec{p_j}\left(1-x\right)\right)^2 &= \left(E_i^2-M^2\right)x^2+2\vec{p_i}\cdot\vec{p_j}x\left(1-x\right)+\left(E_j^2-m^2\right)\left(1-x\right)^2 \\
&= \left(E_i x+E_j\left(1-x\right)\right)^2-2E_iE_j x\left(1-x\right) \\
&\quad +2\vec{p_i}\cdot\vec{p_j}x\left(1-x\right)-M^2x^2-m^2\left(1-x\right)^2 \\
&= \left(E_i x+E_j\left(1-x\right)\right)^2-2p_i\cdot p_j x\left(1-x\right)-M^2x^2-m^2\left(1-x\right)^2
\end{aligned} \tag{2.108}$$

one obtains

$$\begin{aligned}
B_{ij} &= \frac{1}{4\pi^2}\int_0^1 \mathrm{d}x \frac{1}{2p_i\cdot p_j x\left(1-x\right)+M^2x^2+m^2\left(1-x\right)^2} \\
&\quad \cdot \left(\frac{2}{\epsilon_{IR}}+\gamma+\log\frac{k_{max}^2}{\pi\mu^2}+\frac{E_i x+E_j\left(1-x\right)}{\left|\vec{p_i}x+\vec{p_j}\left(1-x\right)\right|}\log\frac{\left(E_i x+E_j\left(1-x\right)\right)-\left|\vec{p_i}x+\vec{p_j}\left(1-x\right)\right|}{\left(E_i x+E_j\left(1-x\right)\right)+\left|\vec{p_i}x+\vec{p_j}\left(1-x\right)\right|}\right)
\end{aligned} \tag{2.109}$$

Finally, performing the x integration,

$$\begin{aligned}
B_{ij} &= \frac{1}{4\pi^2}\frac{1}{\left(M^2+m^2-2p_i\cdot p_j\right)\left(x_+-x_-\right)} \\
&\quad \cdot \left(\log\frac{x_+-1}{x_+}-\log\frac{x_--1}{x_-}\right)\left(\frac{2}{\epsilon_{IR}}+\gamma+\log\frac{k_{max}^2}{\pi\mu^2}\right)
\end{aligned}$$

$$+b_{ij} \tag{2.110}$$

where $x_\pm$ are the two roots of $2p_i \cdot p_j x\left(1-x\right) + M^2x^2 + m^2\left(1-x\right)^2$ and

$$\begin{aligned} b_{ij} &\equiv \frac{1}{4\pi^2}\int_0^1 \mathrm{d}x \frac{1}{2p_i \cdot p_j x\left(1-x\right) + M^2x^2 + m^2\left(1-x\right)^2} \\ &\quad \frac{E_i x + E_j\left(1-x\right)}{|\vec{p_i}x + \vec{p_j}\left(1-x\right)|}\log\frac{\left(E_i x + E_j\left(1-x\right)\right) - |\vec{p_i}x + \vec{p_j}\left(1-x\right)|}{\left(E_i x + E_j\left(1-x\right)\right) + |\vec{p_i}x + \vec{p_j}\left(1-x\right)|} \end{aligned} \tag{2.111}$$

is convergent.

The result for b_{ij} is taken from [28]. In the case $m^2 \approx 0$, $M^2 \neq 0$

$$\begin{aligned} B_{ij} &= \frac{1}{4\pi^2 p_i \cdot p_j}\left(\frac{1}{2}\left(\log\frac{2p_i\cdot p_j}{M^2} + \log\frac{2p_i\cdot p_j}{m^2}\right)\left(\frac{2}{\epsilon_{IR}} + \gamma + \log\frac{k_{max}^2}{\pi\mu^2}\right)\right. \\ &\quad + \frac{1}{4}\log^2\frac{M^2}{\left(E_i + |\vec{p_i}|\right)^2} - \frac{1}{4}\log^2\frac{m^2}{4E_j^2} + \mathrm{Li}_2\left(1 + 2\left(E_i + |\vec{p_i}|\right)\left(\frac{E_j}{2p_i\cdot p_j} + \frac{E_i}{M^2}\right)\right) \\ &\quad - \mathrm{Li}_2\left(1 + 4E_j\left(\frac{M^2E_j}{4\left(p_i\cdot p_j\right)^2} - \frac{E_i}{2p_i\cdot p_j}\right)\right) \\ &\quad \left. + \mathrm{Li}_2\left(1 + 2\left(E_i - |\vec{p_i}|\right)\left(\frac{E_j}{2p_i\cdot p_j} + \frac{E_i}{M^2}\right)\right) - \frac{\pi^2}{6}\right) \end{aligned} \tag{2.112}$$

In the case $M^2 = m^2 \approx 0$ this becomes

$$\begin{aligned} B_{ij} &= \frac{1}{4\pi^2 p_i\cdot p_j}\left(\left(\frac{2}{\epsilon_{IR}} + \gamma + \log\frac{k_{max}^2}{\pi\mu^2}\right)\log\frac{2p_i\cdot p_j}{m^2}\right. \\ &\quad \left. -\frac{1}{4}\log^2\frac{m^2}{4E_i^2} - \frac{1}{4}\log^2\frac{m^2}{4E_j^2} - \mathrm{Li}_2\left(1 - \frac{2E_iE_j}{p_i\cdot p_j}\right) - \frac{\pi^2}{3}\right) \end{aligned} \tag{2.113}$$

Finally, to compare the regularization of collinear divergences by a mass or by dimensional regularization, consider (2.105) in the case $M^2 = m^2 \approx 0$, $E_i = E_j = E$, $p^2 \equiv \vec{p_i}^2 = \vec{p_j}^2 = E^2 - m^2 \approx E^2$:

$$B_{ij} = \frac{1}{4\pi^2\Gamma\left(1+\epsilon_{IR}/2\right)\epsilon_{IR}}\left(\frac{k_{max}^2}{4\pi\mu^2}\right)^{\epsilon_{IR}/2}\int_0^1 \mathrm{d}x\int_{-1}^1 \mathrm{d}z \frac{\left(1-z^2\right)^{\epsilon_{IR}/2}}{\left(E - |\vec{p_i}x + \vec{p_j}\left(1-x\right)|\, z\right)^2} \tag{2.114}$$

and there is now a collinear divergence. To treat this, break up the x integral into three regions of integration. Expand in ϵ_{IR} in the middle region and expand the denominators in x in the other two regions:

$$B_{ij} \approx \frac{1}{4\pi^2E^2\Gamma\left(1+\epsilon_{IR}/2\right)\epsilon_{IR}}\left(\frac{k_{max}^2}{4\pi\mu^2}\right)^{\epsilon_{IR}/2}\int_0^{\delta_2}\mathrm{d}x\int_{-1}^1 \mathrm{d}z\frac{\left(1-z^2\right)^{\epsilon_{IR}/2}}{\left(1+b-\left(1-ax\right)z\right)^2}$$

$$+\frac{1}{4\pi^2\epsilon_{IR}}\left(1+\frac{\gamma\epsilon_{IR}}{2}\right)\left(1+\frac{\epsilon_{IR}}{2}\log\frac{k_{max}^2}{4\pi\mu^2}\right)\int_{\delta_2}^{1-\delta_2}\mathrm{d}x\int_{-1}^{1}\mathrm{d}z\frac{1+\frac{\epsilon_{IR}}{2}\log\left(1-z^2\right)}{\left(E-\sqrt{E^2+q^2x\left(1-x\right)}z\right)^2}$$
$$+\frac{1}{4\pi^2E^2\Gamma\left(1+\epsilon_{IR}/2\right)\epsilon_{IR}}\left(\frac{k_{max}^2}{4\pi\mu^2}\right)^{\epsilon_{IR}/2}\int_{1-\delta_2}^{1}\mathrm{d}x\int_{-1}^{1}\mathrm{d}z\frac{\left(1-z^2\right)^{\epsilon_{IR}/2}}{\left(1+b-\left(1-a\left(1-x\right)\right)z\right)^2} \tag{2.115}$$

where here $q\equiv(p_i-p_j)$, $a\equiv\frac{-q^2}{2E^2}$, $b\equiv\frac{m^2}{2p^2}\approx\frac{m^2}{2E^2}$. The third integral in (2.115) is equal to the first:

$$\begin{aligned}&\frac{1}{4\pi^2E^2\Gamma\left(1+\epsilon_{IR}/2\right)\epsilon_{IR}}\left(\frac{k_{max}^2}{4\pi\mu^2}\right)^{\epsilon_{IR}/2}\int_{1-\delta_2}^{1}\mathrm{d}x\int_{-1}^{1}\mathrm{d}z\frac{\left(1-z^2\right)^{\epsilon_{IR}/2}}{\left(1+b-\left(1-a\left(1-x\right)\right)z\right)^2}\\ =\;&\frac{1}{4\pi^2E^2\Gamma\left(1+\epsilon_{IR}/2\right)\epsilon_{IR}}\left(\frac{k_{max}^2}{4\pi\mu^2}\right)^{\epsilon_{IR}/2}\int_{0}^{\delta_2}\mathrm{d}x_2\int_{-1}^{1}\mathrm{d}z\frac{\left(1-z^2\right)^{\epsilon_{IR}/2}}{\left(1+b-\left(1-ax_2\right)z\right)^2}\end{aligned} \tag{2.116}$$

where $x_2=1-x$. Performing the x integration in the first integral in (2.115),

$$\begin{aligned}&\frac{1}{4\pi^2E^2\Gamma\left(1+\epsilon_{IR}/2\right)\epsilon_{IR}}\left(\frac{k_{max}^2}{4\pi\mu^2}\right)^{\epsilon_{IR}/2}\int_{-1}^{1}\mathrm{d}z\left(1-z^2\right)^{\epsilon_{IR}/2}\int_{0}^{\delta_2}\mathrm{d}x\frac{1}{\left(1+b-z+azx\right)^2}\\ =\;&\frac{1}{4\pi^2E^2a\Gamma\left(1+\epsilon_{IR}/2\right)\epsilon_{IR}}\left(\frac{k_{max}^2}{4\pi\mu^2}\right)^{\epsilon_{IR}/2}\int_{-1}^{1}\mathrm{d}z\left(1-z^2\right)^{\epsilon_{IR}/2}\\ &\left(\frac{1}{z}\frac{1}{1+b-z}-\frac{1}{z}\frac{1}{1+b-\left(1-a\delta_2\right)z}\right)\end{aligned} \tag{2.117}$$

Decompose this into partial fractions and let b and δ_2 go to 0 where allowable:

$$\begin{aligned}&\frac{1}{4\pi^2E^2a\Gamma\left(1+\epsilon_{IR}/2\right)\epsilon_{IR}}\left(\frac{k_{max}^2}{4\pi\mu^2}\right)^{\epsilon_{IR}/2}\\ &\cdot\int_{-1}^{1}\mathrm{d}z\left(1-z^2\right)^{\epsilon_{IR}/2}\left(\frac{1}{1+b}\left(\frac{1}{z}+\frac{1}{1+b-z}\right)-\frac{1}{1+b}\left(\frac{1}{z}+\frac{\left(1-a\delta_2\right)}{1+b-\left(1-a\delta_2\right)z}\right)\right)\\ \approx\;&\frac{1}{4\pi^2E^2a\Gamma\left(1+\epsilon_{IR}/2\right)\epsilon_{IR}}\left(\frac{k_{max}^2}{4\pi\mu^2}\right)^{\epsilon_{IR}/2}\int_{-1}^{1}\mathrm{d}z\left(1-z^2\right)^{\epsilon_{IR}/2}\left(\frac{1}{1+b-z}-\frac{1}{1-\left(1-a\delta_2\right)z}\right)\end{aligned} \tag{2.118}$$

The next step depends on the regularization method used for the collinear divergence. If $m^2\neq0$, expand in ϵ_{IR}:

$$\begin{aligned}&\frac{1}{4\pi^2E^2a\Gamma\left(1+\epsilon_{IR}/2\right)\epsilon_{IR}}\left(\frac{k_{max}^2}{4\pi\mu^2}\right)^{\epsilon_{IR}/2}\int_{-1}^{1}\mathrm{d}z\left(1-z^2\right)^{\epsilon_{IR}/2}\left(\frac{1}{1+b-z}-\frac{1}{1-\left(1-a\delta_2\right)z}\right)\\ =\;&\frac{1}{4\pi^2E^2a\epsilon_{IR}}\left(1+\frac{\gamma\epsilon_{IR}}{2}\right)\left(1+\frac{\epsilon_{IR}}{2}\log\frac{k_{max}^2}{4\pi\mu^2}\right)\int_{-1}^{1}\mathrm{d}z\left(1+\frac{\epsilon_{IR}}{2}\log\left(1-z^2\right)\right)\end{aligned}$$

$$\left(\frac{1}{1+b-z}-\frac{1}{1-(1-a\delta_2)\,z}\right) \tag{2.119}$$

Performing the z integral, substituting for a and b, and simplifying:

$$\begin{aligned}
& \frac{1}{4\pi^2E^2a\epsilon_{IR}}\left(1+\frac{\gamma\epsilon_{IR}}{2}\right)\left(1+\frac{\epsilon_{IR}}{2}\log\frac{k_{max}^2}{4\pi\mu^2}\right) \\
& \int_{-1}^{1}\mathrm{d}z\left(1+\frac{\epsilon_{IR}}{2}\log\left(1-z^2\right)\right)\left(\frac{1}{1+b-z}-\frac{1}{1-(1-a\delta_2)\,z}\right) \\
= \; & \frac{-1}{4\pi^2q^2}\left(\left(\frac{2}{\epsilon_{IR}}+\gamma+\log\frac{k_{max}^2}{\pi\mu^2}\right)\log\frac{-q^2}{m^2}-\frac{1}{2}\log^2\frac{m^2}{4E^2}\right. \\
& \left.+\left(\frac{2}{\epsilon_{IR}}+\gamma+\log\frac{k_{max}^2}{\pi\mu^2}\right)\log\delta_2+\frac{1}{2}\log^2\frac{-q^2\delta_2}{4E^2}\right)
\end{aligned} \tag{2.120}$$

Continuing from (2.118) if instead $m^2=0$,

$$\begin{aligned}
& \frac{1}{4\pi^2E^2a\Gamma\left(1+\epsilon_{IR}/2\right)\epsilon_{IR}}\left(\frac{k_{max}^2}{4\pi\mu^2}\right)^{\epsilon_{IR}/2}\int_{-1}^{1}\mathrm{d}z\left(1-z^2\right)^{\epsilon_{IR}/2}\left(\frac{1}{1+b-z}-\frac{1}{1-(1-a\delta_2)\,z}\right) \\
= \; & \frac{1}{4\pi^2E^2a\Gamma\left(1+\epsilon_{IR}/2\right)\epsilon_{IR}}\left(\frac{k_{max}^2}{4\pi\mu^2}\right)^{\epsilon_{IR}/2}\int_{-1}^{1}\mathrm{d}z\left(1-z^2\right)^{\epsilon_{IR}/2}\left(\frac{1}{1-z}-\frac{1}{1-(1-a\delta_2)\,z}\right)
\end{aligned} \tag{2.121}$$

For the first term in the integrand, break up the z integral into two regions:

$$\begin{aligned}
\approx \; & \frac{1}{4\pi^2E^2a\Gamma\left(1+\epsilon_{IR}/2\right)\epsilon_{IR}}\left(\frac{k_{max}^2}{4\pi\mu^2}\right)^{\epsilon_{IR}/2} \\
& \left(\int_{-1}^{\delta_1}\mathrm{d}z\frac{\left(1-z^2\right)^{\epsilon_{IR}/2}}{1-z}+\int_{\delta_1}^{1}\mathrm{d}z\frac{\left(2\left(1-z\right)\right)^{\epsilon_{IR}/2}}{1-z}-\int_{-1}^{1}\mathrm{d}z\frac{\left(1-z^2\right)^{\epsilon_{IR}/2}}{1-(1-a\delta_2)\,z}\right)
\end{aligned} \tag{2.122}$$

(Note that $\left(1-z^2\right)\approx 2\left(1-z\right)$ when $z\approx 1$.) Perform the z integral in the middle integral and then expand in ϵ_{IR}:

$$\begin{aligned}
= \; & \frac{1}{4\pi^2E^2a\Gamma\left(1+\epsilon_{IR}/2\right)\epsilon_{IR}}\left(\frac{k_{max}^2}{4\pi\mu^2}\right)^{\epsilon_{IR}/2} \\
& \left(\int_{-1}^{\delta_1}\mathrm{d}z\frac{\left(1-z^2\right)^{\epsilon_{IR}/2}}{1-z}+\frac{2}{\epsilon_{IR}}\left(2-2\delta_1\right)^{\epsilon_{IR}/2}-\int_{-1}^{1}\mathrm{d}z\frac{\left(1-z^2\right)^{\epsilon_{IR}/2}}{1-(1-a\delta_2)\,z}\right) \\
= \; & \frac{1}{4\pi^2E^2a}\left(1+\gamma\frac{\epsilon_{IR}}{2}+\left(\frac{\gamma^2}{2}-\frac{\pi^2}{12}\right)\left(\frac{\epsilon_{IR}}{2}\right)^2\right)\frac{1}{\epsilon_{IR}} \\
& \left(1+\frac{\epsilon_{IR}}{2}\log\frac{k_{max}^2}{4\pi\mu^2}+\frac{1}{2}\left(\frac{\epsilon_{IR}}{2}\right)^2\log^2\frac{k_{max}^2}{4\pi\mu^2}\right) \\
& \cdot\left(\int_{-1}^{\delta_1}\mathrm{d}z\frac{1+\frac{\epsilon_{IR}}{2}\log\left(1-z^2\right)}{1-z}+\frac{2}{\epsilon_{IR}}+\log\left(2-2\delta_1\right)\right.
\end{aligned}$$

$$+\frac{1}{2}\frac{\epsilon_{IR}}{2}\log^2\left(2-2\delta_1\right)-\int_{-1}^{1}\mathrm{d}z\frac{1+\frac{\epsilon_{IR}}{2}\log\left(1-z^2\right)}{1-\left(1-a\delta_2\right)z}\Bigg) \tag{2.123}$$

Performing the remaining z integrals, substituting for a, and simplifying:

$$\begin{aligned}
= \quad & \frac{-1}{4\pi^2q^2}\left(\frac{2}{\epsilon_{IR}^2}+\left(\frac{2}{\epsilon_{IR}}+\gamma+\log\frac{k_{max}^2}{\pi\mu^2}\right)\log\frac{-q^2}{4E^2}+\frac{1}{2}\left(\frac{2}{\epsilon_{IR}}+\gamma+\log\frac{k_{max}^2}{\pi\mu^2}\right)^2+\frac{\pi^2}{12}\right.\\
& \left.+\left(\frac{2}{\epsilon_{IR}}+\gamma+\log\frac{k_{max}^2}{\pi\mu^2}\right)\log\delta_2+\frac{1}{2}\log^2\frac{-q^2\delta_2}{4E^2}\right)
\end{aligned} \tag{2.124}$$

Comparing this with (2.120), one sees that it can be obtained by substituting $\log m^2 \to \log E^2 - {}^2/_{\epsilon_{IR}} - \gamma - \log {}^{k_{max}^2}/_{4\pi\mu^2}$ and adding an additional term ${}^{-1}/_{4\pi^2q^2}\left({}^2/_{\epsilon_{IR}^2}+\frac{\pi^2}{12}\right)$.

Performing the z integration in the middle integral in (2.115),

$$\begin{aligned}
& \frac{1}{4\pi^2\epsilon_{IR}}\left(1+\frac{\gamma\epsilon_{IR}}{2}\right)\left(1+\frac{\epsilon_{IR}}{2}\log\frac{k_{max}^2}{4\pi\mu^2}\right)\int_{\delta_2}^{1-\delta_2}\mathrm{d}x\int_{-1}^{1}\mathrm{d}z\frac{1+\frac{\epsilon_{IR}}{2}\log\left(1-z^2\right)}{\left(E-\sqrt{E^2+q^2x\left(1-x\right)}z\right)^2}\\
& =\frac{1}{4\pi^2\epsilon_{IR}}\left(1+\frac{\gamma\epsilon_{IR}}{2}\right)\left(1+\frac{\epsilon_{IR}}{2}\log\frac{k_{max}^2}{4\pi\mu^2}\right)\int_{\delta_2}^{1-\delta_2}\mathrm{d}x\frac{1}{-q^2x\left(1-x\right)}\\
& \cdot\left(2+\epsilon_{IR}\left(\log 4+\frac{E}{\sqrt{E^2+q^2x\left(1-x\right)}}\log\frac{E-\sqrt{E^2+q^2x\left(1-x\right)}}{E+\sqrt{E^2+q^2x\left(1-x\right)}}\right)\right)\\
& =\frac{1}{-4\pi^2q^2}\int_{\delta_2}^{1-\delta_2}\mathrm{d}x\frac{1}{x\left(1-x\right)}\\
& \left(\frac{2}{\epsilon_{IR}}+\gamma+\log\frac{k_{max}^2}{\pi\mu^2}+\frac{E}{\sqrt{E^2+q^2x\left(1-x\right)}}\log\frac{E-\sqrt{E^2+q^2x\left(1-x\right)}}{E+\sqrt{E^2+q^2x\left(1-x\right)}}\right)
\end{aligned} \tag{2.125}$$

Performing the x integration,

$$\begin{aligned}
= \quad & \frac{1}{-2\pi^2q^2}\left(-\log 2\delta_2+\log 2-2\delta_2\right)\left(\frac{2}{\epsilon_{IR}}+\gamma+\log\frac{k_{max}^2}{\pi\mu^2}\right)+b_{ij}\\
\approx \quad & \frac{1}{-2\pi^2q^2}\left(\frac{2}{\epsilon_{IR}}+\gamma+\log\frac{k_{max}^2}{\pi\mu^2}\right)\log\frac{1}{\delta_2}+b_{ij}
\end{aligned} \tag{2.126}$$

where

$$\begin{aligned}
b_{ij} \quad \equiv \quad & \frac{1}{-2\pi^2q^2}\int_0^{1-2\delta_2}\mathrm{d}x_2\left(\frac{1}{1-x_2}+\frac{1}{1+x_2}\right)\frac{2E}{\sqrt{4E^2+q^2\left(1-x_2^2\right)}}\log\frac{2E-\sqrt{4E^2+q^2\left(1-x_2^2\right)}}{2E+\sqrt{4E^2+q^2\left(1-x_2^2\right)}}\\
= \quad & \frac{1}{-2\pi^2q^2}\left(-\frac{1}{2}\log^2\frac{-q^2\delta_2}{4E^2}-\ \mathrm{Li}_2\left(1-\frac{4E^2}{-q^2}\right)-\frac{\pi^2}{3}\right)
\end{aligned} \tag{2.127}$$

Inserting this and (2.120) into (2.115) cancels the δ_2 and reproduces (2.113).

2.5 Asymptotic Limits

Finally, the asymptotic limits at high and low energy of the scalar integrals in some commonly used cases are collected here for convenience.

2.5.1 Low Energy Limits

The low energy limits, where $q^2 \ll M^2$, are:

$$\begin{aligned} J^{(1)}(p_1,q) &\approx \frac{-i}{32\pi^2 M^2}\left(\log\frac{-q^2}{\mu^2}+\frac{\pi^2 M}{\sqrt{-q^2}}\right) \\ I^{(2)}(p_1,p_1-q) &\approx \frac{i}{16\pi^2}\left(\frac{2}{\epsilon_{UV}}-\gamma-\log\frac{M^2}{4\pi\mu^2}+\frac{q^2}{6M^2}\right) \\ I^{(3)}(p_1) &\approx \frac{i}{16\pi^2}\left(\frac{2}{\epsilon_{UV}}-\gamma-\log\frac{M^2}{4\pi\mu^2}+2\right) \end{aligned} \tag{2.128}$$

The low-energy limit of $J^{(2)}(p_1,p_1-q)$ in the different regularization schemes is:

a) Using a photon mass,

$$J^{(2)}(p_1,p_1-q) \approx \frac{-i}{32\pi^2 M^2}\left(\frac{q^2}{6M^2}\log\frac{M^2}{\lambda^2}-\frac{q^2}{6M^2}+\log\frac{M^2}{\lambda^2}\right) \tag{2.129}$$

b) Using zero photon mass but a nonzero electron mass,

$$\begin{aligned} J^{(2)}(p_1,p_1-q) \approx \frac{-i}{32\pi^2 M^2}&\left(\frac{q^2}{6M^2}\left(\log\frac{M^2}{4\pi\mu^2}+\frac{2}{\epsilon_{IR}}+\gamma\right)-\frac{q^2}{6M^2}\right. \\ &\left.+\log\frac{M^2}{4\pi\mu^2}+\frac{2}{\epsilon_{IR}}+\gamma\right) \end{aligned} \tag{2.130}$$

2.5.2 High Energy Limits

The high-energy limits, where $q^2 \gg M^2$, in the three different regularization schemes, are:

a) Using a photon mass,

$$\begin{aligned} I^{(2)}(p_1,p_1-q) &\approx \frac{i}{16\pi^2}\left(\log\frac{4\pi\mu^2}{-q^2}+2-\gamma+\frac{2}{\epsilon_{UV}}\right) \\ I^{(3)}(p_1) &\approx -\frac{i}{16\pi^2}\left(\log\frac{M^2}{4\pi\mu^2}-\frac{2}{\epsilon_{UV}}+\gamma-2\right) \\ J^{(2)}(p_1,p_1-q) &\approx -\frac{i}{16\pi^2 q^2}\left(\frac{1}{2}\log^2\left(\frac{-q^2}{M^2}\right)-\log\left(\frac{-q^2}{\lambda^2}\right)\log\left(\frac{-q^2}{M^2}\right)+\frac{\pi^2}{6}\right) \\ J^{(1)}(p_1,q) &\approx \frac{i}{16\pi^2 q^2}\left(\frac{1}{2}\log^2\frac{-q^2}{M^2}+\frac{2\pi^2}{3}\right) \end{aligned} \tag{2.131}$$

b) Using zero photon mass but a nonzero electron mass,

$$\begin{aligned}
I^{(2)}\left(p_1, p_1-q\right) &\approx \frac{i}{16\pi^2}\left(\log\frac{4\pi\mu^2}{-q^2}+2-\gamma+\frac{2}{\epsilon_{UV}}\right)\\
I^{(3)}\left(p_1\right) &\approx -\frac{i}{16\pi^2}\left(\log\frac{M^2}{4\pi\mu^2}-\frac{2}{\epsilon_{UV}}+\gamma-2\right)\\
J^{(2)}\left(p_1, p_1-q\right) &\approx \frac{i}{16\pi^2 q^2}\left(-\frac{1}{2}\log^2\frac{-q^2}{M^2}+\left(\gamma+\frac{2}{\epsilon_{IR}}+\log\frac{-q^2}{4\pi\mu^2}\right)\log\frac{-q^2}{M^2}-\frac{\pi^2}{6}\right)\\
J^{(1)}\left(p_1, q\right) &\approx \frac{i}{16\pi^2 q^2}\left(\frac{1}{2}\log^2\frac{-q^2}{M^2}+\frac{2\pi^2}{3}\right)
\end{aligned} \tag{2.132}$$

c) Using zero photon mass and a zero electron mass,

$$\begin{aligned}
I^{(2)}\left(p_1, p_1-q\right) &\approx \frac{i}{16\pi^2}\left(\log\frac{4\pi\mu^2}{-q^2}+2-\gamma+\frac{2}{\epsilon_{UV}}\right)\\
I^{(3)}\left(p_1\right) &\approx \frac{i}{8\pi^2}\frac{1}{\epsilon_{IR}}+\frac{i}{8\pi^2}\frac{1}{\epsilon_{UV}}\\
J^{(2)}\left(p_1, p_1-q\right) &= J^{(1)}\left(p_3, q\right)\\
&\approx \frac{i}{16\pi^2 q^2}\left(\frac{1}{2}\left(\log\frac{-q^2}{4\pi\mu^2}+\gamma+\frac{2}{\epsilon_{IR}}\right)^2+\frac{2}{\epsilon_{IR}^2}-\frac{\pi^2}{12}\right)
\end{aligned} \tag{2.133}$$

Note that $J^{(2)}\left(p_1, p_1-q\right)$ can be obtained from case **b** by substituting $\log M^2 \to \log 4\pi\mu^2 - {}^{2}/_{\epsilon_{IR}} - \gamma$ and adding an additional term ${}^{i}/_{16\pi^2 q^2}\left({}^{2}/_{\epsilon_{IR}^2}+\frac{\pi^2}{12}\right)$.

CHAPTER 3

IR DIVERGENCES IN QED

In order to illustrate many of the features of the gravitational calculations of chapter 4 in a more familiar setting, analogous calculations in QED are first performed in this chapter. The lowest-order quantum corrections to electron scattering in a Coulomb potential are calculated below following [17]. Here the same IR divergences occur as in the gravitational case. Soft divergences arise because of the masslessness of the photon, but can be treated by the inclusion of bremsstrahlung in cross sections. Collinear divergences also arise in the ultra-relativistic limit, where energies are large compared to the electron mass m. Although it will be shown in the next chapter that all collinear singularities cancel in cross sections for gravitational processes in which all external lines are on-shell, this will not be the case for the matrix elements of the energy-momentum tensor and the gravitational field, where the external graviton line is not on shell. To examine the dependance of the results on the regularization method used for these remaining singularities, the integrals are evaluated using the three different IR regularization methods of chapter 2:

a) regularization by using a photon mass λ and an electron mass m,

b) regularization by dimensional regularization in $D = 4 + \epsilon_{IR}$ dimensions and using an electron mass, and

c) dimensional regularization alone.

Since the purpose is to illustrate the treatment of IR divergences, only the IR-divergent pieces are computed here. Also, since QED is renormalizable and not usually treated as an effective field theory, in this chapter all analytic parts are explicitly retained in order to compare the results to the literature.

3.1 Lagrangian and Feynman Rules

The spinor QED Lagrangian is

$$\mathcal{L}_{QED} = -\frac{1}{4}F^{\mu\nu}F_{\mu\nu} + \bar{\psi}\gamma^{\mu}\left(i\partial_{\mu} + eA_{\mu}\right)\psi - m\bar{\psi}\psi \tag{3.1}$$

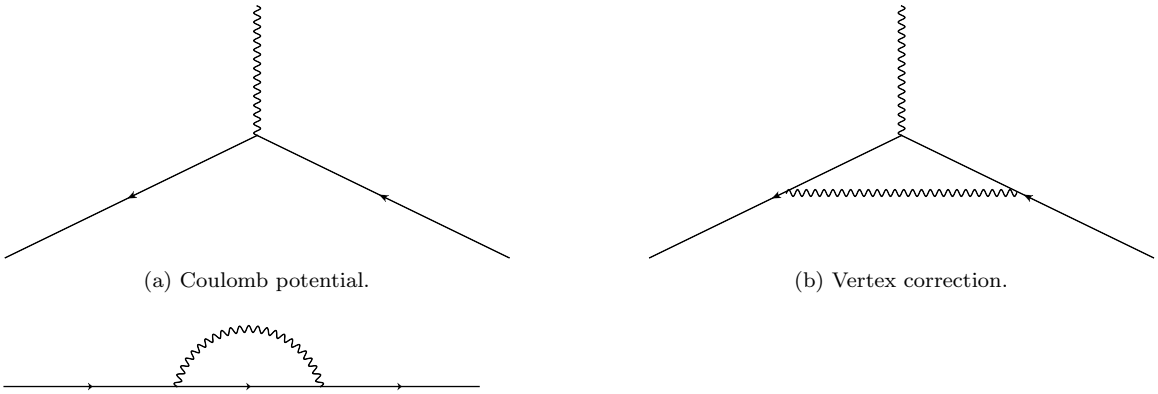

(a) Coulomb potential.

(b) Vertex correction.

(c) Self-energy diagram.

Figure 3.1. Feynman diagrams for the corrections to the Coulomb potential.

plus a gauge fixing Lagrangian which in the Feynman gauge is

$$\mathcal{L}_{gf} = -\frac{1}{2}\left(\partial^{\mu} A_{\mu}\right)^{2} \tag{3.2}$$

where ψ is the electron field, A^{μ} is the photon field, and $F^{\mu\nu} = \partial^{\mu} A^{\nu} - \partial^{\nu} A^{\mu}$ is the field tensor. These result in the photon propagator

$$D^{\mu\nu}\left(k\right) = -i\frac{g^{\mu\nu}}{k^{2}} \tag{3.3}$$

the electron propagator

$$G\left(p\right) = i\frac{\gamma \cdot p + m}{p^{2} - m^{2}} \tag{3.4}$$

and the lowest-order photon-electron vertex

$$ie\Gamma^{\mu}_{(0)} = ie\gamma^{\mu} \tag{3.5}$$

The Born approximation for the scattering of an electron with incoming momentum p_1 and outgoing momentum p_2 by a Coulomb potential of charge Ze is generated by the diagram in figure 3.1a, which evaluates to

$$\mathcal{M}_0 = \bar{u}\left(p_2\right)\gamma^0 u\left(p_1\right)\frac{Ze^2}{\vec{q}^2} \tag{3.6}$$

(Here $q \equiv p_1 - p_2 = (0, \vec{q})$ and of course $p_1^2 = p_2^2 = m^2$.) The IR-divergent corrections in $\mathcal{M}_1$ to the vertex part and electron lines occurring in figure 3.1a are given by figs. 3.1b and 3.1c. The cross section is given by

$$\mathrm{d}\sigma_{el} = 2\pi\delta\left(E_2 - E_1\right)\left|\mathcal{M}\right|^2 \frac{1}{2\left|\vec{p_1}\right|}\frac{\mathrm{d}^3 p_2}{2E_2\left(2\pi\right)^3} \tag{3.7}$$

Integrating with respect to $|\vec{p_1}|$ to eliminate the delta function,

$$\begin{aligned}
\left(\frac{\mathrm{d}\sigma}{\mathrm{d}\Omega}\right)_{el} &= \frac{1}{16\pi^2}\left|\mathcal{M}\right|^2 = \frac{1}{16\pi^2}\left|\mathcal{M}_0 + \mathcal{M}_1 + ...\right|^2 = \left(\frac{\mathrm{d}\sigma}{\mathrm{d}\Omega}\right)_0 + \left(\frac{\mathrm{d}\sigma}{\mathrm{d}\Omega}\right)_1 + ... \\
\left(\frac{\mathrm{d}\sigma}{\mathrm{d}\Omega}\right)_0 &= \frac{1}{16\pi^2}\left|\mathcal{M}_0\right|^2 \\
\left(\frac{\mathrm{d}\sigma}{\mathrm{d}\Omega}\right)_1 &= \frac{1}{16\pi^2}\left(\mathcal{M}_0\mathcal{M}_1^* + \mathcal{M}_0^*\mathcal{M}_1\right) = \frac{1}{8\pi^2}\,\mathrm{Re}\left[\mathcal{M}_0\mathcal{M}_1\right]
\end{aligned} \tag{3.8}$$

3.2 Vertex Function

The integral for the correction to the QED vertex function, fig. 3.1b, is

$$\begin{aligned}
\Gamma^{\mu}_{(1)}\left(p_1, p_2\right) &\equiv F_1\left(q^2\right)\gamma^{\mu} + \frac{i}{2m}F_2\left(q^2\right)\sigma^{\mu\nu}q_{\nu} \\
&= (ie)^2 \int \frac{\gamma^{\rho} i\left(\left(p_2 - k\right)\cdot\gamma + m\right)\gamma^{\mu} i\left(\left(p_1 - k\right)\cdot\gamma + m\right)\gamma^{\sigma}\left(-ig_{\rho\sigma}\right)}{\left(\left(p_2 - k\right)^2 - m^2\right)\left(\left(p_1 - k\right)^2 - m^2\right)k^2}\frac{d^D k}{\left(2\pi\right)^D}
\end{aligned} \tag{3.9}$$

where F_1 and F_2 are two form factors. The numerator of the integrand simplifies to

$$N_{\Gamma} \equiv \gamma^{\mu}\left[4p_1\cdot p_2 + \left(D-2\right)k^2 - 4\left(p_1 + p_2\right)\cdot k\right] + 4\left(p_1 + p_2\right)^{\mu}\gamma\cdot k - k^{\mu}\left[4m + 2(D-2)\gamma\cdot k\right], \tag{3.10}$$

Using the tensor integral reduction methods of chapter 2, contracting with external electron spinors and letting $D \to 4$ where allowable, (3.9) becomes

$$\begin{aligned}
\Gamma^{\mu}_{(1)}\left(p_1, p_2\right) &= -ie^2\left(\left(4m^2 J^{(2)}\left(p_1, p_2\right) - 2q^2 J^{(2)}\left(p_1, p_2\right) + 4I^{(3)}\left(m^2\right) - 3I^{(2)}\left(p_1, p_2\right)\right)\gamma^{\mu}\right. \\
&\quad \left. - \frac{2m}{4m^2 - q^2}\left(I^{(3)}\left(m^2\right) - I^{(2)}\left(p_1, p_2\right)\right)\left(p_1^{\mu} + p_2^{\mu}\right)\right)
\end{aligned} \tag{3.11}$$

Using the Gordon decomposition $\bar{u}\left(p_2\right)\left(p_1 + p_2\right)^{\mu} u\left(p_1\right) = \bar{u}\left(p_2\right)\left(2m\gamma^{\mu} + i\sigma^{\mu\nu}q_{\nu}\right)u\left(p_1\right)$, [17], (3.9) and (3.11) give

$$\begin{aligned}
F_1 &= -ie^2\left(\left(4m^2 - 2q^2\right)J^{(2)}\left(p_1, p_2\right) + 4I^{(3)}\left(m^2\right)\right. \\
&\quad \left. - 3I^{(2)}\left(p_1, p_2\right) - \frac{4m^2}{4m^2 - q^2}\left(I^{(3)}\left(m^2\right)z - I^{(2)}\left(p_1, p_2\right)\right)\right)
\end{aligned} \tag{3.12}$$

3.3 Self-energy

The self-energy diagram 3.1c is

$$-i\Sigma\left(p\right)=\left(ie\right)^{2}\int\frac{\gamma^{\nu}i\left(k\cdot\gamma+m\right)\gamma^{\mu}\left(-ig_{\mu\nu}\right)}{\left(k^{2}-m^{2}\right)\left(p-k\right)^{2}}\frac{d^{D}k}{\left(2\pi\right)^{D}}=-e^{2}\int\frac{N_{\Sigma}}{\left(k^{2}-m^{2}\right)\left(p-k\right)^{2}}\frac{d^{D}k}{\left(2\pi\right)^{D}} \tag{3.13}$$

where now p can be p_1 or p_2 and

$$N_{\Sigma}\equiv\gamma^{\mu}\left(\gamma\cdot k+m\right)\gamma_{\mu} \tag{3.14}$$

Using the anticommutation relations $\gamma^{\mu}\gamma^{\nu}+\gamma^{\nu}\gamma^{\mu}=g^{\mu\nu}$, the numerator becomes

$$N_{\Sigma} \quad = \quad \left(2-D\right)\gamma\cdot k-e^{2}Dm \tag{3.15}$$

After the tensor integral reduction,

$$\begin{aligned}-i\Sigma\left(p\right) &= -e^{2}\left(2-D\right)\gamma^{\mu}I_{\mu}^{(4)}\left(p\right)-e^{2}DmI^{(4)}\left(p\right)\\ &= -e^{2}\left(2-D\right)\left(-\frac{1}{2p^{2}}H_{1}+\frac{1}{2p^{2}}H_{2}+\left(\frac{1}{2}+\frac{m^{2}}{2p^{2}}\right)I^{(4)}\left(p\right)\right)\gamma\cdot p-e^{2}DmI^{(4)}\left(p\right)\end{aligned} \tag{3.16}$$

Since the external electrons are on-shell, the only part needed is the contribution to the electron wave-function renormalization [17]

$$\Sigma_{1}\equiv\frac{d\Sigma}{d\left(\gamma\cdot p\right)}|_{\gamma\cdot p=m} \tag{3.17}$$

which in the case $m\neq0$ evaluates to

$$\begin{aligned}\Sigma_{1} &= \frac{d}{d\left(\gamma\cdot p\right)}\left(-ie^{2}\left(2-D\right)\left(-\frac{1}{2p^{2}}H_{1}+\frac{1}{2p^{2}}H_{2}+\left(\frac{1}{2}+\frac{m^{2}}{2p^{2}}\right)I^{(4)}\left(p\right)\right)\gamma\cdot p\right.\\ &\quad \left.-ie^{2}DmI^{(4)}\left(p\right)\right)|_{\gamma\cdot p=m}\\ &= -ie^{2}\left(2m^{2}\left(2-D\right)\frac{d\left(-\frac{1}{2p^{2}}H_{1}+\frac{1}{2p^{2}}H_{2}+\left(\frac{1}{2}+\frac{m^{2}}{2p^{2}}\right)I^{(4)}\left(p\right)\right)}{dp^{2}}|_{p^{2}=m^{2}}\right.\\ &\quad +\left(2-D\right)\left(-\frac{1}{2p^{2}}H_{1}+\frac{1}{2p^{2}}H_{2}+\left(\frac{1}{2}+\frac{m^{2}}{2p^{2}}\right)I^{(4)}\left(p\right)\right)|_{p^{2}=m^{2}}\\ &\quad \left.+2m^{2}D\frac{dI^{(4)}\left(p\right)}{dp^{2}}|_{p^{2}=m^{2}}\right)\\ &= -ie^{2}\left(4m^{2}\frac{dI^{(4)}\left(p\right)}{dp^{2}}|_{p^{2}=m^{2}}+\left(2-D\right)\frac{1}{2m^{2}}H_{1}\right)\end{aligned}$$

$$= -ie^2\left(2\left(I^{(3)}(m=0)-I^{(3)}(p)\right)+(2-D)\frac{1}{2m^2}H_1\right) \tag{3.18}$$

since

$$\begin{aligned}
\frac{dI^{(4)}(p)}{dp^2} &= \frac{\partial p^\mu}{\partial p^2}\frac{dI^{(4)}(p)}{dp^\mu} \\
&= \frac{\partial p^\mu}{\partial p^2}\int\frac{d}{dp^\mu}\frac{1}{(k^2-m^2)(p-k)^2}\frac{d^Dk}{(2\pi)^D} \\
&= \frac{p^\mu}{2p^2}\int 2(p_\mu-k_\mu)\frac{-1}{(k^2-m^2)(p-k)^2(p-k)^2}\frac{d^Dk}{(2\pi)^D} \\
&= -\int\frac{1}{(k^2-m^2)(p-k)^2(p-k)^2}\frac{d^Dk}{(2\pi)^D}+\frac{1}{2p^2}\int\frac{2p\cdot k}{(k^2-m^2)(p-k)^2(p-k)^2}\frac{d^Dk}{(2\pi)^D} \\
&= \left(-\frac{1}{2}+\frac{m^2}{2p^2}\right)\int\frac{1}{(k^2-m^2)(p-k)^2(p-k)^2}\frac{d^Dk}{(2\pi)^D}-\frac{1}{2p^2}I^{(4)}(p)+\frac{1}{2p^2}I^{(3)}(m=0)
\end{aligned} \tag{3.19}$$

In the case $m=0$,

$$\begin{aligned}
\Sigma_1 &= \left(\frac{d}{d(\gamma\cdot p)}-ie^2\frac{2-D}{2}I^{(4)}(p)\gamma\cdot p\right)|_{\gamma\cdot p=0} \\
&= -ie^2\frac{2-D}{2}I^{(4)}(p)|_{p^2=0}-ie^2\frac{2-D}{2}\left(2p^2\frac{dI^{(4)}(p)}{dp^2}\right)|_{p^2=0} \\
&= -ie^2\frac{2-D}{2}I^{(4)}(p)|_{p^2=0} \\
&\quad -ie^2\frac{2-D}{2}\left(-p^2J^{(3)}(p)-I^{(4)}(p)+I^{(3)}(m=0)\right)|_{p^2=0} \\
&= \frac{e^2}{8\pi^2}\left(-\frac{1}{\epsilon_{IR}}-\frac{1}{\epsilon_{UV}}+1\right)
\end{aligned} \tag{3.20}$$

3.4 Bremsstrahlung

The form factor $F_1(q^2)$, and the self-energy $\Sigma_1(p)$, contain soft infra-red divergences. These can be regularized by introducing a small fictitious photon mass λ, or alternatively by dimensional regularization, but then the results depend on the non-physical parameter λ or ϵ_{IR}. Furthermore, the form of this dependence, as coefficients of non-analytic terms such as $\log\left(\sqrt{-q^2}+\sqrt{4m^2-q^2}\right)$, is such that it can not be absorbed into renormalized parameters occurring in the Lagrangian, and the results are therefore meaningless as they stand.

This occurs because, as is well known [30, 2, 23, 17, 19], soft bremsstrahlung must be included in the cross section for physically measurable quantities. As explained in chapter 2, soft divergences arise from integration over the momentum k of some virtual photon in the range where k is arbitrarily

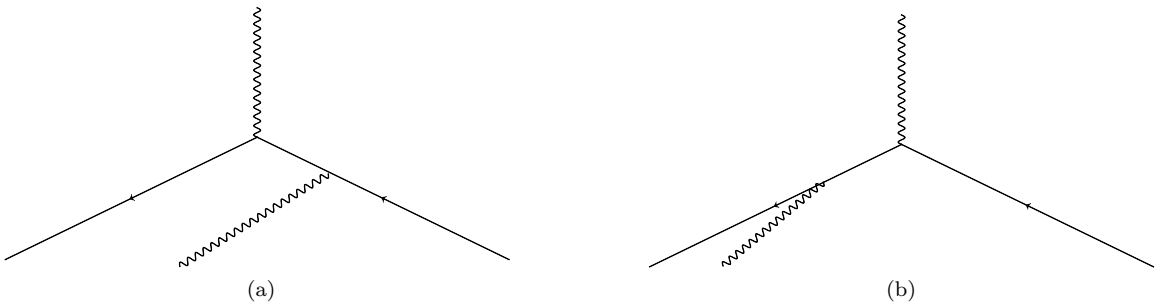

Figure 3.2. Bremsstrahlung diagrams for scattering in the Coulomb potential.

small. However, such virtual low-energy photons can not be distinguished from real low-energy photons emitted as bremsstrahlung during scattering, because any detector of finite size can detect radiation only with some finite energy resolution. The cross section for 'elastic' scattering, without the emission of bremsstrahlung, is therefore not a physically measurable quantity. Instead, it is only the cross section for the elastic process together with the emission of any number of soft photons, having a combined energy less than the detector resolution, which is measurable. The soft divergences in the elastic cross section are canceled by corresponding terms in the bremsstrahlung cross section, and the physical cross section is finite.

To the order considered, the bremsstrahlung amplitude is just the lowest order elastic amplitude $\mathcal{M}_0$ corrected by the emission of only a single photon either from the initial or from the final electron. (See fig.3.2.) However, for comparison with the gravitational calculations, the general case of a diagram with an arbitrary number of external lines is considered. The correction for emission of a photon with momentum k from outgoing electron line i with momentum p_i consists of an electron propagator with momentum $p_i + k$, a vertex factor, and the photon polarization vector ϵ_μ^*, inserted between the outgoing spinor $\bar{u}(p_i)$ and the rest of the expression for $\mathcal{M}_0$:

$$\mathcal{M}_{br,out} = \bar{u}(p_i)\,\epsilon_\mu^*\,(ie\gamma^\mu)\,i\frac{\gamma^\nu\,(p_i+k)_\nu + m}{(p_i+k)^2 - m^2}M_0 \tag{3.21}$$

where M_0 is the expression for $\mathcal{M}_0$ without the external spinor $\bar{u}(p_i)$, $\mathcal{M}_0 = \bar{u}(p_i)\,M_0$. In the limit where k is soft this becomes

$$\mathcal{M}_{br,out} = -e\bar{u}(p_i)\,\epsilon_\mu^*\gamma^\mu\frac{\gamma^\nu\,(p_i)_\nu + m}{2p_i\cdot k}M_0 \tag{3.22}$$

Using $\gamma^\mu\gamma^\nu + \gamma^\nu\gamma^\mu = 2\eta^{\mu\nu}$,

$$\mathcal{M}_{br,out} = -e\bar{u}\left(p_i\right)\left(\frac{-\gamma^{\nu}\left(p_i\right)_{\nu}+m}{2p_i\cdot k}\epsilon_{\mu}^{*}\gamma^{\mu}+\frac{p_i^{\mu}\epsilon_{\mu}^{*}}{p_i\cdot k}\right)M_0 \tag{3.23}$$

Then using $\bar{u}\left(p_i\right)\left(\gamma^{\nu}\left(p_i\right)_{\nu}-m\right)=0$, one finds

$$\mathcal{M}_{br,out} = -e\frac{p_i^{\mu}\epsilon_{\mu}^{*}}{p_i\cdot k}\bar{u}\left(p_i\right)M_0 = -e\frac{p_i^{\mu}\epsilon_{\mu}^{*}}{p_i\cdot k}\mathcal{M}_0. \tag{3.24}$$

Similarly, the correction for emission of a photon with momentum k from an incoming electron line with momentum p_i consists of an electron propagator with momentum p_i-k, a vertex factor, and the photon polarization vector ϵ_{μ}^{*}, inserted between the incoming spinor $u\left(p_i\right)$ and the rest of the expression for $\mathcal{M}_0$, and in the limit of soft k

$$\mathcal{M}_{br,in} = +e\frac{p^{\mu}\epsilon_{\mu}^{*}}{p_i\cdot k}\mathcal{M}_0. \tag{3.25}$$

The total bremsstrahlung amplitude is the sum of (3.24) and (3.25) over all external lines

$$\mathcal{M}_{br} = e\sum_i s_i\frac{p_i^{\mu}\epsilon_{\mu}^{*}}{p_i\cdot k}\mathcal{M}_0, \tag{3.26}$$

with $s_i=-1$ for outgoing lines and $s_i=+1$ for incoming lines. Although the exact form of the correction inserted into $\mathcal{M}_0$ differs for particles of different spin, the limiting form (3.26) for soft k, and all subsequent results, are valid for any spin [19].

The cross section corresponding to (3.26) for the emission of a soft photon with momentum in the range d^3k is

$$\mathrm{d}\sigma_{br} = \left|\mathcal{M}_{br}\right|^2\frac{\mathrm{d}^3k}{2\left|k\right|\left(2\pi\right)^3} = e^2\left(\sum_i\frac{\left|p_i^{\mu}\epsilon_{\mu}\right|^2}{\left(p\cdot k\right)^2}+2\sum_{i<j}s_is_j\frac{\mathrm{Re}\left[p_i^{\mu}\epsilon_{\mu}p_j^{\nu}\epsilon_{\nu}^{*}\right]}{\left(p_i\cdot k\right)\left(p_j\cdot k\right)}\right)\frac{\mathrm{d}^3k}{2\left|k\right|\left(2\pi\right)^3}\mathrm{d}\sigma_0 \tag{3.27}$$

This must be summed over all possible polarization and momentum states of the undetected soft photon.

The sum over polarization states effectively converts the product of polarization vectors $\epsilon_{\mu}\epsilon_{\nu}^{*}$ occurring in (3.27) into the unpolarized density matrix $-\eta^{\mu\nu}$. More precisely, since in an appropriate gauge the two physical polarization states of the photon,

$$\epsilon_{\mu}^{(1)}=\left(0,1,0,0\right),\epsilon_{\mu}^{(2)}=\left(0,0,1,0\right) \tag{3.28}$$

form a basis of the two-dimensional subspace of spacelike vectors orthogonal to $k^{\mu}=\left(k^0,0,0,k^0\right)$, summing $\epsilon_{\mu}\epsilon_{\nu}^{*}$ over these two states produces the projection onto that subspace:

$$\sum_n \epsilon_\mu^{(n)} \epsilon_\nu^{(n)*} = \delta_{\mu\nu}, \tag{3.29}$$

where $\delta_{\mu\nu}$ is

$$\delta_{\mu\nu} \equiv -\eta_{\mu\nu} + \hat{t}_\mu \hat{t}_\nu - \hat{\vec{k}}_\mu \hat{\vec{k}}_\nu = \begin{pmatrix} 0 & 0 & 0 & 0 \\ 0 & 1 & 0 & 0 \\ 0 & 0 & 1 & 0 \\ 0 & 0 & 0 & 0 \end{pmatrix}. \tag{3.30}$$

However, by electromagnetic gauge invariance, one can add to $\delta_{\mu\nu}$ an arbitrary multiple of k_μ without changing the cross section (3.27),

$$\delta_{\mu\nu} \to \delta'_{\mu\nu} \equiv \delta_{\mu\nu} + k_\mu \chi_\nu + k_\nu \chi_\mu. \tag{3.31}$$

Choosing $\chi_\mu = \frac{1}{2}\left(-1/k_0, 0, 0, 1/k_0\right)$ one obtains

$$\delta'_{\mu\nu} = -\eta_{\mu\nu} = \begin{pmatrix} -1 & 0 & 0 & 0 \\ 0 & 1 & 0 & 0 \\ 0 & 0 & 1 & 0 \\ 0 & 0 & 0 & 1 \end{pmatrix} \tag{3.32}$$

(Note that this is the same expression which occurs in the numerator of the photon propagator.) Therefore,

$$\begin{aligned} \sum_n p_i^\mu \epsilon_\mu^{(n)} p_i^\nu \epsilon_\nu^{(n)*} &\to -p_i^2 = -m^2 \\ \sum_n p_i^\mu \epsilon_\mu^{(n)} p_j^\nu \epsilon_\nu^{(n)*} &\to -p_i \cdot p_j \end{aligned} \tag{3.33}$$

and (3.27) becomes

$$\mathrm{d}\sigma_{br} = -e^2 \left(\sum_i \frac{m^2}{\left(p_i \cdot k\right)^2} + 2 \sum_{i<j} s_i s_j \frac{2 p_i \cdot p_j}{\left(p_i \cdot k\right)\left(p_j \cdot k\right)} \right) \frac{\mathrm{d}^3 k}{2\left|k\right|\left(2\pi\right)^3} \mathrm{d}\sigma_0 \tag{3.34}$$

The sum over photon momentum states is an integral up to some maximum magnitude, $k_{\max}$, determined by the resolution of the experimental apparatus. So, finally,

$$\mathrm{d}\sigma_{br} = -e^2 \int_{|k|<k_{\max}} \frac{d^3 k}{\left(2\pi\right)^3} \frac{1}{2k_0} \left(\sum_i \frac{m^2}{\left(p_i \cdot k\right)^2} + 2 \sum_{i<j} s_i s_j \frac{p_i \cdot p_j}{\left(p_i \cdot k\right)\left(p_j \cdot k\right)} \right) \mathrm{d}\sigma_0$$

$$= -e^2 \left(\sum_i \frac{m^2}{2} B_{ii} + \sum_{i<j} s_i s_j p_i \cdot p_j B_{ij} \right) \mathrm{d}\sigma_0 \tag{3.35}$$

where B_{ij} is listed in chapter 2. For the case at hand, fig. 3.2, (3.35) becomes

$$\mathrm{d}\sigma_{br} = e^2 \left(-\frac{m^2}{2} B_{11} + \left(m^2 - \frac{q^2}{2} \right) B_{12} - \frac{m^2}{2} B_{22} \right) \mathrm{d}\sigma_0 \tag{3.36}$$

It can similarly be shown that higher order bremsstrahlung corrections cancel with higher order elastic radiative corrections, and further that the low-energy contributions exponentiate in the sum of the perturbation series, converting the the arguments of the logarithms in B_{ij} into exponents [19, 17].

3.5 Cancellation of IR Divergences and Total Cross Section

The infra-red divergent pieces of $\mathcal{M}_0 + \mathcal{M}_1$ are

$$\begin{aligned} \mathcal{M}_0 + \mathcal{M}_{1,IR} &= \left(1 + \frac{1}{2}\Sigma_1 \right) \bar{u}(p_2) \left(1 + F_1\left(q^2\right) \right) \gamma^0 \left(1 + \frac{1}{2}\Sigma_1 \right) u(p_1) \frac{Ze^2}{\vec{q}^2} \\ &= \left(1 + \Sigma_1 + F_1\left(q^2\right) \right) \bar{u}(p_2) \gamma^0 u(p_1) \frac{Ze^2}{\vec{q}^2} \\ &= \left(1 + \Sigma_1 + F_1\left(q^2\right) \right) \mathcal{M}_0 \end{aligned} \tag{3.37}$$

The total cross section is given by the sum of the elastic cross section (3.8) and the bremsstrahlung cross section (3.27). The infra-red divergent pieces of this sum are

$$\begin{aligned} d\sigma_{tot,IR} &= d\sigma_{el,IR} + d\sigma_{br,IR} \\ &= \left(1 + 2\Sigma_1\left(p^2\right) + 2F_1\left(q^2\right) - e^2 \frac{m^2}{2} B_{11} + e^2 \left(m^2 - \frac{q^2}{2} \right) B_{12} - e^2 \frac{m^2}{2} B_{22} \right) d\sigma_0 \\ &\equiv X d\sigma_0 \end{aligned} \tag{3.38}$$

the factors of 2 multiplying Σ_1 and F_1 coming from squaring $\mathcal{M}_0 + \mathcal{M}_{1,IR}$ to produce $d\sigma_{el,IR}$. X is evaluated in the three different IR regularization schemes **a**, **b**, and **c** below.

In method **b**, dimensional regularization with $m \neq 0$: $2F_1$ is the sum of UV-divergent terms $2F_{1,UV}$ and soft-divergent terms $2F_{1,soft}$, and likewise $2\Sigma_1 = 2\Sigma_{1,UV} + 2\Sigma_{1,soft}$. The UV divergent terms in $2F_1$ are

$$2F_{1,UV} = -2ie^2 \left(4I^{(3)} - 3I^{(2)}(p_1, p_2) - \frac{4m^2}{4m^2 - q^2} \left(I^{(3)} - I^{(2)}(p_1, p_2) \right) \right)$$

$$= \frac{e^2}{8\pi^2}\left(\frac{2}{\epsilon_{UV}}+\gamma-\log\frac{m^2}{4\pi\mu^2}+2+3\frac{\sqrt{4m^2-q^2}}{\sqrt{-q^2}}\log\frac{\left(\sqrt{-q^2}+\sqrt{4m^2-q^2}\right)^2}{4m^2}\right.$$
$$\left.-\frac{4m^2}{\sqrt{4m^2-q^2}\sqrt{-q^2}}\log\frac{\left(\sqrt{-q^2}+\sqrt{4m^2-q^2}\right)^2}{4m^2}\right) \tag{3.39}$$

When $q^2=0$ this becomes

$$2F_{1,UV}=\frac{e^2}{8\pi^2}\left(\frac{2}{\epsilon_{UV}}-\gamma-\log\frac{m^2}{4\pi\mu^2}+2\right) \tag{3.40}$$

which cancels with the UV-divergent term contained in $2\Sigma_1$,

$$2\Sigma_{1,UV}=\frac{e^2}{8\pi^2}\left(-\frac{2}{\epsilon_{UV}}+\gamma+\log\frac{m^2}{4\pi\mu^2}-4\right) \tag{3.41}$$

as it must, by the Ward identity. Therefore the sum of these two parts is

$$2F_{1,UV}+2\Sigma_{1,UV} = \frac{e^2}{8\pi^2}\left(3\frac{\sqrt{4m^2-q^2}}{\sqrt{-q^2}}\log\frac{\left(\sqrt{-q^2}+\sqrt{4m^2-q^2}\right)^2}{4m^2}\right.$$
$$\left.-\frac{4m^2}{\sqrt{4m^2-q^2}\sqrt{-q^2}}\log\frac{\left(\sqrt{-q^2}+\sqrt{4m^2-q^2}\right)^2}{4m^2}-2\right) \tag{3.42}$$

The remaining terms in (3.38) are IR-divergent. $2F_1$ contains the soft IR-divergent term

$$2F_{1,soft} = -ie^2 4\left(2m^2-q^2\right)J^{(2)}(p_1,p_2)$$
$$= \frac{e^2\left(2m^2-q^2\right)}{4\pi^2\sqrt{-q^2}\sqrt{4m^2-q^2}}$$
$$\cdot\left(-\left(\frac{2}{\epsilon_{IR}}+\gamma+\log\frac{\sqrt{-q^2}\sqrt{4m^2-q^2}}{4\pi\mu^2}\right)\log\left(1+\frac{-q^2+\sqrt{-q^2}\sqrt{4m^2-q^2}}{2m^2}\right)\right.$$
$$+\frac{1}{2}\log^2\left(-\frac{1}{2}+\frac{\sqrt{4m^2-q^2}}{2\sqrt{-q^2}}\right)-\frac{1}{2}\log^2\left(\frac{1}{2}+\frac{\sqrt{4m^2-q^2}}{2\sqrt{-q^2}}\right)$$
$$\left.+\ \mathrm{Li}_2\left(\frac{1}{2}+\frac{\sqrt{-q^2}}{2\sqrt{4m^2-q^2}}\right)-\ \mathrm{Li}_2\left(\frac{1}{2}-\frac{\sqrt{-q^2}}{2\sqrt{4m^2-q^2}}\right)\right) \tag{3.43}$$

while

$$e^2\left(m^2-\frac{q^2}{2}\right)B_{12} = \frac{e^2\left(2m^2-q^2\right)}{4\pi^2\sqrt{-q^2}\sqrt{4m^2-q^2}}\left(\frac{2}{\epsilon_{IR}}+\gamma+\log\frac{k_{max}^2}{\pi\mu^2}\right)$$

$$\log\left(1+\frac{-q^2+\sqrt{-q^2}\sqrt{4m^2-q^2}}{2m^2}\right)$$
$$+e^2\frac{\left(2m^2-q^2\right)}{2}b_{12} \tag{3.44}$$

where the convergent term b_{12} is defined in chapter 2, and thus these terms combine to form

$$\begin{aligned}
2F_{1,soft}+e^2\left(m^2-\frac{q^2}{2}\right)B_{12} &= e^2\left(2m^2-q^2\right)\left[-4iJ^{(2)}\left(p_1,p_2\right)+\frac{1}{2}B_{12}\right] \\
&= \frac{-e^2\left(2m^2-q^2\right)}{4\pi^2\sqrt{-q^2}\sqrt{4m^2-q^2}} \\
&\quad\cdot\left(\log\frac{\sqrt{-q^2}\sqrt{4m^2-q^2}}{4k_{max}^2}\log\left(1+\frac{-q^2+\sqrt{-q^2}\sqrt{4m^2-q^2}}{2m^2}\right)\right. \\
&\quad -\frac{1}{2}\log^2\left(-\frac{1}{2}+\frac{\sqrt{4m^2-q^2}}{2\sqrt{-q^2}}\right)+\frac{1}{2}\log^2\left(\frac{1}{2}+\frac{\sqrt{4m^2-q^2}}{2\sqrt{-q^2}}\right) \\
&\quad \left.-\ \mathrm{Li}_2\left(\frac{1}{2}+\frac{\sqrt{-q^2}}{2\sqrt{4m^2-q^2}}\right)+\ \mathrm{Li}_2\left(\frac{1}{2}-\frac{\sqrt{-q^2}}{2\sqrt{4m^2-q^2}}\right)\right) \\
&\quad +e^2\frac{\left(2m^2-q^2\right)}{2}b_{12}
\end{aligned} \tag{3.45}$$

Similarly Σ_1 contains the soft IR-divergent term

$$\Sigma_{1,soft}=\frac{e^2}{8\pi^2}\left(\frac{2}{\epsilon_{IR}}+\gamma+\log\frac{m^2}{4\pi\mu^2}\right) \tag{3.46}$$

while

$$B_{11} = B_{22}=\frac{1}{4\pi^2}\frac{1}{m^2}\left(\frac{2}{\epsilon_{IR}}+\gamma+\log\frac{k_{max}^2}{\pi\mu^2}+\frac{E}{p}\log\frac{(E-p)^2}{m^2}\right) \tag{3.47}$$

and thus the remaining soft IR-divergent terms in (3.38),

$$2\Sigma_{1,soft}-e^2\frac{m^2}{2}B_{11}-e^2\frac{m^2}{2}B_{22}=\frac{e^2}{4\pi^2}\left(\log\frac{m^2}{4k_{max}^2}-\frac{E}{p}\log\frac{(E-p)^2}{m^2}\right) \tag{3.48}$$

All of these results are the same under method **a**, with a photon mass λ, after the substitution $\frac{2}{\epsilon_{IR}}+\gamma+\log 4\pi\mu^2\to\log\lambda^2$. Adding all these terms, the final result for X with a nonzero electron mass, with or without a photon mass, is

$$X = 1+\frac{e^2}{8\pi^2}\left(3\frac{\sqrt{4m^2-q^2}}{\sqrt{-q^2}}\log\frac{\left(\sqrt{-q^2}+\sqrt{4m^2-q^2}\right)^2}{4m^2}\right.$$

$$
\begin{aligned}
&-\frac{4m^2}{\sqrt{4m^2-q^2}\sqrt{-q^2}}\log\frac{\left(\sqrt{-q^2}+\sqrt{4m^2-q^2}\right)^2}{4m^2}-2\Bigg)\\
&-\frac{e^2\left(2m^2-q^2\right)}{4\pi^2\sqrt{-q^2}\sqrt{4m^2-q^2}}\left(\log\frac{\sqrt{-q^2}\sqrt{4m^2-q^2}}{4k_{max}^2}\log\left(1+\frac{-q^2+\sqrt{-q^2}\sqrt{4m^2-q^2}}{2m^2}\right)\right.\\
&-\frac{1}{2}\log^2\left(-\frac{1}{2}+\frac{\sqrt{4m^2-q^2}}{2\sqrt{-q^2}}\right)+\frac{1}{2}\log^2\left(\frac{1}{2}+\frac{\sqrt{4m^2-q^2}}{2\sqrt{-q^2}}\right)\\
&\left.-\ \mathrm{Li}_2\left(\frac{1}{2}+\frac{\sqrt{-q^2}}{2\sqrt{4m^2-q^2}}\right)+\ \mathrm{Li}_2\left(\frac{1}{2}-\frac{\sqrt{-q^2}}{2\sqrt{4m^2-q^2}}\right)\right)\\
&+e^2\frac{\left(2m^2-q^2\right)}{2}b_{12}\\
&+\frac{e^2}{4\pi^2}\left(\log\frac{m^2}{4k_{max}^2}-\frac{E}{p}\log\frac{(E-p)^2}{m^2}\right)
\end{aligned}
\tag{3.49}
$$

and is IR finite. The asymptotic limits of (3.49) are

$$
X\approx\frac{e^2}{4\pi^2}\left(1+\frac{11q^2}{36m^2}+\frac{q^2}{3m^2}\log\frac{m^2}{4k_{max}^2}\right)
\tag{3.50}
$$

at low energy, where $q^2\ll m^2$, and

$$
\begin{aligned}
X\ \approx\ & 1+\frac{e^2}{4\pi^2}\left(\frac{3}{2}\log\frac{-q^2}{m^2}-1+\log\frac{E^2}{k_{max}^2}\right.\\
&\left.-\log\frac{-q^2}{m^2}\log\frac{E^2}{k_{max}^2}-\frac{1}{2}\log^2\frac{-q^2}{4E^2}-\ \mathrm{Li}_2\left(1-\frac{4E^2}{-q^2}\right)-\frac{\pi^2}{6}\right)
\end{aligned}
\tag{3.51}
$$

at high energy, where $q^2\gg m^2$. In the latter case, there are collinear singularities regularized by m. These results agree with the standard results in the literature, for instance, [23, 30].

Note how the IR divergent piece from each elastic diagram cancels with the interference term between the two bremsstrahlung diagrams obtained by cutting the virtual photon line at each of its vertices. Diagrams 3.2a and 3.2b can each be obtained by cutting the photon line at one of the vertices in diagram 3.1b, and it is the cross term B_{12} between diagrams 3.2a and 3.2b that cancels the soft divergence in F_1 from diagram 3.1b. Effectively, the virtual photon in diagram 3.1b is cut off at low energies by the finite resolution of the detector. Similarly, diagram 3.2a can be obtained in two different ways by cutting the photon line at the vertices in diagram 3.1c on the initial electron line, and the soft divergence in Σ_1 is canceled by B_{11} and B_{22}. Similar cancellations can be proven to all orders [19, 17].

In method **c**, with a zero electron mass:

$$X = 1 + 2\Sigma_1\left(p^2\right) + 2F_1\left(q^2\right) - e^2\frac{q^2}{2}B_{12} \tag{3.52}$$

$2F_1$ contains the UV-divergent terms

$$\begin{aligned} 2F_{1,UV} &= -2ie^2\left(4I^{(3)} - 3I^{(2)}\left(p_1,p_2\right)\right) \\ &= \frac{e^2}{8\pi^2}\left(\frac{8}{\epsilon_{IR}} + \frac{2}{\epsilon_{UV}} + 3\gamma + 3\log\frac{-q^2}{4\pi\mu^2} - 6\right) \end{aligned} \tag{3.53}$$

while $2\Sigma_1$ is

$$2\Sigma_1 = \frac{e^2}{8\pi^2}\left(-\frac{2}{\epsilon_{IR}} - \frac{2}{\epsilon_{UV}} + 2\right) \tag{3.54}$$

Both of these terms now also contain collinear divergences represented by $1/\epsilon_{IR}$. The sum of these two parts is

$$2F_{1,UV} + 2\Sigma_1 = \frac{e^2}{8\pi^2}\left(\frac{6}{\epsilon_{IR}} + 3\gamma + 3\log\frac{-q^2}{4\pi\mu^2} - 4\right) \tag{3.55}$$

The remaining terms in (3.38) are soft-IR-divergent. $2F_1$ contains the soft IR-divergent term

$$\begin{aligned} 2F_{1,soft} &= 4e^2q^2iJ^{(2)}\left(p_1,p_2\right) \\ &= -\frac{e^2}{4\pi^2}\left(\frac{2}{\epsilon_{IR}^2} + \frac{1}{2}\left(\log\frac{-q^2}{4\pi\mu^2} + \gamma + \frac{2}{\epsilon_{IR}}\right)^2 - \frac{\pi^2}{12}\right) \end{aligned} \tag{3.56}$$

while

$$\begin{aligned} -e^2\frac{q^2}{2}B_{12} &= \frac{e^2}{4\pi^2}\left(\frac{2}{\epsilon_{IR}^2} + \frac{1}{2}\left(\frac{2}{\epsilon_{IR}} + \gamma + \log\frac{k_{max}^2}{\pi\mu^2}\right)^2 + \right. \\ &\quad \left.\left(\frac{2}{\epsilon_{IR}} + \gamma + \log\frac{k_{max}^2}{\pi\mu^2}\right)\log\frac{-q^2}{4E^2} - \ \mathrm{Li}_2\left(1 - \frac{4E^2}{-q^2}\right) - \frac{\pi^2}{4}\right) \end{aligned} \tag{3.57}$$

and thus these terms combine to form

$$\begin{aligned} & e^2q^2\left[4iJ^{(2)}\left(p_1,p_2\right) - \frac{1}{2}B_{12}\right] \\ &= \frac{e^2}{4\pi^2}\left(\left(\frac{2}{\epsilon_{IR}} + \gamma + \log\frac{k_{max}^2}{\pi\mu^2}\right)\log\frac{k_{max}^2}{E^2} - \frac{1}{2}\log^2\frac{-q^2}{4k_{max}^2} - \ \mathrm{Li}_2\left(1 - \frac{4E^2}{-q^2}\right) - \frac{\pi^2}{6}\right) \end{aligned} \tag{3.58}$$

Adding all these terms, the final result with a zero electron mass is

$$X = 1 + \frac{e^2}{4\pi^2}\left(\frac{3}{2}\left(\frac{2}{\epsilon_{IR}} + \gamma + \log\frac{-q^2}{4\pi\mu^2}\right) - 2\right.$$

$$-\left(\frac{2}{\epsilon_{IR}}+\gamma+\log\frac{-q^2}{4\pi\mu^2}\right)\log\frac{E^2}{k_{max}^2}+\frac{1}{2}\log^2\frac{E^2}{k_{max}^2}-\frac{1}{2}\log^2\frac{-q^2}{4E^2}-\ \mathrm{Li}_2\left(1-\frac{4E^2}{-q^2}\right)-\frac{\pi^2}{6}\right) \tag{3.59}$$

In this case also, the soft divergence in F_1 is canceled by the soft divergence in B_{12}, while the soft divergent terms in Σ_1, B_{11}, and B_{22} have disappeared due to a factor of $m^2 = 0$. The collinear divergences remain.

Compare the results of the two regularization methods for the collinear divergences. After the substitution $\log m^2 \to \log 4\pi\mu^2 + {}^2/_{\epsilon_{IR}} + \gamma$, (3.51) is nearly, but not quite, identical with (3.59). The difference is only in the analytic terms, which in any case are divergent and therefore physically meaningless. Since there are no massless charged particles in nature, this divergence is of no practical concern. Note that the coefficients of the non-analytic terms are the same in both cases and are independent of the regularization parameter m or ϵ_{IR}.

In the following chapters, analogous calculations will be performed for gravitationally interacting massless particles, as well as the calculation of the scattering cross section of two particles.

CHAPTER 4
IR DIVERGENCES IN QUANTUM GRAVITY

The same IR divergences which occur in QED also occur in quantum gravity, including collinear divergences in the case of massless scattering particles. Although massless charged particles do not occur in nature, so that the collinear divergences which arise in QED are purely academic, all particles interact gravitationally, and collinear divergences represent a serious challenge to the theory. Below, it is demonstrated explicitly to first order that these collinear divergences cancel in the final results for scattering cross sections, and the reasons why are examined. The cross section for scattering of a massless scalar particle by a scalar particle of arbitrary mass is calculated first, because all the essential elements are present and the calculation is algebraically much simpler. Then the cross section for photon scattering by a massive scalar source is calculated. Since the analytic parts of the results only renormalize parameters in the Lagrangian, and are meaningless by themselves, only diagrams which contribute non-analytic pieces are shown, and the analytic pieces are truncated.

4.1 Lagrangian and Feynman Rules

As described in chapter 1, although in an effective field theory all terms respecting general covariance must in principal be included, it is known empirically that after renormalization the gravitational Lagrangian,to good approximation, is effectively just the usual Lagrangian of general relativity

$$\mathcal{L}_g \approx \sqrt{-g}\frac{2R}{\kappa^2} \tag{4.1}$$

plus a gauge fixing term. This effective Lagrangian is quantized using the background field method of [13]. The full metric is expanded about a background metric $\bar{g}$ as

$$g_{\mu\nu} \equiv \bar{g}_{\mu\nu} + \kappa h_{\mu\nu} \tag{4.2}$$

(All further indices are raised and lowered with the background metric $\bar{g}$.) The expansion of the gravitational Lagrangian to second order in h is then

$$
\begin{aligned}
\mathcal{L}_g &= \sqrt{-\bar{g}}\left\{\frac{2}{\kappa^2}\bar{R}+\mathcal{L}_g^{(1)}+\mathcal{L}_g^{(2)}+\cdots\right\} \\
\mathcal{L}_g^{(1)} &= \frac{h_{\mu\nu}}{\kappa}\left[\bar{g}^{\mu\nu}\bar{R}-2\bar{R}^{\mu\nu}\right] \\
\mathcal{L}_g^{(2)} &= \frac{1}{2}D_\alpha h_{\mu\nu}D^\alpha h^{\mu\nu}-\frac{1}{2}D_\alpha hD^\alpha h+D_\alpha hD_\beta h^{\alpha\beta}-D_\alpha h_{\mu\beta}D^\beta h^{\mu\alpha} \\
&\quad +\bar{R}\left(\frac{1}{2}h^2-\frac{1}{2}h_{\mu\nu}h^{\mu\nu}\right)+\bar{R}^{\mu\nu}\left(2h^\lambda{}_\mu h_{\nu\alpha}-hh_{\mu\nu}\right)
\end{aligned}
\tag{4.3}
$$

where $\bar{R}$ and D are the scalar curvature and covariant derivative of the background metric [22]. This must be augmented by a gauge fixing Lagrangian, which for harmonic gauge is

$$
\mathcal{L}_{gf}=\sqrt{-\bar{g}}\left\{\left(D^\nu h_{\mu\nu}-\frac{1}{2}D_\mu h^\lambda{}_\lambda\right)\left(D_\sigma h^{\mu\sigma}-\frac{1}{2}D^\mu h^\sigma{}_\sigma\right)\right\}, \tag{4.4}
$$

and a ghost Lagrangian

$$
\mathcal{L}_{gh}=\sqrt{-\bar{g}}\eta^{*\mu}\left[D_\lambda D^\lambda\bar{g}_{\mu\nu}-R_{\mu\nu}\right]\eta^\nu. \tag{4.5}
$$

Because the background field satisfies Einstein's equation, the linear terms in (4.3) will cancel in all matrix elements with the linear terms from the matter Lagrangian. The quadratic terms determine the propagator, which in flat space $\bar{g}_{\mu\nu}=\eta_{\mu\nu}$, in harmonic gauge, is

$$
D_{\alpha\beta,\gamma\delta}(k)=\frac{iP_{\alpha\beta,\gamma\delta}}{k^2}, \tag{4.6}
$$

where

$$
\begin{aligned}
P_{\alpha\beta,\gamma\delta} &= I_{\alpha\beta,\gamma\delta}-\frac{1}{2}\eta_{\alpha\beta}\eta_{\gamma\delta}, &(4.7)\\
I_{\alpha\beta,\gamma\delta} &= \frac{1}{2}\left(\eta_{\alpha\gamma}\eta_{\beta\delta}+\eta_{\alpha\delta}\eta_{\beta\gamma}\right). &(4.8)
\end{aligned}
$$

Expanding (4.3) to second order in h and to first order in the background field yields the three-graviton vertex, which in flat space is [12]:

$$
\begin{aligned}
\tau^{\mu\nu}_{\alpha\beta,\gamma\delta}(k,q) &= i\frac{\kappa}{2}\left\{P_{\alpha\beta,\gamma\delta}\left[k^\mu k^\nu+(k-q)^\mu(k-q)^\nu+q^\mu q^\nu-\frac{3}{2}\eta^{\mu\nu}q^2\right]\right. \\
&\quad +2q_\lambda q_\sigma\left[I^{\lambda\sigma,}_{\alpha\beta}I^{\mu\nu,}_{\gamma\delta}+I^{\lambda\sigma,}_{\gamma\delta}I^{\mu\nu,}_{\alpha\beta}-I^{\lambda\mu,}_{\alpha\beta}I^{\sigma\nu,}_{\gamma\delta}-I^{\sigma\nu,}_{\alpha\beta}I^{\lambda\mu,}_{\gamma\delta}\right] \\
&\quad +\left[q_\lambda q^\mu\left(\eta_{\alpha\beta}I^{\lambda\nu,}_{\gamma\delta}+\eta_{\gamma\delta}I^{\lambda\nu,}_{\alpha\beta}\right)+q_\lambda q^\nu\left(\eta_{\alpha\beta}I^{\lambda\mu,}_{\gamma\delta}+\eta_{\gamma\delta}I^{\lambda\mu,}_{\alpha\beta}\right)\right. \\
&\quad \left.-q^2\left(\eta_{\alpha\beta}I^{\mu\nu,}_{\gamma\delta}+\eta_{\gamma\delta}I^{\mu\nu,}_{\alpha\beta}\right)-\eta^{\mu\nu}q^\lambda q^\sigma\left(\eta_{\alpha\beta}I_{\gamma\delta,\lambda\sigma}+\eta_{\gamma\delta}I_{\alpha\beta,\lambda\sigma}\right)\right] \\
&\quad +\left[2q^\lambda\left(I^{\sigma\nu,}_{\alpha\beta}I_{\gamma\delta,\lambda\sigma}(k-q)^\mu+I^{\sigma\mu,}_{\alpha\beta}I_{\gamma\delta,\lambda\sigma}(k-q)^\nu\right.\right.
\end{aligned}
$$

$$
\begin{aligned}
&- I^{\sigma\nu,}_{\gamma\delta} I_{\alpha\beta,\lambda\sigma} k^{\mu} - I^{\sigma\mu,}_{\gamma\delta} I_{\alpha\beta,\lambda\sigma} k^{\nu} \Big) \\
&+ q^2 \left(I^{\sigma\mu,}_{\alpha\beta} I^{\nu}_{\gamma\delta,\sigma} + I^{\nu}_{\alpha\beta,\sigma} I^{\sigma\mu,}_{\gamma\delta} \right) + \eta^{\mu\nu} q^{\lambda} q_{\sigma} \left(I_{\alpha\beta,\lambda\rho} I^{\rho\sigma,}_{\gamma\delta} + I_{\gamma\delta,\lambda\rho} I^{\rho\sigma,}_{\alpha\beta} \right) \Big] \\
&+ \Bigg[\left(k^2 + (k-q)^2 \right) \left(I^{\sigma\mu,}_{\alpha\beta} I^{\nu}_{\gamma\delta,\sigma} + I^{\sigma\nu,}_{\alpha\beta} I^{\mu}_{\gamma\delta,\sigma} - \frac{1}{2} \eta^{\mu\nu} P_{\alpha\beta,\gamma\delta} \right) \\
&- \left(k^2 \eta_{\gamma\delta} I^{\mu\nu,}_{\alpha\beta} + (k-q)^2 \eta_{\alpha\beta} I^{\mu\nu,}_{\gamma\delta} \right) \Bigg] \Bigg\} \qquad (4.9)
\end{aligned}
$$

The full Lagrangian consists of the gravitational Lagrangian plus the matter Lagrangian. The two types of matter considered are a spin 0 field and the electromagnetic field. The spin 0 Lagrangian is:

$$
\mathcal{L}_s = \frac{\sqrt{-g}}{2} \left(g^{\mu\nu} D_{\mu}\phi D_{\nu}\phi - m^2\phi^2 \right) \qquad (4.10)
$$

where D is the covariant derivative associated with g, which for a scalar is just the same as the partial derivative. Expanding (4.10) about flat space to second order in h determines the lowest-order 2-scalar 1-graviton and 2-scalar 2-graviton vertex factors:

$$
\begin{aligned}
\tau_{\alpha\beta}(p,p') &= -i\frac{\kappa}{2} \left(p_{\alpha}p'_{\beta} + p'_{\alpha}p_{\beta} - \left(p\cdot p' - m^2 \right) \eta_{\alpha\beta} \right) \qquad (4.11) \\
\tau_{\alpha\beta\gamma\delta}(p,p') &= i\kappa^2 \Bigg(I_{\alpha\beta\rho\xi} I^{\xi}_{\sigma\gamma\delta} \left(p^{\rho}p'^{\sigma} + p'^{\rho}p^{\sigma} \right) - \frac{1}{2} \left(\eta_{\alpha\beta} I_{\rho\sigma\gamma\delta} + \eta_{\gamma\delta} I_{\rho\sigma\alpha\beta} \right) p'^{\rho}p^{\sigma} \\
&\quad - \frac{1}{2} \left(I_{\alpha\beta\gamma\delta} - \frac{1}{2} \eta_{\alpha\beta}\eta_{\gamma\delta} \right) \left(p\cdot p' - m^2 \right) \Bigg) \qquad (4.12)
\end{aligned}
$$

The scalar propagator in flat space is

$$
D(k) = \frac{i}{k^2} \qquad (4.13)
$$

The electromagnetic Lagrangian is:

$$
\mathcal{L}_{em} = \frac{\sqrt{-g}}{2} g^{\mu\tau} g^{\nu\sigma} \left(D_{\mu}A_{\nu} - D_{\nu}A_{\mu} \right) \left(D_{\sigma}A_{\tau} - D_{\tau}A_{\sigma} \right) \qquad (4.14)
$$

where

$$
D_{\mu}A^{\nu} = \partial_{\mu}A^{\nu} + \frac{1}{2} g^{\nu\sigma} \left(\partial_{\mu}g_{\sigma\lambda} + \partial_{\lambda}g_{\sigma\mu} - \partial_{\sigma}g_{\mu\lambda} \right) A^{\lambda} \qquad (4.15)
$$

From (4.14) it follows that the lowest-order photon-graviton vertices in flat space are[12]:

$$
\begin{aligned}
\tau^{(1)}_{\beta,\alpha,\mu\nu}(p_1,p_2) &= i\frac{\kappa}{2} \{ \left(p_{1\mu}p_{2\nu} + p_{1\nu}p_{2\mu} \right) \eta_{\alpha\beta} + \eta_{\mu\nu} p_{1\beta} p_{2\alpha} \\
&\quad - p_{1\beta} \left(p_{2\mu}\eta_{\nu\alpha} + p_{2\nu}\eta_{\alpha\mu} \right) - p_{2\alpha} \left(p_{1\mu}\eta_{\nu\beta} + p_{1\nu}\eta_{\beta\mu} \right) \\
&\quad + p_1 \cdot p_2 \left(\eta_{\mu\alpha}\eta_{\nu\beta} + \eta_{\mu\beta}\eta_{\nu\alpha} - \eta_{\mu\nu}\eta_{\alpha\beta} \right) \} \qquad (4.16)
\end{aligned}
$$

$$
\begin{aligned}
\tau^{(2)}_{\beta,\alpha,\mu\nu,\rho\sigma}\left(p_1,p_2\right) &= -i\frac{\kappa^2}{4}\left\{\left[p_{1\beta}p_{2\alpha}-\eta_{\alpha\beta}\left(p_1\cdot p_2\right)\right]\left(\eta_{\mu\rho}\eta_{\nu\sigma}+\eta_{\mu\sigma}\eta_{\nu\rho}-\eta_{\mu\nu}\eta_{\rho\sigma}\right)\right.\\
&+\eta_{\mu\rho}\left[\eta_{\alpha\beta}\left(p_{1\nu}p_{2\sigma}+p_{1\sigma}p_{2\nu}\right)-\eta_{\alpha\nu}p_{1\beta}p_{2\sigma}-\eta_{\beta\nu}p_{1\sigma}p_{2\alpha}\right.\\
&\left.-\eta_{\beta\sigma}p_{1\nu}p_{2\alpha}-\eta_{\alpha\sigma}p_{1\beta}p_{2\nu}+p_1\cdot p_2\left(\eta_{\alpha\nu}\eta_{\beta\sigma}+\eta_{\alpha\sigma}\eta_{\beta\nu}\right)\right]\\
&+\eta_{\mu\sigma}\left[\eta_{\alpha\beta}\left(p_{1\nu}p_{2\rho}+p_{1\rho}p_{2\nu}\right)-\eta_{\alpha\nu}p_{1\beta}p_{2\rho}-\eta_{\beta\nu}p_{1\rho}p_{2\alpha}\right.\\
&\left.-\eta_{\beta\rho}p_{1\nu}p_{2\alpha}-\eta_{\alpha\rho}p_{1\beta}p_{2\nu}+p_1\cdot p_2\left(\eta_{\alpha\nu}\eta_{\beta\rho}+\eta_{\alpha\rho}\eta_{\beta\nu}\right)\right]\\
&+\eta_{\nu\rho}\left[\eta_{\alpha\beta}\left(p_{1\mu}p_{2\sigma}+p_{1\sigma}p_{2\mu}\right)-\eta_{\alpha\mu}p_{1\beta}p_{2\sigma}-\eta_{\beta\mu}p_{1\sigma}p_{2\alpha}\right.\\
&\left.-\eta_{\beta\sigma}p_{1\mu}p_{2\alpha}-\eta_{\alpha\sigma}p_{1\beta}p_{2\mu}+p_1\cdot p_2\left(\eta_{\alpha\mu}\eta_{\beta\sigma}+\eta_{\alpha\sigma}\eta_{\beta\mu}\right)\right]\\
&+\eta_{\nu\sigma}\left[\eta_{\alpha\beta}\left(p_{1\mu}p_{2\rho}+p_{1\rho}p_{2\mu}\right)-\eta_{\alpha\mu}p_{1\beta}p_{2\rho}-\eta_{\beta\mu}p_{1\rho}p_{2\alpha}\right.\\
&\left.-\eta_{\beta\rho}p_{1\mu}p_{2\alpha}-\eta_{\alpha\rho}p_{1\beta}p_{2\mu}+p_1\cdot p_2\left(\eta_{\alpha\mu}\eta_{\beta\rho}+\eta_{\alpha\rho}\eta_{\beta\mu}\right)\right]\\
&-\eta_{\mu\nu}\left[\eta_{\alpha\beta}\left(p_{1\rho}p_{2\sigma}+p_{1\sigma}p_{2\rho}\right)-\eta_{\alpha\rho}p_{1\beta}p_{2\sigma}-\eta_{\beta\rho}p_{1\sigma}p_{2\alpha}\right.\\
&\left.-\eta_{\beta\sigma}p_{1\rho}p_{2\alpha}-\eta_{\alpha\sigma}p_{1\beta}p_{2\rho}+p_1\cdot p_2\left(\eta_{\alpha\rho}\eta_{\beta\sigma}+\eta_{\beta\rho}\eta_{\alpha\sigma}\right)\right]\\
&-\eta_{\rho\sigma}\left[\eta_{\alpha\beta}\left(p_{1\mu}p_{2\nu}+p_{1\nu}p_{2\mu}\right)-\eta_{\alpha\mu}p_{1\beta}p_{2\nu}-\eta_{\beta\mu}p_{1\nu}p_{2\alpha}\right.\\
&\left.-\eta_{\beta\nu}p_{1\mu}p_{2\alpha}-\eta_{\alpha\nu}p_{1\beta}p_{2\mu}+p_1\cdot p_2\left(\eta_{\alpha\mu}\eta_{\beta\nu}+\eta_{\beta\mu}\eta_{\alpha\nu}\right)\right]\\
&+\left(\eta_{\alpha\rho}p_{1\mu}-\eta_{\alpha\mu}p_{1\rho}\right)\left(\eta_{\beta\sigma}p_{2\nu}-\eta_{\beta\mu}p_{2\sigma}\right)\\
&+\left(\eta_{\alpha\sigma}p_{1\nu}-\eta_{\alpha\nu}p_{1\sigma}\right)\left(\eta_{\beta\rho}p_{2\mu}-\eta_{\beta\mu}p_{2\rho}\right)\\
&+\left(\eta_{\alpha\sigma}p_{1\mu}-\eta_{\alpha\mu}p_{1\sigma}\right)\left(\eta_{\beta\rho}p_{2\nu}-\eta_{\beta\nu}p_{2\rho}\right)\\
&\left.+\left(\eta_{\alpha\rho}p_{1\nu}-\eta_{\alpha\nu}p_{1\rho}\right)\left(\eta_{\beta\sigma}p_{2\mu}-\eta_{\beta\mu}p_{2\sigma}\right)\right\} \qquad (4.17)
\end{aligned}
$$

Finally, the photon propagator in the (electromagnetic) Feynman gauge is

$$
D_{\mu\nu}\left(k\right)=\frac{-i\eta_{\mu\nu}}{k^2} \qquad (4.18)
$$

4.2 IR Divergences in Quantum Gravity

The results for the cross section and for the metric may be expected to contain infra-red divergences arising from the masslessness of both the graviton and the photon (or massless scalar particle). Since these arise from low-energy regions of virtual momenta, they can not be ascribed to the integrated degrees of freedom of the underlying high-energy theory, and since they are non-analytic, they can not be removed by renormalization of parameters in the Lagrangian. Therefore they are not resolved by effective field theory.

Just as soft divergences occur in QED because of the masslessness of the photon, they occur in quantum gravity because of the masslessness of the graviton. By the same reasoning as presented in chapter 3 for QED, they can be treated in gravity in the analogous way, by including soft gravitational bremsstrahlung in the final state of the system, and they present no additional difficulty. However, as described in chapter 2, there may also be collinear divergences in diagrams with more than one massless propagator. Such divergences occurs for hard virtual gravitons as well as for soft, as long as they are on-shell, and can not be removed just by the inclusion of real soft bremsstrahlung in the final state.

Collinear divergences are known from other quantum field theories, wherein they are treated in a number of ways. However, none of these ways seem physically relevant to the case at hand. As seen in chapter 3, these divergences occur in the theory of massless QED, but are physically irrelevant, since there are no massless charged particles in nature. However there do exist massless gravitating particles, namely photons. Collinear divergences also occur in QCD [16, 1, 17]. There they are treated by the inclusion of jets of particles in cross sections, but jets are not expected to occur in gravitational scattering. Alternatively, the KLN theorem [18] proves that collinear singularities in the elastic cross section do cancel with singularities in the cross sections for processes that include additional real, collinear gravitons. However, these real gravitons must include hard gravitons as well as soft and must appear in both the final and initial states. The physical meaning of this is unclear in this case [19, 1, 17]. While it is impossible to detect a graviton of sufficiently low wavelength with a finite detector, it is unclear that a hard collinear graviton could never be detected. In particular, if a significant amount of the energy of the system were carried by the graviton, it does not seem obvious that a photon detector would be unable to discriminate between the energy carried by the graviton and the energy carried by the photon.

Thus, the occurrence of collinear divergences could present a serious problem for quantum gravity of massless particles, even in the energy range where effective field theory is expected to be valid.

However, Weinberg [19] shows that, at least in the region of soft virtual graviton momentum, the collinear divergences that appear in individual diagrams of quantum gravity actually cancel between different diagrams for any process in which all external lines are on-shell. He traces the reason to the fact that gravity couples to the energy-momentum tensor, which in the massless case implies that each vertex contains factors of momentum. Consider a diagram $\mathcal{M}_{soft}$ formed from a lower order diagram $\mathcal{M}_0$ by adjoining a soft, on-shell virtual graviton to two external particles with momenta p_i, p_j:

$$\begin{aligned}
\mathcal{M}_{soft} &= \int \frac{\mathrm{d}^4k}{(2\pi)^4} \frac{i}{(p_i-k)^2-m_i^2} \tau^{\mu\nu}(p_i, p_i-k) \frac{iP_{\mu\nu,\rho\sigma}}{k^2} \frac{i}{(p_j+k)^2-m_j^2} \tau^{\rho\sigma}(p_j, p_j+k) \mathcal{M}_0 \\
&= \int \frac{\mathrm{d}^4k}{(2\pi)^4} \frac{i}{(p_i-k)^2-m_i^2} \frac{-i\kappa\left(p_i^\mu (p_i-k)^\nu + p_i^\nu (p_i-k)^\mu + p_i\cdot k\eta^{\mu\nu}\right)}{2} \frac{iP_{\mu\nu,\rho\sigma}}{k^2} \\
&\quad \cdot \frac{i}{(p_j+k)^2-m_j^2} \frac{-i\kappa\left(p_j^\rho (p_j+k)^\sigma + p_j^\rho (p_j+k)^\sigma - p_j\cdot k\eta^{\rho\sigma}\right)}{2} \mathcal{M}_0
\end{aligned} \tag{4.19}$$

In the region of soft k,

$$\begin{aligned}
\mathcal{M}_{soft} &\approx i\kappa^2 \int \frac{\mathrm{d}^4k}{(2\pi)^4} \frac{p_i^\mu p_i^\nu}{-2p_i\cdot k} \frac{P_{\mu\nu,\rho\sigma}}{k^2} \frac{p_j^\rho p_j^\sigma}{2p_j\cdot k} \mathcal{M}_0 \\
&= -i\kappa^2 \int \frac{\mathrm{d}^4k}{(2\pi)^4} \frac{(p_i\cdot p_j)^2 - \frac{m_i^2 m_j^2}{2}}{(2p_i\cdot k)\, k^2\, (2p_j\cdot k)} \mathcal{M}_0
\end{aligned} \tag{4.20}$$

If a collinear divergence is also to be present, then at least one of the m_i must be zero, and

$$\mathcal{M}_{soft} \approx -i\kappa^2 \int \frac{\mathrm{d}^4k}{(2\pi)^4} \frac{(p_i\cdot p_j)^2}{(2p_i\cdot k)\, k^2\, (2p_j\cdot k)} \mathcal{M}_0 \tag{4.21}$$

The integral over k_0 leaves a residue from the pole in k^2

$$\mathcal{M}_{soft} \approx \frac{\kappa^2}{2} \int \frac{\mathrm{d}^3k}{(2\pi)^3} \frac{(p_i\cdot p_j)^2}{2\left|\vec{k}\right|^3 \left(2p_i\cdot\hat{k}\right)\left(2p_j\cdot\hat{k}\right)} \mathcal{M}_0 \tag{4.22}$$

Comparing the similar integral (2.22), one sees these contain an IR-singular term of the form

$$\mathcal{M}_{soft} \sim \pi\frac{\kappa^2}{8} p_i\cdot p_j \log m_i^2 \log\lambda^2 \mathcal{M}_0 \tag{4.23}$$

for each of the m_i equal to zero. But each p_i will be joined by the soft photon to each other p_j in some diagram, so summing over all diagrams gives

$$\begin{aligned}
\mathcal{M}_{soft,total} &\sim \pi\frac{\kappa^2}{8} p_i\cdot \sum_{j\neq i} p_j \log m_i^2 \log\lambda^2 \mathcal{M}_0 \\
&= \pi\frac{\kappa^2}{8} p_i^2 \log m_i^2 \log\lambda^2 \mathcal{M}_0 \\
&= \pi\frac{\kappa^2}{8} m_i^2 \log m_i^2 \log\lambda^2 \mathcal{M}_0
\end{aligned} \tag{4.24}$$

As a result of this, the $\log m_i^2$ singularity occurs in the combination $m_i^2 \log m_i^2$, which goes to zero smoothly with m_i. Note that each term has an additional factor of $p_i\cdot p_j$ compared to the QED

case, originating in the momentum in the matter-graviton vertex, and it is these additional factors which are responsible for quelling the collinear divergences. It is shown in (4.90) below that the contribution from the soft real gravitons to the bremsstrahlung cross section also has the form shown in (4.24), so that when the contributions from all diagrams are added, the corresponding collinear divergences vanish.

Weinberg [19] considers only soft collinear gravitons, but there are no further collinear divergences from hard collinear gravitons either, also for the reason that gravity couples to momentum. Collinear divergences occur whenever an on-shell virtual graviton becomes collinear with an external massless particle to which it is coupled. Since gravity couples to energy-momentum, any such virtual graviton line occurring in any diagram is multiplied by the four-momentum of the massless particle to which it attaches. For example, in fig. 4.2, every term in the numerator has two factors of the momentum $p_2 + k$, one from each of the graviton-scalar vertices. These factors remove the troublesome singularity.

To see this, consider that when evaluating the diagram, each of these factors of $p_2 + k$ is either contracted with one of the momenta p_2, k, or q, either in the diagram itself or in the tensor reduction process. In either case the integrand reduces to a two-point form free from collinear divergences. For example, consider the integral

$$\begin{aligned} I &\equiv \int \frac{(k+p_2)\cdot p_2}{(k+p_2)^2 (q-k)^2 k^2} \mathrm{d}^4 k \\ &= \int \frac{k\cdot p_2 + p_2^2}{(k+p_2)^2 (q-k)^2 k^2} \mathrm{d}^4 k \\ &= \int \frac{\frac{1}{2}\left((k+p_2)^2 + p_2^2 - k^2\right)}{(k+p_2)^2 (q-k)^2 k^2} \mathrm{d}^4 k \end{aligned} \tag{4.25}$$

But in the massless case $p_2^2 = 0$, and the remaining two terms in the numerator each cancel one of the propagators, leaving the IR-convergent integral:

$$I = -\frac{1}{2} \int \frac{\mathrm{d}^4 k}{(q-k)^2 k^2} + \text{analytic terms} \tag{4.26}$$

In the massive case, $p_2^2 = m^2 \neq 0$, the integral

$$\frac{1}{2} \int \frac{m^2}{(k+p_2)^2 (q-k)^2 k^2} \mathrm{d}^4 k \tag{4.27}$$

containing collinear divergences, would remain. Similarly, the integral

$$I \equiv \int \frac{(k+p_2)\cdot k}{(k+p_2)^2 (q-k)^2 k^2} \tag{4.28}$$

is equal to

$$I = \int \frac{\frac{1}{2}\left((k+p_2)^2 + k^2 - p_2^2\right)}{(k+p_2)^2 (q-k)^2 k^2} = \frac{1}{2}\int \frac{1}{(q-k)^2 k^2} + \text{analytic terms} \tag{4.29}$$

Finally, the integral

$$I \equiv \int \frac{(k+p_2)\cdot q}{(k+p_2)^2 (q-k)^2 k^2} \tag{4.30}$$

is equal to

$$I = \int \frac{\frac{1}{2}\left(k^2 - (q-k)^2 + (q+p_2)^2 - p_2^2\right)}{(k+p_2)^2 (q-k)^2 k^2} \tag{4.31}$$

$(q+p_2)^2 = p_4^2 = 0$, and the result for this integral (4.30) is

$$I = 0 + \text{analytic terms} \tag{4.32}$$

As a result of these cancellations, the diagram of fig. 4.2 is completely infra-red convergent.

Similar cancellations can be seen in other diagrams. For instance, the box diagram fig. (4.5), in the case that both scattering particles were massless, would contain an additional massless propagator, but would also contains two additional graviton-scalar vertices, and these vertex factors cancel the additional collinear divergences produced by the additional propagator in exactly the same way. Indeed, anytime an additional massless propagator appears, an additional vertex carrying factors of momentum appears with it. The only collinear divergences which do survive in individual diagrams are those that occur together with soft divergences, and these are exactly the ones that were shown to cancel between diagrams in total cross sections for on-shell processes by [19]. Thus, after the inclusion of final-state soft bremsstrahlung, the scattering cross section will be free of all infra-red divergences.

4.3 Elastic Cross Section

Turning to the problem of the scattering of two scalar particles of mass m and M respectively, the Feynman diagrams which contribute to the scattering cross section to order κ^6 are those shown in figures 4.2 through 4.10, where the heavy solid lines represent a scalar of mass M, the thin solid lines a scalar of mass m, and the double wavy lines a graviton, as well as the "mirror images" of figs. 4.2, 4.3, 4.4, and 4.7, where the radiative corrections are on the side of the heavy scalar particle. The integrals in these diagrams are extremely complicated, even by the standards of quantum field theory, because gravity is a rank-two tensor and because it couples to the momentum of the matter field. Each graviton propagator is a tensor of rank four, and each vertex is a tensor of rank two per

graviton line, involving the momenta of all the lines entering it symmetrized appropriately. Each diagram contains several vertices and propagators, and as the tensor rank and number of lines in a diagram grows, the number of different terms in the diagram becomes enormous. Evaluation of the diagrams is therefore a considerable part of the total effort.

To accomplish this, the diagrams are evaluated largely by computer. All the scalar products are evaluated using the Mathematica [34] program FeynCalc [15] and the results simplified in Mathematica using the kinematic relations between on-shell external momenta: $p_1^2 = p_3^2 = M^2$, $p_2^2 = p_4^2 = m^2$, $p_1+p_2 = p_3+p_4$, $q \equiv p_1-p_3 = p_4-p_2$, $s \equiv (p_1+p_2)^2 = M^2+m^2+2p_1\cdot p_2$, $t \equiv q^2 = 2p_1\cdot q = -2p_2\cdot q$, $u \equiv (p_1-p_4)^2$, $s+t+u = 2M^2+2m^2$. The integrals are then evaluated by the methods of chapter 2 using FeynCalc and proprietary Mathematica programs written by the author for this purpose.

The elastic (non-bremsstrahlung) cross section is determined from the elastic matrix element by [23]

$$\mathrm{d}\sigma_{el} = (2\pi)^4 \delta(p_1+p_2-p_3+p_4) \frac{|\mathcal{M}|^2}{4\sqrt{(p_1\cdot p_2)^2 - M^2m^2}} \frac{\mathrm{d}^3p_3\mathrm{d}^3p_4}{(2\pi)^3 2E_3 (2\pi)^3 2E_4} \tag{4.33}$$

Eliminating the delta functions in the center-of-mass frame, this becomes

$$\mathrm{d}\sigma_{el} = \frac{|\mathcal{M}|^2}{64\pi^2} \frac{|\vec{p_3}|}{|\vec{p_1}|(E_1+E_2)^2} \mathrm{d}\Omega \tag{4.34}$$

Using $\mathrm{d}t = 2|\vec{p_1}||\vec{p_3}|\,\mathrm{d}\cos\theta$, this becomes

$$\mathrm{d}\sigma_{el} = \frac{|\mathcal{M}|^2}{64\pi} \frac{\mathrm{d}(-t)\,\mathrm{d}\phi}{\vec{p_1}^{\,2}(E_1+E_2)^2 2\pi} = \frac{|\mathcal{M}|^2}{16\pi} \frac{\mathrm{d}(-t)\,\mathrm{d}\phi}{\left(s^2-2s(M^2+m^2)+(M^2-m^2)^2\right)2\pi} \tag{4.35}$$

If the cross section is azimuthally invariant then in a frame where the center of mass is moving either parallel or perpendicular to the relative motion of the two particles,

$$\begin{aligned}
\left(\frac{d\sigma}{d(-t)}\right)_{el} &= \frac{|\mathcal{M}_0+\mathcal{M}_1+...|^2}{16\pi\left(s^2-2s(M^2+m^2)+(M^2-m^2)^2\right)} = \left(\frac{d\sigma}{d(-t)}\right)_0 + \left(\frac{d\sigma}{d(-t)}\right)_1 + \dots \\
\left(\frac{d\sigma}{d(-t)}\right)_0 &= \frac{|\mathcal{M}_0|^2}{16\pi\left(s^2-2s(M^2+m^2)+(M^2-m^2)^2\right)} \\
\left(\frac{d\sigma}{d(-t)}\right)_1 &= \frac{\mathcal{M}_0\mathcal{M}_1^* + \mathcal{M}_0^*\mathcal{M}_1}{16\pi\left(s^2-2s(M^2+m^2)+(M^2-m^2)^2\right)} \\
&= \frac{\mathrm{Re}\left[\mathcal{M}_0\mathcal{M}_1^*\right]}{8\pi\left(s^2-2s(M^2+m^2)+(M^2-m^2)^2\right)}
\end{aligned} \tag{4.36}$$

The contributions to the elastic matrix element from the individual diagrams are given below in terms of the scalar integrals I, J, and K listed in chapter 2. The results are first given for arbitrary

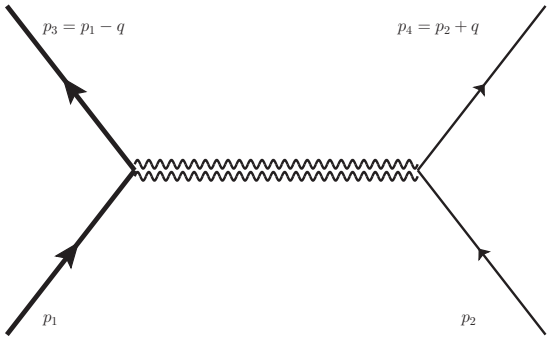

Figure 4.1. Lowest order gravitational scalar-scalar scattering.

values of m and M and then examined in various limits. Since the results for the non-relativistic limit have previously been computed [6, 7], these are compared to provide a check on the calculations. Finally, results are given for the massless case $m = 0$ (or for m infinitesimal to regulate the collinear divergences).

4.3.1 Lowest Order

The lowest order matrix element is given by the tree diagram fig. 4.1:

$$\begin{aligned} -i\mathcal{M}_0 &= \tau_1^{\kappa\lambda}\left(p_1, p_1 - q, M\right)\frac{iP_{\kappa\lambda,\mu\nu}}{q^2}\tau^{\mu\nu}\left(p_2, p_2 + q, m\right) \\ &= -i\kappa^2\left(\frac{m^4 - 2sm^2 + \left(s - M^2\right)^2}{4t} + \frac{s - M^2 - m^2}{4}\right) \end{aligned} \tag{4.37}$$

In the non-relativistic limit where $s = (m + M)^2$, $t \ll m^2, M^2$, this becomes

$$\mathcal{M}_0 \approx \frac{\kappa^2 m^2 M^2}{2t} \tag{4.38}$$

which agrees with [7] while in the case $m = 0$ it becomes

$$\mathcal{M}_0 = \frac{\kappa^2\left(s - M^2\right)\left(s - M^2 + t\right)}{4t} \tag{4.39}$$

(4.39) results in the lowest-order cross section

$$\left(\frac{d\sigma}{d\left(-t\right)}\right)_0 = \kappa^4\frac{\left(s - M^2 + t\right)^2}{256\pi t^2} \tag{4.40}$$

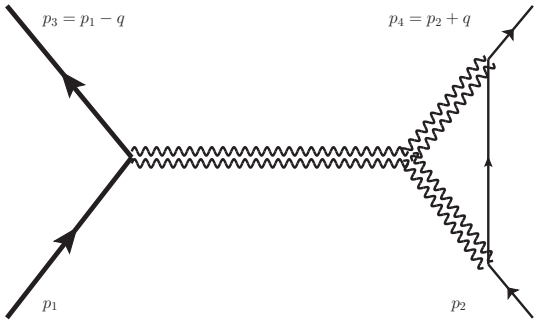

Figure 4.2. Gravitational vertex diagram.

4.3.2 Vertex Corrections

Those matrix elements which produce corrections to the vertex part fall into three categories. One, fig. 4.4, has a structure familiar from QED. The other two, figs. 4.2 and 4.3, are new to gravity. For each of these, there is also a mirror-image diagram correcting the heavy scalar vertex. The results are:

Fig. 4.2:

$$\begin{aligned}
-i\mathcal{M}_1 &= \int \tau_1^{\kappa\lambda}\left(p_1, p_1-q, M\right)\frac{iP_{\kappa\lambda,\mu\nu}}{q^2} \\
&\quad \cdot\frac{\tau_3^{\mu\nu,\rho\sigma,\epsilon\zeta}\left(k,-q\right) iP_{\epsilon\zeta,\alpha\beta}\tau^{\alpha\beta}\left(p_2+q, p_2-k, m\right) i\tau^{\gamma\delta}\left(p_2-k, p_2, m\right) iP_{\gamma\delta,\rho\sigma}}{\left(k^2-\lambda^2\right)\left(\left(k+q\right)^2-\lambda^2\right)\left(\left(p_2-k\right)^2-m^2\right)}\frac{\mathrm{d}^4k}{\left(2\pi\right)^4} \\
&= \kappa^4\left(\frac{9m^6\left(s+m^2-M^2\right)^2}{4\left(t-4m^2\right)^2}+\frac{13m^8+20m^6s-14m^6M^2+m^4\left(s-M^2\right)^2}{8\left(t-4m^2\right)}\right. \\
&\quad \left.+\frac{2m^6+3m^4\left(s-M^2\right)-m^2\left(s-M^2\right)\left(s-M^2+t\right)}{8}\right)J^{(1)}\left(p_2,-q\right) \\
&\quad +\kappa^4\left(\frac{9m^4\left(s+m^2-M^2\right)^2}{8\left(t-4m^2\right)^2}+\frac{5m^6-4m^4M^2+7m^4s-m^2\left(s-M^2\right)^2}{8\left(t-4m^2\right)}\right. \\
&\quad \left.+\frac{9m^4-8m^2M^2-6m^2s-7m^2t+2t^2+4M^2t}{48}\right)I^{(1)}\left(q\right)
\end{aligned} \tag{4.41}$$

In the nonrelativistic limit, this becomes

$$-i\mathcal{M}_1 \approx -\frac{\kappa^4m^4M^2}{4}J^{(1)}\left(p_2,q\right)+\frac{\kappa^4m^2M^2}{48}I^{(1)}\left(q\right) \tag{4.42}$$

which agrees with [7] while in the case $m=0$ it becomes

$$-i\mathcal{M}_1 = \kappa^4\frac{t\left(2M^2+t\right)}{24}I^{(1)}\left(q\right) \tag{4.43}$$

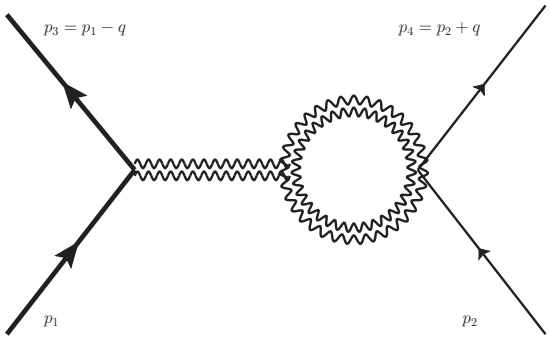

Figure 4.3. Gravitational vertex diagram.

The result for the mirror-image diagram is given by interchanging m and M in (4.41). In the nonrelativistic limit, this becomes

$$\begin{aligned} -i\mathcal{M}_1 &= \int \frac{iP_{\epsilon\zeta,\alpha\beta}\tau^{\alpha\beta}\left(p_1-q,p_1-k,M\right)i\tau^{\gamma\delta}\left(p_1-k,p_1,M\right)iP_{\gamma\delta,\rho\sigma}\tau_3^{\rho\sigma,\epsilon\zeta,\kappa\lambda}\left(k,q\right)}{\left(k^2-\lambda^2\right)\left(\left(p_1-k\right)^2-M^2\right)\left(\left(k-q\right)^2-\lambda^2\right)} \\ &\quad \cdot\frac{iP_{\kappa\lambda,\mu\nu}}{q^2}\tau^{\mu\nu}\left(p_2,p_2+q,m\right)\frac{\mathrm{d}^4k}{\left(2\pi\right)^4} \\ &\approx -\frac{\kappa^4M^4m^2}{4}J^{(1)}\left(p_1,q\right)+\frac{\kappa^4M^2m^2}{48}I^{(1)}\left(q\right) \end{aligned} \tag{4.44}$$

In the case $m = 0$ it becomes:

$$\begin{aligned} -i\mathcal{M}_1 &= \kappa^4\left(\frac{9M^6\left(s+M^2\right)^2}{4\left(t-4M^2\right)^2}+\frac{13M^8+20M^6s+M^4s^2}{8\left(t-4M^2\right)}\right. \\ &\quad \left.+\frac{2M^6+3M^4s-M^2s\left(s+t\right)}{8}\right)J^{(1)}\left(p_1,q\right) \\ &\quad +\kappa^4\left(\frac{9M^4\left(s+M^2\right)^2}{8\left(t-4M^2\right)^2}+\frac{5M^6+7M^4s-M^2s^2}{8\left(t-4M^2\right)}\right. \\ &\quad \left.+\frac{9M^4-6M^2s-7M^2t+2t^2}{48}\right)I^{(1)}\left(q\right) \end{aligned} \tag{4.45}$$

Fig. 4.3:

$$\begin{aligned} -i\mathcal{M}_1 &= \frac{1}{2}\int\tau_1^{\kappa\lambda}\left(p_1,p_1-q,M\right)\frac{iP_{\kappa\lambda,\mu\nu}}{q^2} \\ &\quad \cdot\frac{\tau_3^{\mu\nu,\rho\sigma,\epsilon\zeta}\left(-k,-q\right)iP_{\epsilon\zeta,\alpha\beta}\tau_2^{\alpha\beta,\gamma\delta}\left(p_2+q,p_2,m\right)iP_{\gamma\delta,\rho\sigma}}{\left(k^2-\lambda^2\right)\left(\left(k-q\right)^2-\lambda^2\right)}\frac{\mathrm{d}^4k}{\left(2\pi\right)^4} \\ &= \kappa^4\frac{13m^2\left(2M^2+t\right)}{48}I^{(1)}\left(q\right) \end{aligned} \tag{4.46}$$

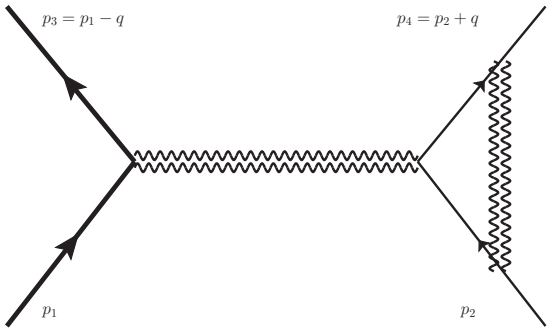

Figure 4.4. Gravitational vertex diagram.

In the non-relativistic case this becomes

$$-i\mathcal{M}_1 \approx \kappa^4 \frac{13m^2M^2}{24} I^{(1)}(q) \tag{4.47}$$

which agrees with [7]. In the case $m = 0$ it becomes

$$-i\mathcal{M}_1 = 0 \tag{4.48}$$

The mirror-image diagram in the nonrelativistic case is also

$$\begin{aligned} -i\mathcal{M}_1 &= \frac{1}{2}\int \frac{iP_{\epsilon\zeta,\alpha\beta}\tau_2^{\alpha\beta,\gamma\delta}(p_1-q,p_1,M)\, iP_{\gamma\delta,\rho\sigma}\tau_3^{\kappa\lambda,\epsilon\zeta,\rho\sigma}(k,q)}{(k^2-\lambda^2)\left((k-q)^2-\lambda^2\right)} \frac{iP_{\kappa\lambda,\mu\nu}}{q^2}\tau^{\mu\nu}(p_2,p_2+q,m)\frac{\mathrm{d}^4k}{(2\pi)^4} \\ &\approx \kappa^4\frac{13m^2M^2}{24}I^{(1)}(q) \end{aligned} \tag{4.49}$$

and in the case $m = 0$ is

$$-i\mathcal{M}_1 = \kappa^4\frac{13M^2t}{48}I^{(1)}(q) \tag{4.50}$$

Fig. 4.4:

$$\begin{aligned} -i\mathcal{M}_1 &= \int \tau_1^{\kappa\lambda}(p_1,p_1-q,M)\frac{iP_{\kappa\lambda,\mu\nu}}{q^2}\frac{\tau_1^{\mu\nu}(p_2+q-k,p_2-k,m)\, i\tau^{\gamma\delta}(p_2-k,p_2,m)}{\left((p_2+q-k)^2-m^2\right)} \\ &\quad \cdot\frac{iP_{\gamma\delta,\alpha\beta}\tau_1^{\alpha\beta}(p_2+q,p_2+q-k,m)\, i}{(k^2-\lambda^2)\left((p_2-k)^2-m^2\right)}\frac{\mathrm{d}^4k}{(2\pi)^4} \\ &= \kappa^4\frac{\left(2m^4-4m^2t+t^2\right)\left(\left(m^2-s\right)\left(m^2-s-t\right)+M^4-M^2(2s+t)\right)}{16t}J^{(2)}(p_2,-p_2-q) \\ &\quad +\kappa^4\left(-\frac{m^2\left(-2M^2\left(m^2+9s\right)+9\left(m^2-s\right)^2+9M^4\right)}{96t}\right. \end{aligned}$$

$$+\frac{14m^4+6m^2\left(M^2-3s+t\right)+9\left(s-M^2\right)^2+9st+t^2-7M^2t}{48}$$
$$+\frac{3m^2\left(m^2-M^2+s\right)^2}{32\left(t-4m^2\right)}\Bigg)I^{(2)}\left(p_2,q+p_2\right) \tag{4.51}$$

Just like the analogous diagram in QED, this diagram has only a threshold singularity at $q^2=4m^2$. It therefore reduces to analytic terms when expanded about $q^2=0$ in the non-relativistic case, while in the case $m=0$ it becomes

$$\begin{aligned}-i\mathcal{M}_1 &= \kappa^4\frac{\left(M^2-s\right)\left(M^2-s-t\right)t}{16}J^{(2)}\left(p_2,-p_2-q\right)\\ &\quad+\kappa^4\frac{9\left(s-M^2\right)^2+7tM^2+9st+t^2}{48}I^{(1)}\left(q\right)\end{aligned} \tag{4.52}$$

The mirror-image diagram also reduces to analytic terms in the nonrelativistic case and in the case $m=0$ is

$$\begin{aligned}-i\mathcal{M}_1 &= \int\frac{\tau_1^{\mu\nu}\left(p_1-q-k,p_1-k,M\right)i\tau^{\gamma\delta}\left(p_1-k,p_1,M\right)iP_{\gamma\delta,\alpha\beta}\tau_1^{\alpha\beta}\left(p_1-q,p_1-q-k,M\right)i}{\left(\left(p_1-q-k\right)^2-M^2\right)\left(k^2-\lambda^2\right)\left(\left(p_1-k\right)^2-M^2\right)}\\ &\quad\cdot\frac{iP_{\mu\nu,\kappa\lambda}}{q^2}\tau_1^{\kappa\lambda}\left(p_2,p_2+q,m\right)\frac{\mathrm{d}^4k}{\left(2\pi\right)^4}\\ &= \kappa^4\frac{\left(2M^4-4M^2t+t^2\right)\left(s-M^2\right)\left(s-M^2+t\right)}{16t}J^{(2)}\left(p_1,q-p_1\right)\\ &\quad+\kappa^4\Bigg(\frac{3M^2\left(s+M^2\right)^2}{32\left(t-4M^2\right)}-\frac{3M^2\left(s-M^2\right)^2}{32t}\\ &\quad+\frac{14M^4-18M^2s+9s^2+9st+6M^2t+t^2}{48}\Bigg)I^{(2)}\left(p_1,p_1-q\right)\end{aligned} \tag{4.53}$$

4.3.3 Box Diagrams

The matrix elements for the box and crossed-box diagrams, figs. 4.5 and 4.6, are:

Fig. 4.5 (box):

$$\begin{aligned}-i\mathcal{M}_1 &= \int\frac{\tau^{\alpha\beta}\left(p_1-q,p_1-k,M\right)i\tau_1^{\gamma\delta}\left(p_1-k,p_1,M\right)iP_{\alpha\beta,\epsilon\zeta}}{\left(\left(p_1-k\right)^2-M^2\right)\left(k^2-\lambda^2\right)}\\ &\quad\cdot\frac{iP_{\gamma\delta,\rho\sigma}\tau_1^{\epsilon\zeta}\left(p_2+q,p_2+k,m\right)i\tau_1^{\rho\sigma}\left(p_2+k,p_2,m\right)}{\left(\left(k-q\right)^2-\lambda^2\right)\left(\left(p_2+k\right)^2-m^2\right)}\frac{\mathrm{d}^4k}{\left(2\pi\right)^4}\\ &= \kappa^4\frac{\left(\left(s-M^2-m^2\right)^2-2M^2m^2\right)^2}{16}K\left(p_1,p_2,q\right)\\ &\quad+\kappa^4\Bigg(\frac{M^2\left(s-m^2-M^2\right)^2\left(s-m^2+M^2\right)}{4\left(t-4M^2\right)}\end{aligned}$$

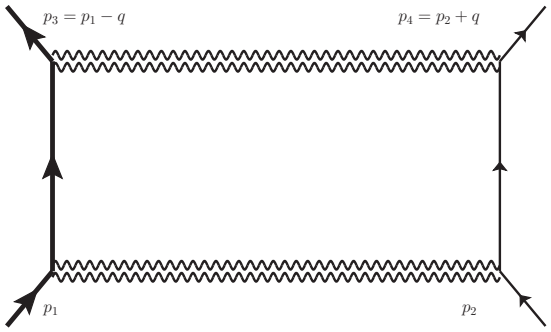

Figure 4.5. Box diagram.

$$
\begin{aligned}
&-\frac{\left(s-M^2-m^2\right)^3}{16}+\frac{M^2\left(s-M^2-m^2\right)\left(s-M^2+m^2\right)}{8}\Bigg) J^{(1)}\left(p_1,q\right)\\
&+\kappa^4\Bigg(\frac{m^2\left(s-M^2-m^2\right)^2\left(s-M^2+m^2\right)}{4\left(t-4m^2\right)}\\
&-\frac{\left(s-M^2-m^2\right)^3}{16}+\frac{m^2\left(s-M^2-m^2\right)\left(s-m^2+M^2\right)}{8}\Bigg) J^{(1)}\left(p_2,q\right)\\
&+\kappa^4\frac{\left(\left(s-m^2-M^2\right)^2-2M^2m^2\right)\left(s-m^2-M^2\right)}{8}J^{(2)}\left(p_1,p_2\right)\\
&+\kappa^4\left(s-m^2-M^2\right)^2\left(\frac{1}{4}+\frac{\left(s+m^2-M^2\right)}{8\left(t-4m^2\right)}+\frac{\left(s-m^2+M^2\right)}{8\left(t-4M^2\right)}\right)I^{(1)}\left(q\right)\\
&+\kappa^4\frac{\left(s-m^2-M^2\right)^2}{16}I^{(2)}\left(p_1,p_2\right) \qquad (4.54)
\end{aligned}
$$

In the non-relativistic case this becomes

$$
\begin{aligned}
-i\mathcal{M}_1 \;\approx\;& \kappa^4\frac{m^4M^4}{4}K\left(p_1,p_2,q\right)-\kappa^4\frac{m^3M^3}{2}J^{(1)}\left(p_1,q\right)-\kappa^4\frac{m^3M^3}{2}J^{(1)}\left(p_2,q\right)\\
&+\kappa^4\frac{m^3M^3}{2}J^{(2)}\left(p_1,p_2\right)+\kappa^4\frac{m^2M^2}{4}I^{(2)}\left(p_1,p_2\right)-\kappa^4\frac{mM\left(m-M\right)^2}{4}I^{(1)}\left(q\right) \qquad (4.55)
\end{aligned}
$$

while in the case $m = 0$ it becomes

$$
\begin{aligned}
-i\mathcal{M}_1 \;=\;& \kappa^4\frac{\left(s-M^2\right)^3}{16}\Big(\left(s-M^2\right)K\left(p_1,p_2,q\right)-J^{(1)}\left(p_2,q\right)+2J^{(2)}\left(p_1,p_2\right)\Big)\\
&-\kappa^4\frac{\left(s-M^2\right)^3}{16}\left(1+\frac{2M^2\left(2\left(s-M^2\right)+t\right)}{\left(s-M^2\right)\left(4M^2-t\right)}\right)J^{(1)}\left(p_1,q\right)+\kappa^4\frac{\left(s-M^2\right)^2}{16}I^{(2)}\left(p_1,p_2\right)\\
&+\kappa^4\frac{\left(s-M^2\right)^2\left(\left(2M^2-t\right)\left(s-M^2+t\right)+M^2t\right)}{4\left(4M^2-t\right)t}I^{(1)}\left(q\right) \qquad (4.56)
\end{aligned}
$$

(For later convenience the collinear divergent terms have been grouped together in the first line.)

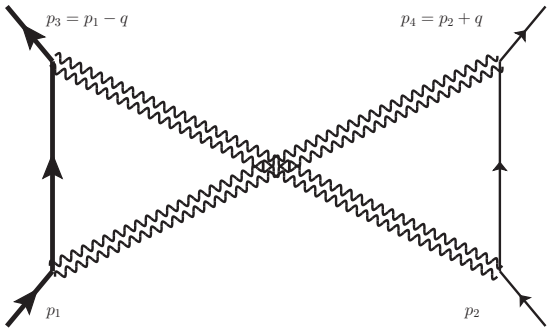

Figure 4.6. Cross box diagram.

Fig. 4.6: The cross box diagram is given by interchanging p_2 and $-p_4$. In the non-relativistic case this becomes

$$\begin{aligned}
-i\mathcal{M}_1 &= \int \frac{\tau_1^{\alpha\beta}\left(p_1-q,p_1-k,M\right) i\tau_1^{\gamma\delta}\left(p_1-k,p_1,M\right) iP_{\gamma\delta,\epsilon\zeta}}{\left(\left(p_1-k\right)^2-M^2\right)\left(k^2-\lambda^2\right)} \\
&\quad \cdot\frac{iP_{\alpha\beta,\rho\sigma}\tau_1^{\epsilon\zeta}\left(p_2+q,p_2+q-k,m\right) i\tau_1^{\rho\sigma}\left(p_2+q-k,p_2,m\right)}{\left(\left(k-q\right)^2-\lambda^2\right)\left(\left(p_2+q-k\right)^2-m^2\right)}\frac{\mathrm{d}^4k}{\left(2\pi\right)^4} \\
&\approx \kappa^4\frac{m^3M^3}{2}J^{(1)}\left(p_1,q\right)+\kappa^4\frac{m^3M^3}{2}J^{(1)}\left(p_2,q\right)-\kappa^4\frac{m^3M^3}{2}J^{(2)}\left(p_1,p_2\right)+\frac{m^4M^3}{4}K \\
&\quad +\kappa^4\frac{mM}{4}I^{(1)}\left(q\right)\left(m+M\right)^2+\kappa^4\frac{m^2M^2}{4}I^{(2)}\left(p_1,p_2\right) \qquad (4.57)
\end{aligned}$$

while in the case $m = 0$ it becomes

$$\begin{aligned}
-i\mathcal{M}_1 &= \kappa^4\frac{\left(s-M^2+t\right)^3}{16} \\
&\quad \left(J^{(1)}\left(-p_2-q,q\right)-2J^{(2)}\left(p_1,-p_2-q\right)+\left(s-M^2+t\right)K\left(p_1,-p_2-q,q\right)\right) \\
&\quad +\kappa^4\frac{\left(s-M^2+t\right)^3}{16}\left(1+\frac{2M^2\left(2\left(s-M^2\right)+t\right)}{\left(s-M^2+t\right)\left(4M^2-t\right)}\right)J^{(1)}\left(p_1,q\right) \\
&\quad +\kappa^4\frac{\left(s-M^2+t\right)^2}{16}I^{(2)}\left(p_1,-p_2-q\right) \\
&\quad -\kappa^4\frac{\left(s-M^2+t\right)^2\left(\left(2M^2-t\right)\left(s-M^2\right)-M^2t\right)}{4\left(4M^2-t\right)t}I^{(1)}\left(q\right) \qquad (4.58)
\end{aligned}$$

The sum of the box and cross diagrams agrees in the non-relativistic limit agrees with [7].

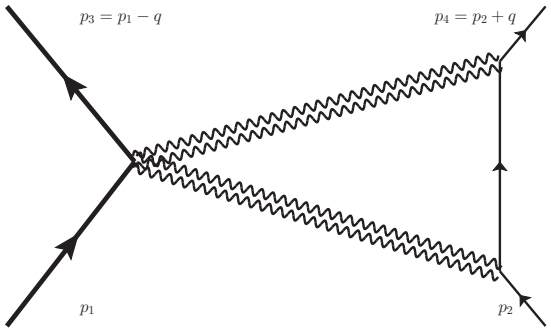

Figure 4.7. Triangle diagram.

4.3.4 Triangle Diagrams

There are two non-vertex triangle diagrams. One, represented by fig. 4.7, has the radiative corrections on the light scalar side and the other, mirror-image, diagram has them on the heavy scalar side.

Fig. 4.7:

$$\begin{aligned}
-i\mathcal{M}_1 &= \int \tau_2^{\rho\sigma,\epsilon\zeta}\left(p_1, p_1-q, M\right)\frac{iP_{\epsilon\zeta,\alpha\beta}\tau_1^{\alpha\beta}\left(p_2+q, p_2+k, m\right)i\tau_1^{\gamma\delta}\left(p_2+k, p_2, m\right)iP_{\gamma\delta,\rho\sigma}}{\left((k-q)^2-\lambda^2\right)\left(\left(p_2+k\right)^2-m^2\right)\left(k^2-\lambda^2\right)}\frac{\mathrm{d}^4k}{\left(2\pi\right)^4} \\
&= \kappa^4\left(\frac{m^2M^2t+m^4\left(14s+2t-12M^2\right)+4m^6}{8}\right. \\
&\quad \left.+\frac{15m^8+m^6\left(-22M^2+26s\right)+7m^4\left(s-M^2\right)^2}{4\left(t-4m^2\right)}+\frac{3m^6\left(m^2+s-M^2\right)^2}{\left(t-4m^2\right)^2}\right)J^{(1)}\left(p_2,q\right) \\
&\quad +\kappa^4\left(\frac{2m^4+m^2\left(32s-36M^2+6t\right)-6\left(s-M^2\right)^2-6st+8M^2t-t^2}{32}\right. \\
&\quad \left.+\frac{3m^4\left(m^2+s-M^2\right)^2}{2\left(t-4m^2\right)^2}+\frac{13m^6-18M^2m^4+22m^4s+5m^2\left(s-M^2\right)^2}{8\left(t-4m^2\right)}\right)I^{(1)}\left(q\right) \quad (4.59)
\end{aligned}$$

In the nonrelativistic case this becomes

$$-i\mathcal{M}_1 \approx -\kappa^4M^2m^4J^{(1)}\left(p_2,q\right)-\frac{5}{4}\kappa^4m^2M^2I^{(1)}\left(q\right) \quad (4.60)$$

which agrees with [7] while in the case $m=0$ it becomes

$$-i\mathcal{M}_1 = -\kappa^4\frac{6\left(s-M^2\right)^2+6st-8M^2t+t^2}{32}I^{(1)}\left(q\right) \quad (4.61)$$

The mirror-image diagram is given in the nonrelativistic case by

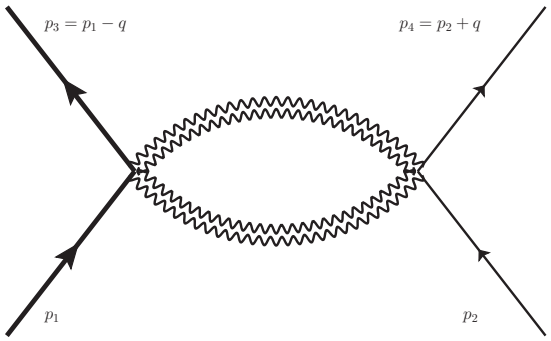

Figure 4.8. Double-seagull diagram.

$$\begin{aligned} -i\mathcal{M}_1 &= \int \frac{iP_{\epsilon\zeta,\alpha\beta}\tau_1^{\alpha\beta}\left(p_1-q,p_1-k,M\right)i\tau_1^{\gamma\delta}\left(p_1-k,p_1,M\right)iP_{\gamma\delta,\rho\sigma}}{\left(\left(p_1-k\right)^2-M^2\right)\left(\left(k-q\right)^2-\lambda^2\right)\left(k^2-\lambda^2\right)}\tau_2^{\rho\sigma,\epsilon\zeta}\left(p_2,p_2+q,m\right)\frac{\mathrm{d}^4k}{\left(2\pi\right)^4} \\ &\approx -\kappa^4 m^2 M^4 J^{(1)}\left(p_1,q\right)-\frac{5}{4}\kappa^4 M^2 m^2 I^{(1)}\left(q\right) \end{aligned} \tag{4.62}$$

and in the case $m = 0$ by

$$\begin{aligned} -i\mathcal{M}_1 &= \kappa^4\left(\frac{7M^4s+M^4t+2M^6}{4}+\frac{15M^8+26M^6s+7M^4s^2}{4\left(t-4M^2\right)}+\frac{3M^6\left(M^2+s\right)^2}{\left(t-4M^2\right)^2}\right)J^{(1)}\left(p_1,q\right) \\ &+\kappa^4\left(\frac{2M^4+M^2\left(32s+6t\right)-6s^2-6st-t^2}{32}\right. \\ &\left.+\frac{13M^6+22M^4s+5M^2s^2}{8\left(t-4M^2\right)}+\frac{3M^4\left(M^2+s\right)^2}{2\left(t-4M^2\right)^2}\right)I^{(1)}\left(q\right) \end{aligned} \tag{4.63}$$

4.3.5 Double Seagull

The double-seagull diagram is:

Fig. 4.8:

$$\begin{aligned} -i\mathcal{M}_1 &= \frac{1}{2}\int \frac{\tau_2^{\rho\sigma,\epsilon\zeta}\left(p_1,p_1-q,M\right)iP_{\epsilon\zeta,\alpha\beta}iP_{\gamma\delta,\rho\sigma}\tau_2^{\gamma\delta,\alpha\beta}\left(p_2,p_2+q,m\right)}{\left(k^2-\lambda^2\right)\left(\left(k-q\right)^2-\lambda^2\right)}\frac{\mathrm{d}^4k}{\left(2\pi\right)^4} \\ &= \frac{\kappa^4}{8}\left(4m^4+m^2\left(14M^2-8s-2t\right)+4\left(s-M^2\right)^2+\left(4s-2M^2+t\right)t\right)I^{(1)}\left(q\right) \end{aligned} \tag{4.64}$$

In the non-relativistic case this is

$$-i\mathcal{M}_1 \approx \kappa^4\frac{11}{4}m^2M^2I^{(1)}\left(q\right) \tag{4.65}$$

which agrees with [7] while in the case $m = 0$ it becomes

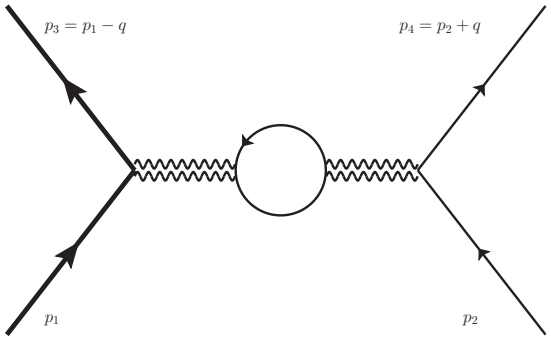

Figure 4.9. Scalar loop vacuum polarization.

$$-i\mathcal{M}_1 = \kappa^4 \left(\frac{\left(s - M^2\right)^2}{2} + \frac{\left(4s - 2M^2 + t\right) t}{8} \right) I^{(1)}(q) \tag{4.66}$$

4.3.6 Vacuum Polarization

There are two gravitational vacuum polarization diagrams figs. 4.9 and 4.10, one with a scalar loop and the other with a graviton loop. The results are:

Fig. 4.9 (scalar loop):

$$\begin{aligned} -i\mathcal{M}_1 &= \int \tau_1^{\kappa\lambda}(p_1, p_1 - q, M) \frac{iP_{\kappa\lambda,\alpha\beta}}{q^2} \frac{\tau^{\alpha\beta}(i)(i)\tau_1^{\gamma\delta}}{(k^2 - m^2)\left((k+q)^2 - m^2\right)} \\ &\quad \cdot \frac{iP_{\gamma\delta,\mu\nu}}{q^2} \tau_1^{\mu\nu}(p_2, p_2 + q, m) \frac{\mathrm{d}^4 k}{(2\pi)^4} \\ &= \kappa^4 \left(\frac{19m^4 + 16M^2m^2 + m^2(3t - 10s) + \left(s - M^2\right)^2 + st + M^2 t + t^2}{480} \right. \\ &\quad - \frac{3m^6 - M^2m^4 - 8m^4 s + 2m^2\left(s - M^2\right)^2}{120t} \\ &\quad \left. + \frac{3M^2m^6 + 2m^8 - 4m^6 s + 2m^4\left(s - M^2\right)^2}{60t^2} \right) I^{(0)}\left(q^2, m^2, m^2\right) \end{aligned} \tag{4.67}$$

Just like the analogous diagram in QED, this diagram has only a threshold singularity at $q^2 = 4m^2$. It therefore reduces to analytic corrections to the graviton propagator when expanded about $q^2 = 0$ in the non-relativistic case, while in the case $m = 0$ it becomes

$$-i\mathcal{M}_1 = \kappa^4 \frac{\left(s - M^2\right)^2 + \left(s + M^2\right) t + t^2}{480} I^{(1)}(q) \tag{4.68}$$

Fig. 4.10 (graviton loop):

$$\mathcal{M}_1 = \tau_1^{\kappa\lambda}(p_1, p_1 - q, M) \frac{iP_{\kappa\lambda,\alpha\beta}}{q^2} \Pi^{\alpha\beta,\gamma\delta}(q) \frac{iP_{\gamma\delta,\mu\nu}}{q^2} \tau^{\mu\nu}(p_2, p_2 + q, m)$$

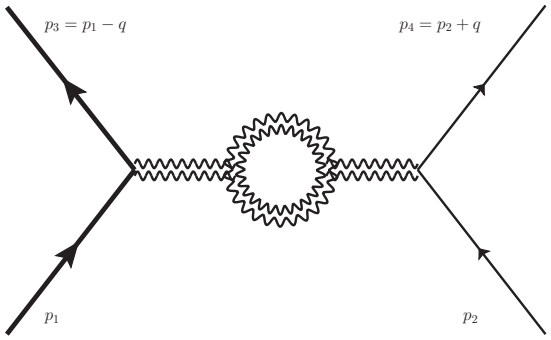

Figure 4.10. Graviton loop vacuum polarization diagram.

$$= \quad -\kappa^4 \frac{21\left(s-M^2\right)^2 + tM^2 + 11t^2 + 21st}{480} \frac{\log\left(-t\right)}{16\pi^2} \tag{4.69}$$

where the graviton polarization operator $\Pi^{\alpha\beta,\gamma\delta}\left(q\right)$ is taken from [7], and includes the effect of the diagram like 4.10 with ghost lines comprising the loop.

4.4 Bremsstrahlung Cross Section

To the elastic cross section (4.36) must be added the bremsstrahlung cross section, computed analogously to QED [19].

To the order considered, the bremsstrahlung amplitude is the lowest order elastic amplitude $\mathcal{M}_0$, (4.39), corrected to first order by the emission of only a single soft graviton either from one of the initial or from one of the final matter particles. (See fig.4.11) For simplicity, consider massless scalar particles. The correction for emission of a graviton with momentum k, from outgoing scalar line i with momentum p_i and mass m_i, consists of a scalar propagator with momentum $p_i + k$, a vertex factor, and a graviton wave function $\epsilon^*_{\mu\nu}$ multiplying the expression for $\mathcal{M}_0$:

$$\mathcal{M}_{br,out} = \frac{i}{\left(p_i+k\right)^2 - m_i^2} \frac{-i\kappa}{2} \left(p_i^\mu \left(p_i+k\right)^\nu + p_i^\nu \left(p_i+k\right)^\mu - p_i \cdot k \eta^{\mu\nu}\right) \epsilon^*_{\mu\nu} \mathcal{M}_0 \tag{4.70}$$

In the limit where k is soft this becomes

$$\mathcal{M}_{br,out} = \frac{\kappa}{2} \frac{p_i^\mu p_i^\nu \epsilon^*_{\mu\nu}}{p_i \cdot k} \mathcal{M}_0 \tag{4.71}$$

Similarly, the correction for emission of a graviton with momentum k from an incoming scalar line with momentum p_i is a scalar propagator with momentum $p_i - k$, a vertex factor, and a graviton

wave function $\epsilon^*_{\mu\nu}$ multiplying $\mathcal{M}_0$:

$$\mathcal{M}_{br,in} = \frac{i}{(p_i - k)^2 - m_1^2} \frac{-i\kappa}{2} \left(p_i^\mu (p_i - k)^\nu + p_i^\nu (p_i - k)^\mu + p_i \cdot k \eta^{\mu\nu} \right) \epsilon^*_{\mu\nu} \mathcal{M}_0 \tag{4.72}$$

which in the limit of soft k becomes

$$\mathcal{M}_{br,in} = -\frac{\kappa}{2} \frac{p_i^\mu p_i^\nu \epsilon^*_{\mu\nu}}{p_i \cdot k} \mathcal{M}_0 \tag{4.73}$$

The total bremsstrahlung amplitude is the sum of these over all external lines

$$\mathcal{M}_{br} = \frac{\kappa}{2} \sum_i s_i \frac{p_i^\mu p_i^\nu \cdot \epsilon^*_{\mu\nu}}{p_i \cdot k} \mathcal{M}_0 \tag{4.74}$$

with $s_i = -1$ for outgoing lines and $s_i = +1$ for incoming lines. As in the electromagnetic case, although the exact form of the correction multiplying $\mathcal{M}_0$ differs for matter particles of different spin, this limiting form for soft k, and all subsequent results, are valid for any spin [19]. For instance, the correction for emission of a graviton with momentum k, from outgoing an photon line i with momentum p_i and polarization vector $\epsilon^*_\alpha(p_i)$, consists of a photon propagator with momentum $p_i + k$, a vertex factor, and a graviton wave function $\epsilon^*_{\mu\nu}$ inserted between the photon polarization vector and the rest of the expression for $\mathcal{M}_0$:

$$\begin{aligned} \mathcal{M}_{br,out} &= \epsilon^*_\alpha (p_i + k) \frac{\eta^{\alpha\beta}}{(p_i + k)^2} \frac{\kappa}{2} \{ ((p_{i\mu} + k_\mu) p_{i\nu} + (p_{i\nu} + k_\nu) p_{i\mu}) \eta_{\delta\beta} + \eta_{\mu\nu} (p_{i\beta} + k_\beta) p_{i\delta} \\ &\quad - (p_{i\beta} + k_\beta) (p_{i\mu} \eta_{\nu\delta} + p_{i\nu} \eta_{\delta\mu}) - p_{i\delta} ((p_{i\mu} + k_\mu) \eta_{\nu\beta} + (p_{i\nu} + k_\nu) \eta_{\beta\mu}) \\ &\quad + k \cdot p_i (\eta_{\mu\delta} \eta_{\nu\beta} + \eta_{\mu\beta} \eta_{\nu\delta} - \eta_{\mu\nu} \eta_{\delta\beta}) \} \epsilon^{*\mu\nu}(k) M^\delta \end{aligned} \tag{4.75}$$

where M^δ is the matrix element without the photon polarization vector: $\mathcal{M}_0 \equiv \epsilon^*_\delta(p_i) M^\delta$. Using $\epsilon^*_\alpha(p_i) p_i^\alpha = 0$ and $p_\delta M^\delta = 0$, in the limit of soft k this becomes

$$\mathcal{M}_{br,out} = \frac{\kappa}{2} \frac{p_i^\mu p_i^\nu}{p_i \cdot k} \epsilon^*_{\mu\nu}(k) \epsilon^*_\delta(p_i) M^\delta = \frac{\kappa}{2} \frac{p_i^\mu p_i^\nu}{p_i \cdot k} \epsilon^*_{\mu\nu}(k) \mathcal{M}_0 \tag{4.76}$$

and similarly for emission from an incoming photon.

The cross section corresponding to this for the emission of a soft graviton with momentum in the range d^3k is:

$$\mathrm{d}\sigma_{br} = \frac{\kappa^2}{4} \sum_{i,j} s_i s_j \frac{p_i^\mu p_i^\nu \epsilon_{\mu\nu}}{(p_i \cdot k)} \frac{p_j^\rho p_j^\sigma \epsilon^*_{\rho\sigma}}{(p_j \cdot k)} \frac{\mathrm{d}^3k}{2k_0 (2\pi)^3} \mathrm{d}\sigma_0$$

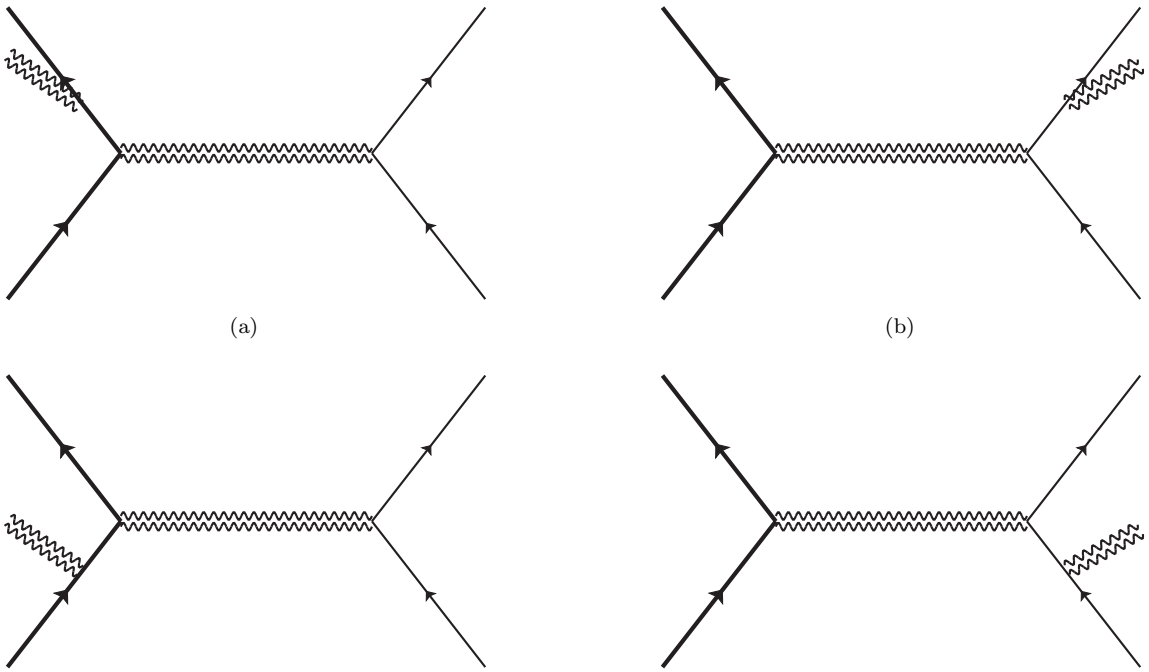

Figure 4.11. Gravitational bremsstrahlung diagrams.

$$= \frac{\kappa^2}{4}\left(\sum_i \frac{\left|p_i^\mu p_i^\nu \epsilon_{\mu\nu}\right|^2}{\left(p_i\cdot k\right)^2} + 2\sum_{i<j} s_i s_j \frac{\mathrm{Re}\left[p_i^\mu p_i^\nu \epsilon_{\mu\nu} p_j^\rho p_j^\sigma \epsilon_{\rho\sigma}^*\right]}{\left(p_i\cdot k\right)\left(p_j\cdot k\right)}\right)\frac{\mathrm{d}^3k}{2k_0\left(2\pi\right)^3}\mathrm{d}\sigma_0 \qquad (4.77)$$

This must be summed over all possible polarization and momentum states of the undetected soft graviton.

The sum over polarization states effectively converts the product of polarization tensors $\epsilon_{\mu\nu}\epsilon_{\rho\sigma}^*$ occurring in (4.77) into the unpolarized density matrix $P_{\mu\nu,\rho\sigma} = {}^1\!/_2\left(\eta_{\mu\sigma}\eta_{\nu\rho} + \eta_{\mu\rho}\eta_{\nu\sigma} - \eta_{\mu\nu}\eta_{\sigma\rho}\right)$. More precisely, since in an appropriate gauge the two physical polarization states of the graviton

$$\epsilon_{\mu\nu}^{(1)} = \begin{pmatrix} 0 & 0 & 0 & 0 \\ 0 & 1 & 0 & 0 \\ 0 & 0 & -1 & 0 \\ 0 & 0 & 0 & 0 \end{pmatrix}, \epsilon_{\mu\nu}^{(2)} = \begin{pmatrix} 0 & 0 & 0 & 0 \\ 0 & 0 & 1 & 0 \\ 0 & 1 & 0 & 0 \\ 0 & 0 & 0 & 0 \end{pmatrix} \qquad (4.78)$$

form a basis of the space of all traceless, symmetric, spacelike tensors orthogonal to $k^\mu = \left(k^0, 0, 0, k^0\right)$ [24], summing $\epsilon_{\mu\nu}\epsilon_{\rho\sigma}^*$ over these two states produces the projection onto that space:

$$\sum_n \epsilon_{\mu\nu}^{(n)}\epsilon_{\rho\sigma}^{(n)*} = \frac{1}{2}\left(\delta_{\mu\sigma}\delta_{\nu\rho} + \delta_{\mu\rho}\delta_{\nu\sigma} - \delta_{\mu\nu}\delta_{\sigma\rho}\right) \qquad (4.79)$$

where $\delta_{\mu\nu}$ is

$$\delta_{\mu\nu} \equiv -\eta_{\mu\nu} + \hat{t}_\mu \hat{t}_\nu - \hat{\vec{k}}_\mu \hat{\vec{k}}_\nu = \begin{pmatrix} 0 & 0 & 0 & 0 \\ 0 & 1 & 0 & 0 \\ 0 & 0 & 1 & 0 \\ 0 & 0 & 0 & 0 \end{pmatrix} \tag{4.80}$$

However, by gravitational gauge invariance, on can add to $\delta_{\mu\nu}$ an arbitrary multiple of k_μ without changing the cross section (4.77),

$$\delta_{\mu\nu} \to \delta'_{\mu\nu} \equiv \delta_{\mu\nu} + k_\mu \chi_\nu + k_\nu \chi_\mu \tag{4.81}$$

Choosing $\chi_\mu = \frac{1}{2}\left(-1/k_0, 0, 0, 1/k_0\right)$ one obtains

$$\delta'_{\mu\nu} = -\eta_{\mu\nu} = \begin{pmatrix} -1 & 0 & 0 & 0 \\ 0 & 1 & 0 & 0 \\ 0 & 0 & 1 & 0 \\ 0 & 0 & 0 & 1 \end{pmatrix} \tag{4.82}$$

and

$$\sum_n \epsilon^{(n)}_{\mu\nu} \epsilon^{(n)*}_{\rho\sigma} \quad \to \quad \frac{1}{2}\left(\eta_{\mu\sigma}\eta_{\nu\rho} + \eta_{\mu\rho}\eta_{\nu\sigma} - \eta_{\mu\nu}\eta_{\sigma\rho}\right) = P_{\mu\nu,\rho\sigma} \tag{4.83}$$

(Note that this is the same expression which occurs in the numerator of the graviton propagator.) Therefore,

$$\begin{aligned} \sum_n p_i^\mu p_i^\nu \epsilon^{(n)}_{\mu\nu} p_i^\rho p_i^\sigma \epsilon^{(n)*}_{\rho\sigma} &= \frac{1}{2}\left(p_i \cdot p_i\right)^2 = \frac{m_i^4}{2} \\ \sum_n p_i^\mu p_i^\nu \epsilon^{(n)}_{\mu\nu} p_j^\rho p_j^\sigma \epsilon^{(n)*}_{\rho\sigma} &= \left(p_i \cdot p_j\right)^2 - \frac{1}{2}\left(p_i \cdot p_i\right)\left(p_j \cdot p_j\right) = \left(p_i \cdot p_j\right)^2 - \frac{m_i^2 m_j^2}{2} \end{aligned} \tag{4.84}$$

and (4.77) becomes

$$\mathrm{d}\sigma_{br} = \frac{\kappa^2}{4}\left(\sum_{i<j} s_i s_j \frac{\left(p_i \cdot p_j\right)^2}{\left(p_i \cdot k\right)\left(p_j \cdot k\right)}\right) \frac{\mathrm{d}^3 k}{\left(2\pi\right)^3 k_0} \mathrm{d}\sigma_0 \tag{4.85}$$

The sum over graviton momentum states is an integral up to some maximum magnitude, k_{max}, determined by the resolution of the experimental apparatus. So, finally,

$$\mathrm{d}\sigma_{br} \quad = \quad \frac{\kappa^2}{8}\int \frac{d^3k}{\left(2\pi\right)^3}\frac{1}{k_0}\left(\sum_i \frac{m_i^4}{2\left(p_i \cdot k\right)^2} + \sum_{i<j} s_i s_j \frac{2\left(p_i \cdot p_j\right)^2 - m_i^2 m_j^2}{\left(p_i \cdot k\right)\left(p_j \cdot k\right)}\right) \mathrm{d}\sigma_0$$

$$= \frac{\kappa^2}{8}\left(\sum_i \frac{m_i^4}{2}B_{ii} + \sum_{i<j} s_i s_j \left(2\left(p_i\cdot p_j\right)^2 - m_i^2 m_j^2\right) B_{ij}\right) \mathrm{d}\sigma_0 \tag{4.86}$$

where B_{ij} is listed in chapter 2.

As in QED, it can be shown that soft divergences in the higher order bremsstrahlung corrections cancel with higher order elastic corrections, and that the low-energy contributions exponentiate in the sum of the perturbation series, converting the arguments of the logarithms in B_{ij} into exponents [19].

If one of the $m_i \approx 0$, then the corresponding terms in (4.86) are

$$\mathrm{d}\sigma_{br,col} \sim \frac{\kappa^2}{8}\left(\sum_{j\neq i} s_i s_j \left(p_i\cdot p_j\right)^2 B_{ij}\right)\mathrm{d}\sigma_0 \tag{4.87}$$

and the B_{ij} contain collinear divergences. Note that each of these terms has an additional factor of $p_i \cdot p_j$ compared to the QED case, originating in the momentum in the matter-graviton vertex, and it is these additional factors which are responsible for quelling the collinear divergences in the total cross section. The collinear divergent terms in B_{ij} are

$$B_{ij,col} \sim \frac{1}{\left(2\pi\right)^3}\frac{4\pi}{2p_i\cdot p_j}\left(-\frac{1}{2}\log m_i^2 \log\frac{4k_{max}^2}{\lambda^2} - \frac{1}{4}\log^2\frac{m_i^2}{4E_i^2}\right) \tag{4.88}$$

Thus

$$\begin{aligned}\mathrm{d}\sigma_{br,col} &\sim \frac{\kappa^2}{4}\left(\sum_{j\neq i} s_i s_j \frac{1}{\left(2\pi\right)^2} p_i\cdot p_j\left(-\frac{1}{2}\log m_i^2\log\frac{4k_{max}^2}{\lambda^2} - \frac{1}{4}\log^2\frac{m_i^2}{4E_i^2}\right)\right)\mathrm{d}\sigma_0 \\ &= \frac{\kappa^2}{4}\frac{1}{\left(2\pi\right)^2} s_i p_i\cdot\left(\sum_{j\neq i} s_j p_j\right)\left(-\frac{1}{2}\log m_i^2\log\frac{4k_{max}^2}{\lambda^2} - \frac{1}{4}\log^2\frac{m_i^2}{4E_i^2}\right)\mathrm{d}\sigma_0 \end{aligned} \tag{4.89}$$

By conservation of momentum, $\sum_{j\neq i} s_j p_j = -s_i p_i$, and so

$$\begin{aligned}\mathrm{d}\sigma_{br,col} &= -\frac{\kappa^2}{4}\frac{1}{\left(2\pi\right)^2} p_i^2\left(-\frac{1}{2}\log m_i^2\log\frac{4k_{max}^2}{\lambda^2} - \frac{1}{4}\log^2\frac{m_i^2}{4E_i^2}\right)\mathrm{d}\sigma_0 \\ &= -\frac{\kappa^2}{4}\frac{1}{\left(2\pi\right)^2} m_i^2\left(-\frac{1}{2}\log m_i^2\log\frac{4k_{max}^2}{\lambda^2} - \frac{1}{4}\log^2\frac{m_i^2}{4E_i^2}\right)\mathrm{d}\sigma_0 \\ &\approx 0 \end{aligned} \tag{4.90}$$

Thus the sum of all the collinear divergences in the bremsstrahlung diagrams vanishes. As shown above, the contribution from the region of soft virtual photons to the corresponding elastic cross

section also has the form shown in (4.88), so that when the contributions from all diagrams are added, the corresponding collinear divergences vanish. This is illustrated in the present case below.

For the case at hand, fig. 4.11, (4.86) becomes

$$\begin{aligned} \mathrm{d}\sigma_{br} &= \frac{\kappa^2}{8}\left(\frac{M^4}{2}B_{11}+\frac{m^4}{2}B_{22}+\frac{M^4}{2}B_{33}+\frac{m^4}{2}B_{44}+\left(2\left(p_1\cdot p_2\right)^2-M^2m^2\right)B_{12}\right. \\ &\quad -\left(2\left(p_1\cdot p_3\right)^2-M^4\right)B_{13}-\left(2\left(p_1\cdot p_4\right)^2-M^2m^2\right)B_{14}-\left(2\left(p_2\cdot p_3\right)^2-M^2m^2\right)B_{23} \\ &\quad \left.-\left(2\left(p_2\cdot p_4\right)^2-m^4\right)B_{24}+\left(2\left(p_3\cdot p_4\right)^2-M^2m^2\right)B_{34}\right)\mathrm{d}\sigma_0 \end{aligned} \tag{4.91}$$

and if $m \approx 0$ this becomes

$$\begin{aligned} \mathrm{d}\sigma_{br} &= \frac{\kappa^2}{8}\left(\frac{M^4}{2}B_{11}+\frac{M^4}{2}B_{33}\right. \\ &\quad +2\left(p_1\cdot p_2\right)^2B_{12}-\left(2\left(p_1\cdot p_3\right)^2-M^4\right)B_{13}-2\left(p_1\cdot p_4\right)^2B_{14} \\ &\quad \left.-2\left(p_2\cdot p_3\right)^2B_{23}-2\left(p_2\cdot p_4\right)^2B_{24}+2\left(p_3\cdot p_4\right)^2B_{34}\right)\mathrm{d}\sigma_0 \end{aligned} \tag{4.92}$$

and B_{12}, B_{13}, B_{14}, B_{23}, B_{24}, and B_{34} contain collinear divergences.

4.5 Cancellation of Infrared Divergences

Just as in QED, the soft IR divergent piece from each elastic diagram cancels with the interference term between the two bremsstrahlung diagrams obtained by cutting the virtual graviton line at each of its vertices. For example, the bremsstrahlung diagrams figs. 4.11d and 4.11b can be obtained by cutting the graviton line on the right side of fig. 4.4 at one of its vertices, and the soft term from the vertex diagram fig. 4.4 combines with the interference term B_{13} between those two bremsstrahlung diagrams. Similarly, figs. 4.11a and 4.11b can be obtained by cutting the upper graviton line in the box diagram fig. 4.56, and figs. 4.11c and 4.11d by cutting the lower graviton line, and the soft term from fig. 4.56 combines with $B_{12}+B_{34}$. Finally the soft term in the cross-box diagram fig. 4.6 combines with the interference terms $B_{14}+B_{23}$ obtained in a similar way from fig. 4.6.

However, as in massless QED, the collinear divergences which multiply those soft divergences still remain in the limit $m \to 0$. While this is a fundamental problem in QED, as explained above, in quantum gravity these collinear divergences will also cancel, after all the corresponding diagrams are added together [19]. In the intermediate results they may be regularized by maintaining an infinitesimal mass m.

The collinear divergent part of the vertex cross section is, by (4.52) and (4.36)

$$\begin{aligned}\left(\frac{\mathrm{d}\sigma}{\mathrm{d}\left(-t\right)}\right)_{1,v} &= \frac{1}{8\pi\left(s-M^2\right)^2}\,\mathrm{Re}\left[\mathcal{M}_0\left(\kappa^4\frac{\left(s-M^2\right)\left(s-M^2+t\right)t}{16}iJ^{(2)}\left(p_2,-p_2-q\right)\right)\right] \\ &= \frac{\kappa^6}{16\pi}\frac{t}{32\pi^2}\left(\frac{s-M^2+t}{4t}\right)^2\left(\frac{1}{2}\log^2\frac{-t}{m^2}-\log\frac{-t}{\lambda^2}\log\frac{-t}{m^2}\right) \qquad (4.93)\end{aligned}$$

The corresponding term in the bremsstrahlung cross section (4.86) is

$$\begin{aligned}\left(\frac{\mathrm{d}\sigma}{\mathrm{d}\left(-t\right)}\right)_{br,v} &= -\frac{\kappa^2}{4}\left(\frac{-t}{2}\right)^2 B_{24}\left(\frac{\mathrm{d}\sigma}{\mathrm{d}\left(-t\right)}\right)_0 \\ &= \frac{\kappa^6}{16\pi}\frac{t}{32\pi^2}\left(\frac{s-M^2+t}{4t}\right)^2 \\ &\quad\left(\log\frac{4k_{max}^2}{\lambda^2}\log\frac{-t}{m^2}-\frac{1}{4}\log^2\frac{m^2}{4E_2^2}-\frac{1}{4}\log^2\frac{m^2}{4E_4^2}-\ \mathrm{Li}_2\left(1-\frac{4E_2E_4}{-t}\right)\right) \qquad (4.94)\end{aligned}$$

The sum of these two terms is

$$\begin{aligned}\left(\frac{d\sigma}{d\left(-t\right)}\right)_{1,v}+\left(\frac{d\sigma}{d\left(-t\right)}\right)_{br,v} &= \frac{\kappa^6}{16\pi}\left(\frac{s-M^2+t}{4t}\right)^2\left(2\frac{1}{4}t^2iJ^{(2)}\left(p_2+q,-p_2\right)-\frac{1}{16}t^2B_{13}\right) \\ &= -\frac{\kappa^6}{16\pi}\frac{t}{32\pi^2}\left(\frac{s-M^2+t}{4t}\right)^2\left(\frac{1}{4}\log^2\frac{-t}{4E_2^2}+\frac{1}{4}\log^2\frac{-t}{4E_4^2}\right. \\ &\quad\left.+\frac{1}{2}\left(\log\frac{E_2^2}{k_{max}^2}+\log\frac{E_4^2}{k_{max}^2}\right)\log\frac{-t}{m^2}-\ \mathrm{Li}_2\left(1-\frac{4E_2E_4}{-t}\right)\right) \qquad (4.95)\end{aligned}$$

The $\log\lambda^2$ and $\log^2 m^2$ terms cancel, and only single $\log m^2$ terms remain. Note that the same combination of the integrals $J^{(2)}\left(p_2+q,-p_2\right)$ and B_{13} occurs in (4.95) as in (3.45). Just as in QED, the result is the same using $m=0$ and dimensional regularization after the substitution $\log m^2 \to \log 4\pi\mu^2 + {}^2\!/_{\epsilon_{IR}} + \gamma$, except for analytic terms.

The collinear terms in the elastic cross section from the box diagram are given by (4.56):

$$\begin{aligned}&\left(\frac{d\sigma}{d\left(-t\right)}\right)_{1,b} \\ &= \frac{1}{8\pi\left(s-M^2\right)^2} \\ &\ \mathrm{Re}\left[\mathcal{M}_0\left(\kappa^4\frac{\left(s-M^2\right)^3}{16}\left(\left(s-M^2\right)iK\left(p_1,p_2,q\right)-iJ^{(1)}\left(p_2,q\right)+2iJ^{(2)}\left(p_1,p_2\right)\right)\right)\right] \\ &= -\frac{\kappa^6}{16\pi}\frac{\left(s-M^2\right)}{32\pi^2}\left(\frac{s-M^2+t}{4t}\right)^2\end{aligned}$$

$$
\begin{aligned}
&\left(\left(\log\frac{s-M^2}{m^2}+\log\frac{s-M^2}{M^2}\right)\log\frac{s-M^2}{\lambda^2}-\frac{1}{2}\log^2\frac{s-M^2}{m^2}\right)\\
&-\frac{\kappa^6}{16\pi}\frac{\left(s-M^2\right)^2}{32\pi^2}\frac{\left(s-M^2+t\right)}{16t^2}\left(\log\frac{s-M^2}{M^2}\log\frac{-t}{s-M^2}-\frac{1}{2}\log^2\frac{-t}{s-M^2}\right)\\
&+\frac{\kappa^6}{16\pi}\frac{\left(s-M^2\right)}{32\pi^2}\frac{\left(s-M^2+t\right)}{16t}\left(\frac{1}{2}\log^2\frac{s-M^2}{M^2}-2\ \mathrm{Li}_2\frac{s-M^2}{s}-\log^2\frac{s}{s-M^2}\right)
\end{aligned}
\tag{4.96}
$$

There are two corresponding bremsstrahlung diagrams in (4.86):

$$
\begin{aligned}
&\left(\frac{\mathrm{d}\sigma}{\mathrm{d}\left(-t\right)}\right)_{br,b}\\
&=\frac{\kappa^2}{4}\left(\left(\frac{s-M^2}{2}\right)^2B_{12}+\left(\frac{s-M^2}{2}\right)^2B_{34}\right)\left(\frac{\mathrm{d}\sigma}{\mathrm{d}\left(-t\right)}\right)_0\\
&=\frac{\kappa^6}{16\pi}\frac{\left(s-M^2\right)}{32\pi^2}\left(\frac{s-M^2+t}{4t}\right)^2\left(\left(\log\frac{s-M^2}{m^2}+\log\frac{s-M^2}{M^2}\right)\log\frac{4k_{max}^2}{\lambda^2}-\frac{1}{4}\log^2\frac{m^2}{4E_2^2}\right.\\
&-\frac{1}{4}\log^2\frac{m^2}{4E_4^2}+\frac{1}{4}\log^2\frac{M^2}{\left(E_1+|\vec{p_1}|\right)^2}+\ \mathrm{Li}_2\left(1+2\left(E_1+|\vec{p_1}|\right)\left(\frac{E_2}{s-M^2}+\frac{E_1}{M^2}\right)\right)\\
&-\ \mathrm{Li}_2\left(1+4E_2\left(\frac{M^2E_2}{\left(s-M^2\right)^2}-\frac{E_1}{s-M^2}\right)\right)+\ \mathrm{Li}_2\left(1+2\left(E_1-|\vec{p_1}|\right)\left(\frac{E_2}{s-M^2}+\frac{E_1}{M^2}\right)\right)\Big)\\
&+\frac{1}{4}\log^2\frac{M^2}{\left(E_3+|\vec{p_3}|\right)^2}+\ \mathrm{Li}_2\left(1+2\left(E_3+|\vec{p_3}|\right)\left(\frac{E_4}{s-M^2}+\frac{E_3}{M^2}\right)\right)\\
&-\ \mathrm{Li}_2\left(1+4E_4\left(\frac{M^2E_4}{\left(s-M^2\right)^2}-\frac{E_3}{s-M^2}\right)\right)+\ \mathrm{Li}_2\left(1+2\left(E_3-|\vec{p_3}|\right)\left(\frac{E_4}{s-M^2}+\frac{E_3}{M^2}\right)\right)\Big)
\end{aligned}
\tag{4.97}
$$

The sum of these comes out to

$$
\begin{aligned}
&\left(\frac{d\sigma}{d\left(-t\right)}\right)_{1,b}+\left(\frac{d\sigma}{d\left(-t\right)}\right)_{br,b}\\
&=-\frac{\kappa^6}{16\pi}\frac{\left(s-M^2\right)}{32\pi^2}\left(\frac{s-M^2+t}{4t}\right)^2\\
&\left(\frac{1}{4}\log^2\frac{s-M^2}{4E_2^2}+\frac{1}{4}\log^2\frac{s-M^2}{4E_4^2}+\frac{1}{2}\left(\log\frac{E_2^2}{k_{max}^2}+\log\frac{E_4^2}{k_{max}^2}\right)\log\frac{s-M^2}{m^2}\right.\\
&+\log\frac{s-M^2}{4k_{max}^2}\log\frac{s-M^2}{M^2}+\frac{1}{4}\log^2\frac{M^2}{\left(E_1+|\vec{p_1}|\right)^2}+\ \mathrm{Li}_2\left(1+2\left(E_1+|\vec{p_1}|\right)\left(\frac{E_2}{s-M^2}+\frac{E_1}{M^2}\right)\right)\\
&-\ \mathrm{Li}_2\left(1+4E_2\left(\frac{M^2E_2}{\left(s-M^2\right)^2}-\frac{E_1}{s-M^2}\right)\right)+\ \mathrm{Li}_2\left(1+2\left(E_1-|\vec{p_1}|\right)\left(\frac{E_2}{s-M^2}+\frac{E_1}{M^2}\right)\right)\Big)\\
&+\frac{1}{4}\log^2\frac{M^2}{\left(E_3+|\vec{p_3}|\right)^2}+\ \mathrm{Li}_2\left(1+2\left(E_3+|\vec{p_3}|\right)\left(\frac{E_4}{s-M^2}+\frac{E_3}{M^2}\right)\right)\\
&-\ \mathrm{Li}_2\left(1+4E_4\left(\frac{M^2E_4}{\left(s-M^2\right)^2}-\frac{E_3}{s-M^2}\right)\right)+\ \mathrm{Li}_2\left(1+2\left(E_3-|\vec{p_3}|\right)\left(\frac{E_4}{s-M^2}+\frac{E_3}{M^2}\right)\right)\Big)
\end{aligned}
$$

$$
\begin{aligned}
&-\frac{\kappa^6}{16\pi}\frac{\left(s-M^2\right)^2}{32\pi^2}\frac{\left(s-M^2+t\right)}{16t^2}\left(\log\frac{s-M^2}{M^2}\log\frac{-t}{s-M^2}-\frac{1}{2}\log^2\frac{-t}{s-M^2}\right)\\
&+\frac{\kappa^6}{16\pi}\frac{\left(s-M^2\right)}{32\pi^2}\frac{\left(s-M^2+t\right)}{16t}\left(\frac{1}{2}\log^2\frac{s-M^2}{M^2}-2\ \mathrm{Li}_2\frac{s-M^2}{s}-\log^2\frac{s}{s-M^2}\right)
\end{aligned}
\tag{4.98}
$$

Again, the $\log\lambda^2$ and $\log^2 m^2$ terms cancel, leaving only single $\log m^2$ terms, and after the substitution $\log m^2 \to \log 4\pi\mu^2 + 2/\epsilon_{IR} + \gamma$, the results are the same if $m = 0$.

This result can be applied to the cross box diagram by permuting p_2 with $-p_4$ in the radiative corrections. Under this transformation, $s-M^2$ becomes $u-M^2 = M^2-s-t = -\left(s-M^2+t\right)$ and $s-M^2+t$ becomes $M^2-s = -\left(s-M^2\right)$. Thus the final result for the crossed box cross section plus corresponding bremsstrahlung is

$$
\begin{aligned}
&\left(\frac{d\sigma}{d\left(-t\right)}\right)_{1,cros}+\left(\frac{d\sigma}{d\left(-t\right)}\right)_{br,cros}\\
&=\frac{\kappa^6}{16\pi}\frac{\left(s-M^2+t\right)}{32\pi^2}\left(\frac{s-M^2+t}{4t}\right)^2\\
&\cdot\left(\frac{1}{4}\log^2\frac{4E_2^2}{s-M^2+t}+\frac{1}{4}\log^2\frac{4E_4^2}{s-M^2+t}+\frac{1}{2}\left(\log\frac{E_2^2}{k_{max}^2}+\log\frac{E_4^2}{k_{max}^2}\right)\log\frac{s-M^2+t}{m^2}\right.\\
&+\log\frac{s-M^2+t}{4k_{max}^2}\log\frac{s-M^2+t}{M^2}+\frac{1}{4}\log^2\frac{M^2}{\left(E_1+|\vec{p_1}|\right)^2}\\
&+\mathrm{Li}_2\left(1+2\left(E_1+|\vec{p_1}|\right)\left(\frac{E_4}{u-M^2}+\frac{E_1}{M^2}\right)\right)\\
&-\mathrm{Li}_2\left(1+4E_4\left(\frac{M^2E_4}{\left(u-M^2\right)^2}-\frac{E_1}{u-M^2}\right)\right)+\mathrm{Li}_2\left(1+2\left(E_1-|\vec{p_1}|\right)\left(\frac{E_4}{u-M^2}+\frac{E_1}{M^2}\right)\right)\Bigg)\\
&+\frac{1}{4}\log^2\frac{M^2}{\left(E_3+|\vec{p_3}|\right)^2}+\mathrm{Li}_2\left(1+2\left(E_3+|\vec{p_3}|\right)\left(\frac{E_2}{u-M^2}+\frac{E_3}{M^2}\right)\right)\\
&-\mathrm{Li}_2\left(1+4E_2\left(\frac{M^2E_2}{\left(u-M^2\right)^2}-\frac{E_3}{u-M^2}\right)\right)+\mathrm{Li}_2\left(1+2\left(E_3-|\vec{p_3}|\right)\left(\frac{E_2}{u-M^2}+\frac{E_3}{M^2}\right)\right)\Bigg)\\
&+\frac{\kappa^6}{16\pi}\frac{\left(s-M^2+t\right)^4}{32\pi^2}\frac{1}{16\left(s-M^2\right)t^2}\left(\log\frac{s-M^2+t}{M^2}\log\frac{-t}{s-M^2+t}-\frac{1}{2}\log^2\frac{-t}{s-M^2+t}\right)\\
&+\frac{\kappa^6}{16\pi}\frac{\left(s-M^2+t\right)^3}{32\pi^2}\frac{1}{16\left(s-M^2\right)t}\left(\frac{1}{2}\log^2\frac{s-M^2+t}{M^2}-2\ \mathrm{Li}_2\frac{s-M^2+t}{u}-\log^2\frac{u}{s-M^2+t}\right)
\end{aligned}
\tag{4.99}
$$

The sum of the vertex terms (4.95), the box terms (4.98), and the cross-box terms (4.99) is

$$
\begin{aligned}
&\left(\frac{d\sigma}{d\left(-t\right)}\right)_1+\left(\frac{d\sigma}{d\left(-t\right)}\right)_{br}\\
&=-\frac{\kappa^6}{16\pi}\frac{t}{32\pi^2}\left(\frac{s-M^2+t}{4t}\right)^2\left(-\mathrm{Li}_2\left(1-\frac{4E_2E_4}{-t}\right)\right)
\end{aligned}
$$

$$
\begin{aligned}
&-\frac{\kappa^6}{16\pi}\frac{\left(s-M^2\right)}{32\pi^2}\left(\frac{s-M^2+t}{4t}\right)^2\\
&\left(-\frac{1}{2}\log^2\frac{-t}{s-M^2}-\log\frac{s-M^2}{k_{max}^2}\log\frac{-t}{s-M^2}+\log\frac{s-M^2}{k_{max}^2}\log\frac{s-M^2}{M^2}\right.\\
&+\frac{1}{4}\log^2\frac{M^2}{\left(E_1+|\vec{p_1}|\right)^2}+\ \mathrm{Li}_2\left(1+2\left(E_1+|\vec{p_1}|\right)\left(\frac{E_2}{s-M^2}+\frac{E_1}{M^2}\right)\right)\\
&-\ \mathrm{Li}_2\left(1+4E_2\left(\frac{M^2E_2}{\left(s-M^2\right)^2}-\frac{E_1}{s-M^2}\right)\right)+\ \mathrm{Li}_2\left(1+2\left(E_1-|\vec{p_1}|\right)\left(\frac{E_2}{s-M^2}+\frac{E_1}{M^2}\right)\right)\Bigg)\\
&+\frac{1}{4}\log^2\frac{M^2}{\left(E_3+|\vec{p_3}|\right)^2}+\ \mathrm{Li}_2\left(1+2\left(E_3+|\vec{p_3}|\right)\left(\frac{E_4}{s-M^2}+\frac{E_3}{M^2}\right)\right)\\
&-\ \mathrm{Li}_2\left(1+4E_4\left(\frac{M^2E_4}{\left(s-M^2\right)^2}-\frac{E_3}{s-M^2}\right)\right)+\ \mathrm{Li}_2\left(1+2\left(E_3-|\vec{p_3}|\right)\left(\frac{E_4}{s-M^2}+\frac{E_3}{M^2}\right)\right)\Bigg)\\
&-\frac{\kappa^6}{16\pi}\frac{\left(s-M^2\right)^2}{32\pi^2}\frac{\left(s-M^2+t\right)}{16t^2}\left(\log\frac{s-M^2}{M^2}\log\frac{-t}{s-M^2}-\frac{1}{2}\log^2\frac{-t}{s-M^2}\right)\\
&+\frac{\kappa^6}{16\pi}\frac{\left(s-M^2\right)}{32\pi^2}\frac{\left(s-M^2+t\right)}{16t}\left(\frac{1}{2}\log^2\frac{s-M^2}{M^2}-2\ \mathrm{Li}_2\frac{s-M^2}{s}-\log^2\frac{s}{s-M^2}\right)\\
&+\frac{\kappa^6}{16\pi}\frac{\left(s-M^2+t\right)}{32\pi^2}\left(\frac{s-M^2+t}{4t}\right)^2\\
&\cdot\left(\frac{1}{2}\log^2\frac{-t}{s-M^2+t}+\log\frac{-t}{k_{max}^2}\log\frac{s-M^2+t}{-t}+\log\frac{s-M^2+t}{k_{max}^2}\log\frac{s-M^2+t}{M^2}\right.\\
&+\frac{1}{4}\log^2\frac{M^2}{\left(E_1+|\vec{p_1}|\right)^2}+\ \mathrm{Li}_2\left(1+2\left(E_1+|\vec{p_1}|\right)\left(\frac{E_4}{u-M^2}+\frac{E_1}{M^2}\right)\right)\\
&-\ \mathrm{Li}_2\left(1+4E_4\left(\frac{M^2E_4}{\left(u-M^2\right)^2}-\frac{E_1}{u-M^2}\right)\right)+\ \mathrm{Li}_2\left(1+2\left(E_1-|\vec{p_1}|\right)\left(\frac{E_4}{u-M^2}+\frac{E_1}{M^2}\right)\right)\Bigg)\\
&+\frac{1}{4}\log^2\frac{M^2}{\left(E_3+|\vec{p_3}|\right)^2}+\ \mathrm{Li}_2\left(1+2\left(E_3+|\vec{p_3}|\right)\left(\frac{E_2}{u-M^2}+\frac{E_3}{M^2}\right)\right)\\
&-\ \mathrm{Li}_2\left(1+4E_2\left(\frac{M^2E_2}{\left(u-M^2\right)^2}-\frac{E_3}{u-M^2}\right)\right)+\ \mathrm{Li}_2\left(1+2\left(E_3-|\vec{p_3}|\right)\left(\frac{E_2}{u-M^2}+\frac{E_3}{M^2}\right)\right)\Bigg)\\
&+\frac{\kappa^6}{16\pi}\frac{\left(s-M^2+t\right)^4}{32\pi^2}\frac{1}{16\left(s-M^2\right)t^2}\left(\log\frac{s-M^2+t}{M^2}\log\frac{-t}{s-M^2+t}-\frac{1}{2}\log^2\frac{-t}{s-M^2+t}\right)\\
&+\frac{\kappa^6}{16\pi}\frac{\left(s-M^2+t\right)^3}{32\pi^2}\frac{1}{16\left(s-M^2\right)t}\left(\frac{1}{2}\log^2\frac{s-M^2+t}{M^2}-2\ \mathrm{Li}_2\frac{s-M^2+t}{u}-\log^2\frac{u}{s-M^2+t}\right)
\end{aligned}
\tag{4.100}
$$

The $\log m^2$ terms (or $1/\epsilon_{IR}$ terms if $m=0$) cancel, as they should, leaving only an IR finite remainder.

4.6 Final Result

Adding to (4.100) the remaining, IR convergent, pieces from the elastic diagrams (4.43) to (4.86) substituted into the cross section formula (4.36), one obtains the total cross section. The general

result is very long and not very enlightening, but in the case $m = 0$, in the limit of small t, the result becomes simply

$$\begin{aligned}\left(\frac{d\sigma}{d(-t)}\right)_{tot} \approx\ & \frac{\kappa^6}{16\pi}\frac{17\left(s-M^2\right)^2}{192t}\frac{1}{16\pi^2}\log\frac{-t}{\mu^2} - \frac{\kappa^6}{16\pi}\frac{17\left(s-M^2\right)^2}{128t}\frac{1}{32}\frac{M}{\sqrt{-t}} \\ & + \frac{\kappa^6}{16\pi}\frac{\left(s-M^2\right)^2}{1024\pi^2 t}\left(-2\log^2\frac{-t}{s-M^2} + 4\log\frac{k_{max}^2}{s-M^2}\log\frac{s-M^2}{M^2}\right. \\ & -2\log\frac{-t}{k_{max}^2}\log\frac{-t}{s-M^2} + 6\log\frac{s-M^2}{M^2}\log\frac{-t}{s-M^2} \\ & \left. -2\log\frac{k_{max}^2}{s-M^2} + 4\log\frac{-t}{s-M^2}\right) \\ & -\frac{\kappa^6}{16\pi}\frac{\left(s-M^2\right)^3}{1024\pi^2 t^2}\log^2\frac{-t}{s-M^2}\end{aligned} \tag{4.101}$$

This is free of all IR divergences. The $\log\mu^2$ term originates in the UV divergences, and combines with terms in the effective Lagrangian as described in chapter 1. Of (4.101), an amount

$$\left(\frac{d\sigma}{d(-t)}\right)_{tot,heavy} = -\frac{\kappa^6}{16\pi}\frac{9\left(s-M^2\right)^2}{32t}\frac{1}{32\pi^2}\log\frac{-t}{\mu^2} - \frac{\kappa^6}{16\pi}\frac{17\left(s-M^2\right)^2}{128t}\frac{1}{32}\frac{M}{\sqrt{-t}} \tag{4.102}$$

comes from the triangle and vertex diagrams which involve only the heavy scalar in internal lines. These terms are essentially the same as the corresponding terms found in the massive case in [7]. There it was shown that some of these terms could be interpreted as corrections to the energy-momentum tensor of the massive particle. An amount

$$\left(\frac{d\sigma}{d(-t)}\right)_{tot,light} = -\frac{\kappa^6}{16\pi}\frac{\left(s-M^2+t\right)^2}{1024\pi^2 t}\left(\log^2\frac{4E^2}{-t} + 2\log\frac{4E^2}{k_{max}^2}\log\frac{-t}{m^2}\right) \tag{4.103}$$

comes from the triangle and vertex diagrams which involve only the massless scalar in internal lines, and in the next chapter it will be explored whether these terms can be interpreted in an analogous way. An amount

$$\begin{aligned}\left(\frac{d\sigma}{d(-t)}\right)_{tot,box} =\ & \frac{\kappa^6}{16\pi}\frac{\left(s-M^2+t\right)^2}{1024\pi^2 t}\left(\log^2\frac{4E^2}{-t} + 2\log\frac{4E^2}{k_{max}^2}\log\frac{-t}{m^2}\right) + \\ & \frac{\kappa^6}{16\pi}\frac{\left(s-M^2\right)^2}{1024\pi^2 t}\left(-2\log^2\frac{-t}{s-M^2} + 4\log\frac{k_{max}^2}{s-M^2}\log\frac{s-M^2}{M^2}\right. \\ & -2\log\frac{-t}{k_{max}^2}\log\frac{-t}{s-M^2} + 6\log\frac{s-M^2}{M^2}\log\frac{-t}{s-M^2} \\ & \left. -2\log\frac{k_{max}^2}{s-M^2} + 4\log\frac{-t}{s-M^2}\right)\end{aligned}$$

$$-\frac{\kappa^6}{16\pi}\frac{\left(s-M^2\right)^3}{1024\pi^2 t^2}\log^2\frac{-t}{s-M^2} \tag{4.104}$$

comes from the box and cross box diagrams, which involve both the massive and the massless matter particles in the internal lines, and

$$\left(\frac{d\sigma}{d\left(-t\right)}\right)_{tot,pol}=\frac{\kappa^6}{16\pi}\frac{11\left(s-M^2\right)^2}{48t}\frac{1}{16\pi^2}\log\frac{-t}{\mu^2} \tag{4.105}$$

comes from the polarization and double-seagull diagrams, which don't involve any of the initial or final particle lines in the propagators. (4.101) will be used in the next chapter to calculate the deflection of a beam of scalar particles around a massive object.

4.7 Photon-Scalar Scattering

Next consider the gravitational scattering of a photon by a scalar particle. The matrix element for photon-scalar scattering can be written

$$-i\mathcal{M}=H^{\mu\nu}\epsilon_\mu\left(p_2\right)\epsilon_\nu^*\left(p_4\right) \tag{4.106}$$

where $\epsilon_\mu\left(p_2\right)$ and $\epsilon_\nu^*\left(p_4\right)$ are the polarization vectors of the initial and final photons. By Lorentz invariance, H must be expressible in terms of the momenta p_1 and p_3 of the initial and final scalar and p_2 and p_4 of the initial and final photon, respectively, and the metric tensor η. $\epsilon_\mu\left(p_2\right)$ and $\epsilon_\nu^*\left(p_4\right)$ each have two linearly independent components, and by an appropriate (electromagnetic) gauge transformation, both can be made orthogonal to both p_2 and p_4. H is thus effectively a linear operator over the two dimensional space-like surface orthogonal to p_2 and p_4, and there are therefore four linearly independent components of the tensor H. But $\mathcal{M}$ must be invariant under parity transformations, which reverse helicities, so these four components must be related in pairs, bringing the number of independent components down to two. Let

$$\begin{aligned} P &= p_1+p_3-\frac{\left(p_1+p_3\right)\cdot K}{K^2}K \\ K &= p_4+p_2 \\ q &= p_1-p_3=p_4-p_2 \end{aligned} \tag{4.107}$$

P is orthogonal to both K and q, and so also to both p_2 and p_4. It therefore can be used to define one of the directions of polarization. The other direction of polarization must be orthogonal to

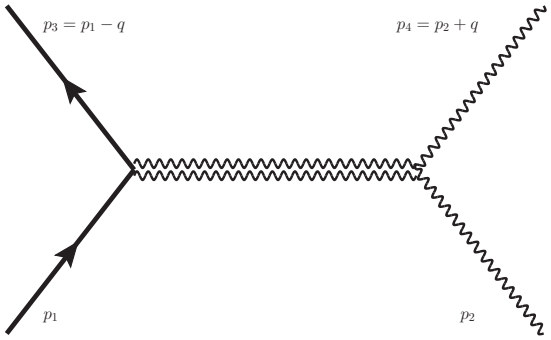

Figure 4.12. Lowest order gravitational photon-scalar scattering.

q, K, and P, and therefore must reverse sign under parity transformations, since P, K, and q do not. Thus by parity invariance there can be no cross terms between the two directions in H, which therefore must be of the form

$$H^{\mu\nu} = H_1 \frac{P^\mu P^\nu}{P^2} + H_2 \left(\eta^{\mu\nu} - \frac{P^\mu P^\nu}{P^2} - \frac{K^\mu K^\nu}{K^2} - \frac{q^\mu q^\nu}{q^2} \right) \tag{4.108}$$

$P^\mu P^\nu / P^2$ is the orthogonal projection operator onto the direction of P. By contracting the expression for $H^{\mu\nu}$ with $P^\mu P^\nu / P^2$, one obtains an expression for the scalar H_1, which can be evaluated independently of H_2. Similarly the other tensor form in (4.108) is a projection onto the other direction of polarization, and contracting $H^{\mu\nu}$ with this form determines an expression for H_2.

In either the center-of-mass frame or the rest frame of p_1, P lies in the plane of scattering. Thus H_1 is the amplitude for scattering of a photon polarized in the plane of scattering, and H_2 the amplitude for a photon polarized in the perpendicular direction. The cross section in either case is still given by (4.36) with $m = 0$:

$$\begin{aligned} \left(\frac{d\sigma}{d(-t)} \right)_{el,\parallel} &= \frac{|H_1|^2}{16\pi (s - M^2)^2} \\ \left(\frac{d\sigma}{d(-t)} \right)_{el,\perp} &= \frac{|H_2|^2}{16\pi (s - M^2)^2} \end{aligned} \tag{4.109}$$

The diagrams determining the matrix element are entirely analogous to the scalar case, including mirror images of figs. 4.13, 4.14, 4.15, and 4.18, where the radiative corrections are on the side of the scalar line. Results for H_1 and H_2 individually are given below.

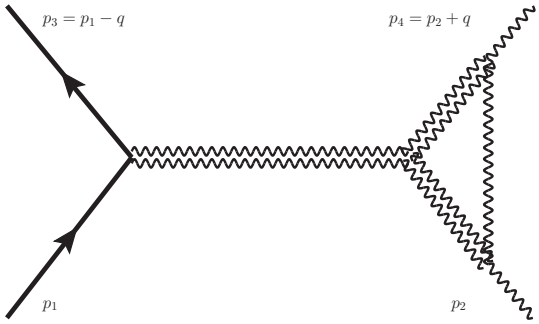

Figure 4.13. Gravitational vertex diagram.

4.7.1 Lowest Order

The lowest order matrix element is given by the tree diagram fig. 4.1, where the heavy solid line represents a scalar of mass M, the double wavy line a graviton, and the single wavy line a photon:

$$\begin{aligned} H^{\alpha\beta} &= \tau^{\kappa\lambda}\left(p_1, p_1-q, M\right)\frac{iP_{\kappa\lambda,\mu\nu}}{q^2}\tau_1^{\alpha,\beta,\mu\nu}\left(p_2, p_2+q\right) \\ H_1 &= -i\kappa^2\frac{\left(s-M^2\right)^2+st}{4t} \\ H_2 &= i\kappa^2\frac{\left(s-M^2\right)^2+st}{4t} \end{aligned} \tag{4.110}$$

This results in the lowest order cross section

$$\left(\frac{\mathrm{d}\sigma}{\mathrm{d}\left(-t\right)}\right)_0 = \frac{\kappa^4}{256\pi\left(s-M^2\right)^2}\frac{\left(\left(s-M^2\right)^2+st\right)^2}{t^2} \tag{4.111}$$

independent of the direction of polarization.

4.7.2 Vertex Corrections

The result for the vertex diagrams are:

fig. 4.13:

$$\begin{aligned} H^{\phi\omega} &= \int \tau_1^{\kappa\lambda}\left(p_1, p_1-q, M\right)\frac{iP_{\kappa\lambda,\mu\nu}}{q^2} \\ &\quad \cdot\frac{\tau_3^{\mu\nu,\rho\sigma,\epsilon\zeta}\left(k,-q\right)iP_{\epsilon\zeta,\alpha\beta}\tau_1^{\phi,\chi,\alpha\beta}\left(p_2+q, p_2-k\right)\left(-i\eta_{\chi\psi}\right)\tau_1^{\psi,\omega,\gamma\delta}\left(p_2-k, p_2\right)iP_{\gamma\delta,\rho\sigma}}{\left(k^2-\lambda^2\right)\left(\left(k+q\right)^2-\lambda^2\right)\left(\left(p_2-k\right)^2-m^2\right)}\frac{\mathrm{d}^4k}{\left(2\pi\right)^4} \\ H_1 &= -\frac{i\kappa^4}{96}\left(41\left(s-M^2\right)^2+\left(41s-\frac{17}{4}M^2\right)t+\frac{137}{8}t^2\right)iI^1\left(q\right) \end{aligned}$$

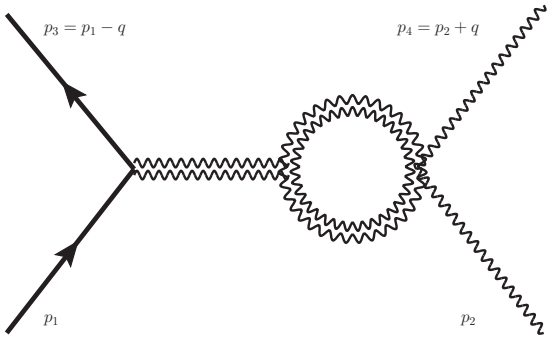

Figure 4.14. Gravitational vertex diagram.

$$H_2 = -\frac{i\kappa^4}{96}\left(36\left(s-M^2\right)^2+\left(36s-\frac{17}{4}M^2\right)t+\frac{137}{8}t^2\right)iI^1(q) \tag{4.112}$$

mirror image:

$$\begin{aligned}
H^{\phi\omega} &= \int \frac{iP_{\epsilon\zeta,\alpha\beta}\tau^{\alpha\beta}\left(p_1-q,p_1-k,M\right)i\tau^{\gamma\delta}\left(p_1-k,p_1,M\right)iP_{\gamma\delta,\rho\sigma}\tau_3^{\rho\sigma,\epsilon\zeta,\kappa\lambda}(k,q)}{\left(k^2-\lambda^2\right)\left(\left(p_1-k\right)^2-M^2\right)\left(\left(k-q\right)^2-\lambda^2\right)} \\
&\quad \cdot\frac{iP_{\kappa\lambda,\mu\nu}}{q^2}\tau_1^{\phi,\omega,\mu\nu}\left(p_2,p_2+q\right)\frac{\mathrm{d}^4k}{\left(2\pi\right)^4} \\
H_1 &= -\frac{\kappa^4M^2\left(2M^4-9M^2t+t^2\right)\left(\left(s-M^2\right)^2+st\right)}{8\left(t-4M^2\right)^2}J^{(1)}(p_1,q) \\
&\quad -\frac{\kappa^4M^2\left(t-13M^2\right)\left(\left(s-M^2\right)^2+st\right)}{8\left(t-4M^2\right)^2}I^1(q) \\
H_2 &= \frac{\kappa^4M^2\left(2M^4-9M^2t+t^2\right)\left(\left(s-M^2\right)^2+st\right)}{8\left(t-4M^2\right)^2}J^{(1)}(p_1,q) \\
&\quad +\frac{\kappa^4M^2\left(t-13M^2\right)\left(\left(s-M^2\right)^2+st\right)}{8\left(t-4M^2\right)^2}I^1(q)
\end{aligned} \tag{4.113}$$

fig. 4.14:

$$\begin{aligned}
H^{\phi\omega} &= \frac{1}{2}\int \tau_1^{\kappa\lambda}\left(p_1,p_1-q,M\right)\frac{iP_{\kappa\lambda,\mu\nu}}{q^2} \\
&\quad \frac{\tau_3^{\mu\nu,\rho\sigma,\epsilon\zeta}\left(-k,-q\right)iP_{\epsilon\zeta,\alpha\beta}\tau_2^{\phi,\omega,\alpha\beta,\gamma\delta}\left(p_2+q,p_2\right)iP_{\gamma\delta,\rho\sigma}}{\left(k^2-\lambda^2\right)\left(\left(k-q\right)^2-\lambda^2\right)}\frac{\mathrm{d}^4k}{\left(2\pi\right)^4} \\
H_1 &= \frac{i\kappa^4}{32}\left(12\left(s-M^2\right)^2+\left(12s-M^2\right)t+\frac{11}{2}t^2\right)iI^1(q) \\
H_2 &= \frac{i\kappa^4}{32}\left(12\left(s-M^2\right)^2+\left(12s-M^2\right)t+\frac{11}{2}t^2\right)iI^1(q)
\end{aligned} \tag{4.114}$$

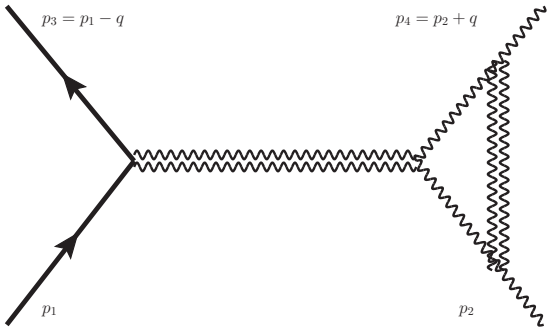

Figure 4.15. Gravitational vertex diagram.

mirror image:

$$\begin{aligned} H^{\phi\omega} &= \frac{1}{2}\int \frac{iP_{\epsilon\zeta,\alpha\beta}\tau_2^{\alpha\beta,\gamma\delta}\left(p_1-q,p_1,M\right)iP_{\gamma\delta,\rho\sigma}\tau_3^{\kappa\lambda,\epsilon\zeta,\rho\sigma}\left(k,q\right)}{\left(k^2-\lambda^2\right)\left(\left(k-q\right)^2-\lambda^2\right)} \\ &\quad \frac{iP_{\kappa\lambda,\mu\nu}}{q^2}\tau_1^{\phi,\omega,\mu\nu}\left(p_2,p_2+q\right)\frac{\mathrm{d}^4k}{\left(2\pi\right)^4} \\ H_1 &= 0 \\ H_2 &= 0 \end{aligned} \tag{4.115}$$

fig. 4.15:

$$\begin{aligned} H^{\phi\omega} &= \int \tau_1^{\kappa\lambda}\left(p_1,p_1-q,M\right)\frac{iP_{\kappa\lambda,\mu\nu}}{q^2}\frac{\tau_1^{\theta,\iota,\mu\nu}\left(p_2+q-k,p_2-k\right)\left(-i\eta_{\iota\chi}\right)\tau^{\chi,\phi,\gamma\delta}\left(p_2-k,p_2\right)}{\left(\left(p_2+q-k\right)^2-m^2\right)} \\ &\quad \frac{iP_{\gamma\delta,\alpha\beta}\tau_1^{\omega,\psi,\alpha\beta}\left(p_2+q,p_2+q-k\right)\left(-i\eta_{\psi\theta}\right)}{\left(k^2-\lambda^2\right)\left(\left(p_2-k\right)^2-m^2\right)}\frac{\mathrm{d}^4k}{\left(2\pi\right)^4} \\ H_1 &= \frac{25i\kappa^4}{96}\left(\left(s-M^2\right)^2+\left(s-\frac{1}{4}M^2\right)t+\frac{1}{8}t^2\right)iI^1\left(q\right) \\ &\quad +\frac{i\kappa^4}{16}\left(\left(s-M^2\right)^2t+st^2\right)iJ^{(2)}\left(p_2,-p_2-q\right) \\ H_2 &= \frac{25i\kappa^4}{96}\left(-\frac{1}{4}M^2t+\frac{1}{8}t^2\right)iI^1\left(q\right) \\ &\quad -\frac{i\kappa^4}{16}\left(\left(s-M^2\right)^2t+st^2\right)iJ^{(2)}\left(p_2,-p_2-q\right) \end{aligned} \tag{4.116}$$

mirror image:

$$\begin{aligned} H^{\phi\omega} &= \int \frac{\tau_1^{\mu\nu}\left(p_1-q-k,p_1-k,M\right)i\tau^{\gamma\delta}\left(p_1-k,p_1,M\right)iP_{\gamma\delta,\alpha\beta}\tau_1^{\alpha\beta}\left(p_1-q,p_1-q-k,M\right)i}{\left(\left(p_1-q-k\right)^2-M^2\right)\left(k^2-\lambda^2\right)\left(\left(p_1-k\right)^2-M^2\right)} \\ &\quad \cdot\frac{iP_{\mu\nu,\kappa\lambda}}{q^2}\tau_1^{\phi,\omega,\kappa\lambda}\left(p_2,p_2+q\right)\frac{\mathrm{d}^4k}{\left(2\pi\right)^4} \end{aligned}$$

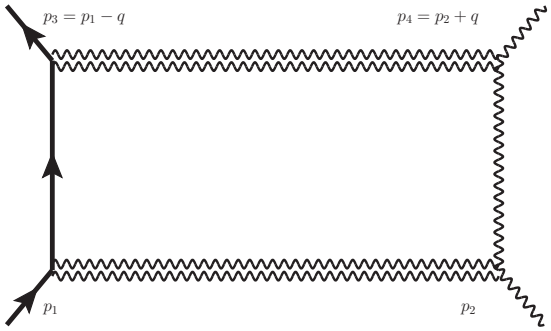

Figure 4.16. Box diagram.

$$
\begin{aligned}
H_1 &= \frac{\kappa^4\left(2M^4-4M^2t+t^2\right)\left(\left(s-M^2\right)^2+st\right)}{16t}J^{(2)}\left(p_1,q-p_1\right)\\
&\quad+\frac{3\kappa^4\left(2M^4-4M^2t+t^2\right)\left(\left(s-M^2\right)^2+st\right)}{16t\left(t-4M^2\right)}I^{(2)}\left(p_1p_1-q\right)\\
H_2 &= -\frac{\kappa^4\left(2M^4-4M^2t+t^2\right)\left(\left(s-M^2\right)^2+st\right)}{16t}J^{(2)}\left(p_1,q-p_1\right)\\
&\quad-\frac{3\kappa^4\left(2M^4-4M^2t+t^2\right)\left(\left(s-M^2\right)^2+st\right)}{16t\left(t-4M^2\right)}I^{(2)}\left(p_1,p_1-q\right)
\end{aligned}
\tag{4.117}
$$

4.7.3 Box Diagrams

The result for the box diagrams are:

fig. 4.16 (box):

$$
\begin{aligned}
H^{\phi\omega} &= \int\frac{\tau^{\alpha\beta}\left(p_1-q,p_1-k,M\right)i\tau_1^{\gamma\delta}\left(p_1-k,p_1,M\right)iP_{\alpha\beta,\epsilon\zeta}iP_{\gamma\delta,\rho\sigma}}{\left(\left(p_1-k\right)^2-M^2\right)\left(k^2-\lambda^2\right)\left(\left(k-q\right)^2-\lambda^2\right)}\\
&\quad\cdot\frac{\tau_1^{\omega,\psi,\epsilon\zeta}\left(p_2+q,p_2+k\right)\left(-i\eta_{\psi\chi}\right)\tau_1^{\chi,\phi,\rho\sigma}\left(p_2+k,p_2\right)}{\left(\left(p_2+k\right)^2-m^2\right)}\frac{\mathrm{d}^4k}{\left(2\pi\right)^4}\\
H_1 &= \frac{\kappa^4}{32}\left(\left(s-M^2\right)^4+st\left(s-M^2\right)^2+\frac{\left(s-M^2\right)^6}{\left(s-M^2\right)^2+st}\right)K\\
&\quad-\frac{\kappa^4}{32}\left(\left(s-M^2\right)^3+st\left(s-M^2\right)+\frac{\left(s-M^2\right)^5}{\left(s-M^2\right)^2+st}\right)J^{(1)}\left(p_2,q\right)\\
&\quad+\frac{\kappa^4}{16}\left(\left(s-M^2\right)^2s+\frac{\left(s-M^2\right)^4s}{\left(s-M^2\right)^2+st}\right)J^{(2)}\left(p_1,p_2\right)\\
&\quad+\kappa^4\left(\frac{2M^6+5M^4s+10M^2s^2-s^3}{32}-\frac{s\left(s-3M^2\right)t}{32}-\frac{\left(s-M^2\right)^4\left(s+M^2\right)}{32\left(\left(s-M^2\right)^2+st\right)}\right.\\
&\quad\left.+\frac{3M^6\left(M^2+s\right)^2}{2\left(t-4M^2\right)^2}+\frac{M^2\left(2M^6+8M^4s+3M^2s^2+s^3\right)}{4\left(t-4M^2\right)}\right)J^{(1)}\left(p_1,q\right)
\end{aligned}
$$

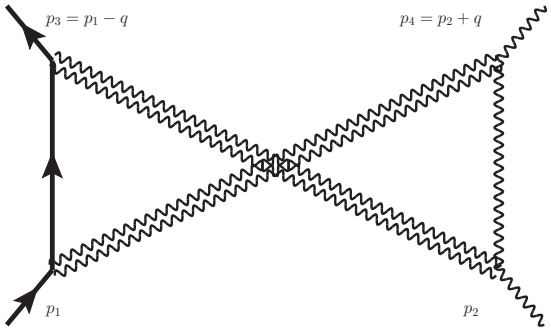

Figure 4.17. Cross box diagram.

$$
\begin{aligned}
& +\kappa^4 \left(\frac{3M^4 - 10M^2 s + 15s^2}{64} + \frac{3st}{32} + \frac{\left(s - M^2\right)^3}{8t} \right. \\
& \left. + \frac{M^6 + 6M^4 s + 2M^2 s^2 + s^3}{8\left(t - 4M^2\right)} + \frac{3M^4 \left(M^2 + s\right)^2}{4\left(t - 4M^2\right)^2} \right) I^{(1)}(q) \\
& + \frac{\kappa^4 s^2}{16} I^{(2)}(p_1, p_2) \\
H_2 \quad = \quad & -\frac{\kappa^4}{32} \left(\left(s - M^2\right)^4 + st\left(s - M^2\right)^2 + \frac{\left(s - M^2\right)^6}{\left(s - M^2\right)^2 + st} \right) K \\
& + \frac{\kappa^4}{32} \left(\left(s - M^2\right)^3 + \left(s - M^2\right) st + \frac{\left(s - M^2\right)^5}{\left(s - M^2\right)^2 + st} \right) J^{(1)}(p_2, q) \\
& - \frac{\kappa^4}{16} \left(\left(s - M^2\right)^2 s + \frac{\left(s - M^2\right)^4 s}{\left(s - M^2\right)^2 + st} \right) J^{(2)}(p_1, p_2) \\
& + \kappa^4 \left(\frac{s\left(3M^4 - 8M^2 s + s^2\right)}{32} + \frac{s\left(s + M^2\right) t}{32} \right. \\
& \left. + \frac{\left(s - M^2\right)^4 \left(M^2 + s\right)}{32\left(\left(s - M^2\right)^2 + st\right)} + \frac{M^2 \left(M^2 \left(s - M^2\right)^2 - 2s^3\right)}{8\left(t - 4M^2\right)} \right) J^{(1)}(p_1, q) \\
& - \kappa^4 \left(\frac{3M^4 - 14M^2 s + 15s^2}{64} + \frac{M^6 - 2M^4 s - M^2 s^2 - 2s^3}{16\left(4M^2 - t\right)} + \frac{\left(s - M^2\right)^3}{8t} \right) I^{(1)}(q) \\
& - \frac{\kappa^4 s^2}{16} I^{(2)}(p_1, p_2)
\end{aligned}
\tag{4.118}
$$

fig. 4.17: The cross box diagram is given by interchanging p_2 and $-p_4$ in the box diagram.

$$
\begin{aligned}
H^{\phi\omega} \quad = \quad & \int \frac{\tau_1^{\alpha\beta}(p_1 - q, p_1 - k, M)\, i\tau_1^{\gamma\delta}(p_1 - k, p_1, M)\, iP_{\gamma\delta,\epsilon\zeta} iP_{\alpha\beta,\rho\sigma}}{\left(\left(p_1 - k\right)^2 - M^2\right)\left(k^2 - \lambda^2\right)\left(\left(k - q\right)^2 - \lambda^2\right)} \\
& \cdot \frac{\tau_1^{\omega,\psi,\epsilon\zeta}(p_2 + q, p_2 + q - k)\left(-i\eta_{\psi\chi}\right)\tau_1^{\chi,\phi,\rho\sigma}(p_2 + q - k, p_2, m)}{\left(\left(p_2 + q - k\right)^2 - m^2\right)} \frac{\mathrm{d}^4 k}{(2\pi)^4}
\end{aligned}
$$

$$
\begin{aligned}
H_1 &= \frac{\kappa^4}{32}\left(\left(u-M^2\right)^4+ut\left(u-M^2\right)^2+\frac{\left(u-M^2\right)^6}{\left(u-M^2\right)^2+ut}\right)K\left(p_1,-p_2-q,q\right)\\
&-\frac{\kappa^4}{32}\left(\left(u-M^2\right)^3+ut\left(u-M^2\right)+\frac{\left(u-M^2\right)^5}{\left(u-M^2\right)^2+ut}\right)J^{(1)}\left(-p_2-q,q\right)\\
&+\frac{\kappa^4}{16}\left(\left(u-M^2\right)^2u+\frac{\left(u-M^2\right)^4u}{\left(u-M^2\right)^2+ut}\right)J^{(2)}\left(p_1,-p_2-q\right)\\
&+\kappa^4\left(\frac{ut\left(3M^2-u\right)}{32}+\frac{2M^6+5M^4u+10M^2u^2-u^3}{32}-\frac{\left(u-M^2\right)^4\left(M^2+u\right)}{32\left(\left(u-M^2\right)^2+ut\right)}\right.\\
&\left.+\frac{3M^6\left(M^2+u\right)^2}{2\left(t-4M^2\right)^2}+\frac{M^2\left(2M^6+8M^4u+3M^2u^2+u^3\right)}{4\left(t-4M^2\right)}\right)J^{(1)}\left(p_1,q\right)\\
&-\kappa^4\left(-\frac{3M^4-10M^2u+15u^2}{64}-\frac{\left(u-M^2\right)^3}{8t}-\frac{3ut}{32}\right.\\
&\left.+\frac{M^6+6M^4u+2M^2u^2+u^3}{8\left(4M^2-t\right)}-\frac{3M^4\left(M^2+u\right)^2}{4\left(t-4M^2\right)^2}\right)I^{(1)}\left(q\right)\\
&+\frac{\kappa^4u^2}{16}I^{(2)}\left(p_1,-p_2-q\right)\\
H_2 &= -\frac{\kappa^4}{32}\left(\left(u-M^2\right)^4+ut\left(u-M^2\right)^2+\frac{\left(u-M^2\right)^6}{\left(u-M^2\right)^2+ut}\right)K\left(p_1,-p_2-q,q\right)\\
&+\frac{\kappa^4}{32}\left(\left(u-M^2\right)^3+\left(u-M^2\right)ut+\frac{\left(u-M^2\right)^5}{\left(u-M^2\right)^2+ut}\right)J^{(1)}\left(-p_2-q,q\right)\\
&-\frac{\kappa^4}{16}\left(\left(u-M^2\right)^2u+\frac{\left(u-M^2\right)^4u}{\left(u-M^2\right)^2+ut}\right)J^{(2)}\left(p_1,-p_2-q\right)\\
&-\kappa^4\left(-\frac{u\left(3M^4-8M^2u+u^2\right)}{32}-\frac{u\left(M^2+u\right)t}{32}\right.\\
&\left.-\frac{\left(u-M^2\right)^4\left(M^2+u\right)}{32\left(\left(u-M^2\right)^2+ut\right)}+\frac{M^2\left(M^2\left(u-M^2\right)^2-2u^3\right)}{8\left(4M^2-t\right)}\right)J^{(1)}\left(p_1,q\right)\\
&-\kappa^4\left(\frac{3M^4-14M^2u+15u^2}{64}+\frac{M^6-2M^4u-M^2u^2-2u^3}{16\left(4M^2-t\right)}+\frac{\left(u-M^2\right)^3}{8t}\right)I^{(1)}\left(q\right)\\
&-\frac{\kappa^4u^2}{16}I^{(2)}\left(p_1,-p_2-q\right) \qquad (4.119)
\end{aligned}
$$

4.7.4 Triangle Diagrams

The result for the triangle diagrams are:

fig. 4.18: The result for the triangle diagram is

$$
H^{\phi\omega} = \int \tau_2^{\rho\sigma,\epsilon\zeta}\left(p_1,p_1-q,M\right)
$$

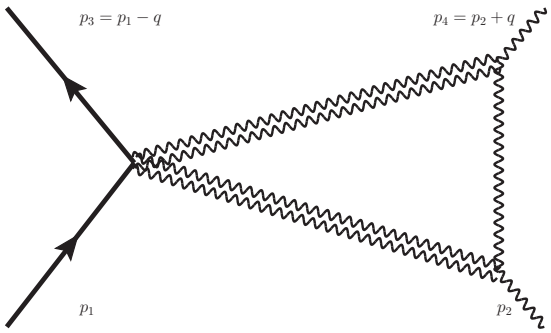

Figure 4.18. Triangle diagram.

$$\frac{iP_{\epsilon\zeta,\alpha\beta}\tau_1^{\omega,\psi,\alpha\beta}\left(p_2+q,p_2+k\right)\left(-i\eta_{\psi\chi}\right)\tau_1^{\chi,\phi,\gamma\delta}\left(p_2+k,p_2,m\right)iP_{\gamma\delta,\rho\sigma}}{\left(\left(k-q\right)^2-\lambda^2\right)\left(\left(p_2+k\right)^2-m^2\right)\left(k^2-\lambda^2\right)}\frac{\mathrm{d}^4k}{\left(2\pi\right)^4}$$

$$\begin{aligned} H_1 &= -\frac{3\kappa^4M^2t}{8}I^{(1)}\left(q\right) \\ H_2 &= -\frac{3\kappa^4M^2t}{8}I^{(1)}\left(q\right) \end{aligned} \tag{4.120}$$

Mirror triangle:

$$\begin{aligned} H^{\phi\omega} &= \int\frac{iP_{\epsilon\zeta,\alpha\beta}\tau_1^{\alpha\beta}\left(p_1-q,p_1-k,M\right)i\tau_1^{\gamma\delta}\left(p_1-k,p_1,M\right)iP_{\gamma\delta,\rho\sigma}}{\left(\left(p_1-k\right)^2-M^2\right)\left(\left(k-q\right)^2-\lambda^2\right)\left(k^2-\lambda^2\right)}\tau_2^{\phi,\omega,\rho\sigma,\epsilon\zeta}\left(p_2,p_2+q\right)\frac{\mathrm{d}^4k}{\left(2\pi\right)^4} \\ H_1 &= \frac{\kappa^4}{16}\left(-M^2\left(5M^4+2M^2s+s^2\right)-M^2\left(3M^2+s\right)t\right. \\ &\quad \left.+\frac{1}{2}M^2t^2-\frac{4M^4\left(5M^4+2M^2s+s^2\right)}{t-4M^2}\right)J^{(1)}\left(p_1,q\right) \\ &\quad +\frac{\kappa^4}{16}\left(-\frac{1}{2}\left(9M^4-6M^2s+5s^2\right)-\frac{5}{2}t\left(M^2+s\right)\right. \\ &\quad \left.+\frac{3t^2}{4}-\frac{2M^2\left(5M^4+2M^2s+s^2\right)}{t-4M^2}\right)I^{(1)}\left(q\right) \\ H_2 &= -\kappa^4\left(\frac{M^2\left(5M^4+14M^2s+s^2\right)}{16}+\frac{M^2\left(3M^2+s\right)t}{16}-\frac{M^2t^2}{32}\right. \\ &\quad \left.+\frac{M^4\left(2M^4+5M^2s+s^2\right)}{t-4M^2}+\frac{3M^6\left(M^2+s\right)^2}{\left(t-4M^2\right)^2}\right)J^{(1)}\left(p_1,q\right) \\ &\quad +\frac{\kappa^4}{2}\left(-\frac{5t\left(M^2-s\right)}{16}+\frac{\left(M^4-18M^2s+5s^2\right)}{16}+\frac{M^2\left(3M^4+8M^2s+s^2\right)}{8M^2-2t}\right. \\ &\quad \left.-\frac{3M^4\left(M^2+s\right)^2}{\left(t-4M^2\right)^2}+\frac{3t^2}{32}\right)I^{(1)}\left(q\right) \end{aligned} \tag{4.121}$$

4.7.5 Double Seagull

The result for the double seagull diagram fig. 4.19is:

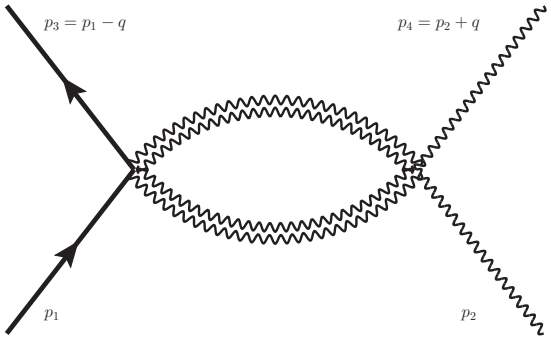

Figure 4.19. Double seagull diagram.

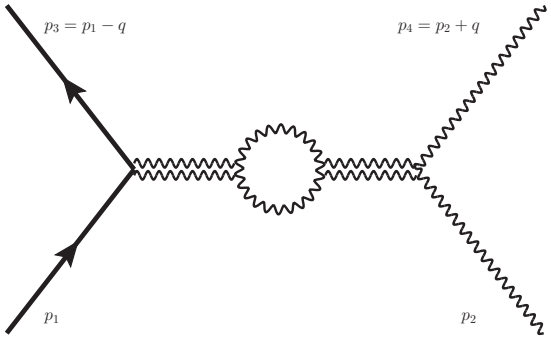

Figure 4.20. Photon loop vacuum polarization.

$$
\begin{aligned}
H^{\phi\omega} &= \frac{1}{2}\int \frac{\tau_2^{\rho\sigma,\epsilon\zeta}\left(p_1, p_1-q, M\right) iP_{\epsilon\zeta,\alpha\beta} iP_{\gamma\delta,\rho\sigma} \tau_2^{\phi,\omega,\gamma\delta,\alpha\beta}\left(p_2, p_2+q\right)}{\left(k^2-\lambda^2\right)\left(\left(k-q\right)^2-\lambda^2\right)} \frac{\mathrm{d}^4k}{\left(2\pi\right)^4} \\
H_1 &= \kappa^4\left(\frac{\left(s-M^2\right)^2}{4}+\frac{\left(3M^2+2s\right)t}{8}\right) I^{(1)}\left(q\right) \\
H_2 &= \kappa^4\left(-\frac{\left(s-M^2\right)^2}{4}+\frac{\left(3M^2-2s\right)t}{8}\right) I^{(1)}\left(q\right)
\end{aligned}
\tag{4.122}
$$

4.7.6 Vacuum Polarization

The result for the vacuum polarization diagrams are:

fig. 4.20 (photon loop):

$$
\begin{aligned}
H^{\phi\omega} &= \int \tau_1^{\kappa\lambda}\left(p_1, p_1-q, M\right) \frac{iP_{\kappa\lambda,\alpha\beta}}{q^2} \frac{\tau_1^{\rho,\sigma,\alpha\beta}\left(-i\eta_{\rho\tau}\right)\left(-i\eta_{\sigma\theta}\right)\tau_1^{\tau,\theta,\gamma\delta}}{\left(k^2-m^2\right)\left(\left(k+q\right)^2-m^2\right)} \\
&\quad \cdot \frac{iP_{\gamma\delta,\mu\nu}}{q^2} \tau_1^{\phi,\omega,\mu\nu}\left(p_2, p_2+q\right) \frac{\mathrm{d}^4k}{\left(2\pi\right)^4} \\
H_1 &= \frac{\kappa^4}{40}\left(\left(s-M^2\right)^2+st\right) I^{(1)}\left(q\right)
\end{aligned}
$$

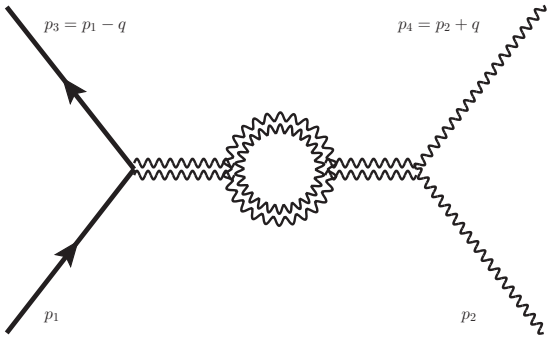

Figure 4.21. Graviton loop vacuum polarization.

$$H_2 = -\frac{\kappa^4}{40}\left(\left(s-M^2\right)^2+st\right)I^{(1)}(q) \tag{4.123}$$

fig. 4.21 (graviton loop):

$$\begin{aligned} H^{\phi\omega} &= \tau_1^{\kappa\lambda}(p_1, p_1-q, M)\frac{iP_{\kappa\lambda,\alpha\beta}}{q^2}\Pi^{\alpha\beta,\gamma\delta}(q)\frac{iP_{\gamma\delta,\mu\nu}}{q^2}\tau_1^{\phi,\omega,\mu\nu}(p_2, p_2+q) \\ H_1 &= \frac{7}{160}\kappa^4\left(\left(s-M^2\right)^2+st\right)\frac{i\log(-t)}{16\pi^2} \\ H_2 &= -\frac{7}{160}\kappa^4\left(\left(s-M^2\right)^2+st\right)\frac{i\log(-t)}{16\pi^2} \end{aligned} \tag{4.124}$$

Where the graviton polarization operator is again taken from [7], and includes the effect of the diagram like with ghost lines comprising the loop.

4.7.7 Bremsstrahlung

As demonstrated above, the bremsstrahlung cross section has the form (4.86) of the lowest order cross section times a correction independent of the spin. Just as in the scalar case, each soft divergent piece in the elastic cross section is canceled by a corresponding piece in the bremsstrahlung cross section. Collinear divergences still remain after this, but again these vanish when the contribution from all diagrams is added together.

The collinear divergent terms in the vertex diagram are

$$\begin{aligned} H_1 = -H_2 &= \frac{i\kappa^4}{16}\left(\left(s-M^2\right)^2 t+st^2\right)iJ^{(2)}(p_2, -p_2-q) \\ &= \left(-i\kappa^2\frac{\left(s-M^2\right)^2+st}{4t}\right)\frac{-\kappa^2 t}{64\pi^2}\left(\frac{1}{2}\log^2\frac{-t}{m^2}-\log\frac{-t}{\lambda^2}\log\frac{-t}{m^2}\right) \end{aligned} \tag{4.125}$$

and their contribution to the elastic cross section is

$$\left(\frac{\mathrm{d}\sigma}{\mathrm{d}\left(-t\right)}\right)_{1,v} = -\frac{\kappa^6}{16\pi\left(s-M^2\right)^2}\frac{t}{32\pi^2}\left(\frac{\left(s-M^2\right)^2+st}{4t}\right)^2\left(\frac{1}{2}\log^2\frac{-t}{m^2}-\log\frac{-t}{\lambda^2}\log\frac{-t}{m^2}\right) \tag{4.126}$$

The corresponding bremsstrahlung terms are

$$\begin{aligned}\left(\frac{\mathrm{d}\sigma}{\mathrm{d}\left(-t\right)}\right)_{br,v} &= -\frac{\kappa^2}{4}\left(\frac{-t}{2}\right)^2 B_{24}\left(\frac{\mathrm{d}\sigma}{\mathrm{d}\left(-t\right)}\right)_0 \\ &= -\frac{\kappa^6}{16\pi\left(s-M^2\right)^2}\frac{t}{32\pi^2}\left(\frac{\left(s-M^2\right)^2+st}{4t}\right)^2 \\ &\quad\cdot\left(\log\frac{4k_{max}^2}{\lambda^2}\log\frac{-t}{m^2}-\frac{1}{4}\log^2\frac{m^2}{4E_2^2}-\frac{1}{4}\log^2\frac{m^2}{4E_4^2}-\ \mathrm{Li}_2\left(1-\frac{4E_2E_4}{-t}\right)\right)\end{aligned} \tag{4.127}$$

and thus the sum is

$$\begin{aligned}&\left(\frac{\mathrm{d}\sigma}{\mathrm{d}\left(-t\right)}\right)_{1,v}+\left(\frac{\mathrm{d}\sigma}{\mathrm{d}\left(-t\right)}\right)_{br,v} \\ &=\frac{\kappa^6}{16\pi\left(s-M^2\right)^2}\frac{t}{32\pi^2}\left(\frac{\left(s-M^2\right)^2+st}{4t}\right)^2 \\ &\cdot\left(\frac{1}{2}\left(\log\frac{E_2^2}{k_{max}^2}+\log\frac{E_4^2}{k_{max}^2}\right)\log\frac{-t}{m^2}+\frac{1}{4}\log^2\frac{-t}{4E_2^2}+\frac{1}{4}\log^2\frac{-t}{4E_4^2}+\ \mathrm{Li}_2\left(1-\frac{4E_iE_j}{-t}\right)\right)\end{aligned} \tag{4.128}$$

independent of polarization.

For the collinear divergent terms in the box diagram,

$$\begin{aligned}H_1=-H_2 &= \frac{\kappa^4}{32}\left(\left(s-M^2\right)^4+st\left(s-M^2\right)^2+\frac{\left(s-M^2\right)^6}{\left(s-M^2\right)^2+st}\right)K \\ &\quad-\frac{\kappa^4}{32}\left(\left(s-M^2\right)^3+st\left(s-M^2\right)+\frac{\left(s-M^2\right)^5}{\left(s-M^2\right)^2+st}\right)J^{(1)}\left(p_2,q\right) \\ &\quad+\frac{\kappa^4}{16}\left(\left(s-M^2\right)^2s+\frac{\left(s-M^2\right)^4s}{\left(s-M^2\right)^2+st}\right)J^{(2)}\left(p_1,p_2\right) \\ &= -\frac{i\kappa^4}{256\pi^2}\left(s-M^2\right)\frac{\left(s-M^2\right)^2+st}{t} \\ &\quad\left(\log\frac{s-M^2}{m^2}\log\frac{s-M^2}{\lambda^2}-\frac{1}{2}\log^2\frac{s-M^2}{m^2}+\log\frac{s-M^2}{M^2}\log\frac{s-M^2}{\lambda^2}\right)\end{aligned}$$

$$
\begin{aligned}
&-\frac{i\kappa^4}{512\pi^2}\left(s-M^2\right)\frac{\left(s-M^2\right)^2+st}{t}\left(1+\frac{\left(s-M^2\right)^4}{\left(\left(s-M^2\right)^2+st\right)^2}\right)\\
&\left(\log\frac{s-M^2}{M^2}\log\frac{-t}{s-M^2}-\frac{1}{2}\log^2\frac{-t}{s-M^2}\right)\\
&-\frac{i\kappa^4}{512\pi^2}\left(s\left(s-M^2\right)+\frac{s\left(s-M^2\right)^3}{\left(s-M^2\right)^2+st}\right)\left(-\frac{1}{2}\log^2\frac{M^2}{s-M^2}-2\ \mathrm{Li}_2\frac{-s}{s-M^2}\right)
\end{aligned}
\tag{4.129}
$$

Thus

$$
\begin{aligned}
\left(\frac{d\sigma}{d\left(-t\right)}\right)_{1,b} &= \frac{\kappa^6}{16\pi\left(s-M^2\right)^2}\frac{\left(s-M^2\right)}{32\pi^2}\left(\frac{\left(s-M^2\right)^2+st}{4t}\right)^2\\
&\cdot\left(\log\frac{s-M^2}{m^2}\log\frac{s-M^2}{\lambda^2}+\log\frac{s-M^2}{M^2}\log\frac{s-M^2}{\lambda^2}-\frac{1}{2}\log^2\frac{s-M^2}{m^2}\right.\\
&+\frac{1}{2}\log\frac{s-M^2}{M^2}\log\frac{-t}{s-M^2}-\frac{1}{4}\log^2\frac{-t}{s-M^2}\\
&\left.+\frac{\left(s-M^2\right)^4}{\left(\left(s-M^2\right)^2+st\right)^2}\left(\frac{1}{2}\log\frac{s-M^2}{M^2}\log\frac{-t}{s-M^2}-\frac{1}{4}\log^2\frac{-t}{s-M^2}\right)\right)
\end{aligned}
\tag{4.130}
$$

The corresponding bremsstrahlung terms are

$$
\begin{aligned}
\left(\frac{\mathrm{d}\sigma}{\mathrm{d}\left(-t\right)}\right)_{br,b} &= \frac{\kappa^2}{4}\left(\left(\frac{s-M^2}{2}\right)^2B_{12}+\left(\frac{s-M^2}{2}\right)^2B_{34}\right)\left(\frac{\mathrm{d}\sigma}{\mathrm{d}\left(-t\right)}\right)_0\\
&= \frac{-\kappa^6}{16\pi\left(s-M^2\right)^2}\frac{\left(s-M^2\right)}{32\pi^2}\left(\frac{\left(s-M^2\right)^2+st}{4t}\right)^2\\
&\cdot\left(\left(\left(\log\frac{s-M^2}{M^2}+\log\frac{s-M^2}{m^2}\right)\log\frac{4k_{max}^2}{\lambda^2}-\frac{1}{4}\log^2\frac{m^2}{4E_2^2}-\frac{1}{4}\log^2\frac{m^2}{4E_4^2}\right.\right.\\
&+\frac{1}{4}\log^2\frac{M^2}{\left(E_1+|\vec{p_1}|\right)^2}+\ \mathrm{Li}_2\left(1+2\left(E_1+|\vec{p_1}|\right)\left(\frac{E_2}{s-M^2}+\frac{E_1}{M^2}\right)\right)\\
&-\mathrm{Li}_2\left(1+4E_2\left(\frac{M^2E_2}{\left(s-M^2\right)^2}-\frac{E_1}{s-M^2}\right)\right)\\
&\left.+\mathrm{Li}_2\left(1+2\left(E_1-|\vec{p_1}|\right)\left(\frac{E_2}{s-M^2}+\frac{E_1}{M^2}\right)\right)\right)\\
&+\frac{1}{4}\log^2\frac{M^2}{\left(E_3+|\vec{p_3}|\right)^2}+\ \mathrm{Li}_2\left(1+2\left(E_3+|\vec{p_3}|\right)\left(\frac{E_4}{s-M^2}+\frac{E_3}{M^2}\right)\right)\\
&-\mathrm{Li}_2\left(1+4E_4\left(\frac{M^2E_4}{\left(s-M^2\right)^2}-\frac{E_3}{s-M^2}\right)\right)
\end{aligned}
$$

$$+\ \mathrm{Li}_2\left(1+2\left(E_3-|\vec{p_3}|\right)\left(\frac{E_4}{s-M^2}+\frac{E_3}{M^2}\right)\right)\Bigg) \tag{4.131}$$

and the sum is

$$\begin{aligned}
&\left(\frac{\mathrm{d}\sigma}{\mathrm{d}\left(-t\right)}\right)_{1,b}+\left(\frac{\mathrm{d}\sigma}{\mathrm{d}\left(-t\right)}\right)_{br,b}\\
&=\frac{\kappa^6}{16\pi\left(s-M^2\right)^2}\frac{\left(s-M^2\right)}{32\pi^2}\left(\frac{\left(s-M^2\right)^2+st}{4t}\right)^2\\
&\cdot\Bigg(\log\frac{s-M^2}{M^2}\log\frac{s-M^2}{4k_{max}^2}+\frac{1}{2}\left(\log\frac{E_2^2}{k_{max}^2}+\log\frac{E_4^2}{k_{max}^2}\right)\log\frac{s-M^2}{m^2}\\
&+\frac{1}{4}\log^2\frac{s-M^2}{4E_2^2}+\frac{1}{4}\log^2\frac{s-M^2}{4E_4^2}+\frac{1}{2}\log\frac{s-M^2}{M^2}\log\frac{-t}{s-M^2}-\frac{1}{4}\log^2\frac{-t}{s-M^2}\\
&+\frac{\left(s-M^2\right)^4}{\left(\left(s-M^2\right)^2+st\right)^2}\left(\frac{1}{2}\log\frac{s-M^2}{M^2}\log\frac{-t}{s-M^2}-\frac{1}{4}\log^2\frac{-t}{s-M^2}\right)\\
&+\frac{1}{4}\log^2\frac{M^2}{\left(E_1+|\vec{p_1}|\right)^2}+\ \mathrm{Li}_2\left(1+2\left(E_1+|\vec{p_1}|\right)\left(\frac{E_2}{s-M^2}+\frac{E_1}{M^2}\right)\right)\\
&-\ \mathrm{Li}_2\left(1+4E_2\left(\frac{M^2E_2}{\left(s-M^2\right)^2}-\frac{E_1}{s-M^2}\right)\right)+\ \mathrm{Li}_2\left(1+2\left(E_1-|\vec{p_1}|\right)\left(\frac{E_2}{s-M^2}+\frac{E_1}{M^2}\right)\right)\Bigg)\\
&+\frac{1}{4}\log^2\frac{M^2}{\left(E_3+|\vec{p_3}|\right)^2}+\ \mathrm{Li}_2\left(1+2\left(E_3+|\vec{p_3}|\right)\left(\frac{E_4}{s-M^2}+\frac{E_3}{M^2}\right)\right)\\
&-\ \mathrm{Li}_2\left(1+4E_4\left(\frac{M^2E_4}{\left(s-M^2\right)^2}-\frac{E_3}{s-M^2}\right)\right)+\ \mathrm{Li}_2\left(1+2\left(E_3-|\vec{p_3}|\right)\left(\frac{E_4}{s-M^2}+\frac{E_3}{M^2}\right)\right)\Bigg)
\end{aligned} \tag{4.132}$$

again independent of polarization.

The collinear terms in the cross box diagram are obtained by replacing p_2 with $-p_4$ and s with u in the radiative corrections (note that the quantity $\left(s-M^2\right)^2+st$ is invariant under this transformation). Thus

$$\begin{aligned}
&\left(\frac{\mathrm{d}\sigma}{\mathrm{d}\left(-t\right)}\right)_{1,c}+\left(\frac{\mathrm{d}\sigma}{\mathrm{d}\left(-t\right)}\right)_{br,c}\\
&=\frac{\kappa^6}{16\pi\left(s-M^2\right)^2}\frac{\left(u-M^2\right)}{32\pi^2}\left(\frac{\left(s-M^2\right)^2+st}{4t}\right)^2\\
&\cdot\Bigg(\log\frac{u-M^2}{M^2}\log\frac{u-M^2}{4k_{max}^2}+\frac{1}{2}\left(\log\frac{E_2^2}{k_{max}^2}+\log\frac{E_4^2}{k_{max}^2}\right)\log\frac{u-M^2}{m^2}\\
&+\frac{1}{4}\log^2\frac{u-M^2}{4E_2^2}+\frac{1}{4}\log^2\frac{u-M^2}{4E_4^2}+\frac{1}{2}\log\frac{u-M^2}{M^2}\log\frac{-t}{u-M^2}-\frac{1}{4}\log^2\frac{-t}{u-M^2}\\
&+\frac{\left(u-M^2\right)^4}{\left(\left(s-M^2\right)^2+st\right)^2}\left(\frac{1}{2}\log\frac{u-M^2}{M^2}\log\frac{-t}{u-M^2}-\frac{1}{4}\log^2\frac{-t}{u-M^2}\right)+
\end{aligned}$$

$$
\begin{aligned}
&+\operatorname{Li}_2\left(1+2\left(E_1+|\vec{p_1}|\right)\left(\frac{E_4}{s-M^2}+\frac{E_1}{M^2}\right)\right)-\operatorname{Li}_2\left(1+4E_4\left(\frac{M^2E_4}{\left(s-M^2\right)^2}-\frac{E_1}{s-M^2}\right)\right)\\
&+\operatorname{Li}_2\left(1+2\left(E_1-|\vec{p_1}|\right)\left(\frac{E_4}{s-M^2}+\frac{E_1}{M^2}\right)\right)+\frac{1}{4}\log^2\frac{M^2}{\left(E_1+|\vec{p_1}|\right)^2}\\
&+\operatorname{Li}_2\left(1+2\left(E_3+|\vec{p_3}|\right)\left(\frac{E_2}{s-M^2}+\frac{E_3}{M^2}\right)\right)-\operatorname{Li}_2\left(1+4E_2\left(\frac{M^2E_2}{\left(s-M^2\right)^2}-\frac{E_3}{s-M^2}\right)\right)\\
&+\operatorname{Li}_2\left(1+2\left(E_3-|\vec{p_3}|\right)\left(\frac{E_2}{s-M^2}+\frac{E_3}{M^2}\right)\right)+\frac{1}{4}\log^2\frac{M^2}{\left(E_3+|\vec{p_3}|\right)^2}\Bigg)
\end{aligned}
\tag{4.133}
$$

independent of polarization.

The sum of the collinear terms in all these diagrams is therefore

$$
\begin{aligned}
&\left(\frac{\mathrm{d}\sigma}{\mathrm{d}\left(-t\right)}\right)_1+\left(\frac{\mathrm{d}\sigma}{\mathrm{d}\left(-t\right)}\right)_{br}\\
&=\frac{\kappa^6}{16\pi\left(s-M^2\right)^2}\frac{1}{32\pi^2}\left(\frac{\left(s-M^2\right)^2+st}{4t}\right)^2\\
&\cdot\Bigg(t\operatorname{Li}_2\left(1-\frac{4E_2E_4}{-t}\right)\\
&+\left(s-M^2\right)\left(\log\frac{s-M^2}{M^2}\log\frac{s-M^2}{4k_{max}^2}+\log\frac{-t}{4k_{max}^2}\log\frac{s-M^2}{-t}+\frac{1}{2}\log^2\frac{s-M^2}{-t}\right.\\
&+\frac{1}{2}\log\frac{s-M^2}{M^2}\log\frac{-t}{s-M^2}-\frac{1}{4}\log^2\frac{-t}{s-M^2}\\
&+\frac{\left(s-M^2\right)^4}{\left(\left(s-M^2\right)^2+st\right)^2}\left(\frac{1}{2}\log\frac{s-M^2}{M^2}\log\frac{-t}{s-M^2}-\frac{1}{4}\log^2\frac{-t}{s-M^2}\right)\\
&+\frac{1}{2}\log^2\frac{M^2}{\left(E_1+|\vec{p_1}|\right)^2}+\operatorname{Li}_2\left(1+2\left(E_1+|\vec{p_1}|\right)\left(\frac{E_2}{s-M^2}+\frac{E_1}{M^2}\right)\right)\\
&-\operatorname{Li}_2\left(1+4E_2\left(\frac{M^2E_2}{\left(s-M^2\right)^2}-\frac{E_1}{s-M^2}\right)\right)+\operatorname{Li}_2\left(1+2\left(E_1-|\vec{p_1}|\right)\left(\frac{E_2}{s-M^2}+\frac{E_1}{M^2}\right)\right)\\
&+\frac{1}{2}\log^2\frac{M^2}{\left(E_3+|\vec{p_3}|\right)^2}+\operatorname{Li}_2\left(1+2\left(E_3+|\vec{p_3}|\right)\left(\frac{E_4}{s-M^2}+\frac{E_3}{M^2}\right)\right)\\
&-\operatorname{Li}_2\left(1+4E_4\left(\frac{M^2E_4}{\left(s-M^2\right)^2}-\frac{E_3}{s-M^2}\right)\right)+\operatorname{Li}_2\left(1+2\left(E_3-|\vec{p_3}|\right)\left(\frac{E_4}{s-M^2}+\frac{E_3}{M^2}\right)\right)\Bigg)\\
&+\left(u-M^2\right)\left(\log\frac{u-M^2}{M^2}\log\frac{u-M^2}{4k_{max}^2}+\log\frac{-t}{4k_{max}^2}\log\frac{u-M^2}{-t}+\frac{1}{2}\log^2\frac{u-M^2}{-t}\right.\\
&+\frac{1}{2}\log\frac{u-M^2}{M^2}\log\frac{-t}{u-M^2}-\frac{1}{4}\log^2\frac{-t}{u-M^2}\\
&+\frac{\left(u-M^2\right)^4}{\left(\left(s-M^2\right)^2+st\right)^2}\left(\frac{1}{2}\log\frac{u-M^2}{M^2}\log\frac{-t}{u-M^2}-\frac{1}{4}\log^2\frac{-t}{u-M^2}\right)\\
&+\operatorname{Li}_2\left(1+2\left(E_1+|\vec{p_1}|\right)\left(\frac{E_4}{s-M^2}+\frac{E_1}{M^2}\right)\right)-\operatorname{Li}_2\left(1+4E_4\left(\frac{M^2E_4}{\left(s-M^2\right)^2}-\frac{E_1}{s-M^2}\right)\right)
\end{aligned}
$$

$$+\ \mathrm{Li}_2\left(1+2\left(E_1-|\vec{p_1}|\right)\left(\frac{E_4}{s-M^2}+\frac{E_1}{M^2}\right)\right)+\ \mathrm{Li}_2\left(1+2\left(E_3+|\vec{p_3}|\right)\left(\frac{E_2}{s-M^2}+\frac{E_3}{M^2}\right)\right)$$
$$-\ \mathrm{Li}_2\left(1+4E_2\left(\frac{M^2E_2}{\left(s-M^2\right)^2}-\frac{E_3}{s-M^2}\right)\right)+\ \mathrm{Li}_2\left(1+2\left(E_3-|\vec{p_3}|\right)\left(\frac{E_2}{s-M^2}+\frac{E_3}{M^2}\right)\right)\Bigg)\Bigg) \tag{4.134}$$

This is free of all IR divergences.

4.7.8 Total

Adding to (4.134) the remaining pieces from the elastic diagrams (4.112) to (4.124), the total cross section at low t is

$$\begin{aligned}\left(\frac{d\sigma}{d\left(-t\right)}\right)_{tot,\parallel} &= \frac{\kappa^6}{\left(16\pi\right)^3}\frac{-\left(s-M^2\right)^2}{4t}\left(\pi^2\frac{17}{4}\frac{M}{\sqrt{-t}}-\frac{76}{15}\log\frac{-t}{4\pi\mu^2}\right.\\ &\quad -4\log^2\frac{-t}{s-M^2}-6\log\frac{M^2}{s-M^2}\log\frac{-t}{s-M^2}-2\log\frac{s-M^2}{k_{max}^2}\log\frac{-t}{s-M^2}\\ &\quad \left.-2\log\frac{s-M^2}{k_{max}^2}\log\frac{M^2}{s-M^2}+5\log\frac{-t}{s-M^2}+4\log\frac{s-M^2}{k_{max}^2}\right)\end{aligned} \tag{4.135}$$

for polarization in the plane of scattering, and

$$\begin{aligned}\left(\frac{d\sigma}{d\left(-t\right)}\right)_{tot,\perp} &= \frac{\kappa^6}{\left(16\pi\right)^3}\frac{-\left(s-M^2\right)^2}{4t}\left(\pi^2\frac{17}{4}\frac{M}{\sqrt{-t}}+\frac{8}{5}\log\frac{-t}{4\pi\mu^2}\right.\\ &\quad -4\log^2\frac{-t}{s-M^2}-6\log\frac{M^2}{s-M^2}\log\frac{-t}{s-M^2}-2\log\frac{s-M^2}{k_{max}^2}\log\frac{-t}{s-M^2}\\ &\quad \left.-2\log\frac{s-M^2}{k_{max}^2}\log\frac{M^2}{s-M^2}+5\log\frac{-t}{s-M^2}+4\log\frac{s-M^2}{k_{max}^2}\right)\end{aligned} \tag{4.136}$$

for polarization perpendicular to the plane of scattering. Note that the total classical correction, the term proportional to $M/\sqrt{-t}$, is independent of the direction of polarization, while the quantum term proportional to $\log -t$ is polarization dependent. As can be seen by adding the $J^{(1)}$ terms in (4.112) through (4.124), this is true to this order of perturbation theory, not just for low t, but for arbitrary values of t.

Just as in the scalar case, some of these terms can be interpreted as corrections to the metric surrounding one of the particles. In the next chapter this possibility will be examined and the full cross section will be used to calculate the bending of light around a massive object.

CHAPTER 5

INTERPRETATION OF RESULTS

The results of chapter 4 are now interpreted and applied in several ways. As pointed out below (4.101), the results can be broken into pieces involving the different particle lines. Those pieces which come strictly from the massive side of the diagram have already been treated in [7]. As was pointed out in [6], the vertex corrections represent corrections to the energy-momentum tensor, and therefore the metric, surrounding the massive particle. It is examined here whether the vertex diagrams from the massless side can be interpreted as corrections to the energy-momentum tensor and metric surrounding a massless particle. When expressing the metric it is more convenient to write λ for the soft IR regulator, but as always this can be changed to dimensional regularization via the substitution $\log \lambda^2 \to \frac{2}{\epsilon_{IR}} + \gamma + \log 4\pi\mu^2$. Finally, the total cross section is used in order to calculate an actual physical observable, the deflection of light by a massive source.

5.1 Metric

5.1.1 Summary of Massive Case

In the limit where the mass of one of the particles in fig. 4.1 becomes very large compared to the momentum transfer, the state of that particle will not be altered much by the interaction, and it will behave as the source of a fixed external field in which the other particle moves. This field is obtained by the cutting the graviton line of the diagram cut at the other particle vertex, as in fig. 5.1. The energy-momentum distribution of the source is given by its vertex part, and the field is determined from the energy-momentum tensor by the graviton propagator.

The lowest-order energy-momentum tensor of a scalar particle is given by the bare vertex in 5.1a [6]:

$$\langle p_4| T_{\mu\nu}(x) |p_2\rangle = \frac{e^{iq\cdot x}}{\sqrt{E_4 E_2}} \left(P_\mu P_\nu - \frac{1}{4}\left(q_\mu q_\nu - \eta_{\mu\nu} q^2\right)\right) \tag{5.1}$$

where $p_4 = (E_4, \vec{p_4})$ and $p_2 = (E_2, \vec{p_2})$ are the momenta of the source particle before and after the collision, $P = \frac{p_4+p_2}{2}$, $q = p_4 - p_2$, and the normalization $\langle p_i|\, p_j\rangle = 2E_i (2\pi)^3 \delta^3(\vec{p_i} - \vec{p_j})$ has been

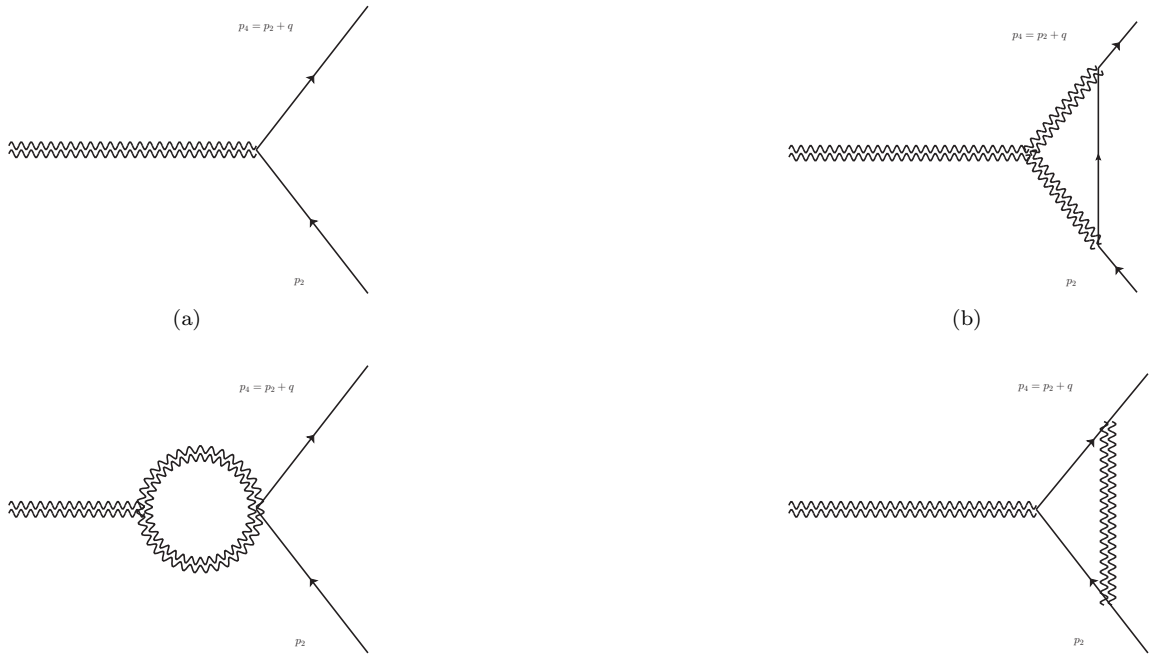

Figure 5.1. The diagrams contributing to the energy-momentum tensor and metric.

used. In the case of a massive particle behaving as a fixed source at rest, $p_4 \approx p_2 \approx P \approx \left(M, \vec{0}\right)$, $q = (0, \vec{q})$, with $\vec{q}^2 \ll M^2$, and so

$$\langle p_4 | \, T_{\mu\nu}(x) \, | p_2 \rangle \approx M \hat{P}_\mu \hat{P}_\nu e^{-i\vec{q}\cdot\vec{x}} \tag{5.2}$$

where $\hat{P} \equiv {}^{P}/_{M} = \left(1, \vec{0}\right)$. Thus, transforming to the position representation,

$$T^{\mu\nu}(x) = \int M \hat{P}_\mu \hat{P}_\nu e^{-i\vec{q}\cdot\vec{x}} \frac{\mathrm{d}^3 q}{(2\pi)^3} = M \delta^3(x) \, \hat{P}^\mu \hat{P}^\nu \tag{5.3}$$

as is appropriate for a point particle at rest.

The linearized Einstein equation is:

$$\Box \psi^{\mu\nu}(x) = -16\pi G T^{\mu\nu}(x) \tag{5.4}$$

where $\psi_{\mu\nu} = h_{\mu\nu} - \frac{1}{2} h^\rho_\rho \eta_{\mu\nu}$, $g_{\mu\nu} = \eta_{\mu\nu} - h_{\mu\nu}$. The solution is determined in the momentum representation by

$$\psi^{\mu\nu}(q) = \frac{16\pi G}{q^2} \langle p_4 | \, T_{\mu\nu}(x) \, | p_2 \rangle \tag{5.5}$$

(This is equivalent to contracting the bare vertex with the graviton propagator.) In the lowest order case these become

$$\begin{aligned} \Box\psi^{\mu\nu} &= -16\pi GM\delta^3\left(\vec{x}\right)\hat{P}^\mu\hat{P}^\nu \\ \psi^{\mu\nu}\left(q\right) &= \frac{16\pi G}{-\vec{q}^2}M\hat{P}_\mu\hat{P}_\nu e^{-i\vec{q}\cdot\vec{x}} \end{aligned} \tag{5.6}$$

Now,

$$\int \frac{e^{-i\vec{q}\cdot\vec{x}}}{\vec{q}^2}\frac{\mathrm{d}^3q}{\left(2\pi\right)^3} = \frac{1}{4\pi r} \tag{5.7}$$

the Green function of the three-dimensional Poisson equation. So, Fourier transforming back to the position representation,

$$\begin{aligned} \psi_{\mu\nu} &= -\frac{4MG}{r}\hat{P}_\mu\hat{P}_\nu \\ h_{\mu\nu} &= -\frac{2MG}{r}\left(2\hat{P}_\mu\hat{P}_\nu - \eta_{\mu\nu}\right) \end{aligned} \tag{5.8}$$

which is the correct Newtonian form, as found by [6].

5.1.2 Aichelburg-Sexl Metric

When the source of the field is massless, it is obviously impossible to consider the limit where the mass becomes infinite. Nevertheless, if the momentum transferred to the source particle is small compared to its momentum and energy in some frame, it is apparent that the source will still be unchanged by the interaction and generate a fixed external field in which the other particle moves. The metric surrounding a massless particle has been given previously by Aichelburg and Sexl [8, 9, 11]. Their result is reproduced here in a new way using Feynman diagrams, following the method used by [6] for the massive case.

The lowest-order energy-momentum tensor of a massless scalar particle is still given by (5.1), now with $E_2 = \|\vec{p_2}\|$, $E_4 = \|\vec{p_4}\|$. For the particle to act like a fixed source, $p_4 \approx p_2 \approx P \gg q$, and so

$$\left\langle p_4\right| T_{\mu\nu}\left(x\right)\left|p_2\right\rangle \approx E\hat{P}_\mu\hat{P}_\nu e^{iq\cdot x} \tag{5.9}$$

where $E \approx E_4 \approx E_2$ is the time component of P and$\hat{P} \equiv {}^{P}/_{E}$. Further,

$$E_2 = \|\vec{p_2}\| = \left\|\vec{P} - \vec{q}/2\right\| = \sqrt{\vec{P}^2 + \vec{P}\cdot\vec{q} + \frac{\vec{q}^2}{4}} \approx \left\|\vec{P}\right\| - \frac{\vec{P}\cdot\vec{q}}{2\left\|\vec{P}\right\|}$$

$$E_4 \quad = \quad \|\vec{p_4}\| = \left\|\vec{P} + \vec{q}/2\right\| = \sqrt{\vec{P}^2 - \vec{P}\cdot\vec{q} + \frac{\vec{q}^2}{4}} \approx \left\|\vec{P}\right\| + \frac{\vec{P}\cdot\vec{q}}{2\left\|\vec{P}\right\|} \tag{5.10}$$

so

$$q_t = E_4 - E_2 \approx \frac{\vec{P}}{\left\|\vec{P}\right\|}\cdot\vec{q} = q_x, \tag{5.11}$$

and $q\cdot x \approx q_x\left(t-x\right) - q_y y - q_z z$, where the x-axis is taken to be in the direction of $\vec{P}$. Thus, transforming to the position representation,

$$T^{\mu\nu}\left(x\right) = \int E\hat{P}_\mu\hat{P}_\nu e^{-i\left(q_x\left(x-t\right)+q_y y+q_z z\right)}\frac{\mathrm{d}^3 q}{\left(2\pi\right)^3} = E\delta\left(x-t\right)\delta\left(y\right)\delta\left(z\right)\hat{P}^\mu\hat{P}^\nu \tag{5.12}$$

which is Aichelburg and Sexl's form for the energy-momentum tensor of a massless particle of energy E moving at the speed of light[8]. Inserting these into (5.5) one obtains

$$\begin{aligned} \Box\psi^{\mu\nu} \quad &= \quad -16\pi G E\delta\left(x-t\right)\delta\left(y\right)\delta\left(z\right)\hat{P}^\mu\hat{P}^\nu \\ \psi^{\mu\nu}\left(q\right) \quad &= \quad \frac{16\pi G}{q^2}Ee^{iq\cdot x}\hat{P}^\mu\hat{P}^\nu \approx -\frac{16\pi G}{q_y^2+q_z^2}Ee^{-i\left(q_x\left(x-t\right)+q_y y+q_z z\right)}\hat{P}^\mu\hat{P}^\nu \end{aligned} \tag{5.13}$$

since $q_t \approx q_x$. Now,

$$\int e^{-iq_x\left(x-t\right)}\frac{\mathrm{d}q_x}{2\pi} = \delta\left(x-t\right) \tag{5.14}$$

and

$$\int \frac{1}{q_y^2+q_z^2}e^{-i\left(q_y y+q_z z\right)}\frac{\mathrm{d}q_y\mathrm{d}q_z}{\left(2\pi\right)^2} = -\frac{\log\rho}{2\pi} \tag{5.15}$$

the Green function of the two-dimensional Poisson equation, where $\rho = \sqrt{y^2+z^2}$ So, Fourier transforming back to the position representation,

$$h^{\mu\nu} = \psi^{\mu\nu} = 8EG\delta\left(x-t\right)\log\left(\rho\right)\hat{P}^\mu\hat{P}^\nu \tag{5.16}$$

which is the form found by Aichelburg and Sexl [8].

For a photon, the lowest order vertex is

$$\begin{aligned} \left\langle p_4,\epsilon_4\right|T_{\mu\nu}\left|p_2,\epsilon_2\right\rangle \quad = \quad & \frac{e^{i\left(p_2-p_1\right)x}}{\sqrt{4E_2E_4}}\left[2P_\mu P_\nu\epsilon_2\cdot\epsilon_4\right. \\ & +P_\mu\left(\epsilon_{4,\nu}\epsilon_2\cdot q - \epsilon_{2,\nu}\epsilon_4\cdot q\right) + P_\nu\left(\epsilon_{4,\mu}\epsilon_2\cdot q - \epsilon_{2,\mu}\epsilon_4\cdot q\right) \\ & -\frac{1}{2}\left(q_\mu q_\nu - \eta_{\mu\nu}q^2\right)\epsilon_2\cdot\epsilon_4 - \eta_{\mu\nu}\epsilon_2\cdot q\epsilon_4\cdot q \\ & \left.+\frac{q_\mu}{2}\epsilon_{4,\nu}\epsilon_2\cdot q + \frac{q_\nu}{2}\epsilon_{4,\mu}\epsilon_2\cdot q + \frac{q_\mu}{2}\epsilon_{2,\nu}\epsilon_4\cdot q + \frac{q_\nu}{2}\epsilon_{2,\mu}\epsilon_4\cdot q\right. \end{aligned}$$

$$-\frac{q^2}{2}\left(\epsilon_{2,\mu}\epsilon_{4,\nu}+\epsilon_{4,\mu}\epsilon_{2,\nu}\right)\Big] \tag{5.17}$$

In the limit of $p_1 \approx p_2 \approx P \gg q$, this becomes

$$\langle p_4,\epsilon_4|\, T_{\mu\nu}\,|p_2,\epsilon_2\rangle \;=\; E\epsilon_2\cdot\epsilon_4\hat{P}_\mu\hat{P}_\nu e^{iqx} \tag{5.18}$$

which is the same as for a scalar, but with an additional factor keeping the initial and final polarizations the same.

5.1.3 Radiative Corrections

The radiative corrections shown in figs. 5.1b-d modify the energy-momentum tensor (5.1) and the metrics (5.8) and (5.16).

The form of the corrected scalar energy-momentum tensor is restricted by several conditions: it must be a symmetric second rank tensor, and it must be compatible with the coordinate invariance of general relativity. The latter requires that it be orthogonal to q, just as does gauge invariance for photons. For a scalar particle, the most general form compatible with these conditions is

$$\langle p_4|\, T_{\mu\nu}\,(x)\,|p_2\rangle = \frac{e^{iq\cdot x}}{\sqrt{4E_4E_2}}\left[2P_\mu P_\nu F_1\left(q^2\right)+\left(q_\mu q_\nu - q^2\eta_{\mu\nu}\right)F_2\left(q^2\right)\right] \tag{5.19}$$

Where F_1 and F_2 are scalar form factors depending on q^2. The lowest order form (5.1) is given by $F_1\left(q^2\right)=1$ and $F_2\left(q^2\right)=-1/2$. The corrected value of $F_1\left(0\right)$ must remain equal to 1 by conservation of energy and momentum [6], but $F_2\left(0\right)$ is unrestricted. The corrected position space representation is again given by the Fourier transform of (5.19).

In the massive case, the radiative corrections were found by [6] to be

$$\begin{aligned} F_1\left(q^2\right) &= \frac{Gq^2}{\pi}\left(-\frac{3}{4}\log\frac{-q^2}{m^2}+\frac{1}{16}\frac{\pi^2 m}{\sqrt{-q^2}}\right) \\ F_2\left(q^2\right) &= \frac{Gm^2}{\pi}\left(-2\log\frac{-q^2}{m^2}+\frac{7}{8}\frac{\pi^2 m}{\sqrt{-q^2}}\right) \end{aligned} \tag{5.20}$$

Substituting these into (5.19) and contracting with a graviton propagator and another scalar vertex reproduces (4.52). Substituting them into (5.19) and Fourier transforming produces both classical corrections and quantum corrections to the energy-momentum tensor in the position representation [6, 7, 21]:

$$T_{00}\left(x\right) \;=\; -\frac{3Gm^2}{8\pi r^4}-\frac{3Gm\hbar}{4\pi^2 r^5}$$

$$
\begin{aligned}
T_{0i}(x) &= 0 \\
T_{ij}(x) &= -\frac{7Gm^2}{4\pi r^4}\left(\frac{r_i r_j}{r^2} - \frac{1}{2}\delta_{ij}\right) + \frac{2Gm\hbar}{\pi^2 r^5}\delta_{ij}
\end{aligned} \tag{5.21}
$$

The square root terms produce classical corrections, which reproduce the leading order corrections in the Schwarzschild solution, while by dimensional analysis the logarithms must have an extra factor of $\hbar$ and therefore produce quantum corrections. The classical corrections were shown in [6] to reproduce the next higher order term in the Schwarzschild solution.

In the massless scalar case, the corrections to the form factors are found to be

$$
\begin{aligned}
\text{Diagram b: } F_1(q^2) &= 0 \\
F_2(q^2) &= \frac{-32\pi G q^2}{3} i I^1(q) \\
\text{Diagram c: } F_1(q^2) &= 0 \\
F_2(q^2) &= 0 \\
\text{Diagram d: } F_1(q^2) &= -24\pi G q^2 i I^1(q) - 8\pi G q^4 i J^{(2)}(p_2, -p_2 - q) \\
F_2(q^2) &= \frac{20\pi G q^2}{3} i I^1(q) - 4\pi G q^4 i J^{(2)}(p_2, -p_2 - q) \\
\text{Totals: } F_1(q^2) &= -24\pi G q^2 i I^1(q) - 8\pi G q^4 i J^{(2)}(p_2, -p_2 - q) \\
F_2(q^2) &= -4\pi G q^2 i I^1(q) + 4\pi G q^4 i J^{(2)}(p_2, -p_2 - q)
\end{aligned} \tag{5.22}
$$

Substituting these results in (5.19) reproduces (4.116). Fig. 5.1d is infrared divergent. Unlike in the cross section, this infrared divergence does not completely vanish, because the box and cross-box diagrams are not included. The implications of this will be considered below.

Notice the absence of classical corrections in (5.22). Aichelburg and Sexl [8] demonstrated explicitly that the linearized solution (5.16) is also an exact solution to Einstein's equation, by beginning with the static Schwarzschild solution, and then applying a kind of improper Lorentz transformation, allowing the rest mass of the particle go to zero as its velocity approaches c. It has in fact been shown [10] that for a general null source the linearized equation is equivalent to the full Einstein equation. Since the lowest order solution is also the exact solution, the classical corrections must vanish. In the present case this can be seen from the Feynman diagrams. Classical corrections are of the form $m/\sqrt{-q^2}$, and require the presence of both massive and massless propagators [21].

The photon energy-momentum tensor depends on more quantities than that in the scalar case, but it also must satisfy additional constraints. The form of the photon energy-momentum tensor may depend on the polarization vectors ϵ_2 and ϵ_4 of the initial and final photon states, in addition

to the momenta P and q. It is constrained by electromagnetic gauge invariance, in addition to the gravitational gauge invariance already present in the scalar and massive vector cases. This requires that when one of the photon momenta is substituted for its polarization vector, the result should equal zero. The most general form of T which satisfies these requirements is

$$\begin{aligned}\langle p_4,\epsilon_4|\,T_{\mu\nu}\,(x)\,|p_2,\epsilon_2\rangle &= \frac{e^{iqx}}{\sqrt{4E_4E_2}}\left[2P_\mu P_\nu\left(\epsilon_2\cdot\epsilon_4-2\frac{\epsilon_2\cdot q\epsilon_4\cdot q}{q^2}\right)F_1\left(q^2\right)\right.\\ &+\left(q_\mu q_\nu-\eta_{\mu\nu}q^2\right)\left(\epsilon_2\cdot\epsilon_4-2\frac{\epsilon_2\cdot q\epsilon_4\cdot q}{q^2}\right)F_2\left(q^2\right)\\ &+\left(4P_\mu P_\nu-q_\mu q_\nu\right)\frac{\epsilon_2\cdot q\epsilon_4\cdot q}{q^2}\\ &+\left(-\left(P_\mu-\frac{q_\mu}{2}\right)\epsilon_{4,\nu}\epsilon_2\cdot q-\left(P_\nu-\frac{q_\nu}{2}\right)\epsilon_{4,\mu}\epsilon_2\cdot q\right.\\ &+\left(P_\mu+\frac{q_\mu}{2}\right)\epsilon_{2,\nu}\epsilon_4\cdot q+\left(P_\nu+\frac{q_\nu}{2}\right)\epsilon_{2,\mu}\epsilon_4\cdot q\\ &\left.\left.-\frac{q^2}{2}\left(\epsilon_{2,\mu}\epsilon_{4,\nu}+\epsilon_{4,\mu}\epsilon_{2,\nu}\right)\right)F_3\left(q^2\right)\right] \qquad (5.23)\end{aligned}$$

where the form factors F_1, F_2, and F_3 are functions of q^2. (Note that although their are divisors of q^2 present in the definition in order to keep the form factors dimensionless, they are canceled by factors of q^2 in the form factors, so that there are no poles in $T_{\mu\nu}\,(q)$.) Electromagnetic gauge invariance reduces the number of form factors from six for a general massive vector particle [12] to three for a photon. From the bare vertex factor (5.17), the lowest order form factors are $F_1=1$, $F_2=-1/2$, $F_3=1$.

These are corrected by the same types of diagrams as in the scalar case. The results are:

$$\begin{aligned}\text{Diagram b: } F_1\left(q^2\right) &= \frac{164}{3}\pi Gq^2iI^1\,(q)\\ F_2\left(q^2\right) &= \frac{55}{3}\pi Gq^2iI^1\,(q)\\ F_3\left(q^2\right) &= \frac{10}{3}\pi Gq^2iI^1\,(q)\\ \text{Diagram c: } F_1\left(q^2\right) &= -48\pi Gq^2iI^1\,(q)\\ F_2\left(q^2\right) &= -20\pi Gq^2iI^1\,(q)\\ F_3\left(q^2\right) &= 0\\ \text{Diagram d: } F_1\left(q^2\right) &= -\frac{100}{3}\pi Gq^2iI^1\,(q)-8\pi Gq^4iJ^{(2)}\,(p_2,-p_2-q)\\ F_2\left(q^2\right) &= \frac{25}{3}\pi Gq^2iI^1\,(q)+4\pi Gq^4iJ^{(2)}\,(p_2,-p_2-q)\\ F_3\left(q^2\right) &= -\frac{50}{3}\pi Gq^2iI^1\,(q)-8\pi Gq^4iJ^{(2)}\,(p_2,-p_2-q)\\ \text{Totals: } F_1\left(q^2\right) &= -\frac{80}{3}\pi Gq^2iI^1\,(q)-8\pi Gq^4iJ^{(2)}\,(p_2,-p_2-q)\end{aligned}$$

$$
\begin{aligned}
F_2\left(q^2\right) &= \frac{20}{3}\pi G q^2 i I^1\left(q\right) + 4\pi G q^4 i J^{(2)}\left(p_2, -p_2 - q\right) \\
F_3\left(q^2\right) &= -\frac{40}{3}\pi G q^2 i I^1\left(q\right) - 8\pi G q^4 i J^{(2)}\left(p_2, -p_2 - q\right)
\end{aligned} \tag{5.24}
$$

Again there are infrared divergences in the diagram of 5.1d.

5.1.4 Fourier Transform and Metric

Substituting (5.22) into (5.19), using the values of $J^{(2)}\left(p_2, -p_2 - q\right)$ and $I^{(1)}\left(q\right)$ from chapter 2, and Fourier transforming, one finds the correction to the energy-momentum tensor in position space is

$$
\begin{aligned}
T^{\mu\nu}\left(x\right) &= \int \frac{e^{-i\left(q_x\left(x-t\right)+q_y y+q_z z\right)}}{2E}\left[2P_\mu P_\nu F_1\left(q^2\right) + \left(q_\mu q_\nu - \eta_{\mu\nu}q^2\right)F_2\left(q^2\right)\right]\frac{\mathrm{d}^3 q}{\left(2\pi\right)^3} \\
&= -\frac{G}{2\pi}E\int e^{-i\left(q_x\left(x-t\right)+q_y y+q_z z\right)}q^2 \\
&\quad \cdot\left(3\log\left(\frac{-q^2}{4\pi\mu^2}\right) + \frac{1}{2}\log^2\left(\frac{-q^2}{m^2}\right) - \log\left(\frac{-q^2}{\lambda^2}\right)\log\left(\frac{-q^2}{m^2}\right)\right)\frac{\mathrm{d}^3 q}{\left(2\pi\right)^3}\hat{P}_\mu\hat{P}_\nu \\
&\quad -\frac{G}{8\pi E}\int e^{-i\left(q_x\left(x-t\right)+q_y y+q_z z\right)}\left(q_\mu q_\nu q^2 - \eta_{\mu\nu}q^4\right) \\
&\quad \cdot\left(\log\left(\frac{-q^2}{4\pi\mu^2}\right) - \frac{1}{2}\log^2\left(\frac{-q^2}{m^2}\right) + \log\left(\frac{-q^2}{\lambda^2}\right)\log\left(\frac{-q^2}{m^2}\right)\right)\frac{\mathrm{d}^3 q}{\left(2\pi\right)^3}
\end{aligned} \tag{5.25}
$$

To lowest order in q (and therefore at long range), this is just

$$
\begin{aligned}
T^{\mu\nu}\left(x\right) &= -\frac{G}{2\pi}E\int e^{-i\left(q_x\left(x-t\right)+q_y y+q_z z\right)}q^2 \\
&\quad \cdot\left(3\log\left(\frac{-q^2}{4\pi\mu^2}\right) + \frac{1}{2}\log^2\left(\frac{-q^2}{m^2}\right) - \log\left(\frac{-q^2}{\lambda^2}\right)\log\left(\frac{-q^2}{m^2}\right)\right)\frac{\mathrm{d}^3 q}{\left(2\pi\right)^3}\hat{P}_\mu\hat{P}_\nu
\end{aligned} \tag{5.26}
$$

Remembering that $-q^2 = q_y^2 + q_z^2$ and using $\log^2\frac{q^2}{m^2} = \log^2\frac{q^2}{\lambda^2} + 2\log\frac{q^2}{\lambda^2}\log\frac{\lambda^2}{m^2} + \log^2\frac{\lambda^2}{m^2}$ this becomes

$$
\begin{aligned}
T^{\mu\nu}\left(x\right) &= -\frac{G}{2\pi}E\int e^{-iq_x\left(x-t\right)}\frac{\mathrm{d}q_x}{2\pi} \\
&\quad \cdot\int e^{i\left(q_y y+q_z z\right)}q^2\left(3\log\left(\frac{-q^2}{4\pi\mu^2}\right) - \frac{1}{2}\log^2\frac{q^2}{\lambda^2} + \frac{1}{2}\log^2\frac{\lambda^2}{m^2}\right)\frac{\mathrm{d}^2 q}{\left(2\pi\right)^2}\hat{P}_\mu\hat{P}_\nu \\
&= -\frac{G}{2\pi}E\delta\left(x-t\right)\int e^{-i\left(q_y y+q_z z\right)}q^2 \\
&\quad \cdot\left(3\log\left(\frac{-q^2}{4\pi\mu^2}\right) - \frac{1}{2}\log^2\frac{q^2}{\lambda^2} + \frac{1}{2}\log^2\frac{\lambda^2}{m^2}\right)\frac{\mathrm{d}^2 q}{\left(2\pi\right)^2}\hat{P}_\mu\hat{P}_\nu
\end{aligned} \tag{5.27}
$$

The Fourier transforms are divergent but can be evaluated as follows. First consider

$$
\int e^{i\left(q_y y+q_z z\right)}\log\left(q\right)\mathrm{d}^2 q = \int e^{iq\rho\cos\theta}\log\left(q\right)\mathrm{d}\theta q\mathrm{d}q
$$

$$= \quad 2\pi \int_0^\infty q J_0\left(q\rho\right) \log\left(q\right) \mathrm{d}q \tag{5.28}$$

where J_n is the Bessel function of order n. The q integral can be evaluated by using the Bessel function identities

$$\begin{aligned} \frac{\partial}{\partial r} J_1\left(q\rho\right) &= \frac{1}{2} q \left(J_0\left(q\rho\right) - J_2\left(q\rho\right)\right) & (5.29) \\ J_1\left(q\rho\right) &= \frac{1}{2} q\rho \left(J_0\left(q\rho\right) + J_2\left(q\rho\right)\right) & (5.30) \end{aligned}$$

so

$$\frac{\partial}{\partial \rho} J_1\left(q\rho\right) + \frac{J_1\left(q\rho\right)}{\rho} = q J_0\left(q\rho\right) \tag{5.31}$$

But the integral

$$\int_0^\infty J_1\left(q\rho\right) \log\left(q\right) \mathrm{d}q = -\frac{\gamma + \log\left(\frac{\rho}{2}\right)}{\rho} \tag{5.32}$$

is convergent. Therefore,

$$\begin{aligned} \int e^{i(q_y y + q_z z)} \log\left(q\right) \mathrm{d}^2 q &= 2\pi \left(\frac{\partial}{\partial \rho} + \frac{1}{\rho}\right) \int_0^\infty J_1\left(q\rho\right) \log\left(q\right) \mathrm{d}q \\ &= -\frac{2\pi}{\rho^2} \end{aligned} \tag{5.33}$$

plus delta-function terms. Similarly

$$\begin{aligned} \int e^{i(q_y y + q_z z)} \log^2\left(q\right) \mathrm{d}^2 q &= 2\pi \int_0^\infty q J_0\left(q\rho\right) \log^2\left(q\right) \mathrm{d}q \\ &= 2\pi \left(\frac{\partial}{\partial \rho} + \frac{1}{\rho}\right) \int_0^\infty J_1\left(q\rho\right) \log^2\left(q\right) \mathrm{d}q \\ &= 2\pi \left(\frac{\partial}{\partial \rho} + \frac{1}{\rho}\right) \frac{\left(\gamma + \log\frac{\rho}{2}\right)^2}{\rho} \\ &= \frac{4\pi}{\rho^2} \left(\gamma + \log\frac{\rho}{2}\right) \end{aligned} \tag{5.34}$$

All the other transforms needed can be found from these by integrating or applying the derivative operator in two dimensions $\nabla \equiv \left(\frac{\partial}{\partial y}, \frac{\partial}{\partial z}\right)$:

$$\begin{aligned} \int e^{-i(q_y y + q_z z)} \frac{q^\mu q^\nu}{q^2} \log\left(q\right) \mathrm{d}^2 q &= -\nabla_\mu \nabla_\nu f\left(\rho\right) \\ &= -\hat{\rho}_\mu \hat{\rho}_\nu \frac{d^2 f}{d\rho^2} - \left(\delta_{\mu\nu} - \hat{\rho}_\mu \hat{\rho}_\nu\right) \frac{1}{\rho} \frac{df}{d\rho} \end{aligned}$$

$$= \hat{\rho}_\mu \hat{\rho}_\nu 2\pi \frac{\log\rho - 1}{\rho^2} - \left(\delta_{\mu\nu} - \hat{\rho}_\mu \hat{\rho}_\nu\right) 2\pi \frac{\log\rho}{\rho^2} \tag{5.35}$$

where

$$\begin{aligned} \nabla^2 f(\rho) &\equiv \nabla^2 \int e^{i(q_y y + q_z z)} \frac{\log(q)}{q^2} \mathrm{d}^2 q \\ &= -\int e^{i(q_y y + q_z z)} \log(q)\, \mathrm{d}^2 q \\ &= \frac{2\pi}{\rho^2} \\ f(\rho) &= \pi \log^2 \rho \end{aligned} \tag{5.36}$$

and $\hat{\rho}$ is the unit vector in the radial direction in the y-z plane.

$$\begin{aligned} \int e^{i(q_y y + q_z z)} q^\mu q^\nu \log(q)\, \mathrm{d}^2 q &= -\nabla_\mu \nabla_\nu \int e^{i(q_y y + q_z z)} \log(q)\, \mathrm{d}^2 q \\ &= \hat{\rho}_\mu \hat{\rho}_\nu \frac{12\pi}{\rho^4} - \left(\delta_{\mu\nu} - \hat{\rho}_\mu \hat{\rho}_\nu\right) \frac{4\pi}{r^4} \end{aligned} \tag{5.37}$$

$$\begin{aligned} \int e^{i(q_y y + q_z z)} q^2 \log(q)\, \mathrm{d}^2 q &= \nabla^2 \int e^{i(q_y y + q_z z)} \log(q)\, \mathrm{d}^2 q \\ &= \frac{1}{\rho} \frac{\mathrm{d}}{\mathrm{d}\rho} \rho \frac{\mathrm{d}}{\mathrm{d}\rho} \left(-\frac{2\pi}{\rho^2}\right) \\ &= -\frac{8\pi}{\rho^4} \end{aligned} \tag{5.38}$$

$$\begin{aligned} \int e^{i(q_y y + q_z z)} q^4 \log(q)\, \mathrm{d}^2 q &= \nabla^2 \int e^{i(q_y y + q_z z)} q^2 \log(q)\, \mathrm{d}^2 q \\ &= \frac{-128\pi}{\rho^6} \end{aligned} \tag{5.39}$$

$$\begin{aligned} \int e^{i(q_y y + q_z z)} q^2 \log^2(q)\, \mathrm{d}^2 q &= \nabla^2 \int e^{i(q_y y + q_z z)} \log^2(q)\, \mathrm{d}^2 q \\ &= \frac{16\pi}{\rho^4} \left(\gamma + \log\frac{\rho}{2} - 1\right) \end{aligned} \tag{5.40}$$

$$\begin{aligned} \int e^{i(q_y y + q_z z)} q^4 \log^2(q)\, \mathrm{d}^2 q &= \nabla^2 \int e^{i(q_y y + q_z z)} q^2 \log^2(q)\, \mathrm{d}^2 q \\ &= \frac{128\pi}{\rho^6} \left(2\gamma + 2\log\frac{\rho}{2} - 3\right) \end{aligned} \tag{5.41}$$

Using these results, (5.27) becomes

$$T^{\mu\nu}(x) = GE\delta(x - t) \frac{8}{\rho^4} \left(1 + 2\gamma + \log\frac{\lambda^2\rho^2}{4}\right) \hat{P}_\mu \hat{P}_\nu \tag{5.42}$$

plus delta-function terms. Substituting (5.22) and (5.19) into (5.5) and Fourier transforming, the long-range correction to the metric is

$$\begin{aligned}
\psi^{\mu\nu}(x) &= -\frac{8\pi G}{E}\int e^{-i(q_x(x-t)+q_y y+q_z z)}\left[2P_\mu P_\nu \frac{F_1(q^2)}{q^2}+\left(\frac{q_\mu q_\nu}{q^2}-\eta_{\mu\nu}\right)F_2(q^2)\right]\frac{\mathrm{d}^3 q}{(2\pi)^3} \\
&\approx 8G^2 E\delta(x-t)\int\left(3\log\frac{-q^2}{4\pi\mu^2}-\frac{1}{2}\log^2\frac{q^2}{\lambda^2}+\frac{1}{2}\log^2\frac{\lambda^2}{m^2}\right)e^{-i(q_y y+q_z z)}\frac{\mathrm{d}^2 q}{(2\pi)^2}\hat{P}_\mu\hat{P}_\nu \\
&= -\frac{8G^2 E}{\pi}\delta(x-t)\frac{1}{\rho^2}\left(3+2\gamma+2\log\frac{\lambda\rho}{2}\right)\hat{P}_\mu\hat{P}_\nu \qquad (5.43)
\end{aligned}$$

plus delta-function terms. The factors of $\log m^2$ which appear in the momentum representation have been absorbed into the local delta-function pieces in the position representation.

Substituting (5.24) into (5.23), the long-range results for the photon are:

$$\begin{aligned}
\langle p_4,\epsilon_4|\,T_{\mu\nu}\,|p_2,\epsilon_2\rangle &= \int\frac{\mathrm{d}^3 q}{(2\pi)^3}\frac{e^{-i(q_x(x-t)+q_y y+q_z z)}}{\sqrt{4E_2E_4}} \\
&\quad\cdot\left[2P_\mu P_\nu\left(\epsilon_2\cdot\epsilon_4-2\frac{\epsilon_2\cdot q\epsilon_4\cdot q}{q^2}\right)\right. \\
&\quad\cdot\left(-\frac{5Gq^2}{3\pi}\log\frac{-q^2}{4\pi\mu^2}-\frac{Gq^2}{4\pi}\log^2\left(\frac{-q^2}{m^2}\right)+\frac{Gq^2}{2\pi}\log\left(\frac{-q^2}{\lambda^2}\right)\log\left(\frac{-q^2}{m^2}\right)\right) \\
&\quad+\left(q_\mu q_\nu-\eta_{\mu\nu}q^2\right)\left(\epsilon_2\cdot\epsilon_4-2\frac{\epsilon_2\cdot q\epsilon_4\cdot q}{q^2}\right) \\
&\quad\cdot\left(\frac{5Gq^2}{12\pi}\log\frac{-q^2}{4\pi\mu^2}+\frac{Gq^2}{8\pi}\log^2\left(\frac{-q^2}{m^2}\right)-\frac{Gq^2}{4\pi}\log\left(\frac{-q^2}{\lambda^2}\right)\log\left(\frac{-q^2}{m^2}\right)\right) \\
&\quad+\left(\left(P_\mu+\frac{q_\mu}{2}\right)\epsilon_{4,\nu}\epsilon_2\cdot q+\left(P_\nu+\frac{q_\nu}{2}\right)\epsilon_{4,\mu}\epsilon_2\cdot q\right. \\
&\quad-\left(P_\mu-\frac{q_\mu}{2}\right)\epsilon_{2,\nu}\epsilon_4\cdot q-\left(P_\nu-\frac{q_\nu}{2}\right)\epsilon_{2,\mu}\epsilon_4\cdot q \\
&\quad\left.-\frac{q^2}{2}\left(\epsilon_{2,\mu}\epsilon_{4,\nu}+\epsilon_{4,\mu}\epsilon_{2,\nu}\right)+\left(4P_\mu P_\nu-q_\mu q_\nu\right)\frac{\epsilon_2\cdot q\epsilon_4\cdot q}{q^2}\right) \\
&\quad\left.\cdot\left(-\frac{5Gq^2}{6\pi}\log\frac{-q^2}{4\pi\mu^2}-\frac{Gq^2}{4\pi}\log^2\left(\frac{-q^2}{m^2}\right)+\frac{Gq^2}{2\pi}\log\left(\frac{-q^2}{\lambda^2}\right)\log\left(\frac{-q^2}{m^2}\right)\right)\right] \\
&\approx \frac{G}{\pi}E\int e^{-i(q_x(x-t)+q_y y+q_z z)} \\
&\quad\cdot\left[\epsilon_2\cdot\epsilon_4 q^2\left(-\frac{5}{3}\log\frac{-q^2}{4\pi\mu^2}-\frac{1}{4}\log^2\left(\frac{-q^2}{m^2}\right)+\frac{1}{2}\log\left(\frac{-q^2}{\lambda^2}\right)\log\left(\frac{-q^2}{m^2}\right)\right)\right. \\
&\quad\left.+\epsilon_2\cdot q\epsilon_4\cdot q\frac{5}{3}\log\frac{-q^2}{4\pi\mu^2}\right]\frac{\mathrm{d}^3 q}{(2\pi)^3}\hat{P}_\mu\hat{P}_\nu \\
&= \frac{G}{\pi^2}E\delta(x-t)\left[\epsilon_2\cdot\epsilon_4\left(-\frac{32}{3}\frac{1}{\rho^4}+\gamma\frac{4}{\rho^4}+\frac{4}{\rho^4}\log\frac{\lambda\rho}{2}\right)\right. \\
&\quad\left.+10\epsilon_2\cdot\hat{\rho}\epsilon_4\cdot\hat{\rho}\frac{1}{\rho^4}-\frac{10}{3}\left(\epsilon_2\cdot\epsilon_4-\epsilon_2\cdot\hat{\rho}\epsilon_4\cdot\hat{\rho}\right)\frac{1}{\rho^4}\right]\hat{P}_\mu\hat{P}_\nu \qquad (5.44)
\end{aligned}$$

$$\begin{aligned}
\psi^{\mu\nu}(q) &= -\frac{16G^2}{\pi}E\delta(x-t)\left[\epsilon_2\cdot\epsilon_4\left(\frac{5}{3}\frac{1}{\rho^2}-\gamma\frac{1}{\rho^2}-\frac{1}{\rho^2}\log\frac{\lambda\rho}{2}\right)\right. \\
&\quad\left.+\left(\frac{5}{3}\epsilon_2\cdot\hat{\rho}\epsilon_4\cdot\hat{\rho}\frac{\log\mu\rho-1}{\rho^2}-\frac{5}{3}\left(\epsilon_2\cdot\epsilon_4-\epsilon_2\cdot\hat{\rho}\epsilon_4\cdot\hat{\rho}\right)\frac{\log\mu\rho}{\rho^2}\right)\right]\hat{P}_\mu\hat{P}_\nu \qquad (5.45)
\end{aligned}$$

5.1.5 Interpretation of Collinear Divergence in Metric

The metrics (5.43) and (5.45) still contain the arbitrary parameters λ and m which regularize the IR divergences. They are written in such a way that the m dependence occurs only in the short-range, delta function terms, but the λ dependence remains even in the long-range terms. In this connection it should be noted that in principal the massive result contains λ dependence too, although only in terms concentrated in a distance of order $1/m$ of the source. At energies well below m, these terms could be expanded in q^2 and would appear like delta-function terms. The same thing would even occur in the radiative corrections to the electromagnetic field of a charge in QED. Just as in QED, the results remain the same using different IR regularization schemes after the appropriate substitutions $\log \lambda^2 \to \frac{2}{\epsilon_{IR}} + \gamma + \log 4\pi\mu^2$ or $\log m^2 \to \log 4\pi\mu^2 + 2/\epsilon_{IR} + \gamma$

If a cross section were computed using these metrics as an external field, and if bremsstrahlung were included, the λ dependence would also disappear, and the m dependence could still be written as a short-range or analytic term, as inspection of (4.95) shows. However the analytic term would occur in combination with E and k_{max}, which are non-covariant or depend on the detector resolution, and which could not be canceled by terms from the Lagrangian, since this is covariant and obviously independent of the detector. It also may seem disturbing that the analytic terms, which correspond to an expansion in q^2 and to the high energy degrees of freedom of the underlying theory, should be affected by the low energy degrees of freedom responsible for the IR divergences.

Thus it may be questionable in the massless case how meaningful the quantum corrections to the metric are. It should be noted that questions about the meaningfulness of the metric in a quantum theory have been raised even in the massive case [20].

5.2 Deflection of Starlight

Although it may be uncertain how meaningful the metrics (5.43) and (5.45) are, the full cross sections calculated in chapter 4, which contain the box and cross box diagrams, contain no infrared divergences, and are perfectly meaningful. Here these are applied to a simple problem, calculating the radiative corrections to the gravitational bending of light following the method of [32]. Classically, the problem consists of calculating the deflection of a beam of radiation in the geometric optics approximation, where light travels along null geodesics [24]. Here the same approximation is used.

Light rays in the geometric optics approximation correspond to photon trajectories in the semi-classical approximation. A beam of semiclassical particles approaching the scattering target with

impact parameter ρ and energy E scatters at an angle θ which is a function of ρ. The semiclassical formula for the scattering cross section is [31]

$$\frac{\mathrm{d}\sigma}{\mathrm{d}\theta} = 2\pi\rho\frac{\mathrm{d}\rho}{\mathrm{d}\theta} = \pi\frac{\mathrm{d}\rho^2}{\mathrm{d}\theta} \tag{5.46}$$

Solving for ρ,

$$\begin{aligned}\rho^2 &= \frac{1}{\pi}\int_\theta^\pi \frac{\mathrm{d}\sigma}{\mathrm{d}\theta}\mathrm{d}\theta \\ &= \frac{1}{\pi}\int_{4E^2\sin^2\frac{\theta}{2}}^{4E^2} \frac{\mathrm{d}\sigma}{\mathrm{d}\,(-t)}\mathrm{d}\,(-t)\end{aligned} \tag{5.47}$$

since $t = q^2 = -\vec{q}^2 = -4E^2\sin^2\frac{1}{2}\theta$.

5.2.1 Lowest Order

From (5.47) and the lowest order cross section in chapter 4, and using $s - M^2 \approx (M+E)^2 - M^2 \approx 2ME$, where E is the energy of the photon in the rest frame of the heavy scattering target, the deflection to lowest order in κ is

$$\begin{aligned}\rho^2 &= \frac{1}{\pi}\int_{4E^2\sin^2\frac{\theta}{2}}^{4E^2} \frac{16\pi G^2M^2E^2}{t^2}\mathrm{d}\,(-t) \\ &= 4G^2M^2\left(\frac{1}{\sin^2\frac{\theta}{2}} - 1\right)\end{aligned} \tag{5.48}$$

In the small angle approximation,

$$\rho^2 \approx \frac{16G^2M^2}{\theta^2} \tag{5.49}$$

$$\theta \approx \frac{4GM}{\rho} \tag{5.50}$$

which is the standard result [24].

5.2.2 Radiative Corrections

From (5.47) and (4.101), the correction to the deflection of a beam of scalar particles is

$$\begin{aligned}\rho^2 = \frac{4G^3M^2E^2}{\pi}\int_{4E^2\sin^2\frac{\theta(\rho)}{2}}^{4E^2}\Bigg(&-\frac{34}{3\,(-t)}\log\frac{-t}{\mu^2} + \pi^2\frac{17}{2\,(-t)}\frac{M}{\sqrt{-t}} \\ &+\frac{4}{(-t)}\log^2\frac{-t}{2ME} - \frac{8}{(-t)}\log\frac{k_{max}^2}{2ME}\log\frac{2E}{M} + \frac{4}{(-t)}\log\frac{-t}{k_{max}^2}\log\frac{-t}{2ME}\end{aligned}$$

$$
\begin{aligned}
&-\frac{12}{(-t)}\log\frac{2E}{M}\log\frac{-t}{2ME}+\frac{4}{(-t)}\log\frac{k_{max}^2}{2ME}+\frac{8}{(-t)}\log\frac{-t}{2ME}-\frac{4ME}{(-t)^2}\log^2\frac{-t}{2ME}\Bigg)\,\mathrm{d}\,(-t)\\
=\;& 4\frac{G^3M^2E^2}{\pi}\left(\frac{17}{3}\log\left(\sin^2\theta\right)\log\frac{16E^4\sin^2\theta}{\mu^2}+\pi^2\frac{17}{2}\frac{M}{E}\left(\frac{1}{\sin\left(\theta\right)}-1\right)\right.\\
&-\left(8\log^2\frac{2E}{M}+12\log\frac{M^2}{k_{max}^2}\log\frac{2E}{M}+4\log\frac{2E}{M}+4\log\frac{k_{max}^2}{M^2}\right)\log\left(\sin^2\theta\right)\\
&-\left(4\log\frac{2E}{M}-2\log\frac{k_{max}^2}{M^2}+4\right)\log^2\left(\sin^2\theta\right)-\frac{8}{3}\log^3\left(\sin^2\theta\right)\\
&-\frac{M}{E}\left(\log^2\frac{2E}{M}+2\log\frac{2E}{M}+2\right)\frac{1}{\sin^2\theta}-\frac{2M}{E}\left(\log\frac{2E}{M}+1\right)\frac{\log\left(\sin^2\theta\right)}{\sin^2\theta}\\
&\left.-\frac{M}{E}\frac{\log^2\left(\sin^2\theta\right)}{\sin^2\theta}+\frac{M}{E}\log^2\frac{2E}{M}+\frac{2M}{E}\log\frac{2E}{M}+\frac{2M}{E}\right)
\end{aligned}
\tag{5.51}
$$

In the small angle approximation

$$
\begin{aligned}
\rho^2 \;\approx\;& 4\frac{G^3M^2E^2}{\pi}\left(\frac{17}{3}\log\left(\frac{\theta^2}{4}\right)\log\frac{4E^4\theta^2}{\mu^2}+\pi^2 17\frac{M}{E}\frac{1}{\theta}\right.\\
&-\left(8\log^2\frac{2E}{M}+12\log\frac{M^2}{k_{max}^2}\log\frac{2E}{M}+4\log\frac{2E}{M}+4\log\frac{k_{max}^2}{M^2}\right)\log\left(\frac{\theta^2}{4}\right)\\
&-\left(2\log\frac{4E^2}{k_{max}^2}+4\right)\log^2\left(\frac{\theta^2}{4}\right)-\frac{8}{3}\log^3\left(\frac{\theta^2}{4}\right)\\
&-4\frac{M}{E}\left(\log^2\frac{2E}{M}+2\log\frac{2E}{M}+2\right)\frac{1}{\theta^2}-8\frac{M}{E}\left(\log\frac{2E}{M}+1\right)\frac{\log\left(\frac{\theta^2}{4}\right)}{\theta^2}\\
&\left.-4\frac{M}{E}\frac{\log^2\left(\frac{\theta^2}{4}\right)}{\theta^2}+\frac{M}{E}\left(\log^2\frac{2E}{M}+2\log\frac{2E}{M}+2\right)\right)
\end{aligned}
\tag{5.52}
$$

The first term represents the effect of higher order terms in the classical Schwarzschild metric. The μ^2 dependence combines with terms from the effective Lagrangian which must be determined empirically. The logarithms of E/M, E/k_{max}, and k_{max}/M which occur in (5.52) are somewhat illusory since they come from the soft-graviton terms in the cross section, which exponentiate in higher orders of perturbation theory. Adding (5.52) to (5.49) and solving for θ would produce a correction to the scattering angle of order GE^2, that is, the square of the Planck length to the wavelength, but this is fantastically small.

From (4.135) and (4.136) the correction to the deflection of a beam of light (photons) in the small angle approximation is

$$
\begin{aligned}
\rho^2 \;=\;& 8\frac{G^3M^2E^2}{\pi}\left(\pi^2\frac{17}{2}\frac{M}{E}\frac{1}{\theta}+\frac{76}{15}\left(\log\frac{E^2}{\pi\mu^2}\log\frac{\theta^2}{4}+\frac{1}{2}\log^2\frac{\theta^2}{4}\right)\right.\\
&\left.+\frac{4}{3}\log^3\frac{\theta^2}{4}+\left(\log\frac{4E^2}{k_{max}^2}-\frac{5}{2}\right)\log^2\frac{\theta^2}{4}\right.
\end{aligned}
$$

$$+\left(-4\log\frac{4E^2}{k_{max}^2}-2\log^2\frac{2E}{M}-\log\frac{2E}{M}\right)\log\frac{\theta^2}{4}\Bigg) \tag{5.53}$$

for polarization in the plane of scattering, and

$$\begin{aligned}\rho^2 &= 8\frac{G^3M^2E^2}{\pi}\left(\pi^2\frac{17}{2}\frac{M}{E}\frac{1}{\theta}-\frac{8}{5}\left(\log\frac{E^2}{\pi\mu^2}\log\frac{\theta^2}{4}+\frac{1}{2}\log^2\frac{\theta^2}{4}\right)\right.\\ &\quad+\frac{4}{3}\log^3\frac{\theta^2}{4}+\left(\log\frac{4E^2}{k_{max}^2}-\frac{5}{2}\right)\log^2\frac{\theta^2}{4}\\ &\quad\left.+\left(-4\log\frac{4E^2}{k_{max}^2}-2\log^2\frac{2E}{M}-\log\frac{2E}{M}\right)\log\frac{\theta^2}{4}\right)\end{aligned} \tag{5.54}$$

for polarization perpendicular to the plane of scattering. Again corrections are of order GE^2. The classical contribution (as well as the quantum contribution from the IR divergent pieces) is the same for both polarizations, but the remaining quantum contribution containing μ^2 is different. Thus while the quantum correction is extremely small, it does make a qualitatively different prediction than the classical result. A beam of unpolarized light incident on the scattering target would bent by a small angle approximately equal to the classical prediction, but in addition it would be split into two polarized beams separated by a very small angle, much as in a birefringent crystal.

CHAPTER 6
CONCLUDING REMARKS

The previous treatment of quantum gravity as an effective field theory has been extended here to massless particles. The lowest order classical predictions of general relativity have been reproduced, in particular the bending of starlight and the Aichelburg-Sexl metric. Just as in the massive case, quantum gravity predicts well-defined and unambiguous long-distance corrections. In agreement with the classical results, higher-order classical corrections to the metric vanish, while quantum corrections remain.

It has been shown explicitly to one loop order that the collinear divergences which usually occur in massless quantum field theories do not occur in scattering cross sections for photons and massless scalars in quantum gravity. An argument of Weinberg has been generalized to suggest that this is due to the special nature of gravity, that it couples to the energy and momentum of its source. The collinear divergences do not disappear from the expressions for the energy-momentum tensor and metric by themselves. This suggests that the concept of the metric of a massless particle may be ambiguous in the quantum case. It should be noted in this connection that it has already been argued [20] for different reasons that the metric of a massive particle is ambiguous in the quantum case, and the present results only compound this ambiguity. Any calculation using these results, however, would also have to include the effect of bremsstrahlung and the radiative corrections to the scattered particle, so all final, observable results would be finite.

As is usual for quantum gravity, the relative order of magnitude of the corrections is Gq^2, where q is the energy scale of the scattered particles. Since $G^{1/2} \sim 10^{-35}$, these corrections are imperceptibly small for any reasonable energy. In the case of the bending of starlight, the quantum corrections predict a qualitatively different result than the lowest-order classical result, that the angle of scattering is dependent on the polarization of the light. This might make verification of the quantum corrections less difficult, since there is no background classical effect obscuring the quantum prediction. Nevertheless the effect is so small that it is difficult to imagine how it ever could be observed. Further, if one were to attempt such an observation, one would have to consider other miniscule corrections, such as diffraction effects, and one would have to determine whether the

classical predictions were truly polarization independent to higher orders. The higher order classical corrections to the metric should certainly be polarization independent, since they depend only on the source of the field, but the author is unaware of any argument why classical terms from diagrams like the triangle diagram of fig. 4.18 should necessarily be polarization independent.

Although these results may remain experimentally inaccessible, they demonstrate that a consistent theory of the quantum gravity of massless particles is possible. As emphasized in [4, 5, 7], because the effective theory of gravity depends only on the low-energy degrees of freedom, it must remain valid at low energies in any theory which reproduces the classical theory of general relativity. Since the IR singularities result from the low energy degrees of freedom, they will still present a challenge to any such theory. For the same reason, however, they will have the same coefficients as calculated above, and hence will cancel in exactly the same way. Thus whatever the true underlying theory of gravity, the results demonstrated here will still be applicable.

APPENDIX

LIST OF CANCELLATION FORMULAE

Below is a list of all scalar product cancellation formulae used in the reduction of integrals:

$$\begin{aligned}
&\int \frac{k\cdot q}{(k^2-\lambda^2)\left((p_1-k)^2-M^2\right)\left((k-q)^2-\lambda^2\right)\left((p_2+k)^2-m^2\right)}\\
&=\frac{1}{2}\int \frac{1}{\left((p_1-k)^2-M^2\right)\left((k-q)^2-\lambda^2\right)\left((p_2+k)^2-m^2\right)}\\
&+\frac{q^2}{2}\int \frac{1}{(k^2-\lambda^2)\left((p_1-k)^2-M^2\right)\left((k-q)^2-\lambda^2\right)\left((p_2+k)^2-m^2\right)}\\
&-\frac{1}{2}\int \frac{1}{(k^2-\lambda^2)\left((p_1-k)^2-M^2\right)\left((p_2+k)^2-m^2\right)}
\end{aligned} \tag{A.1}$$

$$\begin{aligned}
&\int \frac{k\cdot p_1}{(k^2-\lambda^2)\left((p_1-k)^2-M^2\right)\left((k-q)^2-\lambda^2\right)\left((p_2+k)^2-m^2\right)}\\
&=\frac{1}{2}\int \frac{1}{\left((p_1-k)^2-M^2\right)\left((k-q)^2-\lambda^2\right)\left((p_2+k)^2-m^2\right)}\\
&-\frac{1}{2}\int \frac{1}{(k^2-\lambda^2)\left((k-q)^2-\lambda^2\right)\left((p_2+k)^2-m^2\right)}
\end{aligned} \tag{A.2}$$

$$\begin{aligned}
&\int \frac{k\cdot p_2}{(k^2-\lambda^2)\left((p_1-k)^2-M^2\right)\left((k-q)^2-\lambda^2\right)\left((p_2+k)^2-m^2\right)}\\
&=-\frac{1}{2}\int \frac{1}{\left((p_1-k)^2-M^2\right)\left((k-q)^2-\lambda^2\right)\left((p_2+k)^2-m^2\right)}\\
&+\frac{1}{2}\int \frac{1}{(k^2-\lambda^2)\left((p_1-k)^2-M^2\right)\left((k-q)^2-\lambda^2\right)}
\end{aligned} \tag{A.3}$$

$$\int \frac{k^2}{(k^2-\lambda^2)\left((p_1-k)^2-M^2\right)\left((k-q)^2-\lambda^2\right)\left((p_2+k)^2-m^2\right)}$$

$$= \int \frac{1}{\left((p_1-k)^2 - M^2\right)\left((k-q)^2 - \lambda^2\right)\left((p_2+k)^2 - m^2\right)} \tag{A.4}$$

$$\begin{aligned}
&\int \frac{k\cdot q}{(k^2-\lambda^2)\left((k-q)^2-\lambda^2\right)\left((p_1-k)^2-M^2\right)}\frac{d^Dk}{(2\pi)^D} \\
&= \frac{1}{2}\int \frac{1}{\left((k-q)^2-\lambda^2\right)\left((p_1-k)^2-M^2\right)}\frac{d^Dk}{(2\pi)^D} \\
&+\frac{q^2}{2}\int \frac{1}{(k^2-\lambda^2)\left((k-q)^2-\lambda^2\right)\left((p_1-k)^2-M^2\right)}\frac{d^Dk}{(2\pi)^D} \\
&-\frac{1}{2}\int \frac{1}{(k^2-\lambda^2)\left((p_1-k)^2-M^2\right)}\frac{d^Dk}{(2\pi)^D}
\end{aligned} \tag{A.5}$$

$$\begin{aligned}
&\int \frac{k\cdot p_1}{(k^2-\lambda^2)\left((k-q)^2-\lambda^2\right)\left((p_1-k)^2-M^2\right)}\frac{d^Dk}{(2\pi)^D} \\
&= \frac{1}{2}\int \frac{1}{(k^2-\lambda^2)\left((k-q)^2-\lambda^2\right)\left((p_1-k)^2-M^2\right)}\frac{d^Dk}{(2\pi)^D} \\
&-\frac{1}{2}\int \frac{1}{(k^2-\lambda^2)\left((k-q)^2-\lambda^2\right)}\frac{d^Dk}{(2\pi)^D}
\end{aligned} \tag{A.6}$$

$$\begin{aligned}
&\int \frac{k^2}{(k^2-\lambda^2)\left((k-q)^2-\lambda^2\right)\left((p_1-k)^2-M^2\right)}\frac{d^Dk}{(2\pi)^D} \\
&= \int \frac{1}{\left((k-q)^2-\lambda^2\right)\left((p_1-k)^2-M^2\right)}\frac{d^Dk}{(2\pi)^D}
\end{aligned} \tag{A.7}$$

$$\begin{aligned}
&\int \frac{p_1\cdot k}{(k^2-\lambda^2)\left((p_1-k)^2-M^2\right)\left((p_2+k)^2-m^2\right)}\frac{d^Dk}{(2\pi)^D} \\
&= \frac{1}{2}\int \frac{1}{\left((p_1-k)^2-M^2\right)\left((p_2+k)^2-m^2\right)}\frac{d^Dk}{(2\pi)^D} \\
&-\frac{1}{2}\int \frac{1}{(k^2-\lambda^2)\left((p_2+k)^2-m^2\right)}\frac{d^Dk}{(2\pi)^D}
\end{aligned} \tag{A.8}$$

$$\int \frac{k^2}{(k^2-\lambda^2)\left((p_1-k)^2-M^2\right)\left((p_2+k)^2-m^2\right)}\frac{d^Dk}{(2\pi)^D}$$

$$= \int \frac{1}{\left((p_1-k)^2 - M^2\right)\left((p_2+k)^2 - m^2\right)} \frac{d^D k}{(2\pi)^D} \tag{A.9}$$

$$\begin{aligned} \int \frac{k\cdot q}{(k^2-\lambda^2)\left((k-q)^2-\lambda^2\right)} \frac{d^D k}{(2\pi)^D} &= \frac{1}{2}\int \frac{1}{(k-q)^2-\lambda^2}\frac{d^D k}{(2\pi)^D} - \frac{1}{2}\int \frac{1}{k^2-\lambda^2}\frac{d^D k}{(2\pi)^D} \\ &\quad + \frac{q^2}{2}\int \frac{1}{(k^2-\lambda^2)\left((k-q)^2-\lambda^2\right)}\frac{d^D k}{(2\pi)^D} \end{aligned} \tag{A.10}$$

$$\int \frac{k^2}{(k^2-\lambda^2)\left((k-q)^2-\lambda^2\right)} \frac{d^D k}{(2\pi)^D} = \int \frac{1}{(k-q)^2-\lambda^2}\frac{d^D k}{(2\pi)^D} \tag{A.11}$$

$$\begin{aligned} &\int \frac{1}{\left((p_1-k)^2 - M^2\right)\left((p_2+k)^2 - m^2\right)} \frac{d^D k}{(2\pi)^D} = \\ &\frac{(p_1+p_2)^2 - M^2 + m^2}{2}\int \frac{1}{\left((p_1+p_2-k)^2-M^2\right)(k^2-m^2)}\frac{d^D k}{(2\pi)^D} \\ &\frac{1}{2}\int \frac{1}{(p_1+p_2-k)^2-M^2}\frac{d^D k}{(2\pi)^D} - \frac{1}{2}\int \frac{1}{k^2-m^2}\frac{d^D k}{(2\pi)^D} \end{aligned} \tag{A.12}$$

$$\begin{aligned} \int \frac{k^2}{\left((p_1+p_2-k)^2-M^2\right)(k^2-m^2)} \frac{d^D k}{(2\pi)^D} &= m^2 \int \frac{1}{\left((p_1+p_2-k)^2-M^2\right)(k^2-m^2)}\frac{d^D k}{(2\pi)^D} \\ &\quad + \int \frac{1}{(p_1+p_2-k)^2-M^2}\frac{d^D k}{(2\pi)^D} \end{aligned} \tag{A.13}$$

BIBLIOGRAPHY

[1] S. Weinberg, Quantum Theory of Fields, volume 1. Cambridge University Press, Cambridge, 1996.

[2] N.N. Bogoliubov and D.V. Shirkov, Introduction to the Quantum Theory of Fields. Interscience Publishers, New York, 1959.

[3] John F. Donoghue, Eugene Golowich, and Barry R. Holstein. Dynamics of the Standard Model, Cambridge University Press, Cambridge, 1994.

[4] J.F. Donoghue Phys. Rev. Lett. **72** 2996 (1994).

[5] J.F. Donoghue Phys. Rev. D **50** 3874 (1994).

[6] N.E.J. Bjerrum-Bohr, J.F. Donoghue, and B.R. Holstein, Phys. Rev. **D68**, 084005 (2003).

[7] N.E.J. Bjerrum-Bohr, J.F. Donoghue, and B.R. Holstein, Phys. Rev. **D67**, 084033 (2003).

[8] P.C. Aichelburg and R.U. Sexl, General Relativity and Gravitation **2** 4 303 (1971).

[9] P.C. Aichelburg and R.U. Sexl, Lettre al Nuovo Cimento **4** 26 1316 (1970).

[10] Basilis, C. Xanthopoulos, J. Math. Phys. **19** (7) 1607 (1978).

[11] C. Barrabes. C. and P.A. Hogan, Singular Null Hypersurfaces in General Relativity, World Scientific Publishing, Singapore, 2003.

[12] Barry Holstein, Phys. Rev. D **74** 084030 (2006).

[13] G. 't Hooft and M. Veltman, Ann. Inst. H. Poincare **A20** 69 (1974). M. Veltman, in Methods in Field Theory Proc. of the Les Houches Summer School, 1975, ed. by R. Balian and J.Zinn-Justin, North Holland, Amsterdam, 1976.

[14] G. Passarino and M. Veltman, Nucl. Phys. B **160** 151 (1979).

[15] Available on the internet at HTTP://www.feyncalc.org/

[16] George Sterman, An Introduction to Quantum Field Theory, Cambridge University Press, Cambridge, 1993.

[17] Stefan Pokorski, Guage Field Theories, 2nd. ed., Cambridge University Press, Cambridge, 2000.

[18] J. Kinoshita, Math. Phys. **3** 650 (1962). Lee, T.D. and Naunberg, M., Phys. Rev. **133** B1549 (1964).

[19] Steven Weinberg, Phys. Rev. **140** B516 (1965).

[20] G.G. Kirilin, Phys. Rev. **D75** 108501 (2007). N.E.J. Bjerrum-Bohr, John F. Donoghue and Barry Holstein, Phys Rev. **D75** 108502 (2007).

[21] J.F. Donoghue and B.R. Holstein, Phys Rev. Lett. **93** 201602 (2004).

[22] Donoghue, Intro to Effective Field Theory Gravity

[23] V. B. Berestetskii, E. M. Lifshitz and L. P. Pitaevskii, Quantum Elecdtrodynamics, 2nd edition, Volume 4 of Course of Theoretical Physics by Landau and Lifshitz. Butterworth-Heinemann, Oxford 1982.

[24] Robert M. Wald, General Relativity. University of Chicago Press, Chicago, 1984.

[25] C. P. Burgess, Quantum Gravity in Everyday Life: General Relativity as an Effective Field Theory. Living. Rev. Rel. **7** 5 (2004). arXiv:gr-qc/0311082v1

[26] Hermann Weyl, Space-Time-Matter. Dover, Mineola, NY, 1952.

[27] J. Simon, Phys. Rev. **D41,** 3720 (1990); **43** 3308 (1991)

[28] G. 'tHooft and M. Veltman, Scalar One-Loop Integrals. Nuclear Physics **B153** 365-401 (1979)

[29] Leonard Llewyn, Polylogarithms and Associated Functions. Elsevier North Holland, New York, 1981

[30] James D. Bjorken and Sydney D. Drell, Relativistic Quantum Mechanics. McGraw-Hill, 1964.

[31] L. D. Landau and E. M. Lifshitz, Mechanics, 3rd edition, Volume 1 of Course of Theoretical Physics. Butterworth-Heinemann, Oxford 1982.

[32] M. D. Scadron, Advanced Quantum Theory. Springer-Verlag, New York (1979).

[33] I.J. Muzinich and S. Vokos, Phys Rev. D **52**, 3472 (1995); H.W. Hamber and S. Liu, Phys. Lett. B **357**, 51 (1995); A.A. Akhundov, S. Bellucci, and A Shiekh, Phys. Lett. B **395**, 16 (1997); I.B. Khirplovich and G.G. Kirilin, Zh. Eksp. Teor. Fiz. **95**, 1139 (2002); N.E.J. Bjerrum-Bohr, Cand. Scient. thesis, University of Copenhagen, 2001.

[34] Wolfram Research, Inc., Mathematica Version 8.0. Champagne, IL (2011).